

NATIONAL AND KAPODISTRIAN UNIVERSITY OF ATHENS  
FACULTY OF NURSING

SECTOR: BASIC SCIENCE

**THESIS: Study of the effects of mutant alpha-synuclein in  
models of Parkinson's disease**

**Ourania Zygogianni MSc**

Biologist

DOCTORAL THESIS

O.Z. was awarded a scholarship from the State Scholarship Foundation (IKY) funded by the Action "Scholarships for post-graduate studies" (Operational Program "Education and Lifelong learning", 2014-2020) and co-financed by the European Social Fund and the Greek government.

HELLENIC PASTEUR INSTITUTE  
LABORATORY OF CELLULAR AND MOLECULAR  
NEUROBIOLOGY- STEM CELLS



ATHENS 2019

**THESIS: Study of the effects of mutant alpha-synuclein in models of Parkinson's disease**

NATIONAL AND KAPODISTRIAN UNIVERSITY OF ATHENS  
FACULTY OF NURSING

SECTOR: BASIC SCIENCE

**THESIS: Study of the effects of mutant alpha-synuclein in  
models of Parkinson's disease**

**Ourania Zygianni MSc**

Biologist

DOCTORAL THESIS

O.Z. was awarded a scholarship from the State Scholarship Foundation (IKY) funded by the Action "Scholarships for post-graduate studies" (Operational Program "Education and Lifelong learning", 2014-2020) and co-financed by the European Social Fund and the Greek government.

HELLENIC PASTEUR INSTITUTE  
LABORATORY OF CELLULAR AND MOLECULAR  
NEUROBIOLOGY- STEM CELLS



ATHENS 2019

**ADVISORY COMMITTEE**

1. EMERITUS PROFESSOR FOTINI STYLIANOPOULOU (SUPERVISOR)
2. RESEARCH DIRECTOR REBECCA MATSAS
3. ASSOCIATE PROFESSOR ANTONIOS STAMATAKIS

**EXAMINATION COMMITTEE:**

1. EMERITUS PROFESSOR FOTINI STYLIANOPOULOU (SUPERVISOR), FACULTY OF NURSING
2. RESEARCH DIRECTOR REBECCA MATSAS, HELLENIC PASTEUR INSTITUTE
3. ASSOCIATE PROFESSOR ANTONIOS STAMATAKIS, FACULTY OF NURSING
4. PROFESSOR SPIROS EFTHIMIOPOULOS, FACULTY OF BIOLOGY
5. PROFESSOR LEONIDAS STEFANIS, FACULTY OF MEDICINE
6. PROFESSOR MARIA PANAYIOTAKOPOULOU, FACULTY OF MEDICINE
7. RESEARCH DIRECTOR DIMITRA THOMAIDOU, HELLENIC PASTEUR INSTITUTE

For the English language all over the world. Intellectual property is obtained without any formulation and without the need for clause prohibiting its infringement. It should be noted, however, that under Law 2387/20 (as amended by Law No. 100/1975 and still in force) and under the International Convention of Berne (as ratified by Law No. 100/1975), republishing is prohibited, the storage in any saving system and generally the reproduction of the present work, in any way or form, in whole or in part, in the original or in translation or other adaptation without the written permission of the author.

"The approval of the Doctoral Thesis by the Department of Nursing of the University of Athens does not mean accepting the views of the author".

(Relevant provisions of Article 50 of Law 1268/82, in combination with the provisions of the University of Athens, Article 202 (2) of Law 5343/3

## **AKNOWLEDGEMENTS**

I would like to express my gratitude to all the people who offered me guidance, help and support during my studies. Without their help, completing the thesis would not be possible.

I would be indebted to **Dr Rebecca Matsas**, my supervisor for giving me the opportunity to join the stem cell research group at her lab, interacting with all these wonderful people that work in the lab. Moreover, I thank her for her support and scientific guidance all these years (from day 1 until day 1930!). Most of all, I thank her for placing her trust with me for such a demanding project.

I would like to thank **Prof. Fotini Stylianopoulou, and Assistant Prof, Antonios Stamatakis**, my co-supervisors for understanding, supporting and guiding me in so many ways as a PhD student and earlier as a Master student. I would also like to thank Prof. Spyros Efthimiopoulos, Prof. Leonidas Stefanis, Prof. Maria Panayiotakopoulou and Dr Dimitra Thomaidou for being members in my examination committee.

I would be grateful to the following three scientists: **Dr Era Taoufik, Dr Georgina Kouroupi and Dr Florentia Papastefanaki**. I consider myself lucky working with them! Era guided me and gave me scientific perspective in times I was losing hope! I thank her for her time, and for teaching me all these things, technical and scientific. I also thank her for helping me writing the thesis! I thank Georgina for introducing me in the induced pluripotent stem cell world, and for the guidance that provided me with. For her trust to work with her in the Human Stem Cell Unit of Hellenic Pasteur Institute (HPI). Importantly, I consider I have gained a valuable friend! I feel indebted to Florentia, who is a great person and scientist. I thank her for her professionalism, her calm approach, her immunohistochemical and so many other technical expertises! I also thank her for her time working with me in the animal house. She is an irreplaceable coworker.

It is important for me to thank **Nasia Antoniou**, my lab-mate in the craziness that we have lived from time to time! I thank her for listening to my complaints, always trying to support me. I also thank her for our scientific and not at all scientific talks in and out of the lab. Lastly, I thank her for our cooperation in this

project during the last year. Nasia the floor is yours, I am waiting for you in the “Dr side”!!!

I would like also to thank **Maria Kalomoiri**, the former Master student of the lab, for participating in this project. Her time was valuable in a year that I really needed help with the analysis of the mouse model. I also want to thank the other members of Dr Matsas lab, **Dr Katerina Segklia**, **Dr Kanella Prodromidou**, **Dr Konstantinos Tsioras** and the former Master student of the lab **Maria Koronaïou** for the fruitful discussions, and the amazing time we had in the lab the last five years. I also thank the other members of the lab, **Dr Maria Gaitanou**, and **Nick Kokorakis**, as well as **Dr Thomaidou** and the members of her lab, **Elsa Papadimitriou**, **Katerina Aravantinou**, **Eirini Thanou**, **Pari Koutsoudaki** for providing help as well as a pleasant and fun environment in the lab!

Furthermore, I would like to thank the members of the Department of Animal Models for Biomedical Research (DAMBR) of the HPI for the technical support with the animals during these years.

It is also important to mention that I wouldn't be able to complete my thesis without the financial support by the **State Scholarship Foundation (IKY)**. The last one and a half year of my thesis, I was awarded a scholarship which was essential for me to continue with my studies and completing them on time.

Most importantly I would like to thank my parents, Nickos and Sophie, for their endless love, support and the faith they put on me, as well as my siblings, Jane and George, for being there.

*To my first teachers, my parents*

## CONTENTS

AKNOWLEDGEMENTS .....	6
CONTENTS .....	9
ABBREVIATIONS.....	12
1. INTRODUCTION.....	16
1.1 Parkinson’s disease.....	16
1.1.1 General.....	16
1.1.2 Clinical features of PD.....	16
1.1.3 Neuropathological features .....	18
1.1.4 Etiology of PD.....	20
1.1.5 Mechanisms involved in PD pathogenesis .....	26
1.2 A-synuclein .....	30
1.2.1 Localization and structure of $\alpha$ Syn.....	30
1.2.2 Physiological function of $\alpha$ Syn.....	32
1.2.3 Pathological role of $\alpha$ Syn.....	34
1.2.4 $\alpha$ Syn secretion and transmission .....	40
1.3 Modeling PD .....	41
1.3.1 Animal models.....	42
1.3.2 Cellular models.....	55
1.4 Induced Pluripotent Stem Cells .....	57
1.4.1 iPSC applications.....	59
1.4.2 Modeling PD using an <i>in vitro</i> human iPSC model.....	64
1.5 PD treatment .....	72
1.5.1 Pharmacological treatment.....	73
1.5.2 Surgical procedures: Deep Brain Stimulation.....	75
1.5.4 Cell replacement approaches .....	76
2. AIM OF THE THESIS/ OBJECTIVES .....	81
3. MATERIALS.....	84
3.1 Lab equipment.....	84
3.1.1 Instruments and devices.....	84
3.1.2 Microscopes and Image analysis software .....	84
3.1.3 Consumables.....	84
3.2 Reagents .....	85
3.2.1 Chemical reagents.....	85

3.2.2 Cell culture .....	86
3.2.3 Enzymes.....	88
3.2.4 Primer sequences.....	89
3.2.5 Antibodies .....	90
3.2.6 Buffers .....	91
3.3 Laboratory animals .....	92
4. METHODS.....	93
4.1 Human iPSC culture and maintenance.....	93
4.1.1 Human iPSC culture and passaging.....	93
4.1.2 Thawing iPSCs.....	94
4.1.3 Freezing iPSCs.....	94
4.1.4 Detection of the G209A (A53T) mutation in patient-derived genomic DNA.....	95
4.2 Dopaminergic differentiation of human iPSCs.....	95
4.3 Magnetically activated cell sorting (MACS) of PSA-NCAM-positive DAergic cells.....	96
4.4 Primary culture of mouse astrocytes.....	97
4.5 RNA isolation.....	97
4.6 RNA cleaning cDNA Synthesis.....	98
4.7 Real time quantitative PCR.....	99
4.8 Immunofluorescence.....	99
4.9 Electrophysiology.....	100
4.10 Calcium Imaging.....	100
4.11 6-OHDA lesioned mice.....	100
4.12 Behavioral analysis.....	101
4.13 Intrastratial transplantation.....	101
4.14 Euthanasia and Immunohistochemistry.....	102
4.15 Image acquisition and image analysis.....	102
4.16 Statistical analysis.....	103
5. RESULTS .....	104
5.1 iPSC characterization from healthy and PD patients.....	104
5.2 DAergic differentiation and characterization of iPSC-derived neurons .....	106
5.3 Establishment of the 6-OHDA- induced lesion in the medial forebrain bundle of immunodeficient mice and pilot cell transplantation.....	110
5.4 Magnetic Cell Sorting and characterization of the iPSC-derived immature neurons ..	112
5.5 Characterization of long-term DAergic neuronal cultures .....	115
5.5.1 Morphological alterations.....	115
5.5.2 Electrophysiological analysis .....	118

5.5.3 Dysregulated calcium activity in PD neurons .....	118
5.6 Establishment and characterization of the 6-OHDA-induced striatal lesion model in immunodeficient mice .....	120
5.7 <i>In vivo</i> engraftment of iPSC-derived immature neurons.....	124
5.7.1 Investigation of cell survival and differentiation.....	124
5.7.2 Investigation of microglial response.....	132
5.7.3 Conclusions from the <i>in vivo</i> modeling of PD neuronal phenotypes in the 6-OHDA mouse model .....	133
6. DISCUSSION.....	135
6.1 Main findings and discussion.....	135
6.2 Limitations of the study.....	139
6.3 Future research directions .....	141
7. EXTENDED ABSTRACT .....	143
8. ΕΚΤΕΤΑΜΕΝΗ ΠΕΡΙΛΗΨΗ .....	148
9. REFERENCES .....	154

## **ABBREVIATIONS**

**AA** Ascorbic Acid

**AD** Alzheimer's disease

**$\alpha$ Syn** alpha synuclein

**BBB** Blood- Brain Barrier

**BDNF** Brain-derived neurotrophic factor

**BMP** Bone Morphogenic Protein

**cAMP** dibutyryl cyclic adenosine monophosphate

**CMV** Cytomegalovirus

**CNS** Central Nervous System

**CSF** Cerebrospinal fluid

**DA** Dopamine

**DAergic** Dopaminergic

**DAT** Dopamine Transporter

**DBS** Deep Brain Stimulation

**DCX** Doublecortin

**DRP1** Dynamin related protein 1

**EB** Embryoid body

**ER** Endoplasmic Reticulum

**ESC** embryonic stem cell

**FDA** Food and Drug Administration

**FOXA2** Forkhead Box Protein A2

**fVM** fetal ventral mesencephalic

**GBA1**  $\beta$ -Glucocerebrosidase gene

**GCCase**  $\beta$ -Glucocerebrosidase

**GDNF** Gial-derived neurotrophic factor

**GFP** Green Fluorescent Protein

**GI** Gastrointestinal

**GMP** Good Manufacturing Practice

**GPi** internal globus pallidus

**GWASs** Genome Wide Association Studies

**HSYP** Human Synaptophysin

**iPSC** induced pluripotent stem cell

**KO** Knock-out

**LBs** Lewy Bodies

**LMX1A** LIM Homeobox Transcription Factor 1 alpha

**LRRK2** Leucine rich repeat kinase 2

**LSD** Lysosomal Storage Disorders

**OMM** Outer Mitochondrial Membrane

**MAM** Mitochondria-associated membrane

**MAO-B** Monoamine oxidase- B

**MAP2** Microtubule-associated protein 2

**MEA** Multi-electrode array

**MFB** Medial Forebrain Bundle

**MPTP** 1-methyl-4-phenyl-1,2,3,6-tetrahydropyridine

**MPPP** 1-methyl-4-phenyl-4-propionoxypiperidine

**MSA** Multiple System Atrophy

**NAC** non-amyloid- $\beta$  component

**NMDA** N-methyl-D-aspartate

**PD** Parkinson's disease

**PDGF- $\beta$**  platelet-derived growth factor subunit  $\beta$

**PGC-1 $\alpha$**  peroxisome proliferator-activated receptor  $\gamma$  coactivator-1 $\alpha$

**PNS** Peripheral Nervous System

**REM** Rapid Eye Movement

**ROS** reactive oxygen species

**PrP** Prion Protein

**PSA-NCAM** Polysialic Neural Cell Adhesion Molecule

**SERT** serotonin transporter

**SMA** Smooth Muscle Actin

**SNARE** SNAP Receptor

**SNpc** Substantia Nigra pars compacta

**SSEA3-4** Stage-specific embryonic antigen 3-4

**STR** striatum

**Tg** Transgenic

**TGF- $\beta$**  Transforming growth factor beta

**TH** Tyrosine hydroxylase

**TNT** tunneling nanotubes

**TOM** Translocase of outer membrane

**TUJ1** Tubulin beta III

**VMAT2** vesicular monoamine transporter 2

**VIM** ventral medial nucleus of the thalamus

**VTA** Ventral Tegmental Area

**WT** wild type

**6-OHDA** 6-hydroxy-dopamine

## **1. INTRODUCTION**

### **1.1 Parkinson's disease**

#### **1.1.1 General**

Parkinson's disease (PD) is the second most common neurodegenerative disease, after Alzheimer's (AD), with a prevalence of about 1–2% in adults over 60 years of age in industrialized countries and 4% in the population over 85 years [1]. The worldwide incidence rate varies greatly depending on geographical distribution of the population, on ethnicity and sex [2, 3].

Although traditional Indian and ancient Chinese texts refer to PD-like clinical features, the first description of the disorder is credited to the British physician James Parkinson in his monograph *Essay on the Shaking Palsy*, in 1817 [4]. However, it was not until 65 years later that Jean Martin Charcot named the disease in his honor as PD, and further established its fundamental features [5]. Furthermore, it took more than a century until the neuronal loss of the specific anatomical brain region of substantia nigra (SN) to be correlated with the disease [6] and one and a half century to unravel the functional role of dopamine (DA) [7].

PD is the most common cause of Parkinsonism, a wider disorder that accounts for any clinical condition characterized by tremor at rest, rigidity, slowness or absence of voluntary movement, postural instability, and freezing [8]. Unfortunately, despite the remarkable advances in our understanding of the disease in the past 200 years, there is still no cure. For this reason, efforts should continue in order to address this unmet medical need.

#### **1.1.2 Clinical features of PD**

##### **1.1.2.1 Motor symptoms**

PD is a common yet complex and heterogeneous disorder that manifests with a broad range of symptoms, both motor and non-motor. Motor symptoms are of utmost importance for the diagnosis of the disease. The onset is gradual and the earliest symptoms might be unnoticed or misinterpreted for a long time leading to a lag of 2-3 years from the first symptoms to diagnosis. In the beginning, impairment of dexterity or slight dragging of one foot can be observed [9-11].

In most cases, symptoms start in one side of the body with contralateral symptoms appearing within a few years. The body posture becomes stooped, there is axial and limb rigidity with or without “cogwheel” phenomenon, tendency for a shuffling gait and lack of arm swing while walking, as well as limb tremor (rev. by [12]). Speech disturbances and swallowing problems have also been reported [13]. According to United Kingdom Parkinson’s Disease Society Brain Bank clinical diagnostic criteria (UKPDSBB), the first step towards diagnosis of a parkinsonian syndrome is the detection of bradykinesia (slowness of initiation of voluntary movement with progressive reduction in speed and amplitude or repetitive actions), along with either muscular rigidity, 4–6 Hz rest tremor or postural instability [14, 15]. The second step towards diagnosis of PD is to exclude symptoms indicative of other parkinsonian syndromes. Lastly, at least three supportive criteria for PD, such as unilateral onset of symptoms, persistent asymmetry of clinical symptoms, good response to levodopa treatment and induction of dyskinesias by the dopaminergic treatment should be applied [14].

#### **1.1.2.2 Non-motor symptoms**

Non-motor symptoms may exist 10 or even more years before diagnosis of PD [16], during the prodromal phase of the disease. They can be categorized as disturbances in autonomic function, sensory stimulation, sleep, and cognitive abilities (rev. by [12]).

Autonomic dysfunction may appear prior to diagnosis or become apparent with disease progression [17, 18]. Orthostatic hypotension affects one-third of PD patients, leading to hypoperfusion of the brain, dizziness, visual disturbances and impaired cognition that may precede loss of consciousness (rev. by [12, 19]). Gastrointestinal (GI) symptoms may appear with slow-transit constipation that occurs in 70-80% of the patients [20]. Urinary control disturbances are also common, including urinary urgency, frequency, and incontinence (rev. by [19]). Autonomic dermatological symptoms like excessive sweating (hyperhidrosis) have also been reported [21].

Reduced or lost sense of smell constitutes a major sensory symptom found in at least four out of five patients, appearing years before the onset of

motor symptoms [22]. Odor identification tests are used to assess olfaction in PD with the University Of Pennsylvania Smell Identification Test (UPSIT) being arguably the one used worldwide [23].

Sleep disturbances affect two-thirds of PD patients [24]. Fractionated sleep is the most common, including shallow sleep, frequent awakenings in the night and nocturia [25]. Sleep-associated syndromes, like rapid eye movement (REM) sleep behavior disorder and restless legs syndrome, appear in PD patients more frequently than in healthy individuals [26].

Among the non-motor symptoms, neuropsychiatric manifestations are very common in PD patients. Illusions and visual hallucinations occur in 30-40% of patients [27]. In later disease stages, patients may develop paranoid illusions as well as psychosis associated with old age, cognitive impairment and history of depression [28].

Cognitive changes in focused attention and planning, thought, language and memory, personality features, and appearance of dementia are common and may occur both in early or late stages (Williams-Gray et al. 2006, 2007). Mood disorders like depression and anxiety are other common symptoms and usually increase with disease progression [29].

Approximately 60% of patients with PD experience pain, and in a minority of these individuals, the problem is so intractable that it becomes the most distressing symptom of PD [30, 31]. It can be categorized in myoskeletal, radicular or neuropathic, central or primary pain, and akathisia [32].

### **1.1.3 Neuropathological features**

A major pathological hallmark of the disease is the region-specific selective degeneration and eventually loss of A9 dopaminergic (DAergic) neuromelanin-containing neurons from the pars compacta of the substantia nigra (SNpc) in the brain (Fig. 1A-D). More specifically, the ventrolateral tier of SNpc containing neurons that project to the dorsal putamen of the striatum (STR) is the most affected area. The neuronal loss in SNpc leads to a prominent DA deficiency in the striatum, directly correlated with motor features like bradykinesia and rigidity [33]. The DAergic neurons, along with other catecholaminergic neurons, are positive for the enzyme tyrosine hydroxylase

(TH), which catalyzes the conversion of the amino acid L-tyrosine to L-3, 4-dihydroxyphenylalanine (L-dopa), the precursor of DA [34]. Loss of DAergic neurons ultimately leads to destruction of the nigrostriatal pathway [35]. However, neuronal degeneration in other brain regions such as the locus coeruleus, the dorsal nuclei of the vagus nerve, the raphe nuclei, the nucleus basalis of Meynert, the amygdala, and the hypothalamus also occurs [36].

Another hallmark of PD, accompanying the specific neuronal degeneration, is the appearance of intraneuronal inclusions, named Lewy bodies (LBs), first described almost a century after the description of the disease (Fig. 1E-G) [37]. A constant proportion of SN neurons (3–4%) contain LBs, irrespective of disease progression. The main component of LBs is a pathological, post-translationally modified and aggregated form of the  $\alpha$ -synuclein ( $\alpha$ Syn) protein. In a misfolded state,  $\alpha$ Syn becomes insoluble and aggregates forming inclusions in the neuronal soma (LBs) and neuronal processes (Lewy neurites) (rev. by [38]).

LB pathology is not restricted to the brain but can also be found in the spinal cord and the peripheral nervous system (PNS), including the vagus nerve, sympathetic ganglia, cardiac plexus, enteric nervous system, salivary glands, adrenal medulla, cutaneous nerves, and the sciatic nerve [39].

Based on their morphology, LBs are subdivided in two categories, the classical brainstem type and the cortical type [40-43]. Brainstem LBs share a spherical structure with a hyaline core surrounded by a peripheral pale-staining halo, and ultrastructurally are composed of filaments with dense granule material and vesicular structures. On the other hand, cortical LBs lack the inner core and the halo and largely appear in small-to-medium-sized pyramidal neurons of layers V and VI of the cortex (rev. by [44]).

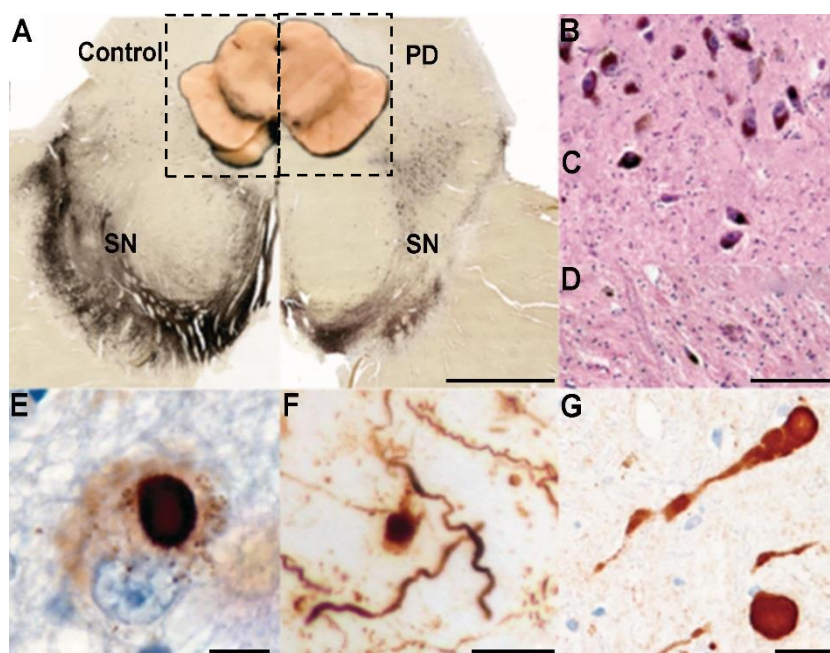


**Figure 1: The main neuropathological features of Parkinson disease (PD).** (A). PD is defined by depigmentation of the substantia nigra (SN) (right panel) compared with control (left panel). Macroscopical (inset) and transverse sections of the midbrain upon immunohistochemical staining for tyrosine hydroxylase (TH), the rate limiting enzyme for the synthesis of dopamine, are shown. Selective loss of the ventrolateral region of the SN with sparing of the more medial and dorsal regions is evident in the histological section (Scale bar, 500  $\mu\text{m}$ ). (B-D). Haematoxylin and eosin staining of the ventrolateral region of the SN showing a normal distribution of pigmented neurons in a healthy control (B) and diagnostically significant moderate (C) or severe (D) pigmented cell loss in PD (Scale bar, 200  $\mu\text{m}$ ). (E-G). Immunohistochemical staining of  $\alpha$ -synuclein ( $\alpha\text{Syn}$ ) shows the round, intracytoplasmic Lewy bodies (E), more diffuse, granular deposits of  $\alpha\text{Syn}$  (E and F), deposits in neuronal cell processes (F), extracellular dot-like  $\alpha\text{Syn}$  structures (F) and  $\alpha\text{Syn}$  spheroids in axons (G) (Scale bar, 10, 50 and 20  $\mu\text{m}$  respectively) (adapted from [45]).

The neuropathology in non-DAergic brain regions is related to the appearance of non-motor symptoms in the disease. For instance, the loss of smell is related to LBs observed in the olfactory bulb and in other brain areas like the amygdala and the perirhinal nucleus [46]. Furthermore, cortical deposits of misfolded proteins contribute to cognitive problems [47].

#### 1.1.4 Etiology of PD

The etiology of the disease remains almost as elusive as when it was first described, whilst it is accepted that it largely depends on genetic and

environmental factors. In about 85-90% of the cases there is no apparent genetic linkage (sporadic forms), and only about 10-15% of the cases are familial forms consequent to genetic mutations, while less than 10% of PD patients suffer from a monogenic form of the disease with Mendelian inheritance (rev. by [48]).

Through the years, there have been several attempts to explain PD propagation and  $\alpha$ Syn transmission in the disease. In 2003, Braak et al, proposed the hypothesis that an unknown pathogen (virus or bacterium) in the gut could be responsible for the initiation of sporadic PD [49], and suggested a staging system for PD based on a specific pattern of  $\alpha$ Syn spreading (Fig. 2) [50].

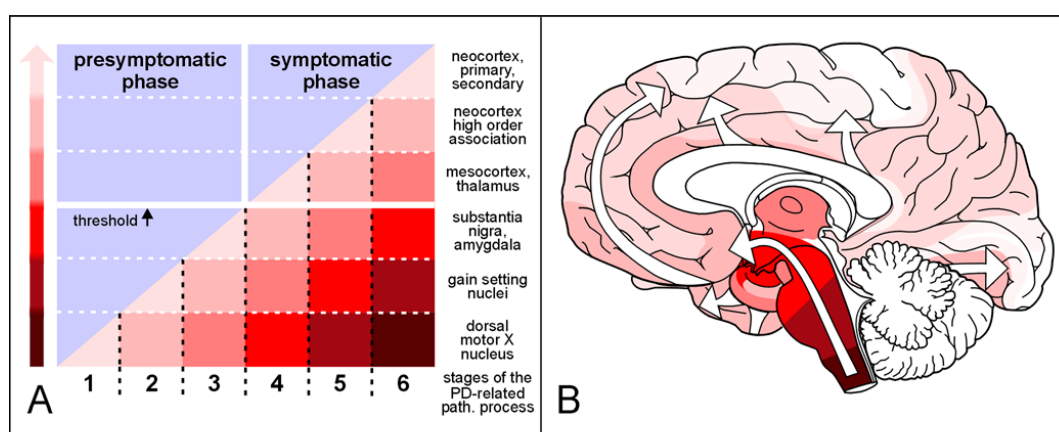


**Figure 2: PD presymptomatic and symptomatic phases according to Braak hypothesis.**  
A. The presymptomatic phase is marked by the appearance of Lewy neurites/ bodies in the brains of asymptomatic persons. In the symptomatic phase, the individual neuropathological threshold is exceeded (black arrow). The increasing slope and intensity of the colored areas below the diagonal indicate the growing severity of the pathology in vulnerable brain regions (right). The severity of the pathology is indicated by darker degrees of shading in the colored arrow (left). B Diagram showing the ascending pathological process (white arrows). The shading intensity of the colored areas corresponds to that in A (rev. by [51]).

The disease begins in structures of the lower brainstem and the olfactory system (stage 1). In particular, a few isolated Lewy neurites may appear in the dorsal motor nucleus of the vagus nerve in the medulla oblongata and the anterior olfactory nucleus are affected. Stage 2 is characterized by additional lesions in the raphe nuclei and gigantocellular reticular nucleus of the medulla oblongata. The disease then moves up the brainstem, traveling from the medullary structures to the locus coeruleus in the pontine tegmentum. At stages

3–4, the substantia nigra and other nuclear grays of the midbrain and forebrain become the focus of initially slight and, then, severe pathological changes. At this point, most individuals probably cross the threshold to the symptomatic phase of the disease. In the end-stages 5–6, LB pathology gradually overruns the entire neocortex, and patients manifest the full range of PD-associated clinical symptoms (Fig.2).

These publications were followed by the more encompassing “dual-hit” hypothesis, stating that sporadic PD is caused by pathogenic invasion either through the nasal cavity and the vagus nerve [52], also known as Braak’s hypothesis.

However, the pathological regional heterogeneity between PD cases suggests that Braak’s proposed pathway is not the only possible route of spread, and pathology may even emerge simultaneously in multiple subcortical and cortical regions. Moreover, the proposed “gut to brain” spread of LB pathology has been challenged [53, 54], with even a “brain to gut” direction of transmission [55]. Furthermore, several cases with inclusions throughout the brain but with preservation of medullary nuclei have been reported [55].

A “multiple hit” hypothesis suggesting that multiple risk factors interact to induce the degenerative processes seen in PD has also been proposed [56]. According to this hypothesis, the primary insult results in cellular stress, while secondary insults result in loss of protective pathways thus inducing neuronal death. Several studies have supported this hypothesis, with both genetic and environmental factors being among the insults [57-61].

In an attempt to explain disease progression in a better way, Engelender and Isacson recently proposed the threshold hypothesis [62]. According to this, PD is believed to be a global systemic disease, affecting different neurons in the central nervous system (CNS) and the PNS. The dysfunction and death of neurons in a particular area depend on their individual vulnerability. Moreover, the appearance of symptoms is a result of the degree to which damaged neurons are functionally connected to and modulated by other neuronal groups. Therefore, the disease progression might be due to a combination of differences in vulnerability and functional reserve of affected neurons. According to this theory, the symptoms only begin when the functional reserve of neurons (and their connecting brain regions) is unable to allow for network

compensation. Consequently, early symptoms of PD reflect a loss of function in the least compensated systems, such as the GI tract, olfactory system, and brainstem, rather than the spread of  $\alpha$ Syn from the PNS to CNS.

In the last few years, it has been noted that during the prodromal phase, which precedes degenerative neuronal loss, the expression levels of a range of proteins involved in synaptic transmission are altered in the prefrontal and cingulate cortex, and the SN [63, 64], suggesting that both non-motor and motor symptoms are caused by impaired synaptic communication. Moreover, evidence coming from animal models of PD supports the hypothesis that pre-synaptic accumulation of  $\alpha$ Syn impinges on synaptic function and axonal integrity leading to degeneration and cell death [65-67]. These data support the notion that neurodegeneration in PD is a dying back-like phenomenon which starts at synaptic terminals in the STR and progresses along the nigrostriatal pathway, ultimately affecting homeostasis and survival of DAergic cell bodies in the SN [35, 68, 69]. Due to these early-onset synaptic alterations observed prior to DAergic neuronal loss, PD has also been classified as a synaptopathy (rev. by [70, 71]).

#### **1.1.4.1 Sporadic form**

The majority of PD cases are defined as idiopathic, due to their largely unknown etiology. Epidemiological studies have revealed a series of risk factors that may be implicated in the development of the disease, with age being the most important one [15]. Gender plays a role in disease susceptibility, with men being more susceptible (rev. by [72]).

A number of environmental factors have been identified to contribute to disease pathogenesis and progression. In the 1980s, drug abusers who self-administered desmethylprodine or 1-methyl-4-phenyl-4-propionoxypiperidine (MPPP) which is an opioid drug, containing 1-methyl-4-phenyl-1,2,3,6-tetrahydropyridine (MPTP) as a major impurity, rapidly developed a syndrome indistinguishable from advanced PD [73]. MPP<sup>+</sup>, the oxidized product of MPTP, appears to be selectively toxic for DAergic neurons, inducing mitochondrial respiration blockade precipitating neuronal death [74]. Exposure to toxic environmental factors especially pesticides and a lifestyle including welding,

farming or rural living are suggestive to be aggravating factors (rev. by [75]). There has been convincing evidence that physical activity negatively correlates with the disease, while constipation is positively correlated [76]. Moreover, there is highly suggestive evidence that head injury [77], anxiety or depression as well as smoking [78] correlate positively with the disease. More recently, microbial and viral infections have been linked to PD, however the studies are largely inconclusive (rev. by [79]). Chronic inflammation or psycho-social factors might contribute to the risk of developing PD (rev. by [80, 81]).

#### 1.1.4.2 Familial forms

Although the possible heritability of PD was raised as early as the turn of the twentieth century by the British neurologist William Gowers [21], it was not until 1997 when Polymeropoulos and his colleagues discovered for the first time that a missense mutation in  $\alpha$ Syn gene (*SNCA*) causes a rare form of familial PD in Italian and Greek families [82]. Since then, substantial progress has been made in identifying the genetic basis of PD, with a significant number of monogenic disease-causing genes having been discovered (rev. by [83]). Up to now, at least 23 loci and 19 genes have been identified and designated as PD-causing genes by the HUGO Gene Nomenclature Committee (HGNC) (Table 1). These include 10 autosomal dominant mutations in genes including *SNCA* and *LRRK2* (Leucine-Rich Repeat Kinase 2), and 9 autosomal recessive genes, like *PARK2*, *PINK1* and *DJ-1*, while association studies have also revealed various genetic risk loci and variants for sporadic PD (rev. by [83]).

As the  $\alpha$ Syn protein is a major component of LBs, the identification of missense mutations in this gene leading to familial forms of the disease is of utmost importance (A53T, A30P, E46K, H50Q, G51D and A53E) [82, 84-87] [88-91]. In addition, duplications and triplications of the *SNCA* locus also cause familial PD and the number of copies correlate with disease severity [92, 93]. Two novel potentially pathogenic substitutions have also been described in sporadic PD patients (A18T and A29S) [94]. Furthermore, positive associations of several single nucleotide polymorphisms (SNPs) in the *SNCA* gene and increased risk for PD have been reported [95]. Additionally, genome-wide association studies (GWASs) have identified common genetic variants close to

the SNCA locus that increase the risk for sporadic PD [96, 97]. Although these studies remain inconclusive and further studies to include populations of different ethnic backgrounds are needed, they all point to the pivotal role of  $\alpha$ Syn in PD.

**Table 1:** Gene locus and disease-causing genes of Parkinson disease (adjusted from [83]. HGNC: HUGO Gene Nomenclature Committee, AD: autosomal dominant, AR: autosomal recessive

Locus (OMIM)	Location	Full Gene Name Approved by HGNC	HGNC Approved Gene Symbol (OMIM)	Inheritance
<i>PARK1</i> (168601)	4q22.1	synuclein alpha	<i>SNCA</i> (163890)	AD
<i>PARK2</i> (600116)	6q26	parkin RBR E3 ubiquitin protein ligase	<i>PRKN</i> (602544)	AR
<i>PARK3</i> (602404)	2p13	Parkinson disease 3	<i>PARK3</i> (Unclear)	AD
<i>PARK4</i> (605543)	4q22.1	synuclein alpha	<i>SNCA</i> (163890)	AD
<i>PARK5</i> (613643)	4p13	ubiquitin C-terminal hydrolase L1	<i>UCHL1</i> (191342)	AD
<i>PARK6</i> (605909)	1p36	PTEN induced putative kinase 1	<i>PINK1</i> (608309)	AR
<i>PARK7</i> (606324)	1p36.23	parkinsonism associated deglycase	<i>PARK7</i> (602533)	AR
<i>PARK8</i> (607060)	12q12	leucine rich repeat kinase 2	<i>LRRK2</i> (609007)	AD
<i>PARK9</i> (606693)	1p36.13	ATPase 13A2	<i>ATP13A2</i> (610513)	AR
<i>PARK10</i> (606852)	1p32	Parkinson disease 10	<i>PARK10</i> (Unclear)	Unclear
<i>PARK11</i> (607688)	2q37.1	GRB10 interacting GYF protein 2	<i>GIGYF2</i> (612003)	AD
<i>PARK12</i> (300557)	Xq21-q25	Parkinson disease 12	<i>PARK12</i> (Unclear)	X-linked inheritance
<i>PARK13</i> (610297)	2p13.1	HtrA serine peptidase 2	<i>HTRA2</i> (606441)	AD
<i>PARK14</i> (612593)	22q13.1	phospholipase A2 group VI	<i>PLA2G6</i> (603604)	AR
<i>PARK15</i> (260300)	22q12.3	F-box protein 7	<i>FBXO7</i> (605648)	AR
<i>PARK16</i> (613164)	1q32	Parkinson disease 16	<i>PARK16</i> (Unclear)	Unclear
<i>PARK17</i> (614203)	16q11.2	VPS35, retromer complex component	<i>VPS35</i> (601501)	AD
<i>PARK18</i> (614251)	3q27.1	eukaryotic translation initiation factor 4 gamma 1	<i>EIF4G1</i> (600495)	AD
<i>PARK19</i> (615528)	1p31.3	DnaJ heat shock protein family (Hsp40) member C6	<i>DNAJC6</i> (608375)	AR
<i>PARK20</i> (615530)	21q22.1	synaptotjanin 1	<i>SYNJ1</i> (604297)	AR
<i>PARK21</i> (616361)	20p13	transmembrane protein 230	<i>TMEM230</i> (617019)	AD
<i>PARK22</i> (616710)	7p11.2	coiled-coil-helix-coiled-coil-helix domain containing 2	<i>CHCHD2</i> (616244)	AD
<i>PARK23</i> (616840)	15q22.2 11p15.4	vacuolar protein sorting 13 homolog C RIC3 acetylcholine receptor chaperone	<i>VPS13C</i> (608879) <i>RIC3</i> (610509)	AR AD

*LRRK2* (leucine-rich repeat serine/threonine-protein kinase 2) autosomal dominant mutations represent the most common cause of familial PD and show age-dependent penetrance (G2019S, M1869T, R1441C, R1441G, R1441H and R1441S) [98, 99]. This kinase is highly expressed in brain areas receiving DA innervations, such as the STR, hippocampus, cortex and cerebellum [100], and has been associated with many aspects of neuronal function including neurogenesis, axonal outgrowth and synaptic function [101-103].

In recent years, 15 GWASs have identified additional genetic risk factors for sporadic PD [104-110]. Although these factors do not necessarily lead to disease appearance, such studies highlight the complexity of the disease and

further support the notion that a combination of genetic and environmental factors do contribute to disease development.

### **1.1.5 Mechanisms involved in PD pathogenesis**

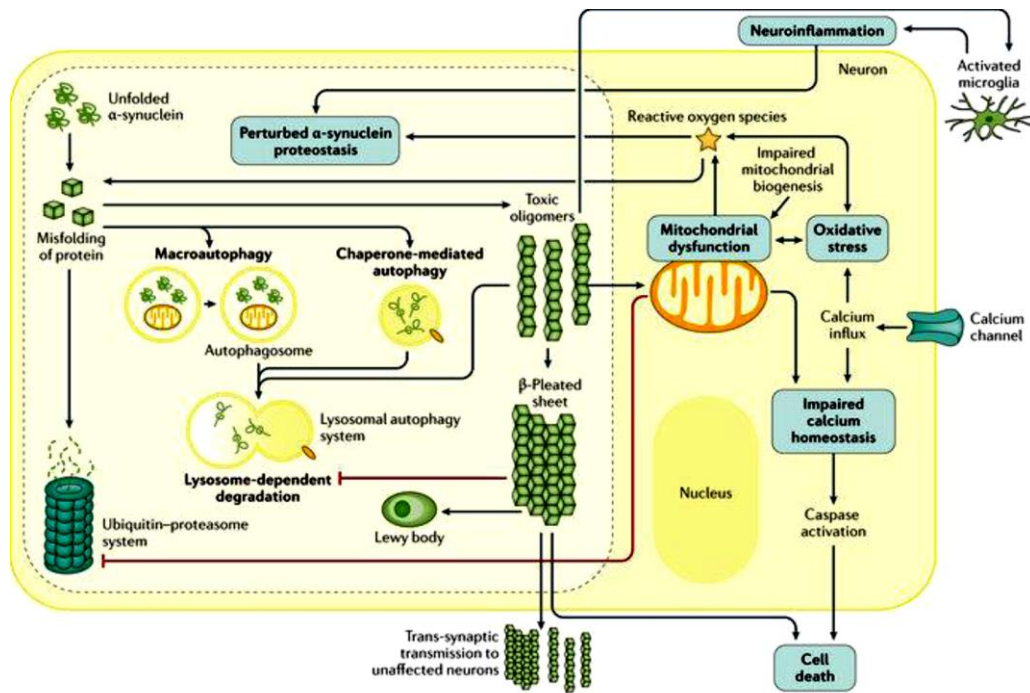
While the cause of PD is still unknown, advances have been made in understanding possible underlying mechanisms. The development of model systems, like toxin-based and genetic animal models as well as cellular models, have given insights into some of the disease mechanisms involved, including the accumulation of misfolded proteins, defects in mitochondrial function, oxidative stress, neuroinflammation and axonal transport (Fig. 3) (rev. by [111]).

#### **1.1.5.1 Accumulation of misfolded proteins**

Interestingly, a number of disrupted pathways have been identified that are shared between neurodegenerative diseases, particularly PD and AD, like the abnormal protein deposition in brain tissue (rev. by [112, 113]). Although the composition and location (intra or extracellular) of these aggregates may differ, it seems that protein aggregation per se leads to neuronal toxicity. It is possible that misfolded proteins may cause damage by deforming the cell or interfering with intracellular trafficking in neurons (rev. by [114, 115]). Intracellular homeostasis of proteins like  $\alpha$ Syn is maintained through the ubiquitin–proteasome system (UPS) and the lysosomal autophagy system (LAS) [116–120], and failure of these systems leads to several neurodegenerative diseases (rev. by [121, 122]).

In addition, both UPS and LAS are thought to decline during ageing and this failure contributes to the development of age-related diseases [123, 124]. In line, dysfunction of the UPS and LAS have been implicated in PD [125, 126].

Moreover, lysosomal impairment has been recognized as a central event in PD pathology, and genetic associations between PD and lysosomal storage disorders, like Gaucher's disease (GD) highlight common risk factors and potential operating disease mechanisms (rev. by [127]). In agreement, genes involved in lysosomal storage disorders like *GBA1*, *SMPD1*, *SCARB2*, and *ATP132* have been also associated with PD (rev. by [128]).



Nature Reviews | Disease Primers

**Figure 3: Mechanisms involved in Parkinson's disease (PD) pathogenesis.** Accumulation of misfolded proteins like  $\alpha$ -synuclein, defects in mitochondrial function, oxidative stress, neuroinflammation, calcium dysregulation and axonal transport are implicated in PD pathogenesis [45].

### 1.1.5.2 Defects in mitochondrial function

Substantial evidence has implicated mitochondrial dysfunction as a key element in PD pathogenesis (rev. by [129]). Studies in which accidental infusions of MPTP selectively inhibited mitochondrial complex I, one of the electron transport chain components, were the first to support mitochondrial defects in PD [73]. Additionally, several studies have shown that mitochondrial dysfunction leads to chronic production of reactive oxygen species (ROS), and causes death of DAergic neurons (rev by [129]). Mitochondrial DNA (mtDNA) mutations with clonally expanded mtDNA deletions in individual cells that cause defects in the respiratory chain in the SN, have also been reported in older PD patients [130]. Recently, advances in the understanding of molecular pathways governed by proteins encoded by PD-linked genes have supported the notion that mitochondrial failure is a key event in the disease. For instance, LRRK2 mutations are associated with mitochondrial impairments, while Parkin and PINK1 play a role in mitophagy (autophagy of mitochondria) (rev. by [45]) as well as in mitochondrial fission and fusion (rev. by [131]).

### **1.1.5.3 Oxidative stress response**

Several lines of evidence support that, increased oxidative stress as a consequence of mitochondrial dysfunction contributes to PD (rev. by [132]). DAergic neurons in SN seem to be particularly vulnerable to metabolic and oxidative stress [133, 134], since they possess particularly long unmyelinated axons, and form a large number of synapses, which require large amounts of energy to be sustained. They also exhibit autonomous pacemaking activity involving cytosolic calcium oscillations and calcium extrusion at the expense of energy [135, 136]. Furthermore, increased levels of cytosolic DA and its metabolites can cause toxic oxidative stress (rev. by [45]). In addition, DJ-1 mutations, resulting in early-onset PD, are associated with increased cellular oxidative stress [137].

### **1.1.5.4 Immune response activation**

Post-mortem analyses of human PD patients and animal studies have shown that neuroinflammation is a common feature of PD pathophysiology [138, 139]. However, its precise role in PD is still not fully understood, and whether it is harmful or beneficial remains elusive. Moreover, the inflammatory responses refer to both microglial activation and peripheral immune cell infiltration, but the relationship between these two different inflammatory pathways remains unclear (rev. by [140-142]). Since both innate and adaptive immune cells have emerged as important contributors in PD, non-cell-autonomous mechanisms have been suggested to be important in participating and/ or modulating disease mechanisms as well (rev. by [141, 143]).

It has been proposed that genetic background and aging, along with environmental factors impact the susceptibility of microglial activation leading to a lack of homeostatic support to the surrounding tissue (increased antigen presentation, phagocytic microglia, pro-inflammatory status and decreased anti-inflammatory status) that may further influence PD pathogenesis (rev. by [144]). Recent understanding of the complex immune-regulatory function of microglia in PD have suggested that strategies aimed at modulating rather than inhibiting microglia activation may represent a promising therapeutic approach in the treatment of disease (rev. by [144, 145]). This year, for instance, an agent

that inhibits the formation of neurotoxic A1 reactive astrocytes (NLY01) has been developed, leading to life prolongation and improved behavioral and neuropathological phenotypes when administered in PD mice [146].

#### **1.1.5.5 Calcium dysregulation**

Dysregulation of calcium signaling seems to lie at the core of multiple neurodegenerative pathologies including PD (rev. by [147, 148]). DAergic neurons in SN are autonomously active generating continuous low-frequency activity in the absence of synaptic input that is dependent on L-type calcium channels [149]. These neurons have a pore-forming Cav1.3 subunit, with low affinity for dihydropyridines and open at more hyperpolarized membrane potentials than Cav1.2 channels do [150]. There is evidence that, over time, DAergic neurons develop an increasing reliance on L-type calcium Cav1.3 channels to maintain their autonomous activity and this comes at a significant bio-energetic cost [135]. The need to maintain calcium homeostasis includes co-ordination of endoplasmic reticular (ER) pumps (rev. by [151]) and the uptake of calcium into mitochondria (rev. by [152]). The Cav1.3 channels generate mitochondrial-mediated oxidative stress during autonomous activity which in turn induces mitochondrial uncoupling as a protective mechanism [137]. The lysosome has also recently been identified as an important participant in intracellular calcium shuttling [153]. In PD patients an increased use of Cav1.3 subtype has been observed, adding to the metabolic burden of cells that rely on this subtype for electrical activity and could therefore make specific neuronal populations more vulnerable to neurodegeneration [154].

#### **1.1.5.6 Axonal transport impairment**

The intracellular transport of organelles/ vesicles along an axon is crucial for the maintenance and function of a neuron and impairment of axonal transport has recently emerged as a common factor in several neurodegenerative disorders (rev. by [155]). Axonal transport analysis in cultured neurons carrying the A53T and A30P mutations mimicking permanent phosphorylation of  $\alpha$ Syn led to a reduced axonal movement of the  $\alpha$ Syn protein [156]. *PARK2*, *PINK1*, and *PARK7* which are also genes associated with

familial forms of PD encode proteins that are involved in the maintenance of mitochondria function, which provides energy for axonal transport [157].

Furthermore, analysis of post-mortem PD brains showed that kinesin and cytoplasmic dynein subunit levels are decreased in sporadic PD, with kinesin levels being affected early on in the disorder, before DAergic neuronal loss [158]. These features were recapitulated in rats with overexpression of human mutant  $\alpha$ Syn (A30P) [158], strongly supporting the notion that neurodegeneration involves disruption of axonal transport in PD.

## **1.2 A-synuclein**

### **1.2.1 Localization and structure of $\alpha$ Syn**

$\alpha$ Syn is a 14 kDa protein (140 amino acids) that was originally identified using an antibody to purified cholinergic vesicles of the Torpedo electric organ, revealing its localization both in the nucleus and the presynaptic terminals [159]. It belongs to the synuclein protein family along with  $\beta$ Syn,  $\gamma$ Syn and synoretin [160].  $\alpha$ Syn,  $\beta$ Syn, and  $\gamma$ Syn share the same domain organization and the same subcellular distribution at presynaptic terminals in neurons [161], with only  $\alpha$ Syn being found in LBs (rev. by [162]).

$\alpha$ Syn localizes preferentially at the nerve terminal, with a relatively small amount in the cell soma, dendrites, or extrasynaptic sites along the axon [163, 164]. More recently  $\alpha$ Syn was found to be localized in mitochondria as shown in several experimental models. However, the exact localization of  $\alpha$ Syn within mitochondria remains unclear, with studies supporting its presence in the outer mitochondrial membrane (OMM) [165], in the inner mitochondrial membrane (IMM) [166], or even the mitochondrial matrix [167]. It has also been shown that most of the membrane-bound  $\alpha$ Syn does not localize to mitochondria but to mitochondria-associated membranes (MAMs), which are the contact sites of ER with mitochondria [168].

Although it is widely expressed in the CNS and the PNS, it is also expressed in several non-neural tissues including red blood cells [169]. Further studies confirmed its abundant expression in all nerve plexuses of the human enteric nervous system (ENS) [170].

Structurally, it is characterized by an amphipathic lysine-rich amino (N)-terminus, which modulates its interactions with membranes (residues 1-60), a central region designated the non-amyloid- $\beta$  component (NAC), which is highly hydrophobic and essential for its aggregation (residues 61-95), and an acidic carboxy (C)-terminal tail, which has been associated with its nuclear localization and many interactions (95-140) (Fig. 4) [171, 172]. It is interesting to note that all missense mutations linked to PD in the *SNCA* gene lie in the N-terminus, potentially disrupting its association with membranes.

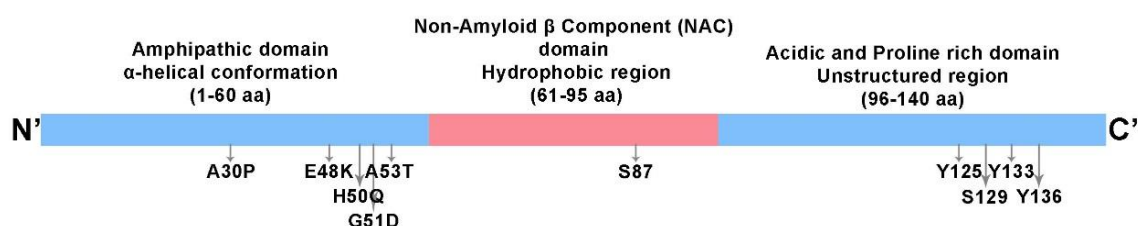


**Figure 4: Primary structure of  $\alpha$ -synuclein ( $\alpha$ Syn).** Schematic representation of the three main regions of human  $\alpha$ Syn. The N-terminus region is an amphipathic domain which contains the PD-associated point mutations (indicated with grey arrows). The central region which is highly hydrophobic and essential for its aggregation. The C-terminal region has an acidic character and is the region where posttranslational modifications (residues S87, S129, Y125, Y133, 139 as indicated with grey arrows) have been observed.

Multiple conformations of native  $\alpha$ Syn might exist physiologically, depending on its cellular localization and membrane interactions. Using different biophysical methods, it was first demonstrated that under native or denaturing conditions  $\alpha$ Syn exists as a monomer, adopting an unfolded extended conformation [173, 174]. Nevertheless, upon binding to synthetic membranes or certain phospholipid surfaces its structure adopts an  $\alpha$ -helical conformation [175]. Its tendency to interact with lipid membranes has consistently been shown both *in vitro* and *in vivo* [175-177].

Several reports suggested that  $\alpha$ Syn also exists normally in  $\alpha$ -helix-rich tetramers and related multimers [178, 179], mediated by its four repeats with a highly conserved hexameric motif (KTKEGV) in its N-terminus [180]. Moreover, the existence of metastable conformers and stable monomer was revealed in the human brain [181].

### 1.2.2 Physiological function of $\alpha$ Syn

Despite recent progress in the field, the physiological role of  $\alpha$ Syn is still not clear. It has been proposed that  $\alpha$ Syn is a curvature-sensing and stabilizing protein [182], and has been added to the class of amphipathic helix-containing proteins that sense and generate membrane curvature [183] suggestive of a physiological role in exocytosis and endocytosis [184].  $\alpha$ Syn seems to be involved in the assembly of the SNARE (SNAP Receptor) complex, a process essential for many membrane fusion events [185-187]. However, there is a controversy on how  $\alpha$ Syn might act on the SNARE complex, with one major study supporting that  $\alpha$ Syn increases SNARE complex assembly [186] and another study suggesting that it inhibits SNARE complex assembly [188].

Further studies to clarify  $\alpha$ Syn contribution to vesicle fusion have also yielded contradictory results. It is hypothesized that  $\alpha$ Syn inhibits vesicle fusion via stabilization of the curvature of synaptic vesicles [189, 190]. On the other hand, it has also been suggested that  $\alpha$ Syn improves the recycling of synaptic vesicles, thus maintaining the exocytotic machinery [191, 192].

It has also been reported that  $\alpha$ Syn affects the vesicle pool, although the underlying mechanisms are still missing.  $\alpha$ Syn overexpression resulted in an increase in synaptic vesicle size [66], in a decrease of vesicle reclustering after endocytosis [193], in decreased motility of synaptic vesicles [194] or even in increased amount of vesicles docked to the membrane [195]. On the other hand, KO of  $\alpha$ Syn was shown to decrease the number of synaptic vesicles, especially of the distal pool, which reduces their availability upon intense stimulation [196]. Additionally, it was shown that calcium binds to the C-terminus of  $\alpha$ Syn increasing its lipid-binding capacity [197]. This way, calcium mediates the localization of  $\alpha$ Syn at the pre-synaptic terminal, and an imbalance in calcium or  $\alpha$ Syn can cause synaptic vesicle clustering.

Synaptic vesicle exo and endocytosis was also monitored and a slowed endocytosis was observed in  $\alpha\beta\gamma$ -Syn triple-KO mice [198]. Expression of each individual Syn isoform on the triple-KO background was found to compensate for this endocytotic failure, demonstrating the complementary function of the Syn isoforms. Its role in synaptic vesicle endocytosis was confirmed by two other studies using patch clamp capacitance measurements [199] [200]. In the first study, Xu et al showed that a mutated form of  $\alpha$ Syn inhibits endocytosis at

the nerve terminals [199]. In the second study, it was shown that when synapses acutely injected with  $\alpha$ Syn protein were stimulated, severe changes in the synaptic vesicle pool were seen, small synaptic vesicles were rare, and bulk membranous structures appeared within the presynaptic terminal in lamprey, indicating that  $\alpha$ Syn induces a failure of synaptic vesicle endocytosis; however, this seems to be dependent on neuronal activity [200]. The exact function of  $\alpha$ Syn in endocytosis is now emerging, with clathrin-mediated endocytosis as well as fast endocytosis like kiss-and-run being considered possible (rev. by [201]).

Due to its presynaptic localization, its role in synaptic activity and neurotransmitter release has also been investigated. *In vivo* models overexpressing wild-type (WT)  $\alpha$ Syn have revealed an inhibitory role of  $\alpha$ Syn on neurotransmitter release [66, 202, 203] while two other studies led to opposite conclusions [204, 205]. Using  $\alpha$ Syn-KO mice, decreased exocytosis [196, 205], no change [192] or even increased exocytosis have been reported [206]. Single- and double-KO mice that lack  $\alpha$ - and/ or  $\beta$ Syn suggested that they are not essential components of the basic machinery for neurotransmitter release, but may contribute to the long-term regulation and/or maintenance of presynaptic function [192]. Furthermore,  $\alpha\beta\gamma$ -Syn triple-KO mice revealed alterations in synaptic structure and transmission, age-dependent neuronal dysfunction, as well as diminished survival [207].

Additionally,  $\alpha$ Syn is considered to be a chaperone protein [208], since it contains regions that are homologous with chaperone 14-3-3 proteins, it interacts with 14-3-3 itself but also with its ligands, such as kinase suppressor of Ras and Ras-related GTPase Rab3a [209]. Moreover,  $\alpha$ Syn is a downregulator of tyrosine hydroxylase (TH) activity and can modulate the production of DA. Therefore,  $\alpha$ Syn-reduced expression or  $\alpha$ Syn aggregation leads to increased DA synthesis, leading to oxidative stress caused by DA metabolism [210].

Overall, the normal function of  $\alpha$ Syn remains elusive, although the current picture points towards a regulatory role in maintaining synaptic homeostasis upon intense neuronal activity (rev. by [201]).

### 1.2.3 Pathological role of $\alpha$ Syn

Although the physiological function of  $\alpha$ Syn is not well understood, the protein become accumulated in PD and a number of neurodegenerative disorders that have been collectively termed synucleinopathies (rev. by [162]). These include PD with dementia (PDD), dementia with Lewy Body pathology (DLB) and multiple system atrophy (MSA). The latter is characterized by oligodendroglial cytoplasmic inclusions [211], with neuronal cytoplasmic and nuclear inclusions to occur less often. Elevated  $\alpha$ Syn levels have been observed in post-mortem brain tissues of AD patients with cognitive decline [212]. Lysosomal storage disorders (LSD) such as GD have also been linked to  $\alpha$ Syn toxicity [213, 214].

$\alpha$ Syn is able to transition between different **conformations** (Fig. 5). Although physiologically,  $\alpha$ Syn seems to be in a monomeric or tetrameric state, fibril formation requires a conformational change in its structure, to  $\beta$ -sheet (rev. by [215]). Once in a  $\beta$ -sheet enriched state, monomeric  $\alpha$ Syn begins to stack and form  $\beta$ -sheet fibril structures. By using electron paramagnetic resonance (EPR) spectroscopy [216] and nuclear magnetic resonance (NMR) spectroscopy [217, 218], it was found that a five-layered  $\beta$ -sandwich of the protein is incorporated into a protofilament.

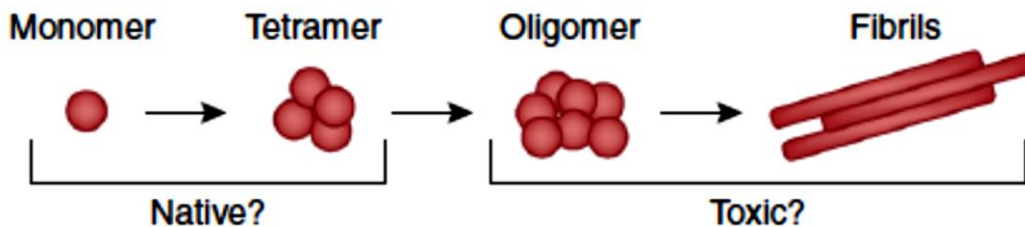


**Figure 5: Native conformations: monomer and tetramer.**  $\alpha$ -synuclein is able to transition between multiple different conformations, including monomers, tetramers, higher-level oligomers (soluble conformations), fibrils (highly ordered insoluble conformations characterized by  $\beta$ -sheet conformation) and aggregates (adapted from [215]).

$\alpha$ Syn fibrillization is affected by several factors that may be relevant to PD. For instance, post-translational modifications (PTMs) of  $\alpha$ Syn have been linked to PD pathology since they seem to favor its oligomerization (rev. by [219]). They include but are not limited to, phosphorylation, nitration, and C-terminal truncation.

A major PTM clearly associated with pathology in PD is the phosphorylation of  $\alpha$ Syn. Using specific antibodies, a major component of LBs in PD post-mortem brain tissue was the phosphorylated  $\alpha$ Syn at serine residue S129 [220] that was later also found in the non-fibrillar (soluble) fraction of PD brain tissue (Anderson, Walker et al. 2006). Phosphorylation in other residues within  $\alpha$ Syn has been reported, such as S87 and tyrosine residues Y125, Y133 and Y136 [221]. The exact effect of these PTMs has not been determined since different studies using different models have shown them to be either toxic or neuroprotective. For example, phosphorylation in residue Y125 has been shown to inhibit  $\alpha$ Syn aggregation [222].

As with phosphorylation, specific antibodies have been used to recognize various forms of 3-nitrotyrosine-modified  $\alpha$ Syn [223]. Further studies have shown four residues of tyrosine nitration Y39, Y125, Y133, and Y136, that are found in LBs, Lewy neurites, glial cell inclusions, and neuroaxonal spheroids in brains from different neurodegenerative disorders [224]. Moreover, C-terminal truncation seems to participate in  $\alpha$ Syn oligomerization [225] whilst reduction of C-terminal truncated  $\alpha$ Syn by immunotherapy has been shown to ameliorate PD-like pathology in animal models mimicking the striatonigral and motor deficits of PD [226].

As already mentioned, there are a number of different  $\alpha$ Syn **species** that have been associated with PD pathogenesis, including oligomers, protofibrils and fibrils. Several studies have tried to demonstrate which particular state is toxic. The fibrillar forms are detected mostly in LBs and are thought to reflect an attempt by the neurons to isolate and/or convert toxic  $\alpha$ Syn oligomers to fibrils, which are stable, less dynamic structures, and exhibit reduced toxicity (rev. by [227]).

It has been suggested that oligomers are more toxic since A53T and A30P  $\alpha$ Syn mutations accelerate oligomerization but not fibrillization [228]. Additionally, it has been shown that  $\alpha$ Syn transgenic (Tg) mice and patient brains have increased levels of soluble, lipid-dependent  $\alpha$ Syn oligomers when compared to controls [229]. Recently though, PD-linked  $\alpha$ Syn mutations, including A53T and E46K, have been shown to decrease its tetrameric conformation and increase its monomeric state, suggesting that the unfolded monomer might be the source of  $\alpha$ Syn toxicity [230].

However, another study suggested that fibrillar  $\alpha$ Syn, rather than its precursor oligomers, is highly cytotoxic [231]. In support of this, another study demonstrated that fibrils of human  $\alpha$ Syn induced the greatest amount of motor impairment, DAergic neuronal loss and synaptic deficits after injection into rat SN [232].

At the same time different species of  $\alpha$ Syn, including ribbons and protofibrils, have been identified demonstrating differences in structure, levels of toxicity, ability to seed, propagate and cross-seed Tau fibrillization both *in vitro* and *in vivo*, with Tau being a microtubule-binding protein that stabilizes and promotes microtubule assembly [233, 234]. In addition, differences in  $\alpha$ Syn species also exist between synucleinopathies, such as PD and MSA [235]. Importantly,  $\alpha$ Syn species differences among patients may contribute to patient variability in terms of onset and rate of disease progression. Therefore, the studies of  $\alpha$ Syn species toxicity are inconclusive, and further investigations are needed to understand  $\alpha$ Syn pathological forms.

Several **pathways** have been implicated in  $\alpha$ Syn toxicity, including cellular organelle dysfunction, defects in inter-organelle contacts and dysfunctional organelle dynamics.  $\alpha$ Syn localizes mainly in the presynaptic terminals, but its oligomers and aggregates localize throughout the neuronal soma and neurites, suggesting that the protein might disrupt cellular function beyond the presynaptic terminal. It also implies retrograde transport of  $\alpha$ Syn species from the terminal to the cell soma. Indeed, multiple organelles are implicated in  $\alpha$ Syn toxicity, including synaptic vesicles, mitochondria, ER and Golgi, lysosomes and autophagosomes as well as the nucleus (Fig. 6). Moreover, interorganelle contacts and organelle axonal transport are also affected.

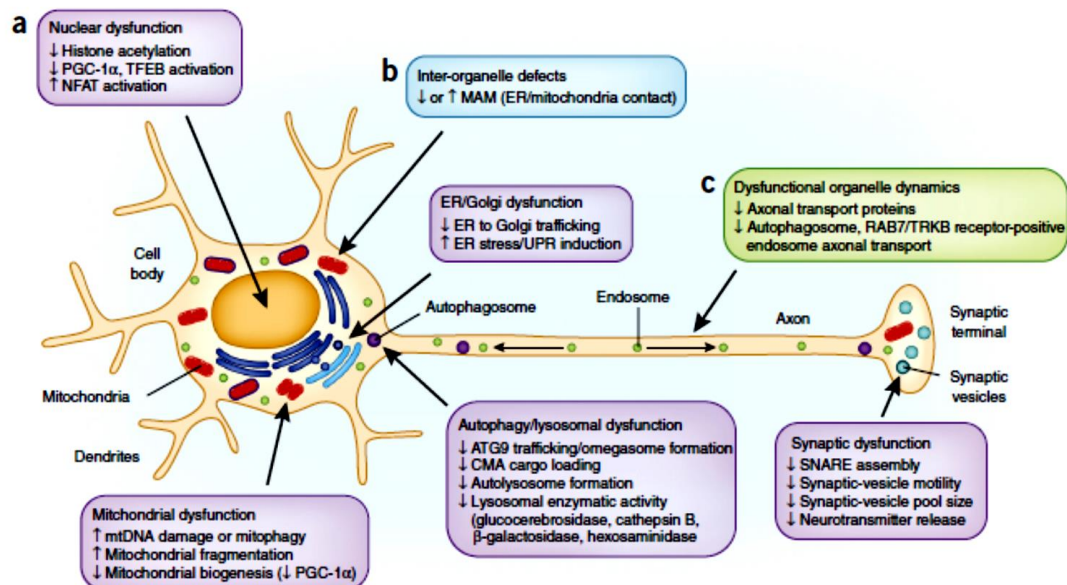


**Figure 6: Pathways implicated in  $\alpha$ -Synuclein toxicity.** (A-C) Organelle dysfunction (a, purple boxes), defects in inter-organelle contacts (B, blue box) and dysfunctional organelle dynamics (c, green box) have all been implicated in  $\alpha$ Syn toxicity (adapted by [215]).

### 1.2.3.1 Synaptic-vesicle trafficking

It has been proposed that  $\alpha$ Syn physiological function might be disrupted in synucleinopathies, since large oligomers preferentially bind to vesicle-associated membrane protein 2 (VAMP2) and disrupt SNARE complex formation, DA release [236] and synaptic-vesicle motility [237]. Furthermore, increased  $\alpha$ Syn levels disrupt neurotransmitter release via decreasing the synaptic-vesicle recycling-pool size and mobility [66, 194]. Other studies however, have suggested that  $\alpha$ Syn physiological role at the synapse is not altered in the disease, with  $\alpha$ Syn oligomers actually promoting SNARE assembly [185]. Additionally, it has been suggested that A53T and E46K  $\alpha$ Syn mutations do not disrupt SNARE assembly [238] or synaptic-vesicle clustering [239].

### 1.2.3.2 Mitochondrial function

As already discussed, mitochondrial function seems also to be disrupted, since mice overexpressing human A53T  $\alpha$ Syn display increased mitochondrial DNA damage [240] and mitophagy [241, 242]. In addition, increased  $\alpha$ Syn levels promote dynamin-related protein 1 (DRP1)-independent mitochondrial

fission in cell lines and in an invertebrate model overexpressing  $\alpha$ Syn [165, 243]. More recently, certain post-translationally modified species of  $\alpha$ Syn have been suggested to disrupt mitochondrial function in PD. In particular, it was shown that  $\alpha$ Syn species (e.g. oligomeric, DA-modified and Ser-129E phosphomimetic) can bind to TOM20, which is a component of the translocase of the Outer Membrane complex (TOM complex) and prevent its interaction with TOM22, thus inhibiting mitochondrial protein import *in vitro* [244].

#### **1.2.3.3 Endoplasmic reticulum, Golgi function, and the endocytic pathway**

Several lines of evidence link ER and Golgi dysfunction to PD. Both WT and mutant  $\alpha$ Syn disrupt ER to Golgi trafficking in yeast [245] and induce ER stress and early secretory-pathway dysfunction, which can be rescued by certain Rab GTPases such as RAB1, RAB3A or RAB8A [189, 190]. Increased  $\alpha$ Syn expression also disrupts endosomal transport events via the yeast E3 ubiquitin ligase RSP5 and its mammalian homolog NEDD4 and endosomal transport can be rescued by the drug N-aryl benzimidazole [246]. Moreover,  $\alpha$ Syn overexpression leads to disrupted dopamine transporter (DAT) trafficking from the ER to Golgi to the cell surface [247].

#### **1.2.3.4 Autophagy or lysosomal pathway**

Two separate lysosomal pathways, namely Chaperone Mediated Autophagy (CMA), a process that targets individual soluble proteins to the lysosome for degradation, and macroautophagy, in which portions of the cytoplasm and organelles are sequestered into multilamellar structures, the autophagosomes, are suggested to mediate  $\alpha$ Syn degradation [248, 249]. Malfunctions in any of these systems lead to increased levels of  $\alpha$ Syn, and evidence for some compensatory crosstalk between the systems exists [250]. Additional proteases, which are not part of the UPS and LAS, like calpains, neurosin, and metalloproteinases, can also cleave  $\alpha$ Syn extracellularly [251].

Additionally, A53T and A30P  $\alpha$ Syn bind to the lysosomal receptor LAMP2A more tightly than the WT protein, which prevents their own degradation and cargo loading of other CMA substrates into lysosomes [252].  $\alpha$ Syn that has been exposed to dopamine (DA-modified  $\alpha$ Syn) also blocks

CMA, which might contribute to selective DAergic vulnerability in PD [253]. Moreover, the lysosomal activity of multiple enzymes, including  $\beta$ -glucocerebrosidase (GCase), cathepsin B,  $\beta$ -galactosidase and hexosaminidase, was found to be reduced in  $\alpha$ Syn triplication PD neurons as compared to control ones, as a result of defective ER to Golgi trafficking [252, 254, 255]. More specifically,  $\alpha$ Syn accumulation disrupts GCase trafficking in sporadic Gaucher's disease (GD)-derived neurons and GD post-mortem brains; leading to reduced GCase lysosomal activity [252, 255].

#### **1.2.3.5 Nuclear dysfunction**

Nuclear dysfunction has also been observed. A30P, A53T, and G51D  $\alpha$ Syn have increased nuclear localization as compared to WT protein [256, 257]. Altered activation of various transcription factors, including decreased activation of the mitochondrial biogenesis factor peroxisome proliferator-activated receptor  $\gamma$  coactivator-1 $\alpha$  (PGC-1 $\alpha$ ) in A53T  $\alpha$ Syn PD neurons and PD neurons in the substantia nigra [258, 259] have been shown. Moreover, increased activation of nuclear factor of activated T cells (NFAT) via calcineurin activation in cell lines overexpressing WT or A53T  $\alpha$ Syn, in DAergic neurons from  $\alpha$ Syn transgenic mice and in PD or DLB brains [260, 261] has also been shown.

#### **1.2.3.6 Disruption of inter-organelle contacts**

In the past few years, defects in inter-organelle contacts have been reported. It has been shown that  $\alpha$ Syn positively affects  $Ca^{2+}$  transfer from the ER to the mitochondria [262]. A30P and A53T point mutations in human  $\alpha$ Syn resulted in its reduced association with mitochondria-associated membranes (MAM), accompanied by a lower degree of apposition of ER with mitochondria, a decrease in MAM function, and an increase in mitochondrial fragmentation compared with WT  $\alpha$ Syn [168]. Moreover, PD-causing  $\alpha$ Syn mutations downregulate ER-mitochondrial apposition, presumably through disrupted interaction with lipid rafts in the case of the A30P  $\alpha$ Syn [177, 263].

### 1.2.3.7 Misregulation of organelle dynamics

Finally,  $\alpha$ Syn toxicity has been recently associated with organelle dynamics and axonal transport.  $\alpha$ Syn fibrils were found to impair the axonal transport of autophagosomes and RAB7- and TrkB-receptor-positive endosomes, but not the transport of synaptophysin or mitochondria, suggesting that  $\alpha$ Syn does not cause a generalized defect in axonal transport [264]. This may be partially due to decreased levels of axonal transport proteins in patients with sporadic PD when compared to age-matched controls [158], or decreased microtubule stability and kinesin-dependent cargo mobility, as observed in cellular models overexpressing  $\alpha$ Syn oligomers [265]. Transport defects might also be mediated by interactions of  $\alpha$ Syn with Tau [233]. Neuronal exposure to extracellular  $\alpha$ Syn also disrupts actin turnover and actin waves along axons, owing to cofilin inactivation [266].

Recently, Ordonez et al, showed that in a new *Drosophila* model of  $\alpha$ -synucleinopathy,  $\alpha$ Syn interacts with spectrin, thereby altering F-actin dynamics, promoting mislocalization of the critical mitochondrial fission protein Drp1, and consequently leading to mitochondrial dysfunction and neuronal death [267]. The results were confirmed in A53T  $\alpha$ Syn mice and in brains with  $\alpha$ -synucleinopathy.

### 1.2.4 $\alpha$ Syn secretion and transmission

The absence of a secretory signal peptide sequence in  $\alpha$ Syn suggested it might be purely an intracellular protein but this view has changed since its detection in biological fluids such as cerebrospinal fluid (CSF) [268] and blood plasma [269] of both normal and PD subjects has been reported. *In vitro*, the first evidence came by Lee et al, who showed that a small percentage of newly synthesized  $\alpha$ Syn was rapidly secreted from cells via unconventional, ER/Golgi-independent exocytosis [270]. Later, it was shown that  $\alpha$ Syn is secreted via an exosomal, calcium-dependent mechanism [271]. It has also been suggested that  $\alpha$ Syn is physiologically secreted by enteric neurons via a conventional ER/Golgi-dependent exocytosis in a neuronal activity-regulated manner [272]. Furthermore, it has been shown that  $\alpha$ Syn fibrils can be

transferred from one neuron to the other through tunneling nanotubes (TNTs) inside lysosomal vesicles [273].

Several studies demonstrating the uptake of fibrillar  $\alpha$ Syn by cells and its ability to produce aggregates composed primarily of the endogenous, host cell protein have followed [274-276].

$\alpha$ Syn is also capable of *in vivo* spreading between cells. For instance, cells transplanted into a human  $\alpha$ Syn overexpressing animal model can acquire misfolded protein from the adjacent host tissue and form aggregates [276]. Direct injection of fibrillar recombinant  $\alpha$ Syn into A53T overexpressing mice also promotes aggregate formation and disease in the host, with  $\alpha$ Syn-KOs being protected against any pathological changes [277]. Furthermore, injection of fibrils consisting of recombinant mouse  $\alpha$ Syn into the striatum of WT mice, results in protein aggregates in the substantia nigra, DAergic neuronal loss, and parkinsonian deficits [278]. However, the precise mechanism of  $\alpha$ Syn exocytosis along with the nature of released  $\alpha$ Syn remain unknown.

### 1.3 Modeling PD

Despite the progress that has been made in the study of PD, the relationship between the genetic targets and the cellular mechanisms that underlie neuronal death is far from understood, making the development of disease-modifying therapies a challenging task. During the last decades, several therapeutic approaches that were promising in a preclinical level, have failed to deliver the same results in clinical trials, underlying the lack of disease models with high predictive power. Furthermore, since several factors contribute to PD, a therapeutic approach might be effective in one form of the disease but not in others.

Moreover, since the available postmortem PD brains come typically from patients at final disease stages, the observed phenotypes most probably do not depict what happens earlier during disease pathogenesis and progression. For all these reasons, there is a need for more precise, even patient-specific disease models that will give us the opportunity to study the disease and test possible protective and/ or therapeutic approaches earlier in the disease progression.

### **1.3.1 Animal models**

Currently available animal models have certainly contributed to better understanding PD etiology, pathology, and molecular mechanisms. PD experimental animal models can be categorized into two main groups: toxin-based and genetic (or combined). Over the years, a number of strategies have been used to produce better animal models recapitulating more faithfully the human disease. Nevertheless, it seems improbable that a single animal model can fully recapitulate the complexity of PD [279].

#### **1.3.1.1 Neurotoxic models**

##### **1.3.1.1.1 6-hydroxydopamine (6-OHDA)**

The 6-OHDA model is the first and most often used, with many animals including rodents, monkeys, cats and dogs being sensitive to 6-OHDA intoxication. It was first used by Ungerstedt et al, more than forty years ago to induce a lesion in the nigrostriatal pathway in rats [280]. As an analog of DA, 6-OHDA is transferred by the dopamine transporter (DAT) into DAergic neurons, accumulates in the mitochondria to inhibit primarily the activity of mitochondrial respiratory chain complex I (Fig. 8) [281]. This compound does not cross the blood-brain barrier (BBB), which makes necessary its direct injection into the brain, either in SNpc, medium forebrain bundle (MFB), or the striatum using a stereotactic device (Fig. 7). The extent of the lesion depends on the amount of 6-OHDA used, the site of injection, and the species under surgery. Usually, it is administered in a unilateral manner with the intact side serving as control. Bilateral administration has also been used, however, it leads to adipsia, aphagia, and eventually premature death, due to the animal's inability to self-sustain [282].

Upon intrastriatal administration, 6-OHDA causes a progressive and retrograde neuronal loss in the SNpc and the ventral tegmental area (VTA). Interestingly, animals with large lesions (>90% neuronal loss) display the typical pattern seen in PD patients, with a greater loss in SNpc as compared to VTA

[283, 284]. It is important to mention that although 6-OHDA interacts with  $\alpha$ Syn, it does not induce LB formation [285].

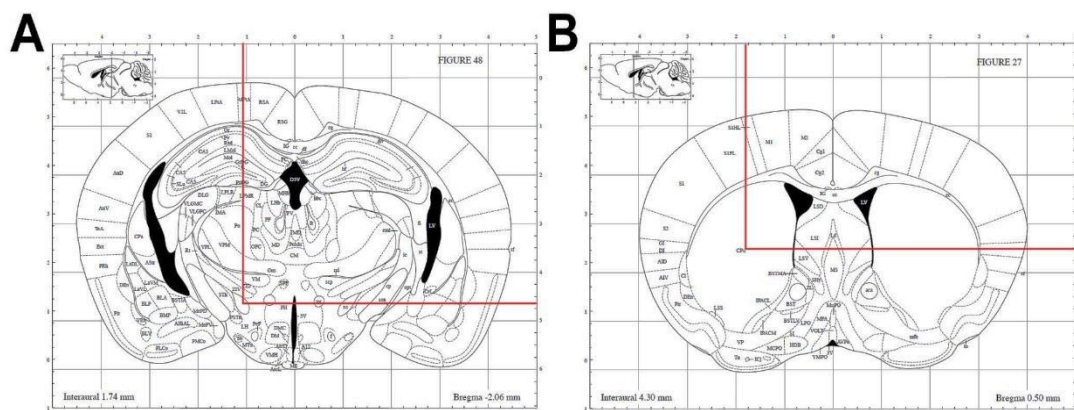


**Figure 7: Coordinates usually used for the 6-OHDA stereotactic injection.** 6-OHDA is usually injected either in the medium forebrain bundle (MFB, A), or the striatum (B) using a stereotactic device.

6-OHDA-treated animals develop motor deficits and the evaluation of motor activity is usually performed after administration of drugs which mimic the effects of dopamine and induce rotational asymmetry. This behavior is related to the degree of the nigrostriatal lesion, although this is not an accurate indicator of the DAergic neuronal loss, since several mechanisms are activated to compensate for the decrease of DA [286]. When DAergic agonists such as apomorphine are administered, the animal exhibits contralateral rotation (turns in a direction opposite to the lesion), but with a drug that stimulates the release of DA, such as amphetamines, the rodent turns in the direction of the lesion. This behavior is based on the fact that the non-lesioned side is able to release more DA than the lesioned one. Lesions to the MFB result in the greatest degree of degeneration (terminal lesion) while lesions within the striatum result in partial lesions. More recently, motor tests without the use of drugs have been developed in rodents, including the stepping test, the paw reaching test, the cylinder test and the spontaneous activity test. These motor tests were initially used in rats, and only recently their effectiveness has been assessed in a unilateral 6-OHDA mouse model [287].

The MFB model is typically used for the study of DAergic neuronal death and for testing therapeutic strategies to treat motor symptoms, while the intrastriatal model, which is more progressive in its symptoms, is useful for earlier PD stages. The 6-OHDA model is a good one since it can replicate

parkinsonian features like DA depletion, nigral DAergic neuronal loss, and behavioral deficits. However, the lesion does not affect other brain regions like olfactory bulbs, lower brainstem areas, or locus coeruleus that have been involved in disease pathogenesis. Additionally, as it has already been mentioned, it cannot induce LB inclusions like those seen in PD patients [288].

#### 1.3.1.1.2 1-methyl-4-phenyl-1,2,3,6-tetrahydropyridine (MPTP)

After it was accidentally discovered, MPTP can be considered a gold standard for toxin-based animal modeling, since it mimics some of the hallmarks of PD such as damage to the nigrostriatal DAergic pathway with a profound loss of DA in the striatum, oxidative stress, and production of reactive oxygen species, energy failure, and inflammation. However, as with 6-OHDA, MPTP injection does not induce LB formation (rev. by [288]). MPTP is highly lipophilic and, unlike 6-OHDA, after systemic administration rapidly crosses the BBB. Once into the brain, MPTP enters astrocytes and is metabolized into MPP<sup>+</sup>, its active metabolite, by monoamine oxidase- B (MAO-B). MPP<sup>+</sup> enters the DAergic neurons through DAT, and can be transported into synaptic vesicles by VMAT2 (vesicular monoamine transporter 2) in the cytoplasm or can interact with complex I mitochondrial proteins thus inhibiting the complex, leading to neuronal death by oxidative stress (Fig. 8). MPTP can be principally used in primates and mice, while it is still unknown why it is not toxic in rats. The classic way of administration is systemic (subcutaneous, intravenous), while unilateral injection in the internal carotid is also used.

Usually, monkeys are treated with high doses of MPTP for a short time (acute model). Recently, however, new protocols have introduced lower doses of the neurotoxin for longer periods of time (subacute to chronic) to replicate more closely the human pathology [289]. This model has also been used for electrophysiological studies, which led to important findings, including the discovery of Deep Brain Stimulation (DBS) as a treatment for PD [290].

#### 1.3.1.1.3 Rotenone and N,N-dimethyl-4,4,4-bypiridinium (Paraquat)

Since pesticides have been implicated in PD pathogenesis, they have been used for developing animal models of the disease [75]. Rotenone is both

an herbicide and an insecticide, with a half-life of 3–5 days depending on its exposure to sunlight, and it is rapidly broken down in soil and in water. It is highly lipophilic, and it can easily cross the BBB. It is mainly used in rats since, so far, since attempts in mice or monkeys have not been successful to induce lesions, with the most commonly used regime typically being the systemic administration using osmotic pumps. Upon intravenous injection, rotenone can lead to loss of DAergic neurons of the SNpc and it is able to induce  $\alpha$ Syn aggregation and LB formation, apart from other features such as oxidative stress or gastrointestinal problems [291]. However, there is not much evidence of DA depletion in the nigrostriatal system, and there are no well-documented cases of PD patients from rotenone intoxication making the model less advantageous than others (rev. by [288]).

Paraquat is an herbicide that exhibits similar structure to MPP<sup>+</sup>, capable to cross the BBB. Typically, it exerts its deleterious effect through oxidative stress mediated by redox cycling and generating reactive oxygen species, more exactly, superoxide radical, hydrogen peroxide, and the hydroxyl radical, which in turn would lead to the damage of lipids, proteins, RNA, and DNA [292]. Importantly, paraquat has the ability to induce LB-like structures in DAergic neurons of the SNpc [293]; although, it is still not known how it leads to oxidative stress and cell death. Additionally, other agricultural compounds like maneb (manganese ethylenebisdithiocarbamate) or ziram lead to greater risk to develop PD, supporting the theory that environmental pesticides can cause PD [288].

### **1.3.1.2 Genetic models**

The aforementioned neurotoxic models have been traditionally used, resulting in severe striatal DA depletion and mirroring mostly later stages of the disease. Although these models recapitulate major motor features of the disease, constituting valuable tools for the development of DA substitution therapies, they do not mimic successfully the progressive nature of the disease.

At the same time, since about 10% of all PD cases are caused by genetic mutations and GWASs have identified genetic risk factors for sporadic PD, the

generation of different genetic models represent a promising approach to study further the disease.

Many different species are amenable to genetic manipulation, including *Mus musculus* (mouse) *Rattus norvegicus* (rat), *Drosophila melanogaster* (fruit fly), and *Caenorhabditis elegans* (nematode). Different strategies have been employed depending on the nature of the gene contributing to PD pathogenesis. In the case of autosomal dominant genes such as *SNCA* or *LRRK2*, overexpression of either WT or mutant forms of the protein has usually been performed. On the other hand, the case of autosomal recessive genes like *PARK2*, *PINK1* and *DJ-1*, where loss of function is caused in PD patients by mutations in one of those genes, KO or knockdown approaches have been used.

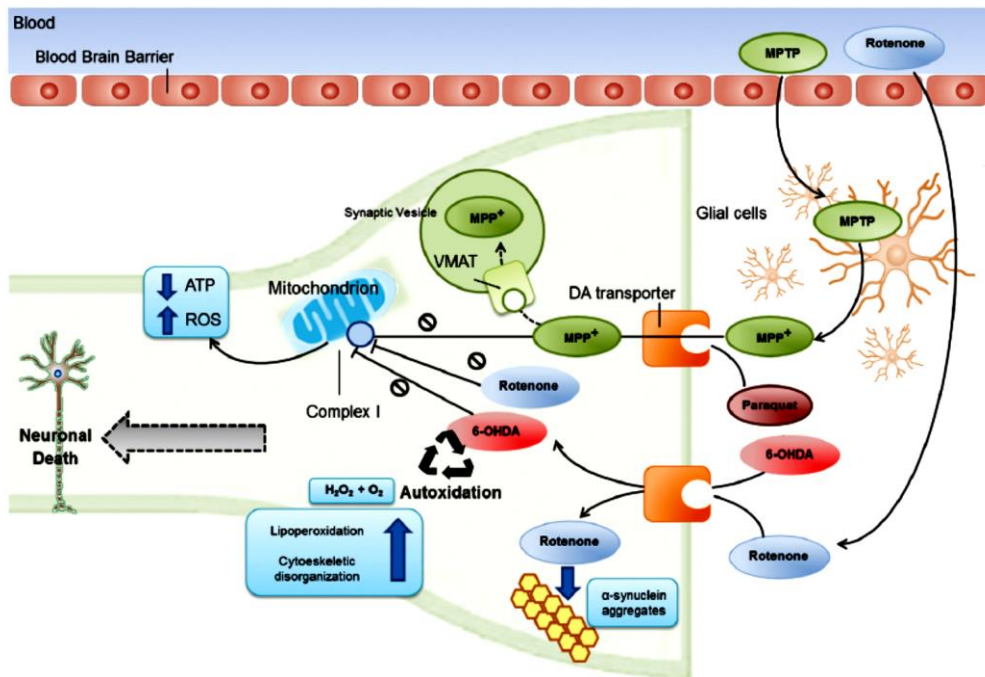


**Figure 8: Pathogenesis of toxin-induced models.** MPTP crosses the blood-brain barrier and is metabolized to 1-methyl-4-phenylpyridinium (MPP<sup>+</sup>) by the enzyme monoamine oxidase B (MAO-B) in glial cells and then to the active toxic compound. MPP<sup>+</sup> is then taken up by dopamine transporter (DAT) where it impairs mitochondrial respiration by inhibiting complex I of the electron transport chain, causing oxidative stress and activation of programmed cell death molecular pathways. Both paraquat and 6-hydroxydopamine (6-OHDA) easily cross cell membrane through the DAT and may also exert their toxicities, in part, by targeting mitochondria with the subsequent production of reactive oxygen species (ROS) and quinones causing the degeneration of the nigrostriatal DAergic neurons. Rotenone is extremely lipophilic and penetrates easily the cellular membrane inducing the formation of α-synuclein (αSyn)

aggregates and mitochondrial impairment with the subsequent production of ROS and quinones [288].

### 1.3.1.2.1 LRKK2

#### 1.3.1.2.1.1 Non-mammalian models

Non-mammalian models provide simple, yet powerful, *in vivo* systems. *C. elegans* has a well-characterized nervous system, consisting of only 6 DAergic neurons, associated with a diversity of behaviors that can be analyzed. It has been used for the study of *LRRK2*, containing only one *lrrk-1* gene encoding a LRRK-like protein. Loss of function studies in *C. elegans* suggest a functional link between LRRK2 and ER stress, as well as its involvement in ER to Golgi trafficking [294]. Overexpression of human WT LRRK2 in *C. elegans* leads to disease related phenotypes such as age-dependent DAergic neurodegeneration, behavioral deficits, and locomotor dysfunction [295]. Moreover, a reduction of DA levels is reported *in vivo*, with several studies suggesting that this is due to mitochondrial dysfunction, autophagy inhibition and ER stress. For instance, neuronal-selective expression of human WT LRRK2 increased nematode survival by protecting against mitochondrial stress, but mutant forms of LRRK2 (G2019S or R1441C) enhanced vulnerability to mitochondrial dysfunction and inhibition of autophagy [156, 296].

The fruit fly has a more complex nervous system with almost 200 DAergic neurons and the ability to display more complex behaviors. LRRK2 drosophila models have also been used to unravel LRRK2-related molecular mechanisms in PD. Using LRRK2-KO and Tg models several *in vivo* LRRK2 interactors have been identified and its role in different signaling pathways like the regulation of protein translation, dendrite degeneration and synaptic function has been illustrated [294].

#### 1.3.1.2.1.2 Mammalian models

Much effort has been placed in developing mouse models for LRRK2. Consistent among the mouse KOs that have been generated is the observation that there is no DAergic neurodegeneration, although some abnormalities are observed outside the nervous system, such as kidney pathology [297-299]. In line with these observations, recently developed LRRK2-KO rat models display

abnormal phenotypes in peripheral organs [300]. Overall, KO studies have suggested that LRRK2 plays little if any role in the development and survival of DAergic neurons under physiological conditions.

Several transgenic techniques for LRRK2 modeling in mice have been utilized, including conventional, bacterial artificial chromosome (BAC) transgenic, tet-inducible systems and mutant LRRK2 knock-in approaches, in which the PDGF- $\beta$  promoter was used to generate G2019S-LRRK2 mouse lines. However, to date only two of the LRRK2 models exhibited age-dependent nigral DAergic neurodegeneration [301, 302]. In parallel, different LRRK2 transgenic rats have been developed and up to now these studies suggest that rats can compensate LRRK2 toxic effects [294].

Regarding viral vector-based models, due to the large size of the *LRRK2* gene and the limited packaging capacity of the different vectors, only two LRRK2 viral models have been developed and characterized. The first carries WT LRRK2 into Herpes simplex virus (HSV) amplicons co-expressing a Cytomegalovirus (CMV)-driven GFP reporter, and induces modest nigral DA neurodegeneration of about 10–20%, whereas the HSV-LRRK2 G2019S induced up to 50% DAergic neuronal loss [303]. Another AAV (adeno-associated virus)-based rat model was developed, carrying either human WT LRRK2 that produced no significant neuronal loss, or G2019S LRRK2 that led to progressive nigral neurodegeneration [304].

Although LRRK2 animal models have provided insights into the potential mechanisms of LRRK2 mediated neurodegeneration, none of them recapitulate all the key features of PD. This might be due to the fact that LRRK2 mutations in humans are partially penetrant, implying that there may be additional factors such as genetic and/ or environmental stressors that are required for the DAergic neurodegeneration. In the future, the development of more robust rodent models and especially of a non-human primate model with the use of viral vectors would be desirable.

#### 1.3.1.2.2 Parkin

Parkin is an E3 ubiquitin ligase that functions in the UPS, and point mutations in *PARK2* gene are the most common cause of autosomal recessive

PD. Several Parkin-KO mice have been generated, showing no substantial DA-related behavioral abnormalities. Some of these KO mice exhibit slightly impaired DA release [305] and some nigrostriatal deficits, including alterations in motor activity, but without DAergic neuronal loss in SNpc [306, 307]. Noteworthy, the Parkin-Q311X-DAT-BAC mice exhibit multiple late onsets and progressive hypokinetic motor deficits, age-dependent DAergic neurodegeneration in the SNpc, and significant reduction in striatal DA and DAergic terminals [308].

#### 1.3.1.2.3 PINK1

PINK1 is a serine/ threonine-protein kinase and point mutations in the *PINK1* gene cause autosomal recessive PD. PINK1-KO mice have an age-dependent, moderate reduction in striatal DA levels accompanied by low locomotor activity, but do not exhibit major abnormalities in the DAergic neurons or striatal DA levels and do not show LB formation [309, 310].

#### 1.3.1.2.4 DJ-1

DJ-1 mutations are linked to an autosomal recessive, early onset PD (Puschmann, 2013). DJ-1-KO mice show decreased locomotor activity, a reduction in the release of evoked DA in the striatum but no loss of SNpc DAergic neurons and no change of the DA levels [311, 312]. However, one DJ-1-KO mouse line shows loss of DAergic neurons in the VTA [313]. Interestingly, a recently described DJ-1-KO mouse, backcrossed on a C57/BL6 background, displayed a dramatically early onset of unilateral loss of DAergic neurons in the SNpc, progressing to bilateral degeneration of the nigrostriatal axis with aging [314]. In addition, this mouse exhibits age-dependent bilateral degeneration in the locus coeruleus, and a mild motor behavioral deficit at specific time points with aging.

#### 1.3.1.2.5 $\alpha$ Syn

##### 1.3.1.2.5.1 Non-mammalian models

Currently, the most commonly used Tg  $\alpha$ Syn *C. elegans* expresses the protein via a muscle-specific or DAergic neuron-specific promoter, together with

a fluorescent reporter. For instance, co-expression of  $\alpha$ Syn and a fluorescent protein in DAergic neurons is associated with neurodegeneration detected as loss of fluorescence (rev. by [315]). Tg lines expressing  $\alpha$ Syn show significant reductions in lifespan, motility and pharyngeal pumping [316].

$\alpha$ Syn has also been extensively studied using fruit flies. The GAL4/UAS system is a powerful tool for targeted Tg expression of WT or mutant  $\alpha$ Syn in all neurons, or in defined neuronal subsets. Feany and Bender first developed Tg *Drosophila* models expressing either WT or familial PD-linked  $\alpha$ Syn mutants (A53T and A30P) [317]. These  $\alpha$ Syn expressing flies replicate several features of PD, including locomotor dysfunction, LB-like inclusion body formation, and age-dependent DAergic neuronal loss and are therefore widely used for studying the molecular pathogenesis of  $\alpha$ Syn-induced neurodegeneration in synucleinopathies. [318].

Fruit flies have unraveled the mechanisms of  $\alpha$ Syn toxicity in terms of misfolding and aggregation, post-translational modifications and oxidative stress (rev. by [319]). For instance, it has been shown that  $\alpha$ Syn mutants including A53T and A30P, which tend to form oligomers, enhance  $\alpha$ Syn toxicity [320]. Another study confirmed that the expression of HSP70, a molecular chaperone, reduces  $\alpha$ Syn toxicity, and vice-versa that a dominant negative form of HSP70 enhances toxicity [321]. Using the same  $\alpha$ Syn overexpressing fruit fly models, it was found that phosphorylated A53T  $\alpha$ Syn was most abundant than WT or A30P  $\alpha$ Syn [322]. Xun et al. performed proteomic analysis in  $\alpha$ Syn flies at different disease stages using liquid chromatography coupled with mass spectrometry [323, 324]. They found cytoskeletal and mitochondrial protein changes in the presymptomatic and early disease stages in the  $\alpha$ Syn A30P expressing flies [323]. They further reported dysregulated expression of proteins associated with membrane, ER, actin cytoskeleton, mitochondria, and ribosome in the presymptomatic  $\alpha$ Syn A53T flies, consistent with the phenotypes of  $\alpha$ Syn A30P flies [324].

More recently, another PD fly model for use in the larval stage expressing A53T  $\alpha$ Syn in DAergic neurons has been developed and characterized [325]. This year, silencing the GBA gene in A53T  $\alpha$ Syn expressing flies resulted in an increase in  $\alpha$ Syn aggregation and DAergic neuronal loss was shown [326].

However, both *C. elegans* and *D. melanogaster* have not been found to have any Syn genes, and a cautious interpretation of the above mentioned results needs to be made as these animals lack pathways and genes present in humans (rev. by [315]).

More recently, Tg vertebrate models using *Danio rerio* (zebrafish) are also being developed. Expression of WT  $\alpha$ Syn in neurons resulted in severe deformities due to neuronal death and lethality during the embryonic stage [327], while its expression in peripheral sensory neurons resulted in dystrophic axons with focal varicosities [328]. While non-mammalian systems are way too simple to model a complex disease as PD, they are useful tools for the study of  $\alpha$ Syn toxicity, bridging between *in vitro* and mammalian studies.

#### 1.3.1.2.5.2 Mammalian models

Mouse models are generally preferred to simulate human genetic disorders, including familial forms of PD. The evolutionary conserved neuronal networks indicate that findings in these models are probable to mirror PD pathology in humans. Importantly,  $\alpha$ Syn-KO mice and those with a naturally occurring deletion of the gene suggest that, as mentioned earlier,  $\alpha$ Syn deletion is not detrimental and that therapeutic suppression would be a viable approach to reducing the accumulation of its toxic assemblies [196, 207].

Numerous mouse models have been developed trying to replicate  $\alpha$ Syn neurodegeneration and propagation. Tg mouse lines overexpressing human WT, A53T, A30P or E46K  $\alpha$ Syn mutant strongly support a toxic gain of function mechanism for  $\alpha$ Syn pathogenesis. Promoters that provide tissue-specific or cell-type-specific expression, like mouse PDGF- $\beta$  (platelet-derived growth factor subunit  $\beta$ ; neuron-specific expression), Thy1 (neuron-specific expression), PrP (prion protein; neuron-specific expression) and rat TH (dopaminergic neuron-specific expression) have been used.

The first Tg mouse line overexpressing human WT  $\alpha$ Syn used PDGF- $\beta$  as a promoter to drive the transgene in neurons [329]. These mice are characterized by ubiquitinated intraneuronal  $\alpha$ Syn inclusions in the temporal neocortex, the CA3 region of the hippocampus, the olfactory bulb, and much

more rarely, in the SN. They also display reduced TH and DA levels in the striatum, as well as decreased number of TH<sup>+</sup> terminals.

Mice overexpressing human WT  $\alpha$ Syn under the Thy1 promoter (mouse line 61) display several features of sporadic PD, including progressive changes in DA release and striatal content,  $\alpha$ Syn pathology, deficits in motor and non-motor functions that are affected in prodromal and later phases of PD, inflammation, and biochemical and molecular changes similar to those observed in PD [330].

Mice overexpressing the A53T  $\alpha$ Syn variant under the Thy1 promoter have severe deficits in motor activity, which begin at 6 months of age and lead to paralysis and death by 12 months [331]. They develop hyperactivity in the dark phase and sleep disorders. They express A53T  $\alpha$ Syn in the cortex, diencephalon, olfactory bulb, striatum, brainstem, cerebellum, and spinal cord, with  $\alpha$ Syn aggregates observed in the hippocampus, brainstem, cerebellum, and spinal cord at 6 months of age and throughout the CNS at 12 months of age. Overall, neurodegeneration in this model is widespread and not limited to brain regions primarily involved in PD.

The best studied Tg mouse is the one overexpressing human A53T  $\alpha$ Syn under the PrP promoter (M83 mouse line). These mice display enhanced  $\alpha$ Syn aggregation, along with more severe pathology and behavioral deficits. They were initially reported to exhibit major pathological changes in their spinal cord motor neurons and develop severe motor impairments, eventually leading to paralysis and death [332]. Elevated DAT levels and reuptake potential in synaptosomal fractions of the striatum at young ages, an age-dependent increase in striatal  $\alpha$ Syn and phospho-Tau accumulation, and nigrostriatal neurodegeneration at 12 months of age were more recently reported [333].

However, since exogenous promoters often fail to mimic the normal spatiotemporal expression of  $\alpha$ Syn in PD, several bacterial artificial chromosome Tg (BAC-Tg) mouse models have more recently been generated that accurately express either the WT or the mutant protein. Thus, BAC-Tg mice harboring the entire human  $\alpha$ Syn gene and its gene expression regulatory regions manifested decreased anxiety-like behaviors which might be due to increased serotonin transporter (SERT) expression, and it is a model useful for the study of gene dosage effects of  $\alpha$ Syn *in vivo* [334].

Finally, unlike the non-mammalian models discussed above, several Tg mouse lines exist on a background that expresses endogenous murine  $\alpha$ Syn, complicating the interpretation of findings in these lines. Janezic et al, though have generated a BAC Tg mouse containing the human *SNCA* gene and a KO allele of the mouse *Snca* gene [203]. These mice display age-dependent nigrostriatal DAergic neuronal loss and motor impairments, deficits in DA transmission in the striatum, as well as age-dependent reduction in firing rates. Furthermore, a BAC-Tg mouse line overexpressing human A53T-  $\alpha$ Syn under the PrP promoter in a  $\alpha$ Syn-KO background has been generated [335]. Significant A53T-  $\alpha$ Syn aggregation is observed in the colonic myenteric plexus, while no widespread aggregation in brain has been reported in these mice. Moreover, subtle motor behavior abnormalities are evident in later ages.

Rodent models have also proved quite useful for the study of the prion-like mechanism of  $\alpha$ Syn propagation. First evidence in the M83 mouse line, overexpressing human A53T  $\alpha$ Syn under the PrP promoter, revealed that intracerebral inoculation of young mice with brain extracts of old mice containing  $\alpha$ Syn aggregates or preformed recombinant  $\alpha$ Syn fibrils induced a progressive, and ultimately lethal, synucleinopathy in injected animals [277, 336]. Further studies demonstrating synucleinopathy in rodent brain after injection of pre-formed  $\alpha$ Syn aggregates have followed, either using WT or mutant  $\alpha$ Syn overexpressing mouse models or non-Tg mice and rats [278, 337]. LB extracts from PD or DLB brains have been inoculated in mice and monkeys [232, 338]. Injection of this LB-fraction into WT mice induced nigrostriatal degeneration and astrogliosis, as well as changes in endogenous  $\alpha$ Syn expression. However, LB extracts did not induce any pathology in  $\alpha$ Syn-KO mice, indicating that the endogenous protein is a prerequisite for LB-induced toxicity. Notably, the injection of brain homogenates from PD patients into TgM83<sup>+/-</sup> mice (hemizygous for the human A53T  $\alpha$ Syn transgene) did not induce CNS dysfunction or  $\alpha$ Syn pathology [235].

A more recent study compared the ability of mutant  $\alpha$ Syn fibril seeds to induce  $\alpha$ Syn pathology in M83 mice. This study showed that H50Q, G51D or A53E mutations in the *SNCA* gene can efficiently cross-seed and induce  $\alpha$ Syn pathology *in vivo*, while E46K  $\alpha$ Syn fibrils are intrinsically inefficient at seeding  $\alpha$ Syn inclusion pathology [339].

Although these models are promising tools for the study of  $\alpha$ Syn propagation, they are not without limitations. Overt synucleinopathy has been observed in studies using Tg mice that greatly overproduce WT or mutant forms of the protein, and highly-concentrated  $\alpha$ Syn species inoculations questioning the translational relevance of these models. Moreover, the long duration to develop a clinically meaningful phenotype which could be highly variable, and, in most cases, the lack of significant DAergic neuronal loss in SNpc, make the interpretation of such studies difficult.

The delivery of  $\alpha$ Syn, both WT and mutant, with viral vectors targeted directly at nigrostriatal DAergic neurons has been considered as an attractive alternative for modeling the disease progression. More recently, a new generation of AAV vectors has been engineered with preferentially neuronal versus glial tropism, and the ability to concentrate to relatively high titers. AAV-vectors- based rodent models of PD were produced that show accumulation of  $\alpha$ Syn aggregates in both the SN and the striatum, dystrophic neurites, loss of striatal DA, DAergic degeneration and parkinsonian phenotypes.

Several molecules with potential disease-modifying role have been identified using such models. Among them, trehalose a natural disaccharide found in invertebrates, fungi, and many plants has been shown to prevent behavioral and neurochemical deficits produced in an AAV human A53T  $\alpha$ Syn rat model [340]. Decreased DAergic neuronal death and ameliorated behavioral deficits have been shown in another AAV human WT- $\alpha$ Syn rat model [341].

Rat models overexpressing either WT or a mutant form of the protein have also been generated. For instance, BAC-Tg rats overexpressing human WT  $\alpha$ Syn develop early changes in novelty-seeking, avoidance and smell before the progressive motor deficit [342]. They also display increased neurogenesis in olfactory bulb in young animals, a strong reduction of striatal DA transmission associated with a severe degeneration of DAergic nerve terminals and astrogliosis in aged animals. Lately, a rat model overexpressing human WT  $\alpha$ Syn by local injection of viral-vectors in midbrain has been reported, leading to early synaptic dysfunction [343]. Progressive aggregation and Ser129-phosphorylated  $\alpha$ Syn was observed in DAergic terminals, in dystrophic swellings that resembled axonal spheroids and contained mitochondria and vesicular proteins.

Furthermore, a Tg rat model overexpressing human A53T  $\alpha$ Syn was created (<https://www.taconic.com/rat-model/alpha-synuclein-a53t>), showing a dramatic decline in general motor activities with age, along with abnormal  $\alpha$ Syn aggregation and DAergic neuronal degeneration [344].

Using viral vectors, recently a non-human primate model for synucleinopathy was produced [345]. In this case, the human A53T *SNCA* gene was delivered in SN, leading to a 50% nigral DAergic neuronal loss and a 60% reduction in striatal DA. However, the validation of this model remains to be fully reported, hopefully providing us with a valuable primate model for potential therapeutic approaches to be tested.

### **1.3.2 Cellular models**

In addition to animal models, several cellular models have been used, which most of the times develop disease-related pathology more quickly, are less costly and do not require ethical approval. Furthermore, genetic or pharmacological manipulations and time-lapse imaging in cellular models are easier and more reliable. In an *in vitro* system, the study of a specific cell type or the interaction of specific cell subtypes are also amenable.

#### **1.3.2.1 Immortalized cell lines**

Immortalized cell lines are genetically modified, easy to be maintained, proliferate rapidly, and enable large scale studies. In PD research, different human and non-human cell lines are commonly used, such as human embryonic kidney 293 (HEK293), or neuroglioma (H4) cells. These lines have been used to address questions related to  $\alpha$ Syn function and subcellular localization as well as the differences between WT and mutant forms of the protein. Using both cell lines, it was shown that A53T  $\alpha$ Syn promoted the strongest increase in the accumulation of  $\alpha$ Syn oligomers in the nucleus compared to other mutants [346]. It was also found using H4 cells that  $\alpha$ Syn mutations (A30P and E46K) promoted a faster shuttling of  $\alpha$ Syn into the nucleus when compared to WT [347].

However, it is important to mention that these cell lines lack a neuronal phenotype. To overcome this, several human and mouse cell lines that can be differentiated into states that display neuronal phenotypes have been used,

including SH-SY5Y and PC12. The human neuroblastoma cell line SH-SY5Y is widely used in PD research, because it is able to differentiate into neuronal-like cells that express DAergic markers, such as TH, DAT, and VMAT2, when exposed to retinoic acid, phorbol esters, dibutyryl cyclic adenosine monophosphate (cAMP). These cells are relatively easy to culture and to expand providing a DAergic system for research studies and screening. They are also vulnerable to oxidative stress, in a similar manner to that observed in DAergic neurons. For instance, using SH-SY5Y cells, the neuron-to-neuron transmission of  $\alpha$ Syn via exocytosis has been shown [274, 276]. However, these are not authentic DAergic neurons, and it is difficult to differentiate them into a post-mitotic mature DAergic state [348].

### 1.3.2.2 Primary cultures

Primary neurons isolated from different mouse brain regions have been extensively used to model PD, after overexpressing the WT or a mutant form of a protein involved in the disease.  $\alpha$ Syn has been thoroughly studied with such systems, and several disease-associated mechanisms have been unraveled. As mentioned earlier, it was first shown in rat embryonic cortical neurons, that a small percentage of newly synthesized  $\alpha$ Syn was rapidly secreted from cells via unconventional, ER/ Golgi-independent exocytosis [270]. Overexpression of A53T  $\alpha$ Syn in rat cortical neurons resulted in CMA dysfunction, followed by a compensatory increase in macroautophagy [250]. Furthermore, hippocampal neurons isolated from mice overexpressing human WT  $\alpha$ Syn showed striking neurotransmitter release deficits and enlarged synaptic vesicles, suggesting that pathologic  $\alpha$ Syn leads to a loss of a number of critical presynaptic proteins, thereby inducing functional synaptic deficits [193]. In another study, WT  $\alpha$ Syn overexpression in hippocampal neurons inhibited neurotransmitter release and increased the synaptic vesicle pool [66].

DAergic neurons are usually prepared from the ventral mesencephalon of mouse or rat embryos at embryonic day 12–15 (E12-15) and they have been extensively used in the study of PD-related molecular mechanisms (rev. by [348]). For instance, overexpression of WT or A53T  $\alpha$ Syn resulted in significant DAergic neuronal death with cytoplasmic  $\alpha$ Syn inclusions appearing only in the

latter [349]. Furthermore, overexpression of A30P or A53T  $\alpha$ Syn using AAVs caused a reduction in DAergic neurite regeneration in a scratch lesion model, while inducing a TH<sup>+</sup> neuronal loss [350]. Rat primary midbrain neurons overexpressing WT or A30P or A53T  $\alpha$ Syn displayed impaired neurite outgrowth and affected neurite branching [65]. Surprisingly, the number of primary neurites per neuron was increased in neurons transfected with either WT or mutant forms of  $\alpha$ Syn in this study.

The propagation of different conformations of  $\alpha$ Syn have also been investigated in primary neuronal cultures. For instance, distinct strains of synthetic  $\alpha$ Syn fibrils efficiently promote cross-seeding of tau aggregation in hippocampal neurons [233]. Furthermore, it was shown that WT and A53T  $\alpha$ Syn fibrils predominantly seed flame-like inclusions in both neurons and astrocytes of mixed primary cultures; whereas the structurally distinct E46K fibrils seed punctate, rounded inclusions [351].

#### **1.4 Induced Pluripotent Stem Cells**

12 years ago, a major technological breakthrough in biomedical research was made, reporting that cells with a gene expression profile and developmental potential similar to embryonic stem cells (ESCs), the so called induced pluripotent stem cells (iPSCs) can be generated from mouse somatic cells, such as fibroblasts, by using a cocktail of four transcription factors [352]. One year later, two research groups independently reported the generation of human iPSCs from fibroblasts [353, 354]. The iPSC induction was achieved after the retrovirus-mediated transduction of four human transcription factors, namely Oct3/4, Sox2, Klf4, and c-Myc into adult human dermal fibroblasts. Using a 30day protocol, human ESC-like colonies were observed. These cells are similar to human ESCs in terms of morphology, feeder dependency, marker expression, spontaneous differentiation and ability to form teratomas.

Subsequent studies have also demonstrated that iPSCs can be generated but with lower efficiency using only three factors (Oct4, Sox2, and Klf4) [355], thus avoiding the use of c-Myc, which is considered to be an oncogene. Therefore, although this procedure is less efficient than the four factor protocol, the resulting iPSC show less clonal variation.

Because iPSCs were initially generated by introducing reprogramming factors via integrating viral vectors, such as retroviral vectors, there was concern about the clinical application of these iPSCs, owing to the potential for insertional mutagenesis caused by the integration of transgenes into the genome of host cells (rev. by [356]). To make iPSCs more clinically applicable, various non-integrating methods have been developed using episomal DNAs, adenoviruses, Sendai viruses, PiggyBac transposons, minicircles, recombinant proteins, synthetically modified mRNAs, microRNAs and small molecules, although the small-molecule approach is not yet applicable to human iPSC derivation (rev. by [357]). Among these approaches, episomal DNAs, synthetic mRNAs and Sendai viruses are commonly applied to derive integration-free iPSCs owing to their relative simplicity and high efficiency (rev. by [358]). Additionally, since 2009, xeno-free conditions have been developed to overcome the problems associated with traditional culture methods and to eliminate undefined animal component. Furthermore, alternative cell sources have been used to produce iPSCs including peripheral blood cells, keratinocytes, liver and stomach cells and even cells from human urine since the collection of urine is non-invasive [359].

The years that followed its discovery, human iPSC technology has led to revolutionary changes in stem cell biology, regenerative medicine, as well as disease modeling and drug discovery (rev. by [357]). Human iPSCs were rapidly applied to generate human 'disease-in-a-dish' models for identification of pathogenic mechanisms and novel therapeutics. These cells have many advantages including their human origin, easy accessibility, expandability, ability to give rise to almost any cell type, avoidance of ethical concerns associated with human ESCs, and the potential to develop personalized medicine solutions using patient-specific iPSCs. The scalability of iPSC production, facilitates assay development and therefore phenotypic screening for drug discovery. Furthermore, recent advances in gene editing technologies like the CRISPR–Cas9 technology, enable the rapid generation of genetically defined human iPSC-based disease models (rev. by [357]).

## 1.4.1 iPSC applications

### 1.4.1.1 Disease modeling

Identifying the pathological mechanisms underlying human diseases has a key role in discovering new therapeutic approaches. Animal models have proved to be valuable tools for modeling human diseases. However, substantial species differences prevent faithful recapitulation of full human disease phenotypes. Disease modeling using patient-derived cells is helpful for studying disease etiology and for developing therapeutic strategies for human diseases. However, the lack of expandable sources of primary cells from patients, especially from hard-to access brain or heart cells is a critical limitation. iPSC technology enabled disease modeling using iPSCs derived from easily accessible cell types, from different patients, paving the way to personalized disease modeling and precision medicine. This technology allowed for modeling of a number of diseases, including brain disorders (rev. by [360, 361]).

The method is particularly attractive for the study of genetic diseases, and especially these caused by a specific mutation. Patient-derived iPSCs can be differentiated into disease relevant cell types while iPSCs derived from non-disease-affected individuals may be used as controls for patient-derived iPSCs. Nowadays, it is even possible to correct the disease-causing gene mutation in patient-derived cells or introduce a mutation in non-affected-derived cells using genome editing approaches. iPSC-based disease modeling is being used for almost a decade studying disorders caused by a single gene mutation (monogenic disorders) with an early onset (rev. by [357]).

Modeling diseases that have a late onset is more challenging because cells differentiated from human iPSCs in general exhibit fetal-like properties (rev. by [362]). Alternative approaches to generate neurons by direct conversion of somatic cells to accelerate maturation by retaining genetic hallmarks of ageing [363] or by inducing cellular aging has been used to aid in the successful modeling of late-onset disease. Additionally, treating the cells with cellular stressors has been attempted [364, 365]. Recent studies though, have suggested that cellular maturation and aging may be distinct events [366]. In an attempt to generate more functionally mature neurons, novel region-specific differentiation protocols [367], and the inclusion of human glial cell

types that support synaptic development and pruning [363] are being employed to facilitate the formation of higher-order neural networks *in vitro*, reflecting stages and activity patterns of relevant developing regions *in vivo*.

Several protocols for the generation of glutamatergic [367-371], GABAergic [372, 373], serotonergic [374] and dopaminergic [375-380] neurons have been described until now. Furthermore, protocols for the generation of non-neuronal brain cells like astrocytes [381-384], oligodendrocytes [385-387], and microglia [375, 377, 380] have been used in an attempt to study several diseases of the CNS.

One major drawback of 2-dimensional neuronal cultures is that they lack the cytoarchitecture of the brain tissue. In line with this, more than one cell type may be required to effectively model some diseases. The co-culture of different cell types enables the investigation of non-cell-autonomous aspect of the disease pathology. For instance astrocyte-motor neuron co-cultures derived from iPSCs from the same patient carrying the M337V TDP-43 mutation have been used to study amyotrophic lateral sclerosis (ALS) [388].

More recently 3-dimensional (3D) iPSC-based culture systems, the so-called organoids, have been used to study cell-to-cell interactions in a context that mimics more closely human development and physiology (rev. by [389]). iPSC-derived organoids appear to recapitulate the brain's 3D cytoarchitectural arrangement thus providing new opportunities to explore disease pathogenesis when derived from patient cells. Organoids can be region-specific, in which case their generation is guided by extrinsic morphogenes and patterning growth factors, yielding forebrain [390], cortical [391], midbrain [392] or hypothalamic structures [393]. Alternatively, organoids can be self-organizing entities with their assembly relying on intrinsic mechanisms of self-organization [389, 394]. Either region-specific or self-organizing, organoids comprise multiple neural and glial identities, and have the potential to reproduce an anatomically relevant human-specific spatial organization with more complex cytoarchitecture, synaptic connections, cell-to-cell and cell-extracellular matrix interactions.

The considerable evolutionary increase in size and complexity of the human brain as compared to other mammalian species, particularly cortical expansion, has been attributed to a greater number and prolonged proliferative potential of neural progenitor cells during development. As iPSC-derived

cortical organoids correspond to human mid-fetal development, they represent suitable models for investigating alterations in individuals with neurodevelopmental disorders (rev. by [395]). Organoids have been used in the study of lissencephaly, a genetic neurological disorder associated with mental retardation and intractable epilepsy and revealed neurodevelopmental disease phenotypes and a mitotic defect in outer radial glia, a cell type that is particularly important for human cortical development [396]. Similarly, human forebrain organoids were used to study congenital microcephaly [397] or microcephaly resulting from Zika virus infection of neural precursor cells [398] and more recently autism spectrum disorders (ASD) [399]. As evidenced from the above paradigms, 3D-organoid modeling of neurodevelopmental diseases is still in its infancy, whilst advances in 3D-modeling of neurodegenerative diseases are lacking far behind [400, 401].

Even though the 3D-cultures present as ideal systems to study the formation and activity of neuronal networks, only two studies published provide relevant in depth information. Detailed electrophysiological analyses of midbrain-like organoid-derived slices revealed action potentials (APs), spontaneous excitatory and inhibitory postsynaptic currents and large-amplitude excitatory postsynaptic potentials indicative of participation of DAergic neurons in network activity [392]. In combination with expression of functional DA receptors, the authors support the potential utility of these systems to evaluate the degree of synaptic competence and connections. However it remains to validate the system using iPSC lines from PD patients. Interestingly, a human 3D brain microphysiological system has been recently developed [402] comprising differentiated mature neurons and glial cells, both astrocytes and oligodendrocytes, that reproduce neuronal-glia interactions and exhibit spontaneous electrical activity as measured by multi-electrode array (MEA), indicative of overall neuronal functionality of the system. Last year, the first attempts to study PD using brain organoids have been reported [403, 404]. Transcriptomic analysis [404] or functional analysis using calcium imaging and MEA were used.

As the 3D systems are still at the early stages of development, complementary use of novel technologies such as 3D printing technologies [393] is expected to improve the scalability and reproducibility of 3D systems,

making this approach even more attractive for studying disease pathogenesis and discovering new drugs.

#### 1.4.1.2 Drug discovery

Many drug screenings are based on targets that are considered to be relevant to the disease mechanisms. However, the low success rates of compounds originating from target-based screening have led to greater interest in phenotypic screening. The scalability of iPSC production, as well as the pluripotency of these cells have made possible the recapitulation of disease relevant phenotypes and pathologies *in vitro*, allowing for phenotyping screening (rev. by [357]). Large-scale drug screenings using human iPSCs have already been performed to evaluate more than 1,000 compounds for several diseases [405-407] and several clinical candidates have been identified [408, 409]. However, the long time needed for iPSCs to differentiate and to develop a disease-relevant phenotype is a concern and faster and more stable differentiation protocols are being sought for this purpose. Moreover, using the right control group is quite important for a drug screening. Comparisons between various groups of iPSCs (healthy, patient and gene-corrected patient iPSCs) can be made to validate the results of a drug screening (rev. by [410]).

Patient-derived iPSCs can also be used in drug repositioning, in which existing drugs already approved for specific diseases are tested to find new applications in other diseases. Generally, using iPSCs in drug discovery is of great value since it allows testing of the drug responsiveness in a broad patient population. By contrast, it is challenging to analyze the effect of a drug in multiple mouse models simultaneously.

The development of new drugs is enormously costly, mostly due to failures, particularly those in late-stage clinical trials, which are in turn partially due to unanticipated side effects. Consequently, there is considerable interest in developing approaches that could more effectively predict the likelihood of candidate drugs to cause serious side effects, thereby enabling the selection of candidates that are less likely to fail owing to toxicity in late-stage trials. iPSCs can be used for reliable preclinical *in vitro* drug testing for cardiac toxicities, and hepatotoxicity. More recently, a platform that assesses adverse drug effects in

the nervous system using PSCs has been developed [411]. The protocol described produces neural tissue constructs with consistent gene expression profiles that are useful for predicting neurotoxicity. However, the extent to which they mimic normal human neural development and function remains currently unexplored.

#### **1.4.1.3 Clinical applications**

iPSC technology's applicability in regenerative medicine has gained much attention with the first clinical study to have initiated in 2014. The study used human iPSC-derived retinal pigment epithelial (RPE) cells to treat macular degeneration, and the treatment was reported to improve the patient's vision. Although the trial was subsequently paused owing to the identification of two genetic variants in the iPSCs of a second patient, it is anticipated to continue (rev. by (Shi, Inoue et al. 2017)). More recently, another study has demonstrated the feasibility of transplanting human ESC-derived cardiac progenitor cells embedded in a fibrin scaffold to patients with severe heart failure (Menasche, Vanneaux et al. 2015).

It is important to mention that there are several issues associated with iPSC-based therapy that will need to be addressed before routine clinical applications can begin. One concern is the risk for tumorigenicity, since iPSCs are maintained in culture for prolonged time periods and, can accumulate karyotypic abnormalities. Although the products differentiated from iPSCs have not been shown to generate teratomas, it is critical to ensure that the final product does not contain undifferentiated cells that have the potential to generate teratomas. Improved differentiation protocols are now applied and approaches to eliminate the risk for tumorigenicity are being used. Moreover, compliance with good manufacturing practice (GMP) is mandatory before human transplantation. Finally, another issue to be considered is the need for an effective immunosuppression method when non-autologous transplantation is performed.

## 1.4.2 Modeling PD using an *in vitro* human iPSC model

### 1.4.2.1 Neuronal modeling

Models of familial PD were among the earliest iPSC-based disease models to be generated since the advent of cellular reprogramming (Fig. 9). Even though iPSCs have been derived from patients with idiopathic PD, the majority of studies have focused on familial PD cases caused by mutations in a single gene (Table 2). Although these are rare forms of PD, they provide a clear advantage: the observed phenotypes are attributable to a specific gene alteration and therefore causality may be established. Today, mutations in 14 genes have been identified to cause familial PD [412]. From those, the best known are implicated in both autosomal and recessive forms causing early disease onset with a generally severe clinical phenotype, and include SNCA, leucine-rich repeat kinase 2 (LRRK2),  $\beta$ -glucocerebrosidase (GBA) and various PARKIN genes. Several studies utilizing hiPSC models reported neuronal dysfunction associated with mutations in LRRK2 [364, 413, 414], GBA [415, 416], PARK2 [417, 418], PARK7 [419] and  $\alpha$ Syn [412, 420-422]. Even though in most PD studies the aim has been to generate and characterize DAergic neurons, few studies have included other types of neurons in the analysis, including glutamatergic and GABAergic neurons [246, 420]. Overall, data derived from these studies confirmed the involvement of various pathways previously implicated in PD pathogenesis such as mitochondrial, lysosomal and ER dysfunction, impaired clearance of autophagosomes, disturbed calcium homeostasis and oxidized dopamine accumulation. However, it has been challenging to identify cellular pathologies in iPSC-derived PD neurons in the absence of oxidative or other cellular stress.

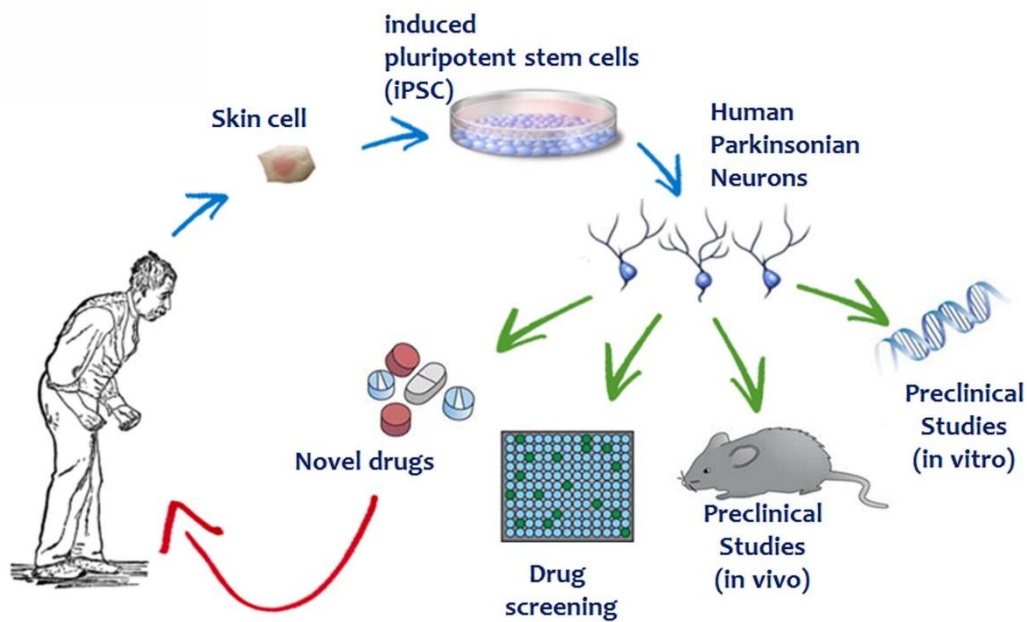


**Figure 9: Induced Pluripotent Stem Cells (iPSCs) as an *in vitro* system to model diseases such as Parkinson's disease and to discover new therapies.**

LRRK2 mutations represent the most common cause of familial PD and are autosomal dominant with age-dependent penetrance [99]. This kinase is highly expressed in brain areas receiving dopamine innervations, such as the striatum, hippocampus, cortex and cerebellum [100] and has been associated with many aspects of neuronal function including neurogenesis, axonal outgrowth and synaptic function [101-103, 423]. iPSC-derived DAergic neurons from LRRK2-G2019S patients were shown to be particularly susceptible to oxidative and mitochondrial stress [364, 413, 414], but RNA-sequencing analysis did not reveal changes in transcript expression associated with synapse formation and function [414]. The only relevant to synapse formation impairment was a diminished neurite outgrowth velocity, a phenomenon not specific to DAergic neurons [414]. Despite the fact that these LRRK2-G2019S mutant neurons also had increased levels of  $\alpha$ Syn and TAU proteins, a phenotype previously associated with axonal degeneration and synaptic alterations, neuropathology was not observed. As this mutation has an age-dependent appearance of the clinical phenotype, it could be that the end time point of analysis was too early to reveal such defects. In a similar way, the iPSC-GBA1 mutation PD systems did not provide a link to dysregulated synaptogenesis or synaptic function [415, 416]. Since the studies performed

are quite limited in number and the focus of the initial analysis might not have been to depict differences in synaptic function, additional work is required to draw safe conclusions about the presence of synaptopathy in LRRK2 and GBA mutant neurons.

**Table 2:** Reports on modeling 2D iPSC-based models of Parkinson's disease (PD) [71].

PD	LRRK2 (G2019S)	Increased susceptibility to oxidative stress	Nguyen et al. 2011 [364]
PD	LRRK2 (G2019S)	Increased susceptibility to proteasomal stress	Liu et al. 2012 [413]
PD	LRRK2 (G2019S)	Increased susceptibility to oxidative and mitochondrial stress; Diminished neurite outgrowth	Reinhardt et al. 2013 [414]
PD	GBA (RecNcil; L444P; N370S)	Autophagic/ lysosomal deficiency; Impaired Ca <sup>2+</sup> homeostasis	Schondorf et al. 2014 [415]
PD	GBA (N370S)	DA homeostasis defects	Woodard et al. 2014 [416]
PD	PARK2 (various mutations)	Impaired dopaminergic differentiation; Mitochondrial alterations	Shaltouki et al. 2015 [418]
PD	PARK2:EX3-5DEL; PARK2:EX3DEL	Reduced complexity of neuronal processes	Ren et al. 2015 [417]
PD	PARK7 (c.192G>C)	Mitochondrial and lysosomal dysfunction	Burbulla et al. 2017 [419]
PD	SNCA (G209A)	N/A	Soldner et al. 2011 [424]
PD	SNCA triplication	Increased susceptibility to oxidative stress	Byers et al. 2011 [425]
PD	SNCA (G209A)	Increased susceptibility to oxidative and nitrosative stress	Ryan et al. 2013 [259]
PD	SNCA (G209A); SNCA triplication	Increased nitrosative stress; ER stress	Chung et al. 2013 [246]
PD	SNCA triplication	Increased susceptibility to oxidative stress	Flierl et al. 2014 [426]
PD	SNCA triplication	Impaired neuronal differentiation; Compromised neurite outgrowth	Oliveira et al. 2015 [427]
PD	SNCA (G209A)	Defective synaptic connectivity; Axonal neuropathology; Altered expression of synaptic transcripts	Kouroupi et al. 2017 [420]
PD	SNCA (G209A)	Fragmented mitochondria and $\alpha$ Syn deposits at mitochondrial membranes in response to cardiolipin	Ryan et al. 2018 [428]

In contrast,  $\alpha$ Syn iPSC-based systems have been far more informative in providing clues for early synaptic deficits in pathology initiation and progression. Even though mutations in  $\alpha$ Syn account for a small number of familial PD

cases, they have received particular attention and have been employed extensively by researchers to create both animal models (rev. by [429]) and iPSC-based cellular platforms of neurons and progenitor cells (rev. by [421]). The reason is that the first genetic cause of PD to be identified was the G209A mutation in the  $\alpha$ Syn gene *SNCA*, leading to synthesis of the pathological p.A53T- $\alpha$ Syn mutant protein [82].  $\alpha$ Syn protein was soon after discovered to be the major component of Lewy bodies, the pathological hallmark of both familial and sporadic PD [430]. Since then a number of point  $\alpha$ Syn mutations have been identified: A30P, E46K, H50Q, G51D and A53E [85, 88, 91, 431-433] as well as duplication or triplication of the  $\alpha$ Syn gene locus that also cause dominant and severe forms of PD [434, 435].

In a first study by Jaenisch and colleagues [424] successful derivation of iPSC-derived p.A53T and p.E46K lines and isogenic gene corrected controls was reported, without further characterization. This p.A53T-hiPSC line was used in a later study by Ryan et al [259] to produce cultures of midbrain DAergic neurons that displayed aggregated  $\alpha$ Syn 35 days after differentiation in both the cell soma and neurites, features similar to those previously identified in post-mortem brains from p.A53T patients [436, 437]. Despite the presence of  $\alpha$ Syn oligomeric aggregates, DAergic neurons did not show axonal damage or defective neuronal network formation. In a more recent study the p.A53T neurons displayed fragmented mitochondria and  $\alpha$ Syn deposits at mitochondrial membranes in response to cardiolipin, a mitochondrial membrane lipid [428]. Cortical neurons generated from the same set of p.A53T iPSC lines by Lindquist and colleagues were also susceptible to induced ER stress [246]. These studies support a “two-hit” hypothesis where the mutant background facilitates induction of a PD phenotype by environmental toxins.

The first observation of damaged neurites and axonal fragmentation with multi-electrode arrays revealing asynchronous firing and a reduction in the number of active channels was identified in LRRK2 neurons. RNA-sequencing data from all PD lines showed a consistent upregulation of the RNA-binding protein fox-1 homolog (RBFOX1), a neuron specific factor that regulates neuronal splicing networks and controls neuronal excitation [438]. Interestingly, when the authors mapped significant differential splicing products they generated a list of 41 genes with a profound enrichment in GO terms related to

neuron projection and neuronal activity. From those, they confirmed that GRIN1 (an NMDA receptor subunit) and SNAP25 (a key component of the SNARE complex) specific isoforms were altered in PD neurons, demonstrating for the first time that differential splicing events are regulated by RBFOX1 in these cellular systems.

Recently, a study from our group [420] further enhanced the hypothesis that synaptopathy is an early event in familial PD cases. This work was focused on the analysis of newly generated lines from two p.A53T patients with different clinical progression and severity [420]. At 35 days of differentiation to DAergic neurons following a dual SMAD inhibition protocol [376, 439], cells exhibited clear features of neurodegeneration, including extensive neuritic pathology,  $\alpha$ Syn<sup>+</sup> and Tau<sup>+</sup> swollen varicosities and large spheroid inclusions highly similar to the dystrophic neurites identified in the brain of p.A53T patients [436, 440]. Astonishingly, the severity of the cellular phenotype was directly correlated with the clinical picture of the two different patients. In a similar manner to the observations of Ryan et al [259], thioflavin-positive aggregates started to be visible at 35 days of differentiation while they became more prominent and widespread at 50 days, with  $\alpha$ Syn protein also being co-detected. A connection of the degenerative phenotype to  $\alpha$ Syn pathology was established in our study, since small molecules inhibiting  $\alpha$ Syn aggregation reverted the neurodegenerative phenotype, indicating a potential treatment strategy for PD and other related disorders.

An intriguing observation was that the extensive p.A53T pathology appeared without the need for external neurotoxic or oxidative stress. Axonal degeneration was evident in DAergic, but also in glutamatergic and GABAergic neurons present in our culture system, as well as in  $\beta$ III-tubulin-positive neurons prior to subtype specification. We presume that the simultaneous presence of all three major neuronal subtypes might be the key for the strong intrinsic and widespread p.A53T degenerative phenotype. This notion is also supported by the observation that when using the Kriks et al [379] differentiation protocol to enrich for DAergic neurons, the fraction of GABAergic cells is clearly diminished and the p.A53T-related axonal degeneration is also less noticeable (submitted). Even though we cannot exclude the possibility that different patient lines may yield neurons with variable phenotypic characteristics, it is also likely

that differences in the ratio of excitatory to inhibitory neurons within a culture may be a decisive factor for the phenotypic outcome.

Transcriptional profiling of p.A53T neurons in Kouroupi et al [420] also revealed dysregulated molecular pathways in the absence of external stress conditions. Presynaptic vesicle formation and trafficking molecules (SYN3, SV2C, RPHA3, DOC2B), vesicular and plasma membrane neurotransmitter transporters, synaptic cell adhesion (SLITRKs, Cadherins) and post synaptic density (DLGAP2, GRIN2D, GRIP2)-associated mRNAs were all decreased in the p.A53T neurons. This correlated well with compromised neuritic growth and defective synaptic connectivity. Notably both axonal guidance molecules and WNT family members associated with synaptogenesis were significantly altered, suggesting perturbations during synaptogenesis. From our data we cannot infer defects at a specific part of the synapse in p.A53T pathology and ultrastructural analysis is needed for such correlations. However considering the localization of  $\alpha$ Syn at the pre-synaptic area and previous observations from overexpression studies in animal models where “vacant synapses” were formed [193], it could be that an original misorganization of the pre-synaptic area might affect the overall organization of the trans- and postsynaptic sites. As the most striking mis-expression was noted in transynaptic adhesion molecules, we could also assume that correct alignment for proper synaptogenesis and maturation could not be achieved, further affecting the pre- and postsynaptic regions. Although this remains an open question, our study clearly indicates synaptopathy as a major feature in p.A53T-pathology that is initiated early (Fig. 10).

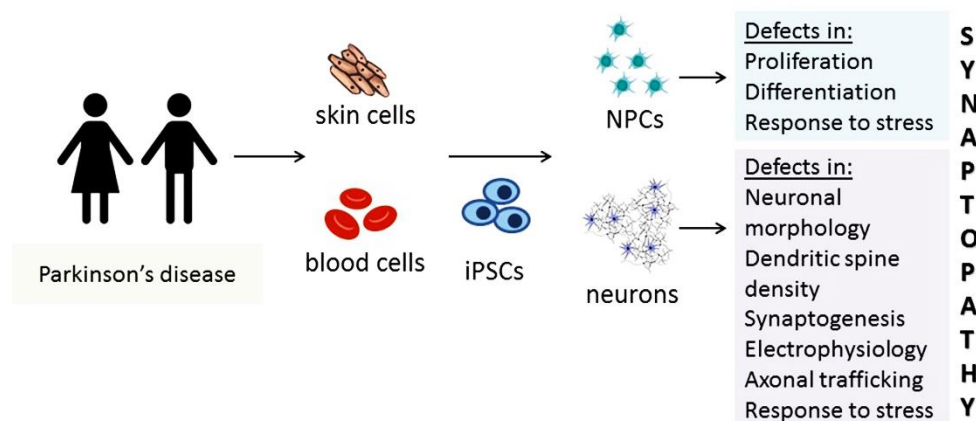


**Figure 10: Scheme of Parkinson's disease modelling using induced pluripotent stem cell reprogramming technology (adapted by [71]).**

Evidence for aberrant neurogenesis in PD has come from the analysis of iPSC-derived neuronal progenitors (NPCs) and neurons from PD patients harboring a triplication of the  $\alpha$ Syn locus. These progenitors demonstrated relevant susceptibilities to oxidative [259, 425] and nitrosative stress [246] and had reduced capacity to differentiate into dopaminergic or GABAergic neurons, while they displayed compromised neurite outgrowth and lower neuronal activity as compared to control cultures. This is the first report to show a link between  $\alpha$ Syn and developmental processes in iPSC-derived cell systems. Molecular profiling indicated lower levels of differentiation markers such as TH, NURR1, GABABR2 and DLK but also lower GIRK2, consistent with the lower potassium currents observed. Even though isogenic control lines were not included in this experimental setting and someone could argue that this effect is not  $\alpha$ Syn dependent as the triplication of the locus affects the expression of 3 up to 12 genes, knocking down  $\alpha$ Syn with a lentivirus rescued the differentiation defects in one out of the two lines used. Nevertheless, such differentiation distortions were not reported in a follow up study using a different set of triplication lines [441], probably due to the clonal variation and differentiation propensity of the lines generated. This follow up study [441] also included a Parkin and six LRRK2 mutant lines and despite the neurite outgrowth defects observed in midbrain DAergic neurons, the number of TH<sup>+</sup> neurons was unaffected.

#### **1.4.2.2 Non-neuronal modeling**

It is important to mention that, until recently, iPSC technology tended to focus on neuronal phenotypes in order to model neurodegenerative diseases, such as PD. However, other brain cell types, have been implicated in PD pathogenesis and more recently effort has been made towards modeling these diseases with non-neuronal iPSC-derived cells. Hopefully, this approach will help us understand in deep cell to cell interactions and underlying mechanisms towards disease-modifying therapies. Astrocytes, for instance, are the most abundant cell type in the CNS and perform a wide variety of functions, including synaptogenesis and synaptic transmission, response to inflammation, wound healing, and the formation and maintenance of the BBB. They are involved in

recycling of glutamate and molecular regulation of ion, neurotransmitter and neurohormone concentrations (rev. by [442]). Strategies for the directed differentiation of astrocytes from iPSCs can either rely on a neural progenitor cell (NPC) or an oligodendrocyte progenitor cell intermediate [443]. Up to now, Serio et al have shown that astrocytes from iPSCs carrying the M337V TDP-43 mutation associated with ALS, had decreased survival, increased TDP-43 levels, and intracellular mislocalization of the protein [388].

Oligodendrocytes envelope neuronal axons in a thick membrane of myelin, enabling rapid conductance of electrical signals through neural networks. Although human oligodendrocytes can be generated from iPSCs (Goldman and Kuypers, 2015) and are seemingly highly active once transplanted *in vivo* (Windrem et al., 2014), they myelinate less than 3% of axons *in vitro* (Kerman et al., 2015). iPSC-derived oligodendrocytes have been generated from MSA patients and a PD patient carrying the SNCA triplication in which the expression  $\alpha$ Syn protein decreases over time [444].

Microglia are brain-resident macrophages, and are professional phagocytes, responsible for the homeostatic clearance of cellular debris, dying cells, incompetent synapses and aggregation-prone proteins. However, they can be transition into a damaging, reactive state by inflammatory stimuli, triggering cytokine release, potentially leading to increased neuronal damage and creating a vicious cycle of cytokine production and neuronal destruction. Three recent reports have described the creation of microglia from iPSCs via a hematopoietic progenitor-like intermediate cell [375, 380, 445]. Furthermore, the first attempt to generate iPSC-derived macrophages carrying either the A53T mutation or the SNCA triplication has been reported [446]. SNCA triplication macrophages, but not A53T, have significantly increased intracellular  $\alpha$ Syn versus controls and release significantly more  $\alpha$ Syn to the medium. SNCA triplication macrophages also showed significantly reduced phagocytosis capability. While the protocols differed in their reliance on EB differentiation and/ or fluorescent-activated cell sorting (FACS), all methods yielded immature microglia-like cells expressing canonical microglial markers and demonstrating phagocytic and migratory functionality.

### **1.4.2.3 Three-dimensional modeling**

Along with the above mentioned 2D models, only a few studies using 3D iPSC models have been reported. In the first one, phase-guided, 3D microfluidic cell culture bioreactors were used, and iPSCs were differentiated into DAergic neurons for 30 days [447]. These neurons showed spontaneous electrophysiological activity with propagation of APs along neurites, supporting the robustness of the model. In another study, detailed electrophysiological analyses of midbrain-like organoid-derived slices revealed APs, spontaneous excitatory and inhibitory postsynaptic currents and large-amplitude excitatory post-synaptic potentials indicative of participation of DAergic neurons in network activity [392]. In combination with expression of functional DA receptors, the potential utility of these systems to evaluate the degree of synaptic competence and connections is supported. However it remains to validate the system using PD patient-derived iPSC lines.

Last year, two other improved organoid approaches to model familial PD were reported [403, 404]. Son et al generated neuroectodermal spheres and intestinal organoids from iPSCs carrying the G2019S mutation and healthy individuals [404]. Gene expression analysis revealed differences between PD and healthy mainly in synaptic transmission, and specifically synaptic vesicle trafficking. Monzel et al. were able to generate midbrain-specific cultures from neuroepithelial stem cells [403]. After neuronal differentiation they were able to obtain DAergic neurons, astrocytes and oligodendrocytes. Neurons were able to secrete DA, form spatially patterned and organized networks, and show synaptic connections and spontaneous neuronal activity. Myelination of neurites was also observed, highlighting the complexity of the model.

## **1.5 PD treatment**

The current medical management of the disease aims at controlling symptoms for as long as possible while minimizing adverse effects. Symptomatic or palliative therapies, including pharmacological and surgical approaches, notably improve quality of life and functional capacity, but they do not cure or halt disease progression and are not quite effective with non-motor

manifestations of the disease. Overall, slowing and preventing disease progression in PD constitutes an unmet medical need.

### **1.5.1 Pharmacological treatment**

Since DAergic neuronal loss constitutes the major hallmark of the disease, DA replacement approaches have been used to restore mainly motor functions, including DAergic and non-DAergic agents. Among the variety of DAergic agents, levodopa (L-dopa), a precursor of DA able to cross the BBB, remains the "gold standard" treatment for PD motor symptoms. Once in the brain, L-dopa exerts its symptomatic benefits through its conversion to DA, by the enzyme L-amino acid decarboxylase. This strategy leads to the restoration of DA levels in the striatum and leads, in many cases, to the improvement of motor symptoms [448]. To date, L-dopa is routinely orally administered in combination with a decarboxylase inhibitor (benzerazide, carbidopa), in order to prevent the formation of DA in the peripheral tissues, which can result in adverse effects such as nausea and vomiting.

L-dopa treatment is well known to improve motor symptoms and patients' quality of life. Most people can be maintained over the first 5 years of the disease on 300-600 mg/ day of L-dopa, and motor symptoms initially improve by 20-70%, depending on the patient's condition (rev. by [15]). However, L-dopa has a short half-life in plasma, which eventually results in short-duration responses with a "wearing-off" effect (a gradual waning of the effect of DAergic treatment on motor symptoms before the next dose). Moreover, after 4-6 years of chronic treatment, severe motor complications arise comprising "on-off" fluctuations (when symptoms can reappear and disappear randomly) and dyskinesias (involuntary movements and tics). Non-motor side effects such as confusion, hallucinations, and sleep disorders are also present in some patients. In individual studies, the percentage of fluctuations and dyskinesia may range from 10 to 60% of patients at 5 years of treatment, and up to 80-90% in later years. More recently, different ways of L-dopa administration are being used. For instance, percutaneous infusion of L-dopa (L-dopa-carbidopa intestinal gel) is clinically useful for certain patients with severe motor

fluctuations, although it requires appropriate clinical support, restricting use to specialized centers.

The non-ergoline DAergic agonists (pramipexole, ropinirole, rotigotine, and piribedil) are efficacious drugs that, in contrast to L-dopa, when used as monotherapy do not provoke dyskinesias. They are being used in younger patients (under 55 years of age); although L-dopa is usually necessary within 3 years of diagnosis. DAergic agonists could lead to troublesome adverse effects like early gastrointestinal and psychiatric side-effects, ankle oedema, sleep attacks, and impulse control disorders necessitating drug withdrawal in few patients (rev. by [15]). Nevertheless, to date new formulations of DAergic agonists such as apomorphine are currently under different clinical trials. This year it was shown that apomorphine infusion resulted in a reduction in off time (periods when antiparkinsonian drugs have no effect) in PD patients with persistent motor fluctuations despite optimized oral or transdermal therapy [449].

The selective type B monoamine oxidase (MAO-B) inhibitors, selegiline and rasagiline, as a symptomatic monotherapy, are well tolerated and can be administered once daily but they are less efficacious than either L-dopa or DAergic agonists (rev. by [15]). Among them, only rasagiline has been proven efficacious for the treatment of motor fluctuations [450].

Catechol-O-methyl transferase (COMT) inhibitors, especially entacapone, have also been used for treating motor fluctuations efficiently. Moreover, enhancing L-dopa duration of action with enzyme inhibition using COMT and/ or MAO-B inhibition remains an effective approach for reducing motor fluctuations.

Amantadine, which is an N-methyl-D-aspartate (NMDA) antagonist, is also an effective anti-dyskinetic agent in some patients [451], and anticholinergic drugs can reduce painful dystonic phenomena in young onset cases.

### **1.5.3 Targeted therapies**

It has already been stated that currently there are no therapies slowing PD progression. The discovery of genetic variants causing and/ or increasing

the risk for the disease, over the last 20 years however, has provided the field with potential disease-modifying therapies ready to be tested in clinical trials (rev. by [452]).

To begin with, a large body of evidence supports the accumulation of  $\alpha$ Syn plays a pivotal role in PD pathogenesis. The last decade, several methods have been developed to target  $\alpha$ Syn accumulation, including reducing  $\alpha$ Syn production, by gene silencing mechanisms targeting its mRNA level, or reducing intracellular  $\alpha$ Syn aggregation, using specific antibodies against monomeric  $\alpha$ Syn. Another approach is to increase intracellular  $\alpha$ Syn degradation, by enhancing autophagy. Furthermore, degradation of extracellular  $\alpha$ Syn by immunotherapy is also considered. Lastly, inhibiting neuronal uptake of extracellular  $\alpha$ Syn could be an attractive approach, although there are currently no clinical trials.

However, the challenges associated with therapies targeting  $\alpha$ Syn accumulation are still numerous. To begin with, there is no animal model that naturally replicates  $\alpha$ -synucleinopathy in humans. Second, there is currently no established method to assess target engagement in the brain for potential therapeutic approaches that target  $\alpha$ Syn. Third, there is no biofluid-based biomarker that can assess the level of  $\alpha$ Syn pathology in patient brains. Fourth, it is not known when during the PD progression, intracerebral  $\alpha$ Syn pathology appears and whether there is a “point of no return” beyond which the neuronal damage can no longer be rescued (rev. by [452]).

At the same time, therapeutic approaches targeting the GBA pathway are being considered, either by increasing in GCCase activity or by modulating GBA-related glycosphingolipids. The development of LRRK2-related therapeutics is also of interest, and LRRK2 kinase inhibitors are already being clinically tested (rev. by [452]).

### **1.5.2 Surgical procedures: Deep Brain Stimulation**

A better understanding of basal ganglia physiology has led to the development of surgical treatments in PD, known as Deep Brain Stimulation (DBS). DBS is a surgical treatment involving the implantation of a medical device, which can send electrical impulses in a region of the basal ganglia,

mainly the internal globus pallidus (GPi), and the subthalamic nucleus (STN). At its fundamental core, the general purpose of electrical stimulation therapy in the SN is to use the applied electric field to manipulate the opening and closing of voltage-gated sodium channels on neurons, generate stimulation-induced action potentials, and subsequently, control the release of neurotransmitters in the targeted pathway [453].

DBS can provide additional help for specific patients whose symptoms are not controlled sufficiently by DAergic medications and until recently was used only in advanced stages of PD. It is effective in ameliorating motor fluctuations and dyskinesia, as well as non-motor features of the disease, including non-motor fluctuations, sleep-related symptoms, and behavioral abnormalities. DBS in the ventral medial nucleus of the thalamus (VIM) is also an option for treatment of tremor.

A couple of years ago, Food and Drug Administration (FDA) approved DBS for earlier PD patients, although there are many challenges towards its clinical implementation, including patient selection, prediction of outcomes and adverse effects of the treatment [454]. Moreover, improved hardware and software (rechargeable battery, multipolar electrodes) now offer a higher flexibility and precision to individually target the different motor symptoms and to avoid stimulation-related side effects.

Another surgical approach that has been used is unilateral or bilateral pallidotomy, where a small area in the GP is destroyed, leading to the reduction of the key symptoms of PD like akinesia, tremor, and rigidity as well as L-dopa-induced dyskinesias [455]. Although the procedure has been nearly abandoned due to safety efficacy issues, gamma knife pallidotomy has recently been proposed as an alternative for patients who are not candidates for DBS [456].

## **1.5.4 Cell replacement approaches**

### **1.5.4.1 First clinical trials and alternative cell sources**

PD is particularly attractive for cell replacement therapies since its core pathology involves the loss only of a specific neuronal subtype, the A9 DAergic neurons. Proof-of-principle studies supporting this approach have already performed in 1980s when the shortcomings of the existing approaches were

not known. In a breakthrough study in Sweden, fetal ventral mesencephalic (fVMs) allografts have been used as a cell source. They were transplanted in the striatum and it has recently been shown that they can release DA, survive for over 20 years in some patients and improve their quality of life and some non-motor features of the disease [457, 458].

In the years that followed these first attempts, however, cell replacement therapy for PD has been questioned for several reasons. Along with the aforementioned successful transplantations, several others took place using for instance tissue from the patients' adrenal medulla. The rationale for this approach was that the adrenal medulla produces catecholamines, including DA (albeit at very low levels). In these early grafted patients, however, the transplants had poor survival and no major clinical benefits with some of them experiencing surgical complications. These findings led to the abandonment of the approach [459].

Although, the above preclinical positive reports in Sweden paved the way for more patients to be grafted in 1990s and overall the patients improved, the results were variable. At the same time, two human VM transplant trials were performed in United States reaching the same conclusion, namely, that these transplants did not lead to significant improvement, producing adverse effects including graft-induced dyskinesias (GIDs). It is very interesting though that, in some grafted patients, many years after transplantation, a fraction of the grafted neurons contained LBs and  $\alpha$ Syn aggregates, suggesting the aforementioned prion-like mechanism of disease progression [225, 457]. It is also worth mentioning that the post-transplantation immunosuppression approaches used varied, with some patients having received immunosuppressant for up to 1 year post-grafting and others not. Lastly, fVM transplants raise issues of tissue availability and ethical problems inherent in using fetal tissue.

For all these reasons, efforts have been focused on improving the transplantation procedure and finding a better source for cell grafting. One promising alternative source is stem cells, given that their use would avoid issues of tissue availability and, depending on the source of the cells, be ethically less disputed. Different stem cell sources have been proposed, and several differentiation protocols towards DAergic neurons have been employed. Mesenchymal stem cells are multipotent cells derived from the bone marrow

that can differentiate into various cells of the mesodermal lineage, but also have the capacity to differentiate into epithelial, endothelial and neuronal cells. *In vitro* studies proved their ability to differentiate into TH-expressing cells [460] but their capacity to make true midbrain DAergic neurons is unproven. Thus, although benefits have been reported in animal models of PD, the quality of the response is insufficient to allow these cells to go to proper clinical trials.

ESCs are pluripotent stem cells derived from the inner cell mass of early-stage preimplantation embryos that provide an unlimited supply of cells. They have been shown to efficiently differentiate into midbrain DAergic neurons [378, 379] and to provide similar efficacy to fVM transplants in preclinical studies, constituting the most promising stem cell source up to date.

The last decade, iPSCs have gained much attention. This cell source would allow autologous grafting and provides an unlimited supply of cells. Furthermore, long-term survival and function of autologous iPSC-derived midbrain DAergic neurons have already been reported in nonhuman primates [461].

Neurons obtained by direct reprogramming of somatic cells by defined factors constitute another cell source for potential replacement therapy. DAergic neurons have already been reprogrammed from fibroblasts [462] or astrocytes [463]. This source would allow autologous grafting, as well as greatly reducing graft overgrowth and/ or tumor formation risks associated with grafts from stem cell sources.

#### **1.5.4.2 Future potential of clinical trials**

It has been almost 30 years since the first evidence that transplanted DAergic neuroblasts can survive in the PD brain and considerable progress has been made in the cell replacement field. For now, TRANSNEURO, which is a European research consortium, is running a clinical trial with 11 patients grafted with fVMs for 3 years now, in an attempt to explore efficacy and safety of the fetal cell replacement approach (rev. by [464]).

More recently, PSCs have gained prominence and 4 separate clinical trials using either ESCs or iPSCs from healthy donors have already started or are about to start the following couple of years in Europe, the US and Japan

(rev. by [464]). In all the cases, PSCs have been produced under Good Manufacturing Practice (GMP) and are compliant with each region's national guidelines. Each group is about to use a different cell source and patients of different disease stage. Moreover, the immunosuppressive regime, as well as the whole trial design will be different. In spite of the setup discrepancies, these trials hold great promise for the future of cell replacement therapy in PD.

#### 1.5.4.3 Autologous cell transplantation

The aforementioned trials, using either fVMs or PSCs, are focusing on non-autologous transplantation, since the transplanted cells are not patient-derived ones. The advent of iPSC though would allow for autologous transplantation, as already mentioned. Nevertheless, it remains an open question whether patient cells constitute a suitable source of donor cells for autologous transplantation to treat PD. Despite the obvious advantage of avoiding the need for immunosuppression, one concern is that patient cells may display disease-related features *in vivo* as they have been shown to do *in vitro* in a number of studies modeling PD.

Preclinical *in vivo* studies are for now limited. In an initial report by Hargus et al, engrafted DA neurons generated from sporadic PD patients survived *in vivo* and ameliorated 6-OHDA-associated behavioral deficits in rats, even though only a few donor-derived neurons projected their axons towards the DA-depleted host striatum [465]. These observations were recently confirmed in a primate model of PD where sporadic PD patient iPSC-derived neurons survived and, in this case, extended dense neurites into the host striatum [466]. This effect was consistent regardless of whether the cells were derived from patients with idiopathic PD or from healthy individuals [467].

Surprisingly similar studies using human iPSC-derived neurons from patients with familial forms of PD have lagged behind, despite the large number of mutation-carrying iPSC lines that have been generated for *in vitro* disease modeling. Given the generally severe clinical phenotype of inherited PD forms and the multitude of disease-relevant features identified in such mutant neurons *in vitro*, it is pertinent to investigate whether similar changes occur also *in vivo*. The only study reported so far used DAergic neurons carrying the G2019S-

LRRK2 mutation, suggested that these cells survive *in vivo* in the mouse brain for 11 weeks, but up-regulate human  $\alpha$ Syn which is believed to be the first step towards induction of pathology [468]. However, the increased human  $\alpha$ Syn levels fail to induce spreading or aggregation in the mouse brain. Further *in vivo* studies are needed to investigate whether the disease-related features displayed in iPSC-models *in vitro*, appear also *in vivo*. These studies would clarify whether autologous transplantation could be a future therapeutic approach for the disease.

## 2. AIM OF THE THESIS/ OBJECTIVES

The cutting-edge technology of human induced pluripotent stem cells (iPSCs) has opened up new prospects for understanding human biology and disease. It has prompted the creation of *in vitro* patient-derived models of disease and has raised hopes for cell replacement therapies (rev. by [464]). A prominent characteristic of Parkinson's disease (PD) is the progressive loss of striatal-projecting dopaminergic neurons of the substantia nigra pars compacta, resulting in debilitating motor deficits (rev. by [15]). Even though it is still unknown whether DAergic neuron degeneration is an initial disease feature or the inevitable consequence of multiple dysfunctions throughout the brain, it represents a common pathological manifestation in PD and is responsible for many of the clinical symptoms. During the past 20 years, mutations causing familial PD have been identified and their study has assisted in gaining valuable insights into PD etiopathology.

$\alpha$ -synuclein ( $\alpha$ Syn, *SNCA* gene) is the major sporadic PD linked gene [110], whereas point mutations [412] and multiplications [93] of the locus cause an autosomal dominant form of the disease, often characterized by early onset and a generally severe phenotype. The best-studied  $\alpha$ Syn mutation is p.A53T (G209A in the *SNCA* gene), first identified in families of Italian and Greek ancestry [82, 469, 470]. In these lines Dr. Matsas' team at the Laboratory of Cellular and Molecular Neurobiology – Stem Cells of the Hellenic Pasteur Institute in collaboration with Dr. Stefanis, Prof. of Neurology at the Athens Medical School, has previously developed a disease-in-a-dish model for familial PD using iPSCs from two patients carrying the p.A53T  $\alpha$ Syn mutation. By directed differentiation, they generated a model that displays disease-relevant phenotypes, including protein aggregation, compromised neuritic outgrowth, axonal neuropathology and synaptic defects [420]. Despite the various mutation-carrying human iPSC lines that have been generated so far for *in vitro* PD modeling, including ours, their engraftment potential has not been addressed. This is an important question as it would allow monitoring their behavior in a more physiological *in vivo* environment, in the presence of other cell types, such as the host neurons and glia.

The purpose of this study is to investigate the phenotype of p.A53T-patient-derived (PD) neurons *in vivo* vis-à-vis healthy-derived (control) neurons

after transplantation in a 6-OHDA lesion mouse model developed in the immunosuppressed NOD/SCID strain. The “disease-in-a dish” model of iPSC-derived neurons from PD patients carrying the p.A53T- $\alpha$ Syn mutation developed by [420], comprised DAergic, GABAergic and glutamatergic neurons, that displayed a number of disease-associated features, including protein aggregation, compromised neuritic outgrowth and contorted or fragmented axons with swollen varicosities containing  $\alpha$ Syn and Tau. Moreover, PD neurons showed disrupted synaptic connectivity and widespread transcriptional alterations in genes involved in synaptic signaling. Interestingly, small molecules that target  $\alpha$ Syn and prevent its aggregation [471] could rescue the impaired synaptic connectivity and axonal neuropathology of PD neurons, providing a direct link between the identified disease-associated phenotypes and pathological  $\alpha$ Syn [420]. Here we aimed to further explore the *in vitro* properties of these PD-iPSCs, differentiated to the DAergic lineage, and investigate if they could survive and differentiate *in vivo* after transplantation into the host mouse brain. To this end, we aimed to generate an enriched population of engraftable cells, consisting of progenitors and early neurons with restricted proliferative capacity, to avoid cellular overgrowth within the graft. For this purpose we sought to apply a floor-based strategy for the generation of engraftable neurons [379] combined with further enrichment in PSA-NCAM-positive neuronal cells. This novel protocol is expected to yield an appropriate population of cells for transplantation studies.

To investigate the *in vivo* phenotype of the PD cells *in vivo*, our objective was to perform transplantation into a lesion model that can support xenograft survival. As such we chose to use a toxin-induced brain lesion model in the immunosuppressed NOD/SCID mouse strain that sustains human graft survival and differentiation. Even though our aim is to use this lesion model as a means for supporting graft survival, and not for therapeutic purposes, we considered necessary to characterize its properties. Therefore characterization of the model was performed before PD and control cells were stereotactically transplanted, while analysis of the grafted mice followed. The potential of PD grafted cells was compared to control cells in terms of survival, differentiation and possible development of disease-related characteristics. These studies are informative as to whether the distinct degenerative characteristics which PD cells develop

*in vitro*, appear also *in vivo* and whether there is spread of pathology from the graft to the host. Overall we expected that our work will provide evidence if this is a valid approach for *in vivo* disease modeling in a hybrid human-mouse environment.

### **3. MATERIALS**

#### **3.1 Lab equipment**

##### **3.1.1 Instruments and devices**

- Laminar hood (Thermo Fisher Scientific)
- CO<sub>2</sub> Incubator (Heracell 150; Marschall Scientific)
- Light Cycler 96 (Roche)
- Pipettes (1-10 µL, 2-20 µL, 20-200 µL, 100-1000 µL; Gilson)
- Pipette filler (Thermo Fisher)
- Freezers -20°C; -80°C
- Freezing container (Thermo Fisher, 5100-0001)
- Mini rocker-shaker (MR-1; Kisker)
- Waterbath (Julabo)
- Laboratory balance (Mettler)
- pH-measurer (Orion 3 Star; Thermo Electron Corporation)
- Neubauer counting chamber (Marienfeld)
- Sterile microsurgery tools: scissors, needle holder, medium and fine forceps (WPI)
- Electric razor (Braun)
- Scalpel (surgical blade, with no.10 or 15 blade)
- Hamilton syringe (10µl; 701N, Hamilton)
- Dental drill or bone drill with small (1- to 1.5-mm) cutting burrs
- Mouse, rat stereotaxic device (Stoelting)
- Inhalation device for anesthesia (Harvard apparatus)
- Video camera

##### **3.1.2 Microscopes and Image analysis software**

- Confocal laser scanning microscopy platform TCS SP8 (Leica)
- Image processing program ImageJ (NIH)
- Adobe Photoshop CS6

##### **3.1.3 Consumables**

- Syringes (1, 5, 10ml)
- Sutures (nonabsorbable silk 5-0 or 6-0 monofilament; BBraun)

- Surgical gloves and mask
- Tissue culture plates, sterile (6-, 12-, 24 well; Corning)
- Serological pipettes, sterile, single wrapped (1, 2, 5, 10ml; Greiner Bio-one)
- VWR Micro Cover Glasses, 24 x 50 mm (VWR, 48393-081)
- Microscope slides B/50, 76 x 26 mm (Knittel)

## **3.2 Reagents**

### **3.2.1 Chemical reagents**

- Agarose (Sigma, A9539)
- TRI reagent (Sigma, T9424) for RNA extraction
- Chloroform (Sigma, 32211)
- Isopropyl alcohol (Fisher Scientific, BP2618212)
- 6-Hydroxydopamine (Sigma, H4381)
- Desipramine (Sigma, D3900)
- Rimadyl (analgesic)
- Baytril (antibiotic)
- L-Ascorbic acid (Sigma, A4544)
- Eye gel Recugel (Bausch and Lomb)
- Hibitane (local antiseptic)
- Betadine (local antiseptic)
- Xylocaine (local anesthetic)
- Dextroamphetamine Sulfate CII (LGC Standards GmbH, USP1180004)
- Normal donkey serum, NDS (S30, Merck)
- Triton X-100 (FLUKA)
- NaCl (0,9% saline)
- Sodium azide or  $\text{NaN}_3$  (Sigma)
- Ethanol (Panreac and Merck)
- Trisodium citrate, dehydrate (BDH)
- Isoflurane or IsoFlo (Abbott)
- Paraformaldehyde (Sigma, 1581127)
- Sodium hydroxide or NaOH (Merck)
- Hydrochloric acid or HCl (Merck)

- Sodium Chloride or NaCl (Panreac)
- Calcium- and magnesium-free Hanks' buffered salt solution (CMF-HBSS); containing 2 g/ liter glucose, ice cold
- 1% (w/v) DNase in CMF-HBSS (store in small aliquots at -20°C)
- PBS, Phosphate buffer saline 1x (Gibco, 11594516)
- HBSS Hank's Balanced Salt Solution, no calcium, no magnesium, no phenol red (Gibco, 14175095)
- Prolong Gold Antifade Reagent with DAPI (CST, 8961)
- Hoechst 33343 Solution (Thermo Scientific, 62249)

### **3.2.2 Cell culture**

#### Basic media, and supplements

Knockout DMEM (Gibco, 10829-018)

KSR (knockout serum replacement) (Gibco, 10828-028)

Penicillin/Streptomycin (Gibco, 11548876)

GlutaMAX Supplement (Gibco, 35050-038)

MEM-Non essential amino acids (Gibco, 11140-035)

Beta-mercaptoethanol (Gibco, 21985-023)

FGF basic rec human (Miltenyi, 130-093-842)

DMEM high glucose (Gibco, 11965092)

Fetal Bovine Serum (Gibco, 10500064)

F12 (Sigma, 51445C)

N2 Supplement (Gibco, 17502048)

B27 supplement (Gibco, 12587010)

Neurobasal (Gibco, 21103049)

LDN193189 (Stemgent, 04-0074)

SB431542 (Tocris, 1614)

SHH C24II (R&D, 1845-SH)

Purmorphamine (Stemgent, 04-0009)

FGF8 (R&D, 423-F8)

CHIR99021 (Stemgent, 04-0004)

BDNF (brain-derived neurotrophic factor; R&D, 248-BD)

GDNF (glial cell line-derived neurotrophic factor; R&D, 212-GD)

TGFβ3 (transforming growth factor type β3; R&D, 243-B3)

Ascorbic acid (Sigma- Aldrich, A92902)  
Dibutryl cAMP (Sigma- Aldrich, P4890)  
DAPT (Tocris, 2634)  
Y-27632 (ROCK inhibitor; Stem Cell Technologies, 72302)  
Synth-a-Freeze (Cryopreservation medium, Gibco, A1254201)

#### iPSC media on feeders

Knockout DMEM  
KSR (knockout serum replacement) 2%  
Pen/Strep 1%  
GlutaMAX 1%  
MEM-Non essential amino acids 1%  
Beta-mercaptoethanol 1000x  
(Filter using Millipore stericup 0.22µm)  
FGF basic rec human 10ng/ml

#### MEF media

DMEM high glucose  
GlutaMAX Supplement 1%  
Fetal Bovine Serum 10%

#### iPSC media feeder-free conditions

TeSR™-E8™ Basal Medium (Stem Cell technologies, 05990)  
Pen/Strep 1%

#### N2 medium

DMEM high glucose /F12  
N2 Supplement 1%  
GlutaMAX Supplement 1%  
Beta-mercaptoethanol 1000x

#### B27 medium

Neurobasal  
B27 Supplement 2%  
GlutaMAX Supplement 1%

#### DAergic differentiation media

DMEM/F12  
KSR 15%,  
GlutaMAX 2mM  
Beta-mercaptoethanol 10 mM  
LDN193189 100 nM  
SB431542 10 mM  
SHH C24II 100 ng/ml  
Purmorphamine 2 mM  
FGF8 100 ng/ml  
CHIR99021 3 mM

#### Maturation media

BDNF 20 ng/ml  
GDNF 20 ng/ml  
TGF $\beta$ 3 1 ng/ml  
Ascorbic acid 0.2 mM  
dibutyryl cAMP 0.5 mM

#### Coating materials

Gelatin solution 0.1 % (Merck, ES-006-B)  
Matrigel (BD, 354230)  
Polyethylenimine (PLE, Sigma, 40877)  
Laminin (Sigma, L2020)  
Fibronectin Bovine Protein, Plasma (Gibco, 33010018)  
Poly-L-ornithine (PLO, Sigma, P3655)

### **3.2.3 Enzymes**

- Tsp45I (NEB, R0583S)
- Collagenase, Type IV (Invitrogen, 17104-019): for the dissociation of iPSC
- ReLesR (StemCell technologies, 05782): for the dissociation of iPSC
- StemPro Accutase Cell Dissociation Reagent (Gibco, A1110501): for the dissociation of iPSC
- RQ1 RNase-free DNase (Promega, M6101), for the removal of DNA in RNA samples

- ImProm-II Reverse Transcriptase (Promega, A3802) and random hexamers (Applied Biosystems, N8080127) for the RT-qPCR

#### Other reagents

- Mouse embryonic fibroblasts (MEFs, Gibco, A34180)
- PCR kit (Qiagen, 201203)
- Molecular Mass Ruler (BioRad, 1708207)
- Clean and Concentrator (Zymo Research, R1018)
- Random Hexamers (50mM) (Applied Biosystems, N8080127)
- Anti-PSA-NCAM magnetic Microbeads (Miltenyi Biotech, 130-092-966)

### 3.2.4 Primer sequences

**Table 1. Primer sequences used for RT-qPCR in the current study**

Gene name	Application	Forward	Reverse
FOXA2	qPCR	CCATGCACTCGGCTTCCAG	TGTTGCTCACGGAGGAGTAG
NURR1	qPCR	TCGACATTTCTGCCTTCTCCTG	GGTTCCTTGAGCCCCTGTCT
PITX3	qPCR	GAGCTAGAGGCGACCTTCC	CCGGTTCTTGAACCACACCC
TH	qPCR	TGTCTGAGGAGCCTGAGATTCG	GCTTGTCCTTGGCGTCACTG
MAP2	qPCR	GAGAATGGGATCAACGGAGA	CTGCTACAGCCTCAGCAGTG
VGLUT1	qPCR	CGACGACAGCCTTTTGTGGT	GCCGTAGACGTAGAAAACAGAG
GAD67	qPCR	GCCAGACAAGCAGTATGATGT	CCAGTTCCAGGCATTTGTTGAT

### 3.2.5 Antibodies

**Table 2. Primary antibodies used in the current study**

<b>Epitope</b>	<b>Host</b>	<b>Dilution</b>	<b>Vendor</b>	<b>Catalog number</b>
NANOG	Goat	1/100	R&D	AF1997
SOX2	Rabbit	1/1000	Abcam	Ab59776
TRA-1-60	Mouse	1/100	Merck-Millipore	MAB4360
SSEA-3	Mouse	1/50	DSHB	MC-631
SSEA-4	Mouse	1/50	DSHB	MC-813-70
A-fetoprotein	Mouse	1/200	Merck-Millipore	2004189
NESTIN	Rabbit	1/200	Merck-Millipore	ABD69
MAP2	Mouse	1/200	Merck-Millipore	MAB3418
Smooth Muscle Actin (SMA)	Mouse	1/200	Merck-Millipore	CBL171
$\alpha$ -Synuclein ( $\alpha$ Syn)	Mouse	1/500	BD Biosciences	610787
$\alpha$ -Synuclein ( $\alpha$ Syn)	Mouse	1/500	Santa Cruz	sc-12767
TH	Rabbit	1/500	Merck-Millipore	AB152
TUJ1	Rabbit	1/1000	Cell Signalling	5568
PSA-NCAM	Mouse	1/100 (ICC); 1:300 (IHC)	Merck-Millipore	MAB5324
doublecortin (DCX)	Goat	1/200 (ICC); 1/500 (IHC)	Santa-Cruz	sc-8066
human cytoplasmic antigen (STEM121)	Mouse	1/500	Clontech	Y40410
human nuclei clone 3E1.3	Mouse	1/500	Merck-Millipore	MAB4383
Synaptophysin (clone EP10)	Mouse	1/200	Thermo Fisher	14-6525-80
DARPP32	Rabbit	1/1000	Abcam	ab40801

**Table 3. Secondary antibodies used in the current study**

Antigen	Conjugate	Host	Dilution	Vendor	Catalog number
goat IgG	Alexa 488	donkey	1/500 (ICC); 1/1000 (IHC)	Molecular Probes	A11055
rabbit IgG	Alexa 488	donkey	1/500 (ICC); 1/1000 (IHC)	Molecular Probes	A21206
mouse IgG	Alexa 647	donkey	1/500 (ICC); 1/1000 (IHC)	Molecular Probes	A31571
rabbit IgG	Alexa 647	donkey	1/500 (ICC); 1/1000 (IHC)	Molecular Probes	A31573
mouse IgG	Alexa 546	donkey	1/500 (ICC); 1/1000 (IHC)	Molecular Probes	A10036
rabbit IgG	Alexa 546	donkey	1/500 (ICC); 1/1000 (IHC)	Molecular Probes	A10040

### **3.2.6 Buffers**

#### 10x Phosphate buffered saline (PBS)

140 mM NaCl

8 mM Na<sub>2</sub>HPO<sub>4</sub> (x2H<sub>2</sub>O)

1.5 mM NaH<sub>2</sub>PO<sub>4</sub> KCl

3 mM KCl

#### 8% paraformaldehyde (PFA STOCK)

80g paraformaldehyde in 1L 1x PBS

#### Antigen retrieval buffer pH 6

10 mM trisodium citrate dehydrate

#### Normal Donkey Serum Blocking solution or blocking buffer

5% (v/v) NDS in 0.01 M PBS (pH ~ 7.4) and 0.02% (v/v) NaN<sub>3</sub>

#### Mowiol (embedding medium)

2.4g MOWIOL 4-88 (Calbiochem)

6g glycerol

6ml ddH<sub>2</sub>O

12ml 2 M Tris pH 8.5

### 3.3 Laboratory animals

All animal procedures were performed in strict compliance with the European and National Laws for Laboratory Animal Use (Directive 2010/63/EU and Greek Law 56/2013), according to FELASA recommendations for euthanasia and the Guide for Care and Use of Laboratory Animals of the National Institutes of Health. All protocols were approved by the Institutional Animal Care and Use Committee of the Hellenic Pasteur Institute (Animal House Establishment Code: EL 25 BIO 013) and the License No 5677/ 25-09-2012 for experimentation was issued by the Greek authorities (Veterinary Department of Athens Prefecture). The preparation of the thesis was made in compliance with ARRIVE guidelines for reporting animal research.

For the 6-OHDA injections, male mice of the [NOD.CB17-Prkdc<sup>scid</sup>/NCrHsd](#) strain were used ([www.envigo.com](http://www.envigo.com)). This strain bears an autosomal recessive, single nucleotide polymorphism with *Prkdc* gene on chromosome 16. This mutations leads to severe combined immunodeficiency affecting T- and B-lymphocyte development accompanied by reduced number and function of the Natural Killer (NK) cell, macrophage and granulocyte populations.

For the isolation of mouse astrocytes, neonatal P0-P1 mice of the C57BL/6J01aHsd strain were used ([www.envigo.com](http://www.envigo.com)).

## 4. METHODS

### 4.1 Human iPSC culture and maintenance.

The PD patient-derived p.A53T-iPSC and healthy donor control lines used in this study were generated and characterized as previously described (Kouroupi et al, 2017).

#### 4.1.1 Human iPSC culture and passaging.

iPSCs were maintained in culture either using feeders or in feeder-free conditions. Regarding feeders, irradiated mouse embryonic fibroblasts (MEFs) were used, which are ideal for supporting healthy undifferentiated human iPSCs. One to three days prior to iPSC passaging or thawing, MEFs were seeded on gelatin-treated 6-well plates at densities ranging from  $2 \times 10^4$ – $5.3 \times 10^4$  cells/cm<sup>2</sup> according to manufacturer's instructions ([www.thermofisher.com](http://www.thermofisher.com)), in MEF medium. The day of the passaging, MEF medium was removed and each well was washed one time with KO-DMEM, before the iPSCs were plated on it. When FGF2 was added, the iPSC medium was used within 5 days.

Regarding feeder-free conditions, matrigel as a surface coating matrix was used. The day of the passaging, matrigel aliquot stored at -20°C was allowed to thaw on ice. Upon thawing, matrigel was added to DMEM medium at 1:200 dilution and the diluted one was seeded immediately on 6-well plates. The plates were then incubated at room temperature for one hour and after gently washes with KO-DMEM, were ready for the plating of the iPSCs. For feeder-free conditions, mTeSR™-E8™ Medium was used. This medium were prepared as indicated ([www.stemcell.com](http://www.stemcell.com)) and stored in 50ml aliquots at -20°C for up to 6 months. The medium in use was stored in 4°C for up to 2 weeks.

iPSCs were passaged whenever full confluent colonies were produced (usually every 5-7 days), while media were changed every day. iPSC colonies were usually passaged using the enzyme-free passaging reagent ReLeSR™, which does not require manual selection of differentiated areas or scraping to remove cell aggregates. After washing the cells once with PBS, 1ml/well of ReLeSR was added and 1 minute later the ReLeSR was removed so that colonies are exposed to a thin film of liquid for additional 5 minutes. Next, 1 ml/well of medium was added and holding the plate with one hand and using

the other hand to firmly tap the side of the plate, the cells were detached from it. The detached cell aggregates were transferred in the new plate containing medium. The plate was then placed in the incubator and was moved in several quick, short, back-and-forth and side-to-side motions to evenly distribute the cell aggregates. The plating density was adjusted each time to maintain the culture at the desired confluence. When the colonies were full confluent with very few spontaneous differentiation in the culture, they were passaged using collagenase IV. More specifically, iPSC colonies were incubated with the enzyme for 10min at 37°C, which was then removed, the cells were gently scraped using a cell scraper, were centrifuged for 5 min at 900 x g and then replated either on feeders or without feeders. After plating the cells, the plates were gently rocked side to side, and back and forth to spread the cells evenly across the well.

#### **4.1.2 Thawing iPSCs.**

Cells were thawed rapidly by placing the cryovial in a water bath set to maintain 37°C. The cryovial were swirled gently to ensure rapid thaw. Upon thawing, the cells then transferred from the cryovial into a 15 mL centrifuge tube. The cryovial was rinsed once with 1 mL of appropriate medium. The cells were centrifuged at 200 x g for 5 minutes. In parallel, the plates were washed with KO-DMEM and 1ml/well of medium was added. The supernatant was discarded and cells were gently resuspended in the appropriate medium volume. After plating the cells, the plates were gently rocked side to side, and back and forth to spread the cells evenly across the well.

#### **4.1.3 Freezing iPSCs.**

The optimal time for harvest is normally when cells are approximately 70-80% confluent. After removing the medium, cells were incubated with collagenase IV, as described above. 1 ml/ well of cryoprotectant (Synth-a-Freeze) was used per cryovial. The cryovial was placed immediately into a pre-chilled freezing container into a -80°C freezer. The next day, the cryovial was transferred to liquid hydrogen container.

#### 4.1.4 Detection of the G209A (A53T) mutation in patient-derived genomic DNA

The primers used are [82]:

Syna3 forward: 5'-GCTAATCAGCAATTTAAGGCTAG-3'

Syna13 reverse: 5'-GATATGTTCTTAGATGCTCAG-3'

(Primer stock 100 $\mu$ M, Working stock 10 $\mu$ M at -20°C)

Reaction	DNA template 200 ng/ $\mu$ l	1
	10x buffer	2
	5x Q Sol	4
	Primer 3 (10 $\mu$ M)	4
	Primer 13 (10 $\mu$ M)	4
	dNTPs (10 mM)	0.4
	Taq polymerase	0.1
	ddH <sub>2</sub> O	4.5
	Total volume	20 $\mu$ l

PCR Cycling Conditions:

- 1) Denaturation 94°C for 4 min
- 2) Denaturation 94°C for 30 sec
- 3) Annealing 50°C for 30 sec
- 4) Elongation 72°C for 1 min
- 5) Go to step 2, 34 times
- 6) 72°C for 5 min

Digestion with Tsp45I enzyme and incubation in 65°C for 5 h was followed:

DNA (PCR product)	20
NEB1	3
BSA	0.3
Tsp45I	1.3
ddH <sub>2</sub> O	5.4
Total volume	30 $\mu$ l

The digestion product was loaded in 3 % agarose gel, using 12  $\mu$ l DNA ladder (Mass Ruler L).

#### 4.2 Dopaminergic differentiation of human iPSCs.

For DAergic differentiation a floor-plate induction protocol was applied [379] with minor modifications. Immediately preceding differentiation, hiPSC

colonies were dissociated into a single cell suspension by incubation with accutase for 20min. The dissociated cells were centrifuged at 500 x g for 5min and resuspended in KO DMEM and their number was determined using a Neubauer counting chamber.

For differentiation, hiPSCs were plated (40,000 cells per cm<sup>2</sup>) on matrigel in DMEM/F12 medium containing KSR, Glutamax and  $\beta$ -mercaptoethanol. Floor-plate induction was performed by addition of 100 nM LDN193189, 10  $\mu$ M SB431542, 100 ng/ml SHH C24II, 2  $\mu$ M purmorphamine, 100 ng/ml FGF8 and 3  $\mu$ M CHIR99021 as summarized in Fig2.1 (differentiation medium). On day 5 of differentiation (5 days in vitro, DIV), KSR medium was gradually changed to N2 medium (25%, 50%, 75%). On 11 DIV, the medium was changed to Neurobasal/B27 50x/ Glutamax 100x supplemented with 100 ng/ml BDNF, ng/ml GDNF, 1 ng/ml TGF $\beta$ 3, 200  $\mu$ M ascorbic acid, 0.5 mM dibutyryl cAMP, and 10 mM DAPT for 9 days (maturation medium). At 20 DIV, cells were dissociated using accutase and replated at high density (300,000 cells per cm<sup>2</sup>) on dishes pre-coated with polyethylenimine (PLE; 15 mg/ml)/ laminin (1 mg/ml)/ fibronectin (2 mg/ml) in differentiation medium until the desired maturation stage. For the coating, the plates were incubated with PLE for 1h at 37°C, washed three times with sterile ddH<sub>2</sub>O, and incubation with laminin and fibronectin for 2h at 37°C followed. The next day, the plates were washed twice with sterile PBS right before the cell plating.

#### **4.3 Magnetically activated cell sorting (MACS) of PSA-NCAM-positive DAergic cells.**

For enrichment in PSA-NCAM-positive immature neurons, human iPSC-derived DAergic cells at 28 DIV were incubated with 10mM Y-27632 (ROCK inhibitor) for 1h to prevent cell death. MACS was performed according to the manufacturer's instructions ([www.miltenyibiotec.com](http://www.miltenyibiotec.com)). Accutase-dissociated cells were treated with 1% BSA followed by incubation with anti-PSA-NCAM magnetic Microbeads for 15 min at 4°C. After extensive washing, the cell suspension was loaded on the separation column (MS column) attached to a magnetic stand. Labeled cells were retained and after removal of the column from the magnetic separator, they were eluted with differentiation medium, counted and replated. After two days (30 DIV) cells were either analyzed by

immunofluorescence and RT-qPCR or were dissociated to single cell suspension for transplantation. Some cultures were maintained in differentiation medium for longer periods of time and were analyzed by immunofluorescence, electrophysiology and calcium imaging at the indicated time points. Cultures grown for more than 50 DIV were replated on a mouse astrocyte feeder layer.

#### **4.4 Primary culture of mouse astrocytes.**

Astrocytes were purified from neonatal P0-P1 mouse cortices and plated in DMEM/10% FBS in poly-D-lysine (PDL)-coated tissue culture flasks as previously described [472]. When confluent, the flasks with adherent cells were shaken in an orbital shaker at 120 rpm, over 20 h at 37°C to remove microglia and oligodendrocyte progenitor cells, resulting in approximately 95% astrocyte purity as determined by GFAP immunostaining. Astrocytes were then detached by incubation with trypsin/EDTA, re-plated on PLO/laminin-coated coverslips and allowed to reach confluence for about one week. This astrocytic feeder layer was used for co-culture with human iPSC-derived neurons.

#### **4.5 RNA isolation.**

Total RNA was extracted from cell pellets using the TRI Reagent. The following steps were followed:

1. Add 1 ml of TRIzol to the cell pellet and transfer the cell suspension in a 2 ml tube.
2. Lyse cells by repetitive pipetting (pipette up and down 4-5 times using insulin syringe).
3. Incubate the samples at RT for 5 min to ensure complete homogenization.
4. Add 0.2 ml of chloroform to each tube and shake vigorously by hand for 15 sec to mix well.
5. Incubate the samples at RT for 2-3 min.
6. Centrifuge samples for 15 min at 12,000 x g at 4°C.
7. Transfer the upper aqueous/clear phase (~500-600 µl) to a new 1.5 ml tube. Be careful not to get any of the intermediate or the lower pink phase!
8. Add 0.5 ml of isopropyl alcohol to precipitate RNA and mix.
9. Incubate the samples at RT for 10 min.
10. Centrifuge at 12,000 x g for 10 minutes at 4°C.

11. Discard the supernatant (reverse the tube).
12. Wash pellet with 1 ml 75% ethanol.
13. Mix sample by vortexing (gently).
14. Centrifuge at 7500 x g for 5 min at 4oC.
15. Remove supernatant.
16. Air dry the pellet for 5-10 minutes. Do not completely dry out the pellet.
17. Dissolve pellet in 30 to 60 µl (50 µl) RNase free water. Do not vortex!
18. Incubate the samples at RT (or 55-60oC) for 10 min.
19. RNA can be frozen (-80oC). Run on a gel to test the RNA quality. Measure the concentration of RNA in each sample (260/280 ratio should be ~1.8-2.2).

#### **4.6 RNA cleaning cDNA Synthesis.**

RNA cleaning was performed using the columns of Clean and Concentrator kit. For the digestion with DNase I, for every µg RNA, 1 µl DNAase I was added, plus 10x buffer and ddH<sub>2</sub>O and incubation at 37°C for 30min was followed.

1 µg of total RNA was used for first strand cDNA synthesis with the ImProm-II Reverse Transcription System (Promega), following the steps:

1. Add 2 volumes RNA Binding Buffer to each sample 1 and mix.
2. Add an equal volume of ethanol (95-100%) and mix.
3. Transfer the sample to the Zymo-SpinII C Column in a Collection Tube and centrifuge for 30seconds. Discard the flow- through.
4. Add 400 µl RNA Prep Buffer to the column and centrifuge for 30 seconds. Discard the flow-through.
5. Add 700 µl RNA Wash Buffer to the column and centrifuge for 30 seconds. Discard the flow-through.
6. Add 400 µl RNA Wash Buffer to the column and centrifuge for 2 minutes to ensure complete removal of the wash buffer. Transfer the column carefully into an RNase-free tube.
7. Add 50 µl DNase/ RNase- Free Water directly to the column matrix and centrifuge for 30 seconds.

1 µg of total RNA was used for first strand cDNA synthesis with the ImProm-II Reverse Transcription System (Promega) according to the following protocol: Target RNA and primer combination and denaturation (total 5 µl/ RT reaction)  
On ice:

- RNA up to 1  $\mu\text{g}$  (1-1.5  $\mu\text{g}$ )
- Random Hexamers 2  $\mu\text{l}$  of 0.5  $\mu\text{M}$  (stock 50  $\mu\text{M}$ ; working dilution 1/100, 0.5  $\mu\text{M}$ )
- Mix well (spin)
- Incubate at 70°C for 5 min (heat block)
- Incubate on ice for 5min
- Spin
- Add 15  $\mu\text{l}$  RT mix

#### Reverse Transcription

*RT mix:*

<i>Nuclease-free water</i>	<i>until 15 <math>\mu\text{l}</math></i>
<i>ImProm-II 5x reaction buffer</i>	<i>4 <math>\mu\text{l}</math></i>
<i>MgCl<sub>2</sub></i>	<i>1.2 <math>\mu\text{l}</math></i>
<i>dNTPs (stock 25 <math>\mu\text{M}</math>)</i>	<i>1 <math>\mu\text{l}</math></i>
<i>RNasin</i>	<i>0.5 <math>\mu\text{l}</math></i>
<i>ImProm-II Reverse Transcriptase</i>	<i>1 <math>\mu\text{l}</math></i>

#### **4.7 Real time quantitative PCR.**

Quantitative PCR analyses were carried out in a Light Cycler 96 (Roche) Real time PCR detection system using KAPA SYBR FAST qPCR Master Mix (KapaBiosystems). The primers used are listed in Table 1. The mix of primers, the enzyme and the 1/10 diluted cDNA.

#### **4.8 Immunofluorescence.**

Cells were fixed with 4% paraformaldehyde (Sigma- Aldrich) for 20 min at room temperature. Samples were blocked with 0.1% Triton X- 100 (Sigma-Aldrich) and 5% donkey serum in PBS for 30 min and were subsequently incubated with primary antibodies (listed in Table 2) at 4°C overnight, followed by incubation with appropriate secondary antibodies (Molecular Probes, Thermo Fisher Scientific) conjugated to AlexaFluor 488 (green), 546 (red) or 647 (blue), for 2 h at room temperature. Protein aggregates were detected with the PROTEOSTAT Aggresome Detection Kit (Enzo) followed by immunolabeling for either DCX or TH. Coverslips were mounted with ProLong Gold antifade reagent containing DAPI (Cell Signaling).

#### **4.9 Electrophysiology.**

Patch-clamp recordings were performed as previously described [15]. Whole-cell voltage clamp recordings were made from hiPSC-derived neurons at 55-60 DIV. The pharmacological inhibitors tetrodotoxin (TTX; final concentration 1  $\mu$ M) and tetraethylammonium (TEA; 10 mM) were applied to block voltage-gated sodium and potassium channels, respectively. Data were acquired at room temperature (22-24°C) using an EPC9 HEKA amplifier and an ITC-16 acquisition system with a patchmaster software (HEKA). Data analysis was performed using OriginPro 8 (OriginLab Software).

#### **4.10 Calcium Imaging.**

At 55-60 DIV hiPSC-derived neurons were incubated with culture medium containing 3  $\mu$ M Fluo-3 (Molecular Probes) for 30 min at 37°C. After washing with extracellular solution (mM: 140 NaCl, 2.8 KCl, 2 CaCl<sub>2</sub>, 4 MgCl<sub>2</sub>, 20 HEPES, 10 glucose, pH 7.4- 7.5), cells were placed into fresh extracellular solution and equilibrated in the microscope chamber at 5% CO<sub>2</sub>, 70–75% humidity, 37 °C for 30 min. Cells were excited at 488 nm with a fluorescein isothiocyanate (FITC) filter; the fluorescence signals were recorded at 10 frames/ sec using a fluorescence Olympus Time lapse IX81 Cell-R microscope. From each field, 20–30 cells were selected for analysis of Ca<sup>2+</sup> responses using ImageJ software. The amplitude of fluorescence signals for each region of interest (ROI) was presented as relative fluorescence changes (DF/F) after background subtraction. The Ca<sup>2+</sup> transient frequency and amplitude were counted manually over a 5-min period.

#### **4.11 6-OHDA lesioned mice.**

Male NOD.CB17-Prkdcscid/NCrHsd mice 9- 10 weeks old were anesthetized using gaseous isoflurane (2–5% in 2:1 O<sub>2</sub>:N<sub>2</sub>) and received 2 X 1  $\mu$ l unilateral stereotactic injections of 4  $\mu$ g/  $\mu$ l 6-hydroxydopamine (6-OHDA) dissolved in physiological saline containing 0.02% ascorbic acid. The mouse's head was shaved using an electric razor, and the mouse was placed in the stereotactic frame. His head was stabilized and the skin was cleaned with a betadine solution. A midline incision was made using a scalpel and infusions were delivered over 1 min via a 30 gauge stainless steel cannula. Lesions were

made in the right mid-striatum (AP= +0.5 mm to bregma, ML= +1.8 mm, DV= -3.0 and -3.5 mm). The cannula was left in place for a further 2 min, before being slowly removed. The wound was cleaned and closed with sutures. Each animal was left to recover in a heating pad and was placed back in its cage afterwards. Animals were monitored daily and for the following 10 days received subcutaneously 0.5 ml of 0.9% saline/glucose solution to prevent dehydration. Behavioral tests were performed 14 days after the lesions, when the animals had fully recovered.

#### **4.12 Behavioral analysis.**

Rotational asymmetry was analyzed at 2, 7, 11 and 15 weeks after 6-OHDA lesioning, using a spontaneous activity test (drug-free asymmetry) and after intraperitoneal (i.p) injection of amphetamine (4mg/ kg; drug-induced asymmetry). *Spontaneous activity test.* Limb-use asymmetry was estimated as follows. A transparent cylinder was placed on a piece of transparent plastic to visualize stepping movement from underneath and overall movement from above. The right hindlimb was marked in order to distinguish left from right steps. Sessions were videotaped for 3 min and scored offline to evaluate the number of steps taken by each limb [ipsilateral and contralateral (the impaired paw), forelimb and hindlimb). The ratio of ipsilateral to contralateral steps was calculated for the forelimbs and hindlimbs [287]. *Amphetamine test.* Amphetamine-induced ipsilateral rotations increase in response to a unilateral lesion. Mice were injected i.p. with 10 mg/kg of d-amphetamine sulphate and were left for 10 min to acclimatize in a plastic box. Rotational activity was measured over a 30 min period [473] and data were expressed as net ipsilateral minus contralateral turns. Mice with >5 net ipsilateral turns were used for transplantation and were analyzed by immunocytochemistry after a further 12 weeks (mice that received control-derived grafts: n= 5; mice that received PD-derived grafts: n= 3).

#### **4.13 Intra-striatal transplantation.**

Three weeks after 6-OHDA injection PSA-NCAM-enriched DAergic cells from control or PD iPSC lines were stereotactically transplanted in mice. Cells were dissociated with accutase and re-suspended in cold HBSS at a density of

100,000 cells/  $\mu$ l. Mice received 2 X 1  $\mu$ l cells at the same coordinates that the lesions were made at a rate of 0.5  $\mu$ l/ min.

#### **4.14 Euthanasia and Immunohistochemistry.**

Animals were perfused intracardially with 0.9% saline solution and 4% paraformaldehyde (pH 7.4). Perfused brains were either cryopreserved in 30% sucrose, frozen in OCT compound for obtaining cryostat 20 $\mu$ m-sections [474], or were embedded in 4% agarose and sectioned (40 $\mu$ m) on a vibrating microtome (Leica), serially collected. Slices were blocked with 0.1% Triton X-100 (Sigma-Aldrich), 2mg/ml BSA and 1.5% donkey serum in PBS for 1-3h and were subsequently incubated with primary antibodies (Table 2) at 4°C either overnight for cryostat sections or for 3 nights for vibratome sections, followed by incubation with appropriate secondary antibodies (Molecular Probes, Thermo Fisher Scientific) conjugated to AlexaFluor 488 (green), 546 (red) or 647 (blue). Cryostat sections were in parallel incubated with Hoechst 33342 for DNA fluorescent staining, while the vibratome sections were incubated for 30min before mounting them. Cryostat sections were mounted with Mowiol and vibratome sections were mounted on microscope slides with ProLong Gold antifade reagent containing DAPI (Cell Signaling).

#### **4.15 Image acquisition and image analysis.**

Digital images, both after immunocytochemistry and immunohistochemistry, were acquired using a Leica TCSSP8 confocal microscope (LEICA Microsystems) and analyzed using ImageJ software (NIH).

For quantification of the graft area as well as the percentage of cells positive for the different markers, 2-5 slices from each animal were analyzed. Quantification of graft-derived human synaptophysin (HSYP) contacts on DARPP32-positive striatal medium spiny neurons of the host was performed as follows: 5 digital images (63x lens, zoomx3) were acquired at the graft-host tissue interphase in 1-2 sections per animal. Within every image, 4 representative regions of interest were selected and the number of contacts between HSYP and DARPP32 was counted.

#### **4.16 Statistical analysis.**

All *in vitro* experiments were replicated at least three times and data from parallel control and PD cultures were acquired. The *in vivo* data for the transplantations of 6-OHDA lesioned mice were obtained from two independent experiments. All data represent mean  $\pm$  standard error of the mean (SEM). Statistical analysis was performed in Microsoft Office Excel 2013. In each case, comparisons between the two groups (control and PD) were performed using the Student's t-test. Probability values less than 0.05 ( $P < 0.05$ ) were considered significant.

## 5. RESULTS

The purpose of this study is to investigate the phenotype of p.A53T-patient-derived neurons *in vivo* vis-à-vis control neurons derived from a healthy individual after transplantation in a 6-OHDA lesion mouse model developed in the immunosuppressed NOD/SCID strain. Towards this goal, one iPSC line from one male PD patient carrying the p.A53T mutation (PD) and one iPSC line from an age-matched healthy individual (control), which have been previously generated [420] were used. A DAergic differentiation protocol and a MACS sorting approach were applied to generate iPSC-derived PSA-NCAM enriched DAergic immature neurons. After their *in vitro* characterization, the main goal of the study was to explore the fate of PD immature neurons after *in vivo* transplantation and to compare them with control cells, focusing on their survival and differentiation capacity *in vivo*. Moreover, after having observed neurodegenerative phenotypes *in vitro*, we wanted to address whether these neurons maintain their phenotypes *in vivo*. For this reason, the 6-OHDA-induced PD mouse model was reproduced and characterized in our laboratory by behavioral and immunohistochemical analyses of the mouse brains up to 12 weeks after transplantation.

### 5.1 iPSC characterization from healthy and PD patients

At the beginning of the study, we analyzed the iPSC clones derived from one healthy donor and two PD patients that would further be used for differentiation. These iPSC lines were generated by Dr Koupouri [420] and showed ESC-like morphology expressing pluripotency markers [354], as shown in Fig. 11A. More specifically, NANOG along with SOX2 are transcription factors critically involved in self-renewal of undifferentiated ESCs/ iPSCs [475, 476]. TRA-1-60 (Podocalyxin) is also a cell surface antigen that is expressed in PSCs [477]. Moreover, the cell surface antigens SSEA3 (Stage-specific embryonic antigen 3) and SSEA4 are glycosphingolipids that are used as pluripotency markers [354].

A prime characteristic of the ESCs/ iPSCs derived from the mammalian inner cell mass is the ability to undergo lineage-specific differentiation into the three germ layers: endoderm, mesoderm and ectoderm which appear during gastrulation in the developing embryo [478]. The differentiation capacity of the iPSC lines was confirmed by the *in vitro* germ-layer differentiation assay of embryoid body (EB) formation. EBs were allowed to form from iPSCs in non-adherent plates in iPSC medium without FGF2 and to differentiate spontaneously. After 8 days, iPSCs formed ball-shaped structures (EBs) which were plated and maintained on gelatin coated dishes for another 12 days. Cells within EBs showed different morphologies and after undergoing spontaneous differentiation for 20 days *in vitro* (DIV), they consisted of endodermal AFP (a-fetoprotein, endodermal marker) positive cells, ectodermal Nestin positive or MAP2 (microtubule associated protein 2) positive cells, and mesodermal SMA ( $\alpha$ -smooth muscle actin, mesodermal marker) positive cells (Fig. 11B).

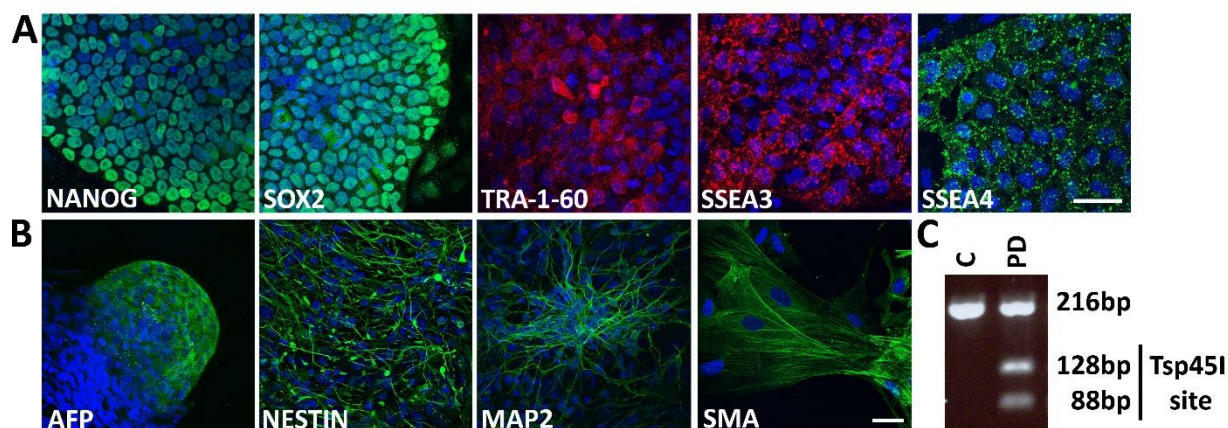


**Figure 11: Characterization of iPSCs from one healthy donor and one PD patient.** (A) Representative images of a PD-iPSC clone expressing pluripotency markers: Nanog, Sox2 (green), TRA-1-60, SSEA3 (red), and SSEA4 (green). Cell nuclei counterstained with TO-PRO-3 (blue). Scale bar, 40  $\mu$ m. (B) *In vitro* spontaneous differentiation (embryoid body formation) of iPSCs to cells representative of each germ layer: a-fetoprotein (AFP, endoderm), NESTIN and MAP2 (ectoderm) and a-smooth muscle actin (SMA, mesoderm); Scale bar: 40  $\mu$ m. (C) Genomic DNA analysis by PCR demonstrating the presence of the heterozygous G209A SNCA mutation in PD-iPSCs but not in control cells.

Their capability to form teratomas consisting of all three germ layer cells *in vivo* as well as the expression of selected pluripotent markers by qRT-PCR (including NANOG and SOX2) have been published [420]. Additionally, their genome-wide pluripotency signature has been confirmed by RNAseq [420].

Finally, the G209A SNCA mutation was detected in PD-derived iPSCs but not in control iPSCs, using PCR and the restriction enzyme Tsp45I (Fig. 11C). This specific mutation results in a novel Tsp45I restriction site which cuts the normal 216 base-pair (bp) PCR product into fragments of 128 and 88 bp and is used to screen for G209A substitution [82].

## 5.2 DAergic differentiation and characterization of iPSC-derived neurons

Several iPSC differentiation protocols have been developed to improve DAergic neuron specification and their *in vivo* performance, particularly in terms of avoiding cellular overgrowth [378, 379, 479-481]. In this study, we applied a floor plate induction protocol [379] to differentiate a previously generated p.A53T-iPSC (PD) line by comparison to a healthy donor (control) line [420] towards the dopaminergic lineage (Fig. 12). The protocol relies on the inhibition of BMP (Bone Morphogenic Protein) and TGF $\beta$  (Transforming Growth Factor beta) signaling pathways. Towards this, a BMP inhibitor (LDN193189) and a Lefty/ Activin/ TGF $\beta$  pathways inhibitor (SB431542) have been used.

Most importantly, the protocol is based on previous studies using rat and chick neural plate explants demonstrating that the floor plate-derived signal sonic hedgehog (SHH) and fibroblast growth factor 8 (FGF8) from the mid-hindbrain boundary are required for the induction of DAergic neurons during embryogenesis [482]. Cells were plated at a high density the first day of differentiation, and the activation of SHH signaling was obtained using the recombinant SHH24II, and purmophamine which is a small molecule agonist. CHIR99021 from 3-13 DIV, which is a potent GSK3 $\beta$  inhibitor which strongly activates WNT signaling was also used. From 11 DIV, cells were maintained in differentiation medium containing Brain-derived neurotrophic factor (BDNF), Glial cell-derived neurotrophic factor (GDNF), ascorbic acid (AA), cyclic adenosine monophosphate (cAMP). This protocol has been shown to lead to a more efficient induction of DAergic fate than the protocols used before for DAergic differentiation [376, 439]. Moreover, the generated immature neurons at around 25 DIV have been shown to engraft better after transplantation in the 6-OHDA mouse model [379, 480].

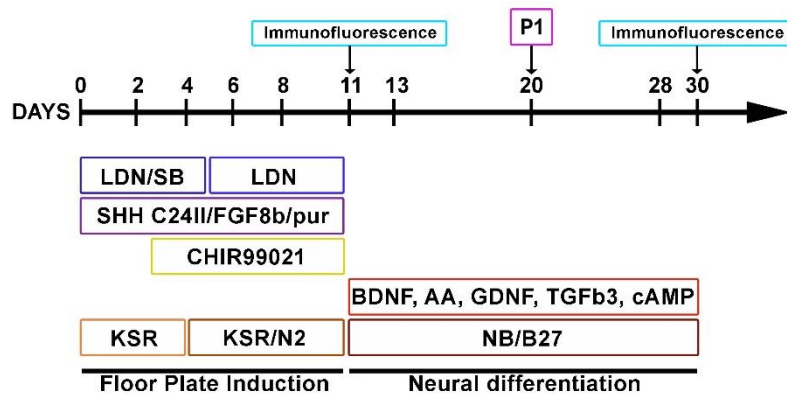


**Figure 12: Schematic drawing of the protocol used for neuronal differentiation of iPSCs and timeline of analysis.** Floor plated induction for 11 days, was followed by neuronal differentiation. Immunocytochemistry was performed at 11 and 30 DIV. At 30 DIV, cells were dissociated and used for transplantation.

At the end of floor plate induction (11 DIV), LMX1A/ FOXA2-positive DAergic precursors were derived (Fig. 13A). LMX1A is a transcription factor which plays a role in the development of DAergic neurons during embryogenesis and FOXA2, is a transcription factor which regulates specification and differentiation of DAergic neurons. At this stage practically all cells were LMX1A-positive floor plate precursors and approximately half were also FOXA2-positive in agreement with a dopaminergic fate (Fig. 13B, C, percentage of FOXA2-positive cells: control  $44.01 \pm 5.67\%$ ,  $n= 3$ ; PD  $48.63 \pm 7.32\%$ ,  $n= 3$ ).

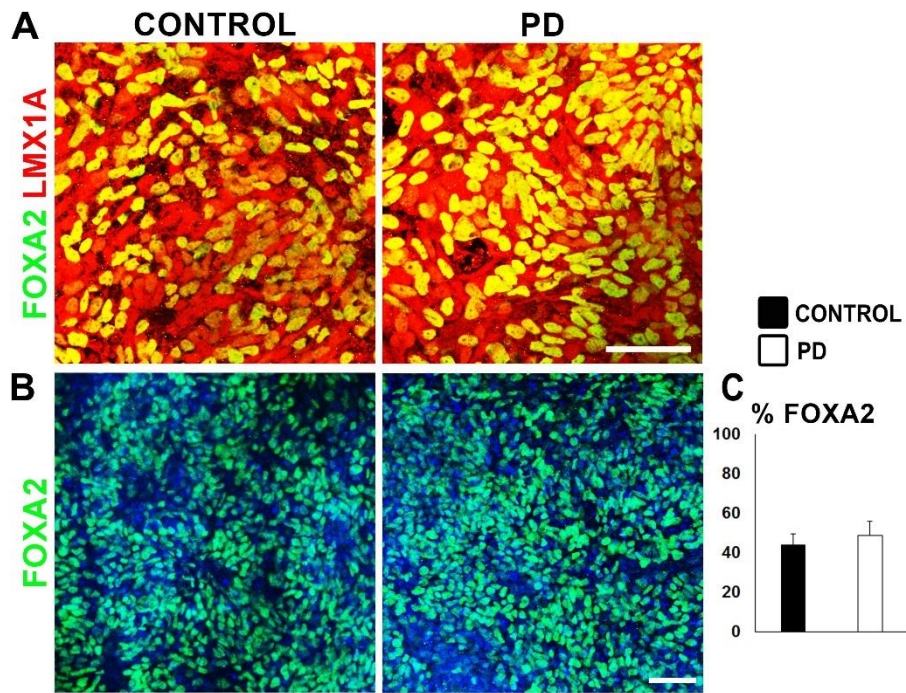


**Figure 13: Immunocytochemical analysis of iPSC-derived midbrain floor-plate precursors 11 DIV.** (A) Double immunofluorescence labeling of control and PD cells at 11 DIV for LMX1A (red) and FOXA2 (green). Scale bar, 50µm. (B) Immunofluorescence labeling for FOXA2 and (B) quantification in control and PD cells at 11 DIV. Nuclei are shown in blue (TOPRO3). Scale bar, 50µm.

At 30 DIV, cells were analyzed by immunocytochemistry for Nurr1 and TH in order to check their differentiation to the DAergic lineage (Fig. 14). Cells expressed Nurr1, which is an essential transcription factor for early differentiation of DAergic neurons [483] while few already expressed the DAergic neuronal marker TH (Fig. 14A; For Nurr1, control  $73.91 \pm 5.04$  %; PD  $70.58 \pm 17.49$  %;  $n=3$ ;  $P=0.863$ . For TH, control  $2.51 \pm 0.63$  %, PD  $1.36 \pm 0.24$  %;  $n=3$ ;  $P=0.166$ ), confirming that they were still at an early stage of DAergic differentiation. They also expressed the immature neuronal markers polysialylated neural cell adhesion molecule (PSA-NCAM) and doublecortin (DCX), with around one third of the cells to express both of them (Fig. 14B, DCX, control  $34.72 \pm 2.58$ %; PD  $33.34 \pm 15.8$ %;  $n=3$ ; Fig. 2.2B). PSA-NCAM is a marker of immature migrating neurons [484, 485]. DCX is a microtubule-associated phosphoprotein required for neuronal migration and differentiation, and it is expressed in migrating neurons throughout the central nervous system during development [486, 487]. For this reason, it has been extensively used as a marker for newly born (immature) neurons and migrating neurons. Some

of cells also express  $\alpha$ Syn (Fig. 2.3C), as well as the neuronal lineage marker  $\beta$ III-tubulin (TUJ1) (Fig.14C; control  $40.13 \pm 4.17\%$ ; PD  $31.23 \pm 7.78\%$ ,  $n= 3$ ;  $P= 0.41$ ).

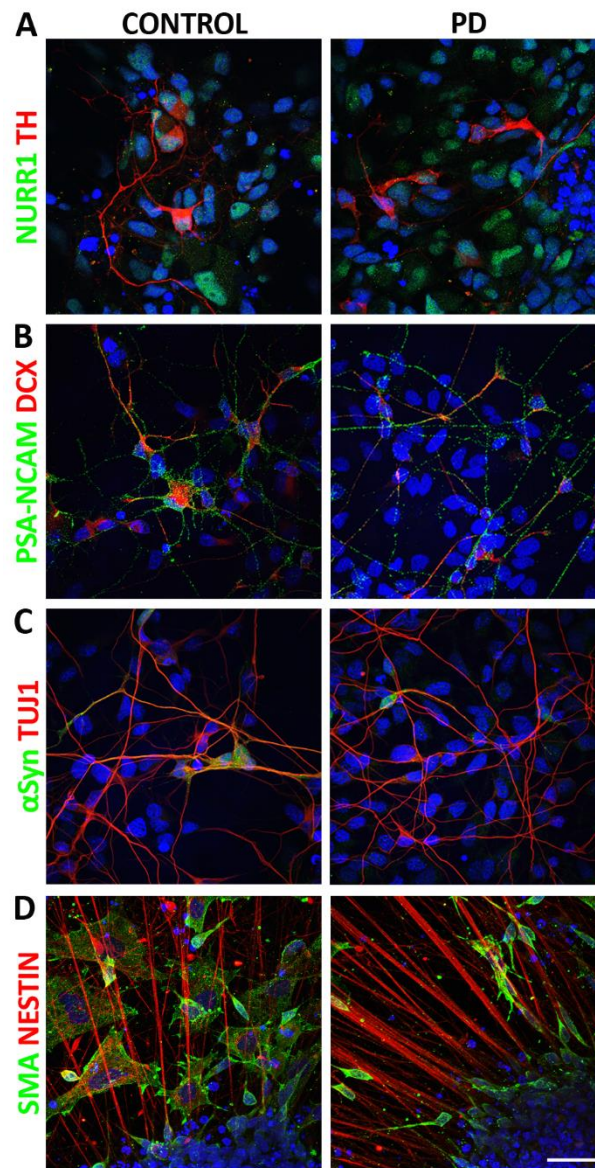


**Figure 14: Immunocytochemical analysis of iPSC-DAergic neurons 30 DIV.** Double immunofluorescence of control and PD cells at 30 DIV for: (A) NURR1 (green) and TH (red); (B) PSA-NCAM (green) and doublecortin (red, DCX); (C)  $\alpha$ Syn (green) and  $\beta$ III-tubulin (TUJ1, red); (D) SMA (green) and Nestin (red). Cell nuclei are in blue; Scale bar:  $40\mu\text{m}$ .

However, at this differentiation stage, a substantial number of Nestin positive neural precursor cells (around 40%) were observed, along with a smaller number of SMA positive cells in the culture (Fig. 14D), which probably corresponded to neural crest cells, as has been recently shown [488]. A large number of cells in culture were also positive for the proliferation nuclear marker

Ki-67 (data not shown, control  $40.94 \pm 7.5 \%$ ; PD  $27.07 \pm 1.98 \%$ ,  $n=3$ ;  $P=0.216$ ), raising concerns about their behavior *in vivo* regarding potential overgrowth activity. In parallel with our observations, several studies have demonstrated that PSC-derived cell populations were posing a risk for tumor formation after transplantation, since these cell populations contain a large number of proliferating non-neural cells [488-491]. Therefore, we checked the cells' proliferative capacity in a pilot study described below.

### **5.3 Establishment of the 6-OHDA- induced lesion in the medial forebrain bundle of immunodeficient mice and pilot cell transplantation**

To investigate the *in vivo* potential of human iPSC-derived DAergic cells at 30 DIV, we developed a parkinsonian mouse model in the NOD/SCID strain that supports xenograft survival [492]. Initially, we performed a unilateral stereotactic injection of 6-OHDA in the medial forebrain bundle (MFB) of 9-10 week old mice (coordinates, anterior posteriorly AP= -2.1; medio laterally ML= 1.1; dorso ventrally DV= -4.6 and -4.9). The MFB lesion has been extensively used for the study of PD, since a major component of it is the mesolimbic pathway, consisting of DAergic neurons that project from the ventral tegmental area to the nucleus accumbens. We chose the MFB lesion paradigm in order to introduce a severe lesion in mice which results in motor deficits. However, injections in MFB led to the death of almost 90% of the mice during the first two weeks after the lesion (injected animals  $n= 22$ ; survived  $n= 3$ ; survival rate 13.64%). Although extensive post-operative care were given to mice, including daily intraperitoneal injection of 5% glucose and access to wet pellets the first two weeks after the lesion, post-operative mortality is high in mice receiving a MFB lesion, as a result of aphagia and adipsia and a decline in general health. These mice also develop rotational asymmetry [493].

Nevertheless, we proceeded with pilot cell transplantation in the surviving mice using human iPSC-derived DAergic neurons (30 DIV) 3 weeks after 6-OHDA lesion in order to investigate graft survival *in vivo*. For this reason, we transplanted only control derived cells in these NOD/SCID mice. Immunohistochemical analysis followed 2 and 8 weeks post transplantation (wpt), confirming survival by immunofluorescence for the human-specific

cytoplasmic antigen (Fig. 15A). However, we observed rosette-rich neural overgrowth in the grafts. Further analysis showed that although many of the grafted cells were positive for the neuronal lineage marker TUJ1 (Fig. 15B), many also expressed the proliferating marker Ki-67 while many cells were also positive for the mitosis- specific marker phospho- histone 3 (PH3) (Fig. 15C, D), indicating a large proliferative capacity of the transplanted cells. These observations came in agreement with other transplantation studies pointing towards the necessity of employing sorting methods to eliminate non- neuronal and, in particular highly proliferating cells in the culture using fluorescence-activated cell sorting (FACS) or magnetic-activated cell sorting (MACS) [480, 490, 494, 495].

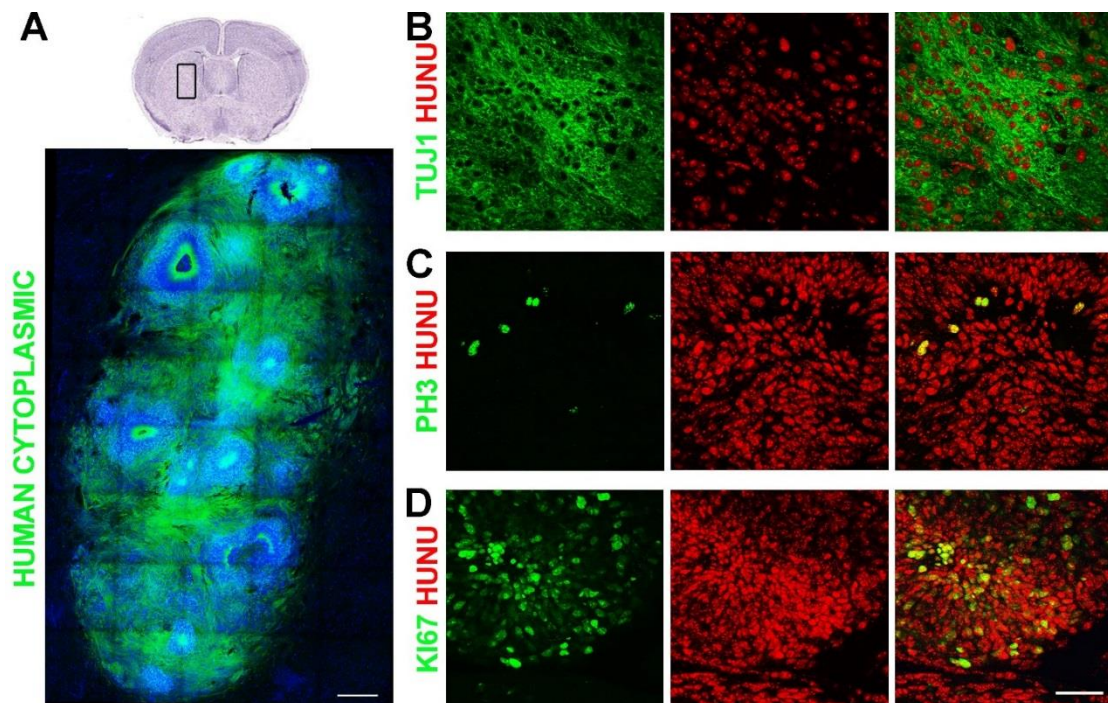


**Figure 15: In vivo engraftment of iPSC-derived control cells 8 wpt.** (A) Immunostaining for the human-specific cytoplasmic antigen (green) in control-derived grafts. Nuclei are shown in blue. Scale bar, 500 $\mu$ m. (B) Double immunostaining for TUJ1 (green) and HuNu (red). (C) Double immunostaining for PH3 (green) and HuNu (red). (D) Double immunostaining for Ki-67 (green) and HuNu (red). Scale bar, 40  $\mu$ m.

From the above pilot study, we concluded that it was necessary to include a cell sorting step before transplantation in order to enrich the iPSC-derived cultures in non-proliferating or minimally proliferating neuronal cells. Moreover, modifications should be made in our lesion model to ensure a higher survival rate of the lesioned animals.

## 5.4 Magnetic Cell Sorting and characterization of the iPSC-derived immature neurons

We reasoned that an enriched population of neuronal cells differentiated to the dopaminergic lineage, consisting of progenitors and early neurons with restricted proliferative capacity, would be appropriate for transplantation studies [466, 467, 480, 492, 494]. Therefore, we applied MACS isolation on the basis of PSA-NCAM immunoreactivity at 28 DIV (Fig. 16).

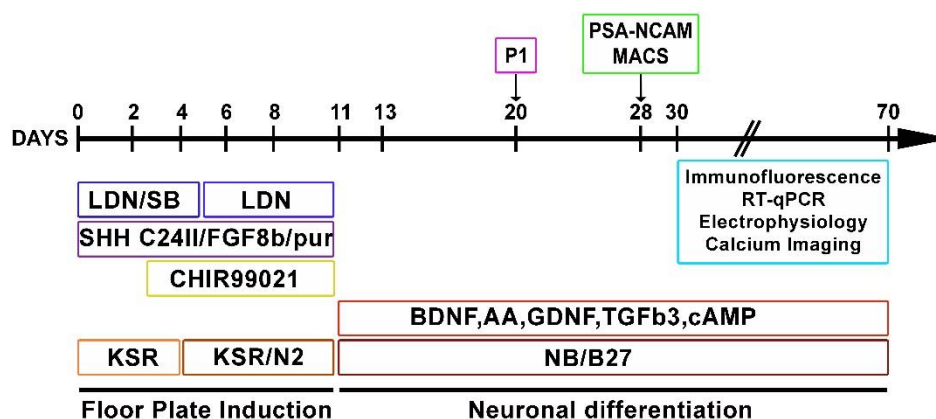


**Figure 16: Schematic drawing of the protocol used for neuronal differentiation of iPSCs and timeline of analysis.** Floor plated induction for 11 days, was followed by neuronal differentiation. At 28 DIV, MACS isolation was performed. At 30DIV, cells were either harvested for gene expression analysis, or cultured further for phenotypic characterization, electrophysiological studies and calcium imaging (up to 70 DIV). Cells from 50-70 DIV were maintained on mouse primary astrocytes.

Two days later, at 30 DIV, sorted cells were analyzed by immunofluorescence to confirm the expression of the immature neuronal markers PSA-NCAM and DCX (Fig. A). Quantification (Fig. 17B) revealed that 60-73% of the cells in the culture expressed PSA-NCAM and 53-65% expressed the marker DCX with no statistically significant differences between control and PD cells (for PSA-NCAM: control  $73.06 \pm 6.89\%$   $n=4$ ; PD  $60.88 \pm 10.26\%$   $n=5$ ;  $P=0.341$ . For DCX: control  $65.60 \pm 7.15\%$   $n=4$ ; PD  $53.57 \pm 12.06\%$   $n=5$ ;  $P=0.397$ ). A similar number of cells in the two types of culture expressed TUJ1 (control  $67.35 \pm 9.41\%$   $n=4$ ; PD  $63.29 \pm 14.19\%$   $n=5$ ;  $P=0.812$ ). The number of TH positive neurons was overall low (control  $10.85 \pm 0.97\%$   $n=3$ ; PD  $9.86 \pm 2.84\%$   $n=4$ ;  $P=0.724$ ), verifying that cells were at an immature differentiation state (Fig. 17C, D).

A significant proportion of Nestin positive cells were also present, more in PD cultures, but without statistical significance as compared to controls (control  $34.17 \pm 11.54\%$ ; PD  $62.36 \pm 14.14\%$ ;  $n= 3$ ;  $P= 0.197$ ) (Fig. 17E, F). Nestin is an intermediate filament protein that is used as a marker for neural stem/progenitor cells [496]. After sorting, proliferating Ki-67 positive cells were less than 10% in both cultures (control  $7.16 \pm 3.73\%$   $n= 4$ ; PD  $9.8 \pm 5.04\%$ ;  $n= 3$ ,  $P= 0.683$ ).

Apart from the immunocytochemical analysis, RT-qPCR analysis followed at 30 DIV to test for the mRNA expression of several DAergic lineage markers. RT-qPCR confirmed mRNA expression of the DAergic lineage markers FOXA2 (early DAergic progenitors), NURR1 (late DAergic progenitors) and TH (mature DAergic neurons) (Fig. 17G) whilst other neuronal markers, including MAP2 (neuron-specific marker), GAD67 (GABAergic neuron marker) and VGLUT1 (glutamatergic neuron marker) were also detected. Overall no marked differences were apparent between PD and control cultures at 30 DIV, either by immunofluorescence or RT-qPCR analysis.

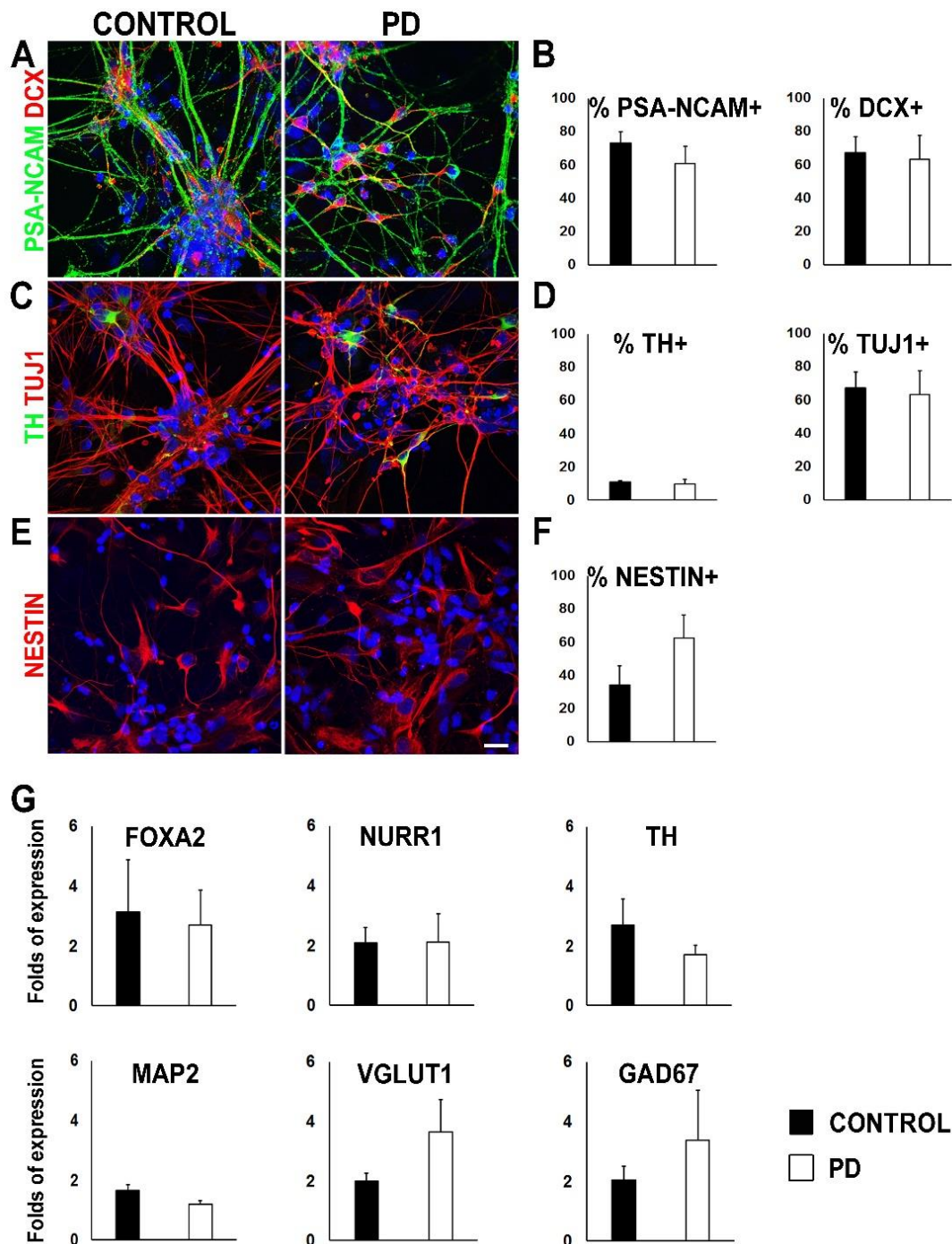


**Figure 17: Dopaminergic differentiation of iPSC-derived cells.** (A) Schematic representation of the differentiation protocol used and timeline of analysis, following MACS isolation at 28 DIV. (B, D) Double immunofluorescence of control and PD cells at 30 DIV for: (B) PSA-NCAM (green) and doublecortin (red, DCX); (D) TH (green) and  $\beta$ III-tubulin (TUJ1, red). Cell nuclei are in blue. (C, E) Quantification of positive cells for each marker in control versus PD cultures is shown as percentage of total nuclei. (F) Immunofluorescence for the neural progenitor marker Nestin (red) and (G) quantification of Nestin-positive cells as percentage of total nuclei. Data represent mean  $\pm$  SEM ( $n = 3-5$ ),  $P > 0.05$ . Scale bar, 10  $\mu$ m. (H) RT-qPCR analysis of mRNA expression at 30 DIV for the indicated neuronal and dopaminergic lineage markers. Data represent mean  $\pm$  SEM ( $n = 3$ ).

## 5.5 Characterization of long-term DAergic neuronal cultures

Previous work from our laboratory has revealed a number of disease-relevant phenotypes in PD neurons derived from the same iPSC line used in this study [420]. These include protein aggregation, compromised neuritic outgrowth, and contorted or fragmented axons with swollen varicosities containing  $\alpha$ Syn and Tau, along with disrupted synaptic connectivity and widespread transcriptional alterations in genes involved in synaptic signaling. As in this study we have been using a different differentiation protocol, before proceeding to *in vivo* transplantation we investigated the presence of similar phenotypes in the PD neurons that were maintained up to 70 DIV. Cells were analyzed between 45-70 DIV, where various degeneration signs became apparent.

### 5.5.1 Morphological alterations

Because the differentiation protocol we used in this study was different from that we previously reported in [420], before proceeding to *in vivo* transplantation we addressed the phenotype of PD cultures maintained for longer periods of time *in vitro*. When cells were analyzed between 45-70 DIV, degeneration signs became apparent. First we noted that DCX-positive cells, which constituted approximately one third of the total population in both cultures at 47 DIV, exhibited morphological differences between control and PD. PD DCX positive cells had significantly more primary neurites per cell (Fig. 18A, B; control  $2.42 \pm 0.04$  and PD  $3.38 \pm 0.16$ ,  $n=3$  per group; \*  $P=0.029$ ) and an increased number of secondary branches per cell (Fig. 18A; control  $0.52 \pm 0.09$  and PD  $1.14 \pm 0.28$ ,  $n=3$ ,  $P=0.179$ ). Moreover, intracellular protein aggregates (aggresomes) were detected in PD DCX-positive neurons at 70 DIV, as indicated with a fluorescence-based assay for detection of aggregated protein cargo [497] (Fig. 18C). Such protein aggregates were hardly observed in control cultures. Additionally mutant TH-positive cells, which formed a dense network at 70 DIV, displayed dystrophic neurites with swollen varicosities that quite often ended up in fragmented processes (Fig. 19A). These features, which were not observed in control TH-positive neurons, were accompanied by detection of intracellular protein aggregates in PD cells (Fig. 19B). Immunofluorescence

indicated that  $\alpha$ Syn was also upregulated in PD cultures (Fig. 20A, B). Thus our analysis revealed new phenotypes in PD neurons related to the morphology of DCX+ cells, and defective neuropathological characteristics similar to those previously reported, including increased  $\alpha$ Syn immunoreactivity, presence of protein aggregates and dystrophic neurites [420].

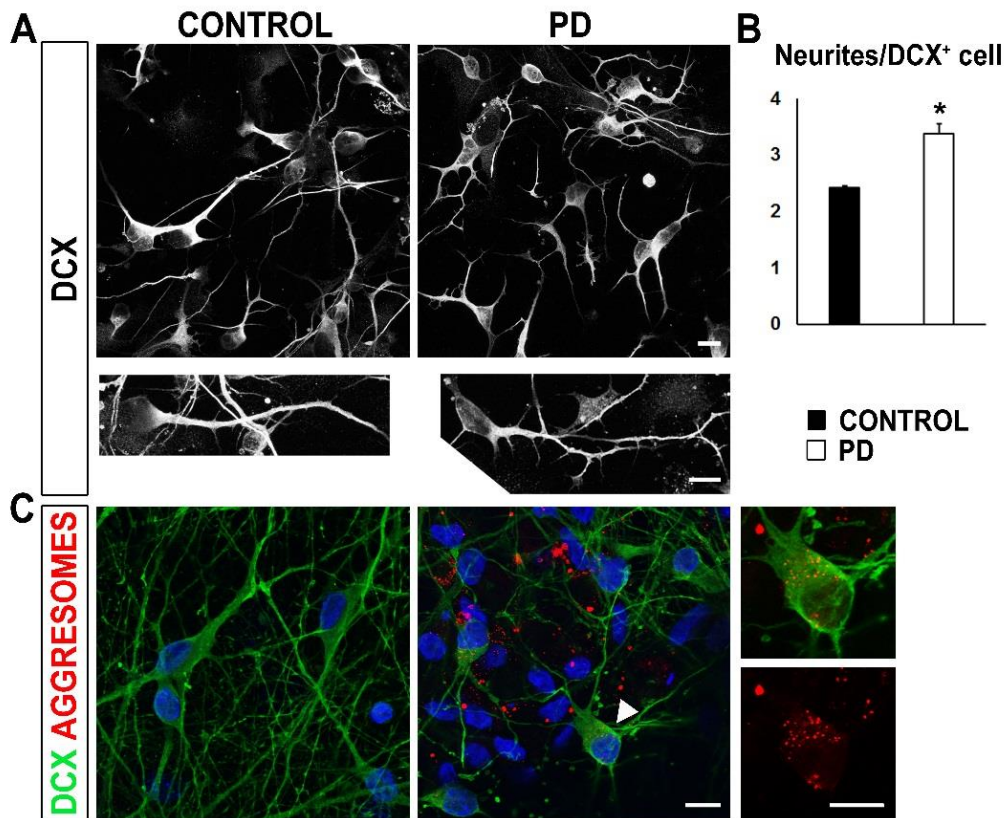


**Figure 18: Pathological phenotypes of iPSC-derived PD neurons in prolonged DAergic cultures.** (A) Representative images in upper and at higher magnification in lower panels, illustrating the more branched morphology of DCX+ cells in PD versus control cultures at 47 DIV. (B) Quantification of the number of total neurites per DCX+ cell (control  $2.42 \pm 0.04$  and PD  $3.38 \pm 0.16$ , \*  $P= 0.029$ ) (C) At 70 DIV protein aggregates (aggresomes, red) are detected throughout in PD cultures and intracellularly in DCX+ cells (green), but not in control cells.

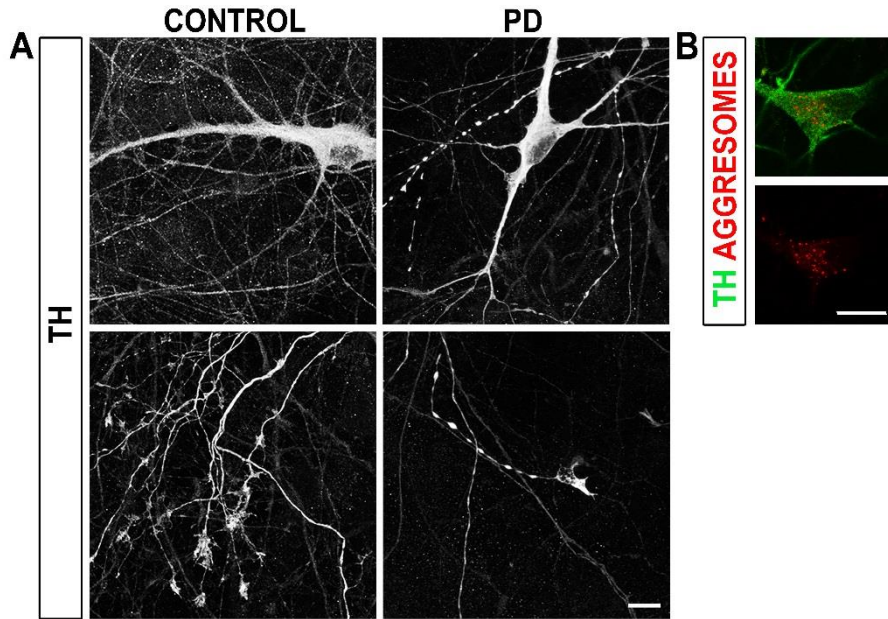


**Figure 19: Pathological phenotypes of hiPSC-derived PD neurons in prolonged DAergic cultures.** (A) Immunostaining for TH at 70 DIV shows PD neurites with swollen varicosities (upper panel) that end up in fragmented processes (lower panel). (B) Intracellular protein aggregates detected in PD TH+ neurons at 70 DIV. Scale bars, 10 $\mu$ m.

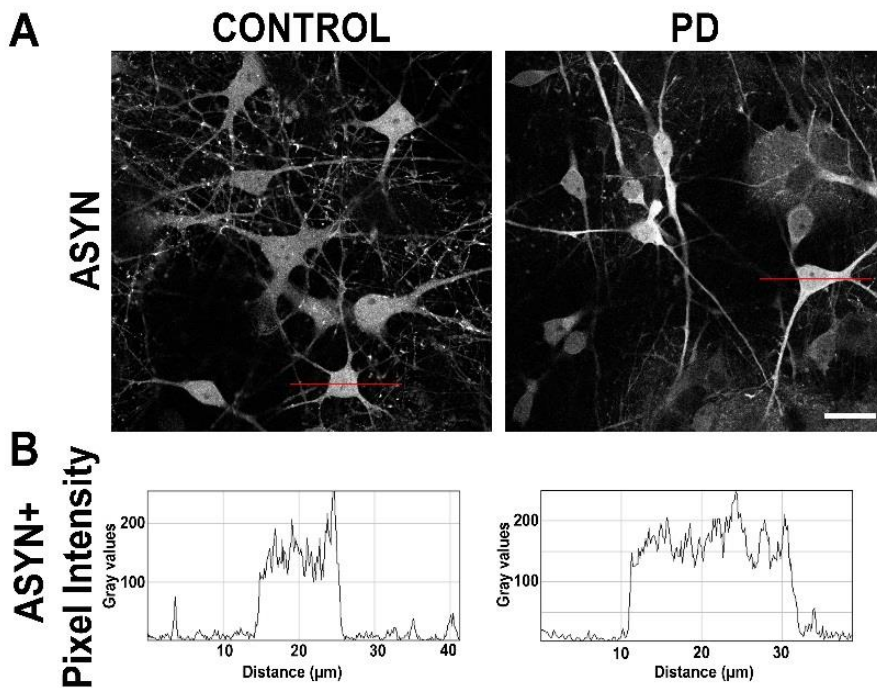


**Figure 20:  $\alpha$ -synuclein ( $\alpha$ Syn) expression is elevated in PD cultures.** (A) Immunofluorescence for  $\alpha$ Syn in hiPSC-derived control and PD cells at 70 DIV. Scale bar, 20 $\mu$ m. (B) Representative plot analysis of pixel intensity in one healthy and one PD  $\alpha$ Syn+ cell [marked with red bar in (A)].

### 5.5.2 Electrophysiological analysis

To assess for possible functional differences between control and PD cultures, whole-cell patch-clamp recordings were performed between 55 and 60 DIV (Fig. 5.4). Voltage-clamp recordings demonstrated the presence of transient inward sodium currents and sustained outward potassium currents (representative traces are shown in Fig. 5.4A) that could be blocked by the Nav-blocker TTX (1  $\mu$ M) and K<sub>v</sub>-blocker TEA (10 mM), respectively (Fig. 21A). Current-voltage relationship curves show the activation of voltage-gated sodium and potassium channels (Figure 21B, C). For control and PD iPSC-derived neurons the passive and active membrane properties were compared. The mean input resistance was  $1.011 \pm 0.186$  G $\Omega$  (n= 14) and  $1.711 \pm 0.397$  G $\Omega$  (n= 9), respectively (Fig. 21D). Resting membrane potential was  $-57.14 \pm 5.34$  mV (n= 14) and  $-74.44 \pm 9.59$  mV (n= 9) respectively (Fig. 21E). In agreement with our previous observations [420], we did not observe statistically significant differences on active and passive membrane properties between control and PD cells.

### 5.5.3 Dysregulated calcium activity in PD neurons

Ca<sup>2+</sup> fluxes across the plasma membrane and between intracellular compartments play critical roles in fundamental neuronal functions [498]. Ca<sup>2+</sup> signals are produced in response to stimuli, such as membrane depolarization, mechanical stretch, noxious insults, extracellular agonists, intracellular messengers, and the depletion of intracellular Ca<sup>2+</sup> stores. Neurite outgrowth, synaptogenesis, synaptic transmission, plasticity, and cell survival are regulated by Ca<sup>2+</sup> dynamics (rev. by [499, 500]). Furthermore, abnormal cellular Ca<sup>2+</sup> load can trigger cell death by activating several catabolic processes as has been shown in many neurological diseases (rev. by [501]). Moreover, spontaneous neuronal activity leads to increases in intracellular calcium levels and activation of signaling pathways that are important for the regulation of neuronal processes [502].

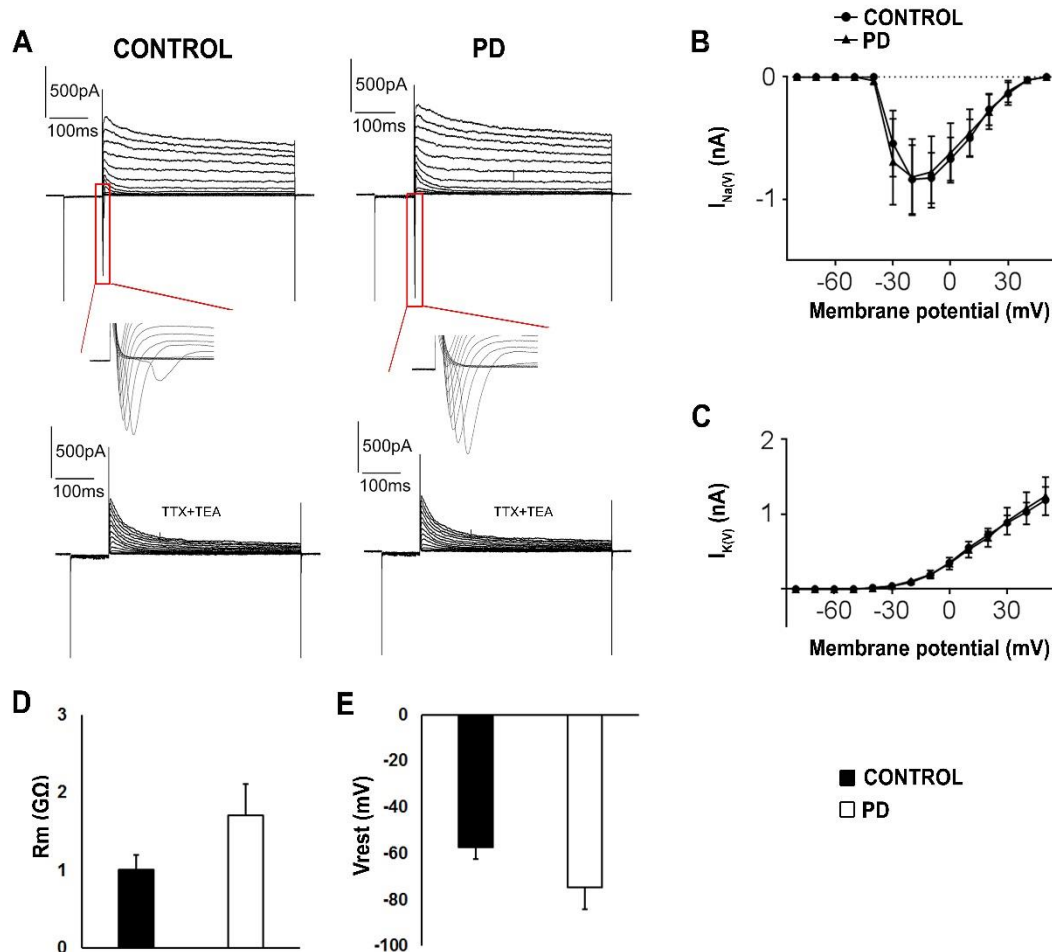


**Figure 21: Electrophysiological properties in control and PD neurons.** (A) Representative traces of voltage clamp recordings showing fast inward currents followed by long-lasting outward currents, due to voltage steps in 10 mV increments. The inset shows a high magnification view of the inward current. Following initial recording, cells were perfused with 1  $\mu$ M TTX to block  $\text{Na}^+$  currents and with 10 mM TEA (tetraethylammonium) to block  $\text{K}^+$  currents. (B, C) The mean current–voltage relations of inward  $\text{Na}^+$  currents [ $I_{\text{Na}}(V)$ , (B)] and outward  $\text{K}^+$  currents [ $I_{\text{K}}(V)$ , (C)] under basal conditions show no difference between control and PD neurons. Passive membrane properties: (D) membrane input resistance ( $R_m$ ) (control  $1.011 \pm 0.186$  G $\Omega$ ;  $n = 14$  and PD  $1.711 \pm 0.397$  G $\Omega$ ;  $n = 9$ ), and (E) resting membrane potential ( $V_{\text{rest}}$ ) (control  $-57.14 \pm 5.34$  mV;  $n = 14$  and PD  $-74.44 \pm 9.59$  mV;  $n = 9$ ) show no difference between control and PD neurons.

In line with these data, we assessed the integrity of the PD neuronal network using calcium imaging to measure spontaneous  $\text{Ca}^{2+}$  transients at 55–60 DIV. We observed significantly more spontaneous  $\text{Ca}^{2+}$  transients in PD as compared to control cultures (Fig. 22A, B; control  $0.01 \pm 0.002$ ,  $n = 20$ ; PD  $0.04 \pm 0.003$ ,  $n = 33$ ; \*\*\*\*  $P = 2.51 \times 10^{-10}$ ) with significantly larger mean amplitude (Fig. 5.5C; control  $1.70 \pm 0.21$ ,  $n = 22$ ; PD  $2.33 \pm 0.15$ ,  $n = 35$ ; \*  $P = 0.02$ ), indicating

an abnormal neuronal network activity that likely influences neuritic growth and synaptic connectivity [499].

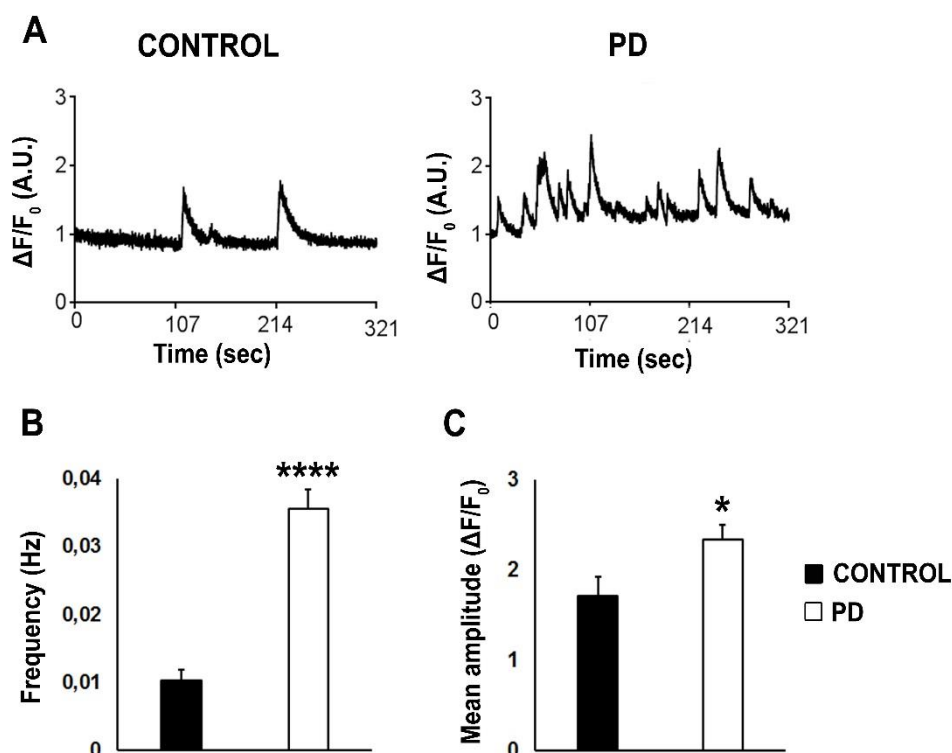


**Figure 22: Spontaneous calcium transients in control and PD neurons** (A) Representative Fluo-3 traces of spontaneous Ca<sup>2+</sup>-transients (A.U. =arbitrary units), normalized to the average response from the first 40 seconds of recording. (B) PD neurons displayed a higher frequency of Ca<sup>2+</sup> spikes (control 0.01 ± 0.002, n= 20; PD 0.04 ± 0.003, n =33; \*\*\*\* P=2.51x10<sup>-10</sup>) and spike amplitude (C) (control 1.70 ± 0.21, n= 22; PD 2.33 ± 0.15, n= 35; \* P= 0.02); (n= 20 for control neurons; n = 33 for PD neurons).

## 5.6 Establishment and characterization of the 6-OHDA-induced striatal lesion model in immunodeficient mice

Since our initial 6-OHDA injections in the MFB led to very low survival of NOD/SCID mice, we proceeded with the induction of a unilateral lesion by intrastriatal injection of 6-OHDA in 9-10 week old mice. The intrastriatal injection causes a milder DAergic depletion in the SN, compared to the TH+ neuronal loss observed after MFB injection. Therefore, we were hoping for a higher survival rate in the lesioned mice, particularly of the compromised NOD/SCID strain that we had to use for xenografting human cells [378, 379, 465]. As in the MFB lesioned mice, extensive post-operative care were given to mice with intrastriatal 6-OHDA lesion, including daily intraperitoneal injection of 5%

glucose and access to wet pellets. This way, we managed to increase the survival rate from 13.64% after the MFB lesion to 56% after the intrastriatal lesion. Specifically, from a total of n= 100 6-OHDA injected animals, 56 animals survived from five independent experiments. Mice with >5 net ipsilateral turns in the amphetamine test, which confirmed successful lesions (Kriks, Shim et al. 2011) were used for further analysis. Among the 56 animals survived, 27 displayed the desired phenotype and were used for the model's characterization (n= 17), or transplanted with either control (n=5) or PD immature neurons (n= 5) as it is described below. The saline injected animals (control group) used were n= 13 that survived throughout the experimental procedure and subsequent analyses.

A robust functional deficit was confirmed 2 weeks after intrastriatal 6-OHDA administration using both drug-induced and drug-free behavioral analysis (Fig. 6.1A- C). For the drug-induced test amphetamine was used which is a substrate for dopamine transporter (DAT) [503] that leads to its phosphorylation, thereby reducing its activity, while it also activates Protein kinase C (PKC) causing DA efflux [504]. Thus, amphetamine administration in a 6-OHDA unilaterally lesioned animal leads to rotational asymmetry as the animal turns contralateral to the side with the greater DAT stimulation which is the non-lesioned side. As a result, the animal rotates ipsilateral to the lesion [505].

Amphetamine-induced rotational asymmetry was assessed over a 15-week period (Fig. 23A). Mice with >5 net ipsilateral turns in the amphetamine test (2 weeks post injection) were used for further analysis. Surprisingly, although 6-OHDA injection led to significantly increased ipsilateral turns per min at 2 weeks post injection (6-OHDA  $8.64 \pm 0.76$ ; n= 16; saline  $0.48 \pm 0.72$  turns per min; n= 13; \*\*\*\* P=  $2.25 \times 10^{-8}$ ), ipsilateral turns were notably decreased over time. At 7 weeks, turns in the 6-OHDA group were  $3.93 \pm 0.43$  per min (n= 5) versus  $0.78 \pm 1.02$  per min in the saline group (n= 6), \* P= 0.025. Finally, at 11 and 15 weeks values were not substantially different between the two groups (11 weeks: 6-OHDA  $2.82 \pm 0.71$  turns, n= 6; saline  $1.09 \pm 0.79$  turns, n= 5, P= 0.138; and 15 weeks; 6-OHDA  $0.47 \pm 0.39$  turns, n= 6 and saline  $-0.32 \pm 0.87$  turns, n= 4, P= 0.453).

Spontaneous forelimb and hindlimb activity was also measured at the same time points (Fig. 23B, C). Spontaneous rotation requires a novel environment and spontaneous testing was carried out before the drug-induced one [493]. Preference for ipsilateral steps was significantly higher in the 6-OHDA group as compared to the saline group at 2 weeks (forelimbs: 6-OHDA  $1.63 \pm 0.10$  ipsi/contralateral steps per min,  $n=12$ ; saline  $1.07 \pm 0.06$ ,  $n=6$ ; \*\*\*  $P=0.0002$ ; hindlimbs: 6-OHDA  $2.68 \pm 0.29$ ,  $n=10$ ; saline  $1.07 \pm 0.24$ ,  $n=6$ ; \*\*\*  $P=0.0007$ ) with the difference leveling out thereafter both for forelimbs (at 7 weeks: 6-OHDA  $0.94 \pm 0.03$ ,  $n=4$ ; saline  $1.06 \pm 0.03$ ,  $n=4$ ; \*  $P=0.037$ ; at 11 weeks: 6-OHDA  $0.86 \pm 0.05$ ,  $n=4$ ; saline  $1.03 \pm 0.07$ ,  $n=4$ ;  $P=0.091$ ; at 15 weeks: 6-OHDA  $0.94 \pm 0.06$ ,  $n=4$ ; saline  $1.13 \pm 0.06$ ,  $n=4$ ;  $P=0.065$ ) and hindlimbs (at 7 weeks: 6-OHDA  $1.44 \pm 0.17$ ,  $n=5$ ; saline  $1.05 \pm 0.31$ ,  $n=4$ ;  $P=0.328$ ; at 11 weeks: 6-OHDA  $1.32 \pm 0.21$ ,  $n=5$ ; saline  $1.03 \pm 0.14$ ,  $n=4$ ;  $P=0.289$  and at 15 weeks: 6-OHDA  $1.15 \pm 0.16$ ,  $n=5$ ; saline  $0.85 \pm 0.19$ ,  $n=4$ ,  $P=0.258$ ). These analyses revealed an unexpected spontaneous behavioral recovery in the lesioned animals, which impeded assessment of functional improvement following transplantation.

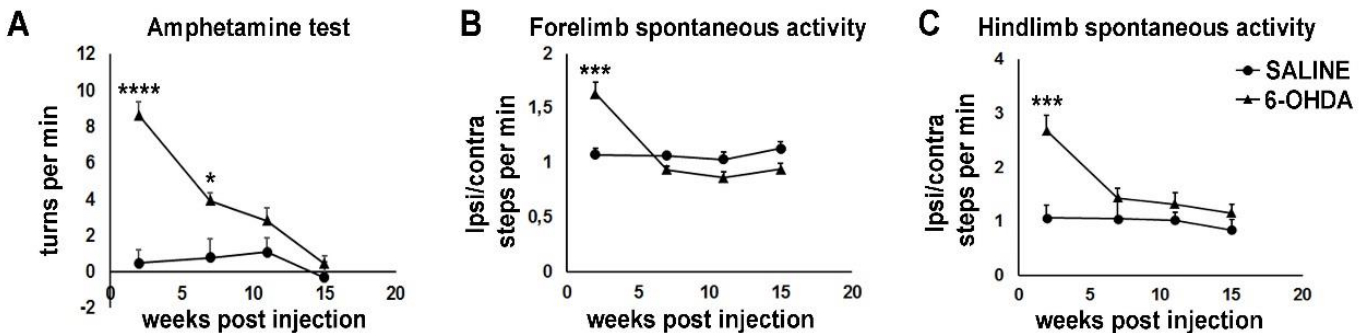


**Figure 23: Behavioral characterization of the 6-OHDA hemi-parkinsonian model in NOD/SCID mice.** (A) Amphetamine-induced rotational asymmetry in 6-OHDA- and saline-injected control mice. Data represent mean  $\pm$  SEM (6-OHDA  $8.64 \pm 0.76$ ;  $n=16$ ; saline  $0.48 \pm 0.72$  turns per min;  $n=13$ ; \*\*\*\*  $P=2.25 \times 10^{-8}$  at 2 weeks;  $3.93 \pm 0.43$  per min;  $n=5$ ; saline  $0.78 \pm 1.02$  per min;  $n=6$ , \*  $P=0.025$  at 7 weeks). (B, C) Spontaneous forelimb (B) and hindlimb (C) activity showing ipsilateral versus contralateral paw preference (forelimbs: 6-OHDA  $1.63 \pm 0.10$  ipsi/contralateral steps per min,  $n=12$ ; saline  $1.07 \pm 0.06$ ,  $n=6$ ; \*\*\*  $P=0.0002$  at 2 weeks; 6-OHDA  $0.94 \pm 0.03$ ,  $n=4$ ; saline  $1.06 \pm 0.03$ ,  $n=4$ ; \*  $P=0.037$  at 7 weeks; hindlimbs: 6-OHDA  $2.68 \pm 0.29$ ,  $n=10$ ; saline  $1.07 \pm 0.24$ ,  $n=6$ ; \*\*\*  $P=0.0007$  at 2 weeks).

At the tissue level, loss of TH-positive neurons in the SN was measured 3 weeks post-lesioning (Fig. 24A). A 65.5% loss was observed (Fig. 24E; saline  $100 \pm 6.03$  %,  $n=3$ ; 6-OHDA  $34.51 \pm 4.84$  %,  $n=3$ ; \*\*  $P=0.0001$ ) which resulted in an extensive striatal DAergic denervation (Fig. 24C). Although loss of TH-positive neurons in the SN remained stable over 15 weeks (saline  $100 \pm 16.61$ ,  $n=3$ ; 6-OHDA  $39.83 \pm 0.7$  %,  $n=3$ ; 60.2%, \*  $P=0.022$ ), striatal DAergic reinnervation was observed (Fig. 24C), in agreement with the concurrent behavioral recovery.

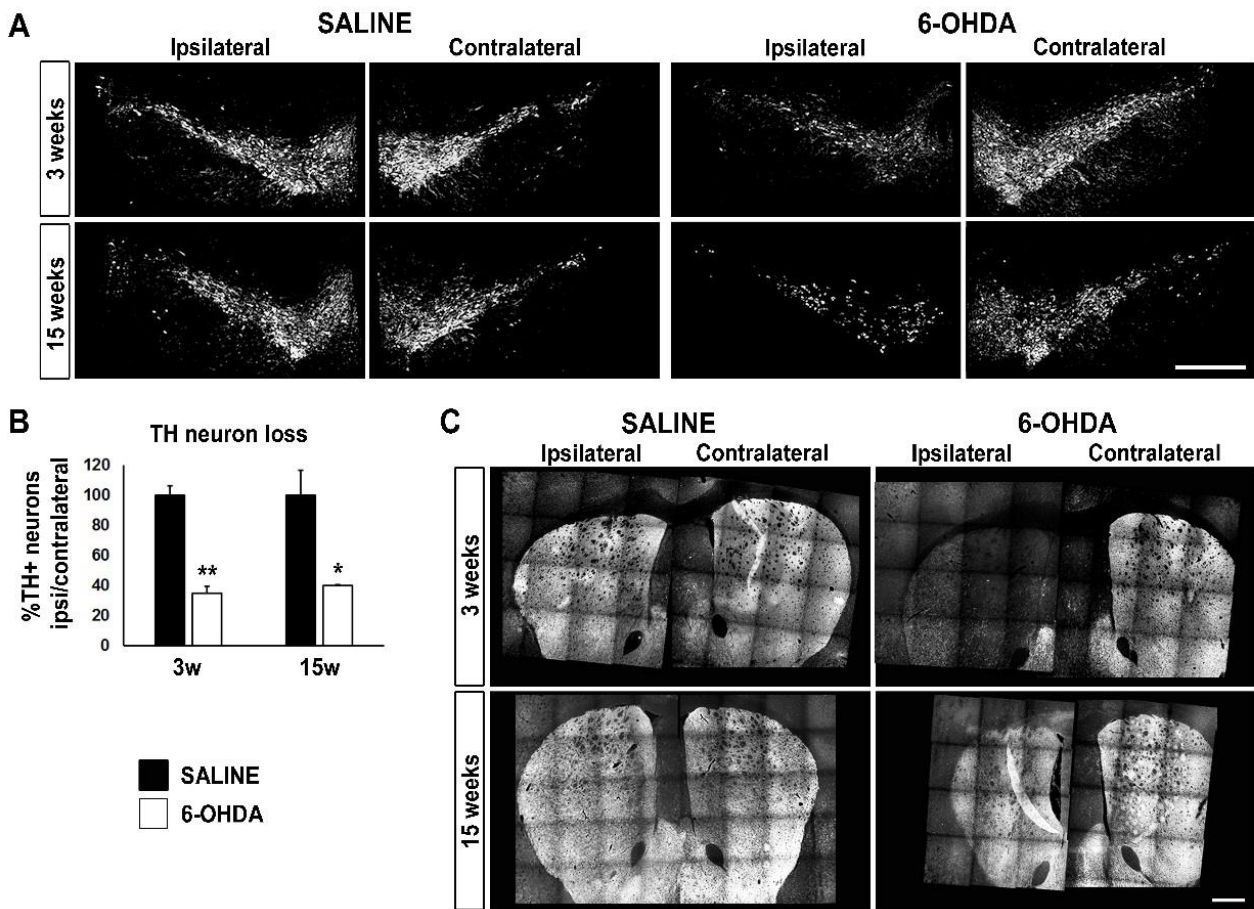


**Figure 24: Immunohistochemical characterization of the 6-OHDA hemi-parkinsonian model in NOD/SCID mice.** (A) Representative confocal images of coronal midbrain sections immunostained for TH (from -2.74 to -3.06 mm from bregma) at 3 and 15 weeks after saline or 6-OHDA injection. A marked reduction of TH+ neurons is evident in the ipsilateral side of 6-OHDA lesioned mice at both time points. Quantification is shown in (B) (saline  $100 \pm 6.03$  %,  $n=3$ ; 6-OHDA  $34.51 \pm 4.84$  %,  $n=3$ ; 65.5 % \*\*  $P=0.0001$  in 2 weeks, saline  $100 \pm 16.61$ ,  $n=3$ ; 6-OHDA  $39.83 \pm 0.7$  %,  $n=3$ ; 60.2%, \*  $P=0.0224$  at 15 weeks). Scale bar, 500 $\mu$ m. (C) Representative confocal images of coronal striatal sections showing TH innervation (+0.945mm from bregma, next to injection level) at 3 and 15 weeks after saline or 6-OHDA injection. Denervation at 3 weeks followed by re-innervation at 15 weeks is apparent in the ipsilateral side of 6-OHDA lesioned animals. Scale bar, 500 $\mu$ m.

## 5.7 *In vivo* engraftment of iPSC-derived immature neurons

### 5.7.1 Investigation of cell survival and differentiation

To investigate their characteristics *in vivo*, control and PD human iPSC-derived PSA-NCAM-enriched DAergic neurons (30 DIV) were transplanted 3 weeks after 6-OHDA injection (Fig. 25A). Although analysis of the 6-OHDA mice had shown spontaneous re-innervation of the striatum beginning 7 weeks after 6-OHDA administration, we proceeded with cell transplantation in this model since lesions have been shown to increase survival and integration of transplanted cells within the host brain [506].

Analysis of grafted animals was performed by immunohistochemistry in 5 control animals and 3 PD grafted animals (two of the PD transplanted died in the meantime), unless stated otherwise. Both control and PD neurons managed to survive in the host striatum, as indicated by human-specific cytoplasmic marker staining, and formed well-defined grafts without signs of cellular overgrowth (Fig. 25B). To assess neural overgrowth in this case, we performed immunohistochemistry for Ki-67. The number of proliferating cells in the grafts were in both cases very low (Fig. 26A, B; control  $1.49 \pm 0.81$  %; PD  $2.08 \pm 0.96$  %,  $P = 0.66$ ). These numbers are in agreement with previous work reporting limited proliferation capacity in PSA-NCAM MACS sorted grafted cells [490].

Quantification of the graft area (mean area in  $\mu\text{m}^2$  from 3-7 sections/ animal) and the number of human nuclei (HuNu) per section (mean number from 3-5 sections/ animal) revealed non-significant differences between control and PD grafts (Fig. 25D; graft area: control  $197.03 \pm 96.16$ ; PD  $61.99 \pm 16.41$   $\mu\text{m}^2$ ,  $P = 0.238$  and Fig. 7.1E; HuNu/ section: control  $543.66 \pm 182.14$ ; PD  $279.06 \pm 180.33$ ,  $P = 0.349$ ).

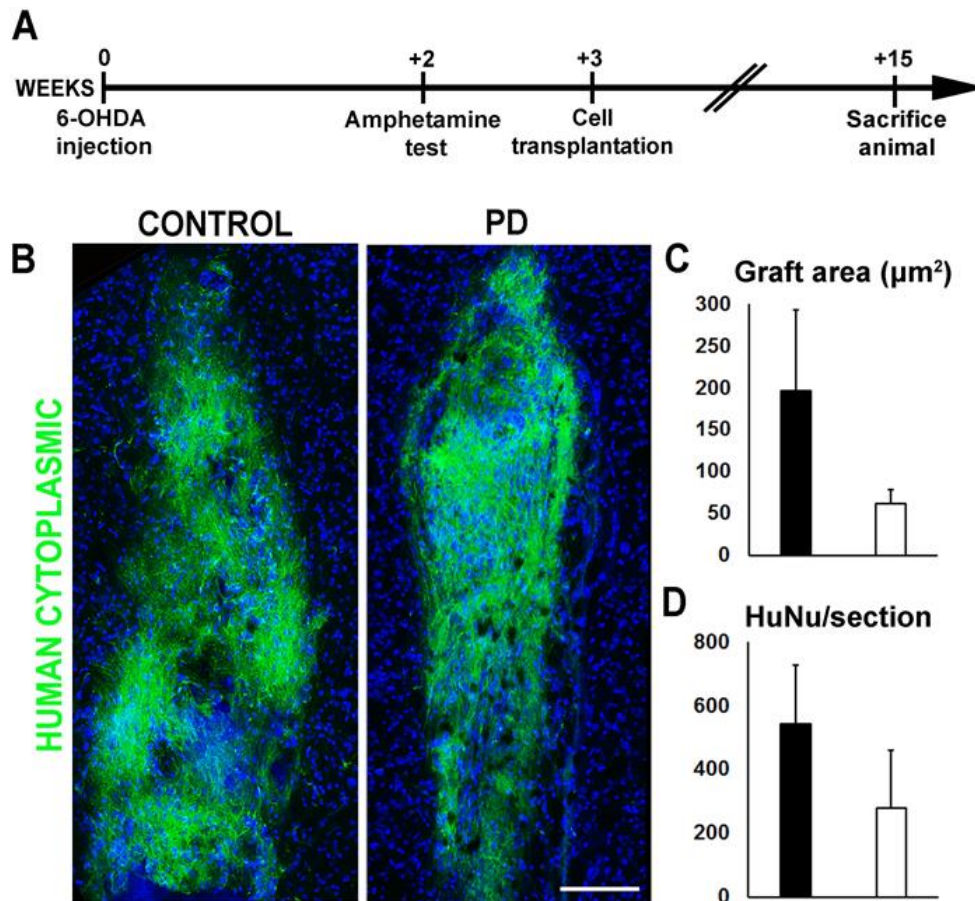


**Figure 25: In vivo engraftment of iPSC-derived control and PD cells.** (A) Schematic drawing of the time course of the *in vivo* experiment. DA differentiated cells were stereotactically transplanted 2 days after MACS enrichment (30DIV), as illustrated in Fig.16. (B) Immunostaining for the human-specific cytoplasmic antigen (green) in control and PD-derived grafts. Nuclei are shown in blue. Scale bar, 100 $\mu\text{m}$ . (C) Quantification of graft area ( $\mu\text{m}^2$ ; control  $197.03 \pm 96.16$ ; PD  $61.99 \pm 16.41\mu\text{m}^2$ ,  $P= 0.238$ ) and (D) quantification of human nuclei+ (HuNu+) per section (control  $543.66 \pm 182.14$ ; PD  $279.06 \pm 180.33$ ,  $P= 0.349$ ). Data represent mean  $\pm$  SEM (control-derived  $n=5$  and PD-derived grafts  $n= 3$ ).

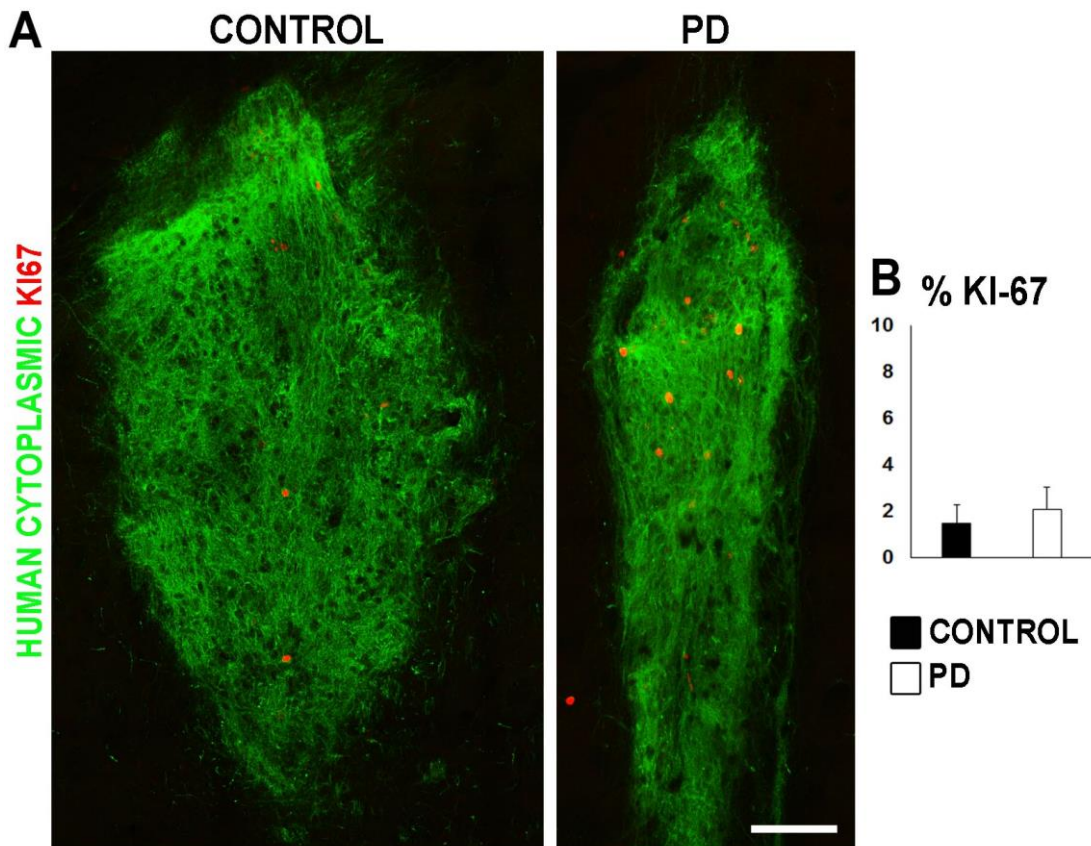


**Figure 26: Low proliferating potential of grafted cells.** (A) Double labeling for human cytoplasmic (green) and Ki-67 (red) shows that both control and PD-derived grafts consist of very low percentage of proliferating cells, with no apparent differences between them. (B) Quantification of % Ki-67<sup>+</sup> cells/human cytoplasmic<sup>+</sup> cells (control 1.71 ± 1.0%; PD 2.08 ± 0.96%,  $P = 0.81$ ). Scale bar, 100µm. Data represent mean ± SEM.

Next we investigated the ability of the grafted cells to differentiate by accessing the expression of various markers. Immunohistochemical analysis at 12 weeks showed that many of the grafted cells were TUJ1-positive neurons (Fig. 27A, B; control 37.59 ± 13.44%; PD 19.09 ± 0.28%,  $P = 0.241$ ), whilst a subpopulation still expressed the neural progenitor cell marker Nestin (Fig. 27E, F; control 32.64 ± 5.81%; PD 44.72 ± 10.68%,  $P = 0.394$ ). The expression of the immature neuronal marker DCX was also significantly higher in PD derived grafts as compared to control (Fig. 27G, H; control 15.85 ± 0.81%; PD 47.28 ± 2.88%; \*\*  $P = 0.009$ ). These results indicate that PD derived cells are in more immature state as compared to controls. Few cells were TH-positive DAergic neurons (Fig. 28A, B; control 0.56 ± 0.32%,  $n = 3$  and PD 0.056 ± 0.056%,  $n = 3$ ;  $P = 0.22$ ) indicating limited DAergic differentiation *in vivo* at 12 wpt. Possibly, this number would be greater at later time points.

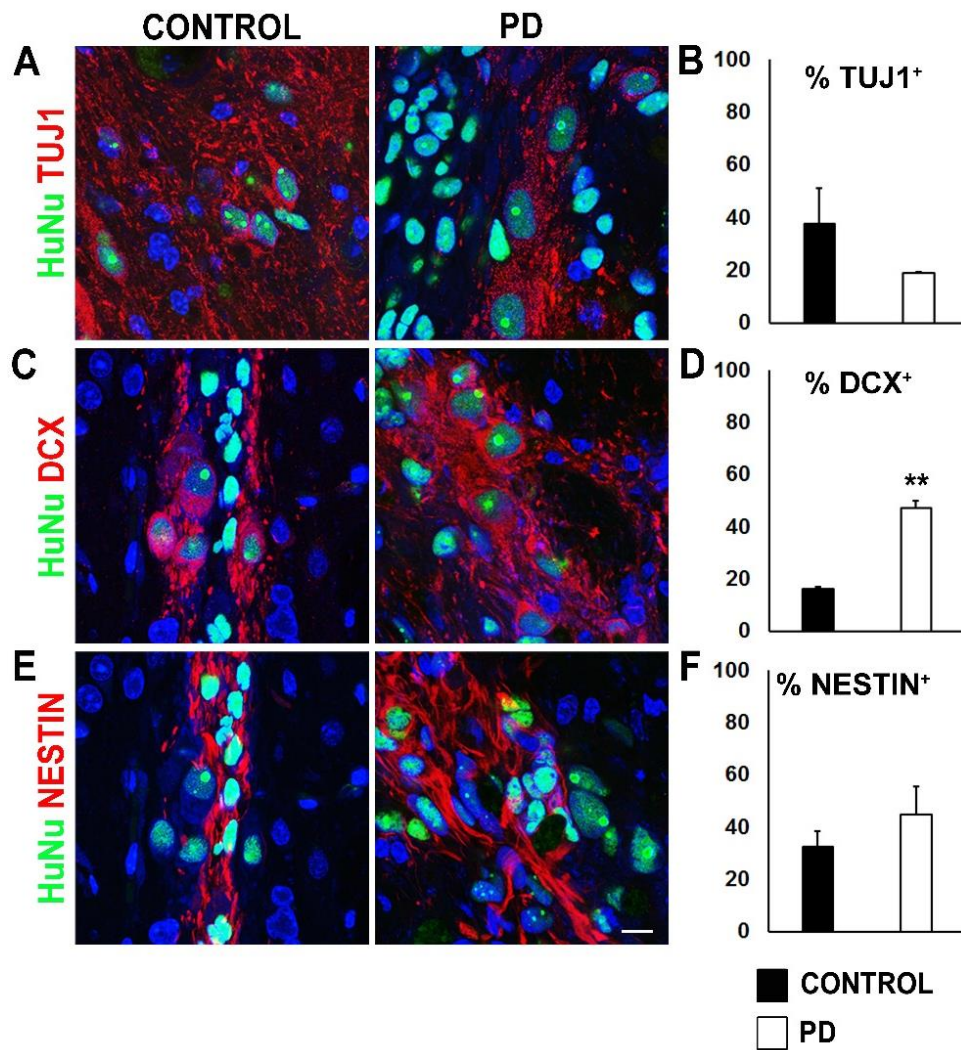


**Figure 27: In vivo engraftment of iPSC-derived control and PD cells** (A) Double immunostaining for HuNu (green) and TUJ1 (red); (B) Quantification of TUJ1+/ HuNu+ cells out of total HuNu+ cells (control  $37.59 \pm 13.44\%$ ; PD  $19.09 \pm 0.28\%$ ,  $P= 0.241$ ). (C) Double immunostaining for HuNu (green) and DCX (red); (D) Quantification of DCX+/ HuNu+ cells out of total HuNu+ cells (control  $15.85 \pm 0.81\%$ ; PD  $47.28 \pm 2.88\%$ ; \*\*  $P= 0.009$ ). (E) Double immunostaining for HuNu (green) and Nestin (red); (F) Quantification of Nestin+/HuNu+ cells out of total HuNu+ cells (control  $32.64 \pm 5.81\%$ ; PD  $44.72 \pm 10.68\%$ ,  $P= 0.394$ ). Nuclei are shown in blue. Scale bar (A, C, E), 10  $\mu\text{m}$ . Data represent mean  $\pm$  SEM (control-derived  $n=5$  and PD-derived grafts  $n= 3$ ).

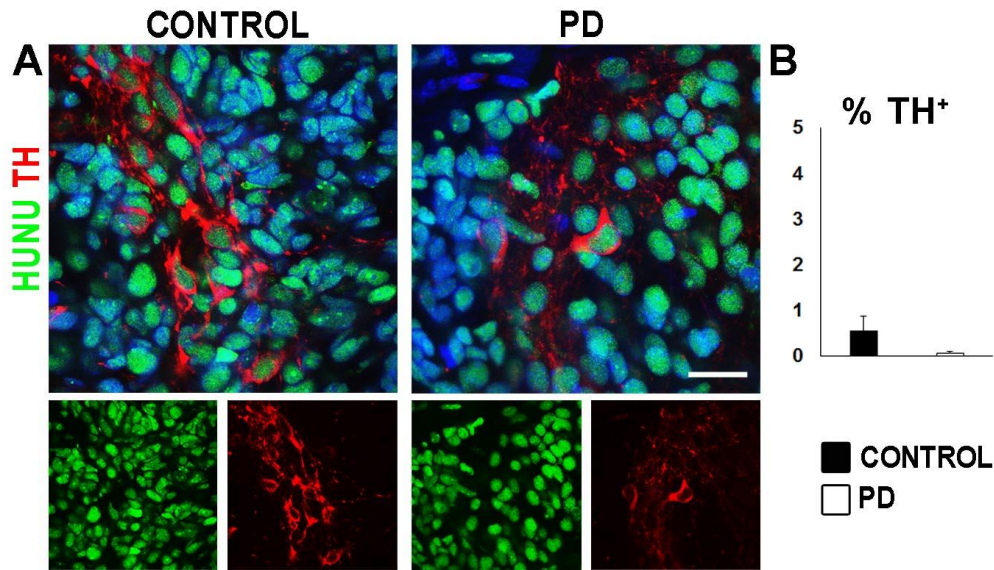


**Figure 28: Both control and PD-derived grafts contain few TH+ DAergic neurons.** (A) Double immunofluorescence for HuNu (green) and TH (red). (B) (control  $0.56 \pm 0.32$  %,  $n=3$  and PD  $0.056 \pm 0.056$  %,  $n= 3$ ). Scale bar, 10  $\mu\text{m}$ .

Interestingly, using an antibody that specifically recognizes the human protein we noted extensive  $\alpha\text{Syn}$  immunoreactivity in PD grafts whilst control grafts, exhibited much lower  $\alpha\text{Syn}$  levels (Fig. 29A). Quantification revealed significantly increased  $\alpha\text{Syn}$  immunofluorescence intensity in PD-derived grafts as compared to control-derived grafts (Fig. 29B; control  $36.744 \pm 16.825$  pixels/ $\mu\text{m}^2$ ,  $n = 3$ ; PD  $207.389 \pm 28.466$  pixels/ $\mu\text{m}^2$ ,  $n= 3$ ; \*  $P= 0.014$ ), indicating a first step towards induction of pathology. This is also in accordance with the higher  $\alpha\text{Syn}$  intensity observed *in vitro*. Human  $\alpha\text{Syn}$  immunoreactivity was not detected outside the grafts, suggesting no spreading to host cells at this time point.

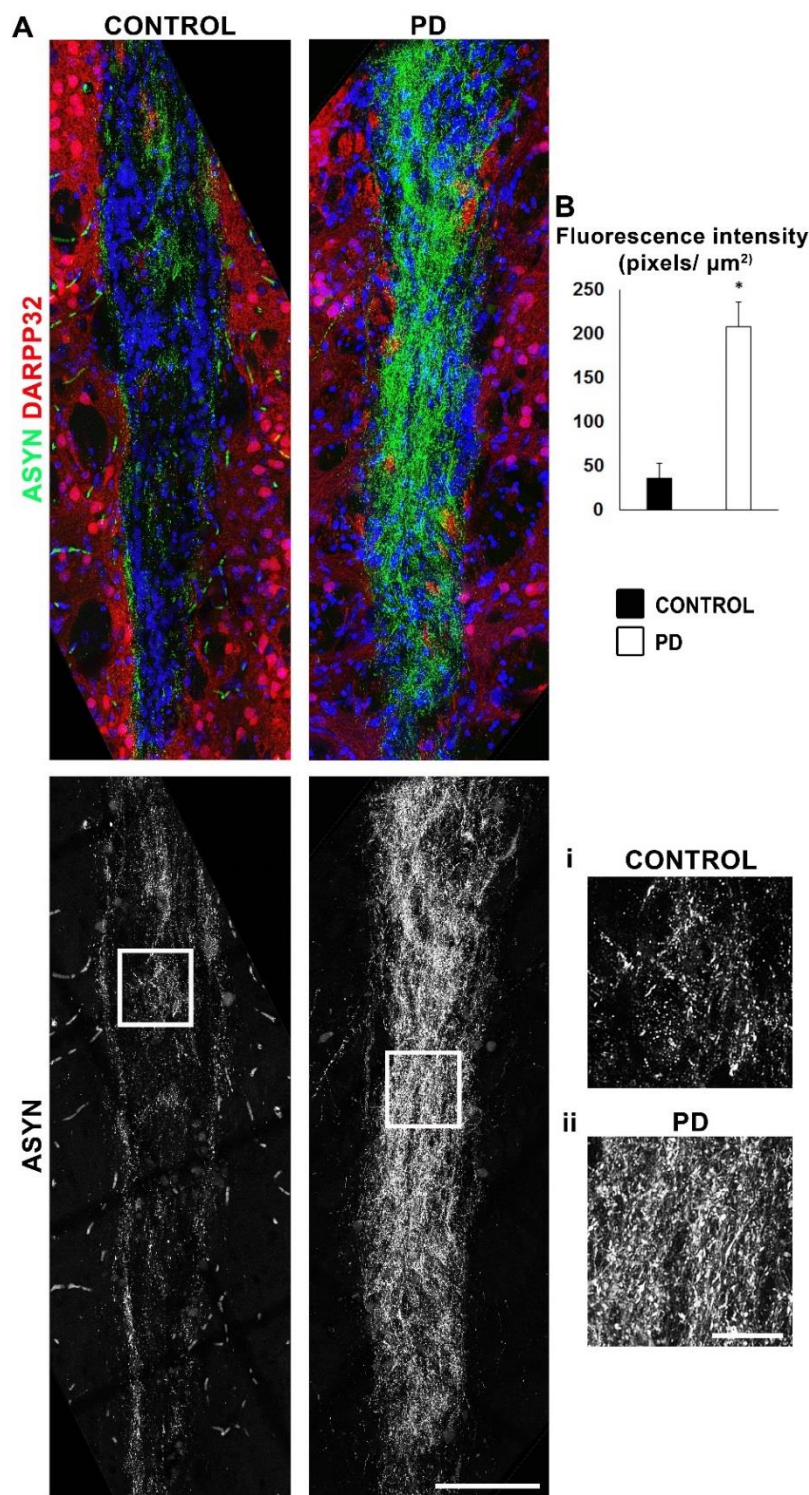


**Figure 29: Increased  $\alpha$ -synuclein ( $\alpha$ Syn) expression in grafted iPSC-derived PD neurons.** (A)

Representative images of striatal sections from mice that received control or PD-derived grafts, labeled for human  $\alpha$ Syn (green, top panel; same fields: white lower panel). Host DARPP32+ medium spiny neurons are stained in red and nuclei are shown in blue (DAPI staining).

Increased levels of  $\alpha$ Syn immunoreactivity are clearly detected in PD-derived grafts. Scale bar, 100  $\mu\text{m}$ . The insets are shown at higher magnification in (i, ii,  $\alpha$ Syn; white). Scale bar in the insets, 25  $\mu\text{m}$ .

(B) Quantification of  $\alpha$ Syn fluorescence intensity (arbitrary units) in control and PD-derived grafts (control  $6.005 \pm$

$2.72$  arbitrary units (A.U.),  $n = 3$ ; PD  $54.792 \pm 9.583$  A.U.,  $n = 3$ ; \*  $P = 0.039$ ).

Despite the rather limited DAergic differentiation of human neurons at 12 weeks *in vivo*, application of a human-specific antibody against synaptophysin (HSYP), showed widespread immunoreactivity throughout the grafts (Fig. 30). Synaptophysin is a presynaptic protein present ubiquitously on presynaptic vesicles [507, 508], frequently used to label and quantify neuronal synapses

[507, 509, 510]. Double labeling for HSYP and DARPP32 that marks the host striatal medium spiny neurons, revealed an intercalated control graft-to-host interphase as opposed to the sharp boundaries demarcating the PD graft-to-host interphase (Fig. 31A). This suggests that control grafts may integrate better in the host tissue. In support of the above, quantification of HSYP<sup>+</sup> contacts onto DARPP32<sup>+</sup> neurons in the graft interphase revealed that PD-derived cells formed significantly less contacts than control (Fig. 31B;  $150.6 \pm 21.39$ ; PD  $85.07 \pm 14.73$ , \*  $P= 0.045$ ). This is also evident by 3D reconstruction of the HSYP<sup>+</sup> contact surfaces onto DARPP32<sup>+</sup> neurons (Fig. 31C).

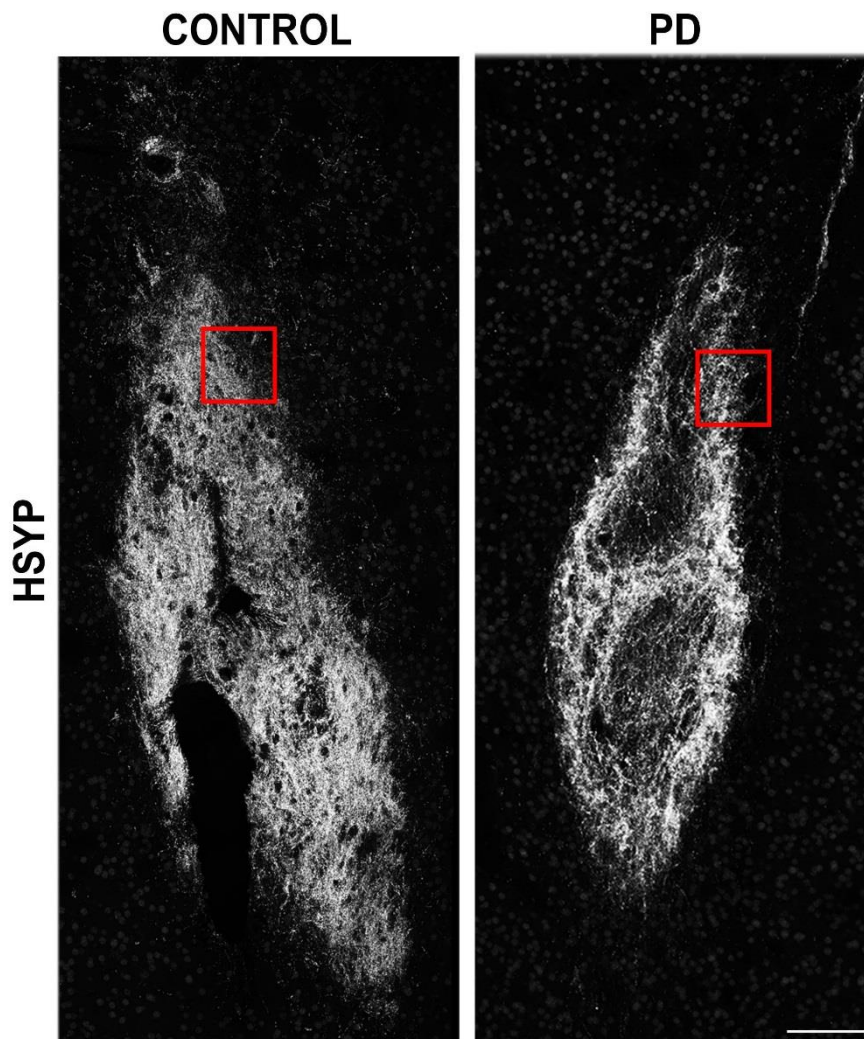


**Figure 30: Widespread expression of human synaptophysin in grafted iPSC-derived control and PD neurons.** (A) Low power view of control and PD-derived grafts immunostained for human synaptophysin (HSYP; white). Scale bar, 100 $\mu$ m.

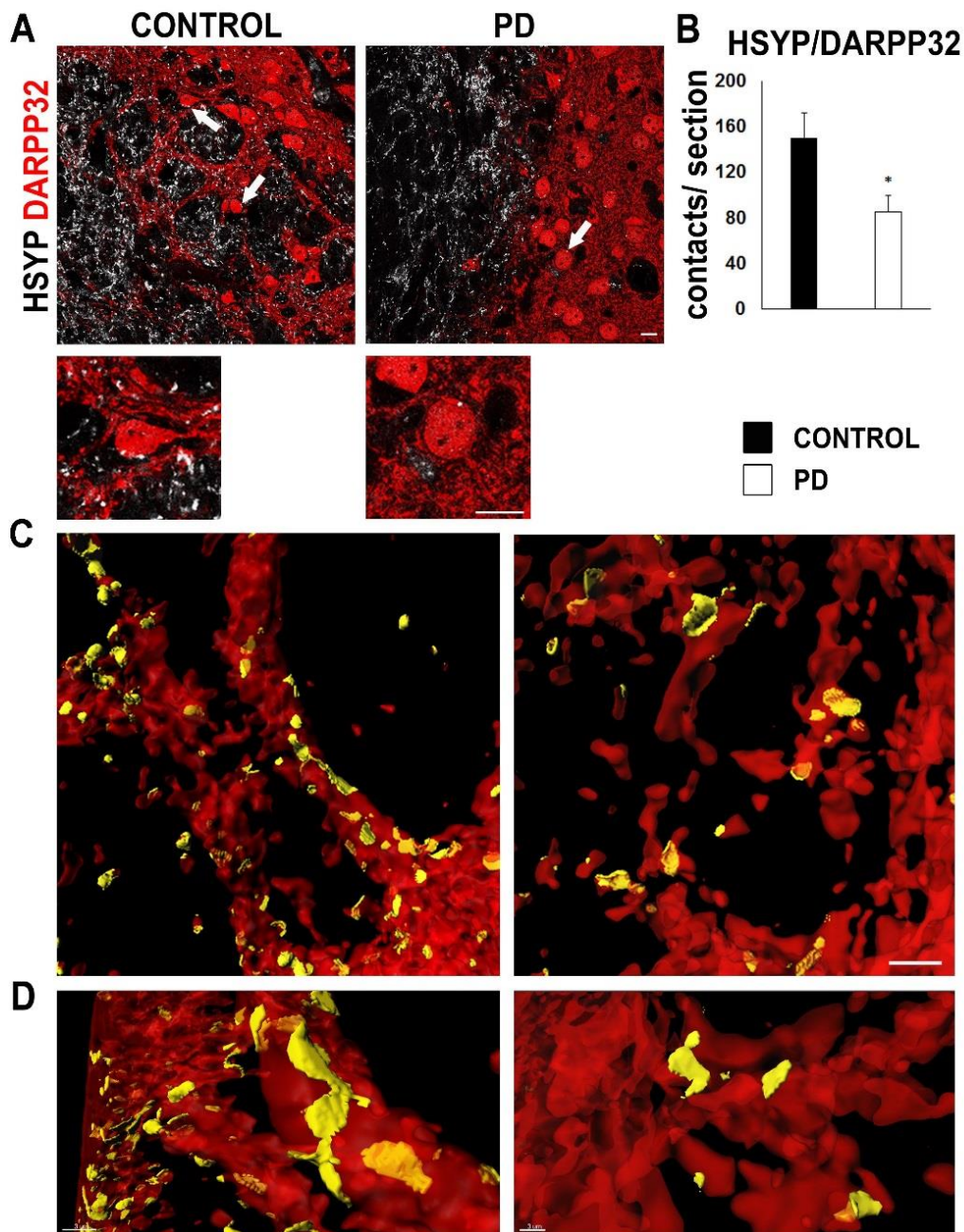


**Figure 31: PD iPSC-derived grafted neurons form fewer contacts onto host DARPP32+ medium spiny neurons in vivo.** (A) At higher magnification, double labeling for HSYP (white) and DARPP32 (red) indicates better integration of control-derived grafts within the host tissue. An intercalated control graft-host interphase is evident versus a sharply demarcated PD graft-host interphase. Arrows (top panel) and arrowheads (lower panel) depict possible synaptic contacts between grafted cells and host neurons. Orthogonal views of the images in the lower panel reveal the close proximity of HSYP/DARPP32 staining. Scale bars, 10 $\mu$ m. (B) Quantification of HSYP/DARPP32 contacts per section in control (n= 5) and PD-derived grafts (n= 3). Data represent mean  $\pm$  SEM (150.6  $\pm$  21.39; PD 85.07  $\pm$  14.73, \* P= 0.0451). (C, D) 3D reconstruction of the contacts of grafted cells (yellow) on DARPP32+ neurons (red). Scale bars, 3 $\mu$ m.

Our *in vivo* results revealed that iPSC-derived PD neurons survive and differentiate over a 12-week period. Yet, up-regulation of  $\alpha$ Syn immunoreactivity was noted in patient-derived grafts, indicative of a first step towards pathology. Moreover, control-derived grafts appeared to become better integrated than PD grafts within the host tissue extending projections that formed more contacts with host striatal neurons.

### 5.7.2 Investigation of microglial response

Microglial activation is an important contributor to PD pathogenesis (rev. by [141]). Microglia have been shown to have both neurotoxic and neuroprotective effects, depending on their activation state (rev. by [511, 512]). For instance, postmortem analysis of PD patients revealed a large number of activated microglia and accumulation of inflammatory mediators in the SN [143]. Moreover, both pro-inflammatory and anti-inflammatory cytokines have been detected in the striatum and SN of PD patients [513-515]. Noninvasive positron emission tomography (PET) imaging studies also confirmed the occurrence of microglial activation in PD [516].

In this study, the host brain immunological response was investigated at 12 weeks post-transplantation by immunofluorescence. Control and PD-derived grafts were surrounded by host Iba1<sup>+</sup> macrophage/microglial cells (Fig. 32A) whilst activated CD68<sup>+</sup> macrophage/microglia had infiltrated within the grafts in similar numbers between control and PD (Fig. 32B, C; control  $129 \pm 21.44$ , PD  $156 \pm 50.17$ ;  $P = 0.653$ ). Such CD68<sup>+</sup> activated cells were not evident outside the grafts. Thus at this stage we did not note a significant microgliosis in the grafted animals. It is possible that such a response might be more evident at earlier or even at later time-points when induction of pathology in PD cells would be more prominent.

It has to be mentioned though that this *in vivo* model was limited to studies up to 12 weeks post transplantation. Further *in vivo* studies were not possible, since a percentage of the NOD/SCID mice become leaky from spontaneous development of functional T- and B-lymphocytes as the mice age

([www.envigo.com](http://www.envigo.com)). Therefore, at longer time points we would not detect presence of the graft.

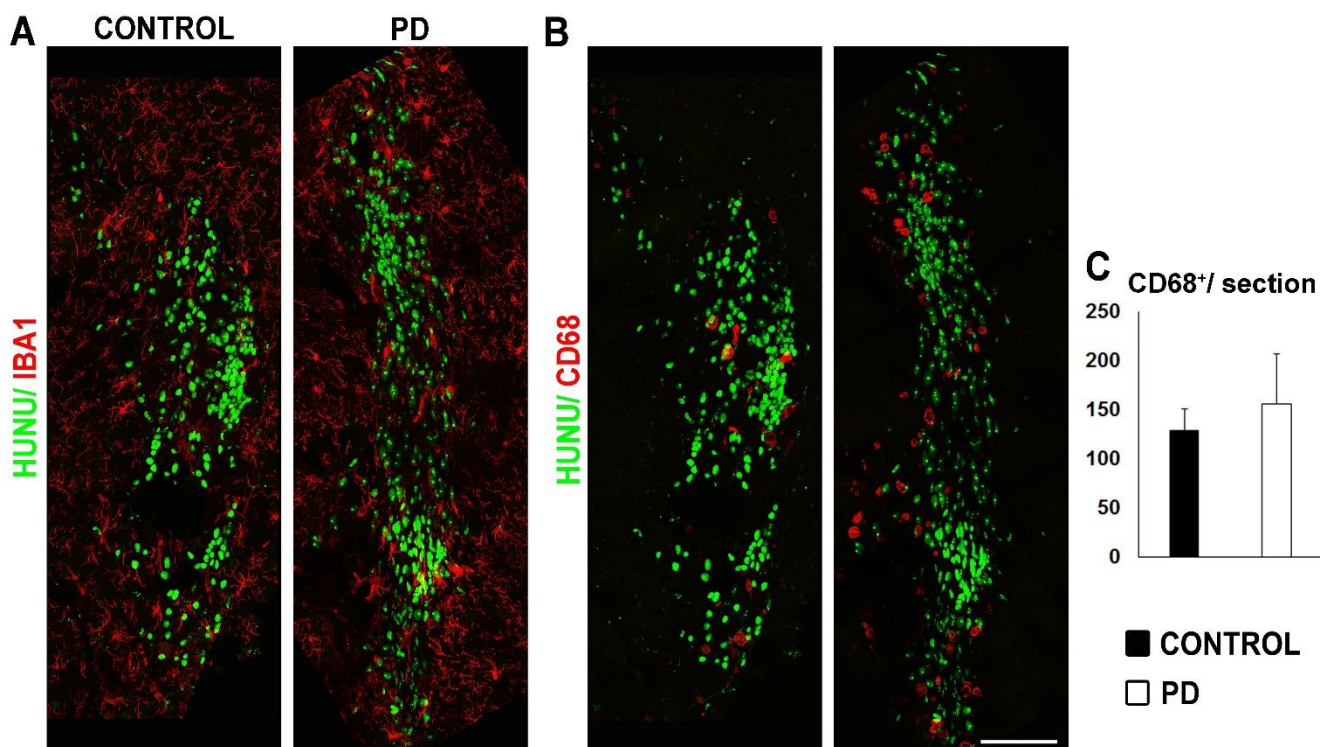


**Figure 32: Host microglial/ macrophage response.** (A) Double labeling for HuNu (green) and Iba1 (red) shows that control and PD-derived grafts are surrounded by host macrophage/microglial, presumably resting, cells. (B) Double labeling for HuNu (green) and CD68+ (red) detects activated macrophage/microglia cells within control and PD-derived grafts with no apparent differences between them. (C) Quantification of CD68+ microglial cells/ per section (control  $129 \pm 21.44$ , PD  $156 \pm 50.17$ ;  $P= 0.653$ ). Scale bar,  $100\mu\text{m}$ . Data represent mean  $\pm$  SEM.

### 5.7.3 Conclusions from the *in vivo* modeling of PD neuronal phenotypes in the 6-OHDA mouse model

Having observed morphological and functional alterations in p.A53T neurons *in vitro* both previously [420] and in the current study, we wanted to investigate whether p.A53T neurons would retain such phenotypes *in vivo*. For this purpose, either control-derived or PD-derived cells were transplanted in 6-OHDA mice. Assessment of the graft at 12 weeks after transplantation suggested that both control and PD cells survived and could differentiate to almost a similar extent. One difference we noted was an increased number of DCX-positive cells in PD grafts, suggesting that PD neurons might be stalled at this immature differentiation state, an observation that might account for their compromised ability to extend neurites and form contacts with host neurons.

Furthermore, increased  $\alpha$ Syn immunoreactivity was seen in PD grafts, as well as decreased contacts with the cells of the surrounding host brain tissue.

## 6. DISCUSSION

### 6.1 Main findings and discussion

Parkinson's disease (PD) is the second most common neurodegenerative disorder. We have previously developed a "disease-in-a-dish" model for familial PD using induced pluripotent stem cells (iPSCs) from two patients carrying the p.A53T  $\alpha$ -synuclein ( $\alpha$ Syn) mutation. By directed differentiation, we generated a model that displays disease-relevant phenotypes, including protein aggregation, compromised neurite outgrowth, axonal neuropathology and synaptic defects. In this work we investigated the *in vivo* phenotypes of iPSCs, derived from one patient, after transplantation in a lesion mouse model. We initially established a medial-forebrain bundle lesion by 6-hydroxydopamine injection, in the immunosuppressed NOD/SCID strain. However, due to high mortality rate, we didn't repeat this experiment and its initial results will not be discussed further. We proceeded by establishing a parkinsonian mouse model by unilateral intrastriatal 6-hydroxydopamine injection in the same strain. Immunohistochemistry revealed that despite the disease-related characteristics that mutant cells displayed when maintained up to 70 days *in vitro*, they could survive and differentiate *in vivo* over a 12-week period. However, some differences were noted between patient-derived and control grafts, including a significant rise in  $\alpha$ Syn immunoreactivity that might signal a first step towards pathology. Moreover, control-derived grafts appeared to integrate better than PD grafts within the host tissue extending projections that formed more contacts with host striatal neurons. Our data suggest that the distinct disease-related characteristics which p.A53T cells develop *in vitro*, may be attenuated or take longer to emerge *in vivo* after transplantation within the mouse brain. Further analysis of the phenotypes that patient cells acquire over longer periods of time as well as the use of multiple iPSC clones from different patients should extend our current proof-of-concept study and provide additional evidence for *in vivo* disease modeling.

A decade ago improved neurodegenerative disease modeling was largely dependent on the development of novel animal models in an effort to recapitulate more faithfully human pathology. Nowadays disease modeling can be performed in a human setting and in a patient-specific manner using iPSC-

derived systems. The use of human iPSCs has been instrumental in uncovering new disease phenotypes and tracking cellular responses to drugs (for review see [71]). To date a large number of hiPSC-based models have been developed by directed differentiation of patient-derived iPSCs to the appropriate neuronal phenotypes. Especially for PD, attempts have largely focused on the generation of midbrain DAergic neurons not only from patients but also from healthy subjects or even from human embryonic stem cells, with the prospect of utilizing them for transplantation therapies [466, 467, 480, 494]. As a result several protocols have been developed with varying efficiency, whilst not all iPSC clones are capable to differentiate equally well to a particular neuronal population, in this case into DAergic cells, even when the same protocol is used [378, 379, 480, 481].

Along this course, we generated several iPSC lines from two patients with familial PD, carrying the p.A53T  $\alpha$ Syn mutation. We thus developed a robust PD model characterized *in vitro* by protein aggregates, severe axonal neuropathology and defective synaptic connectivity [420]. Importantly, these disease-related characteristics could be reverted by small molecules that target  $\alpha$ Syn and prevent its aggregation. In the absence of isogenic gene-corrected control lines, the protective effects of these small molecules provide a direct link between the disease-associated phenotypes and pathological  $\alpha$ Syn [420]. The aim of the present study was to investigate the phenotype of these cells *in vivo* after transplantation in the mouse brain and investigate if the vulnerability of iPSC-derived PD neurons is retained in an *in vivo* setting or whether it might be rescued under the supportive influence of the host environment. To this end, we directed p.A53T-iPSC and corresponding control lines [420] to differentiate to the DAergic lineage by applying an efficient floor plate induction protocol that yielded approximately 50% LMX1a/FOXA2-positive progenitors at 11 DIV, a percentage compatible with previous reports [480]. To remove unwanted cells that might cause graft overgrowth, we performed an enrichment in PSA-NCAM-expressing cells, which is known to result in a neuronal population with constrained proliferation potential and enhanced transplantation efficacy [488, 490, 517]. This work is the first description of an *in vivo* assessment of patient-derived cells carrying the p.A53T mutation, with the limitation that a single clone from a patient and a control subject were used. It therefore represents a proof-

of concept or in other words, a “case study” of the survival and behavior of the mutant cells in the lesioned striatum of immunocompromised mice.

Because in the current study we applied a different differentiation protocol to that previously reported in [420], we considered it necessary to assess the emergence of disease phenotypes in our cultures. *In vitro* characterization revealed similar profiles between control and p.A53T cells at the time of their transplantation (30 DIV) in 6-OHDA lesioned immunodeficient mice. However in more prolonged cultures up to 70 DIV, PD cells displayed significant morphological and functional alterations. This analysis uncovered both novel and previously identified defective phenotypes. In particular, we showed here for the first time that DCX-positive neurons showed abnormal neurite patterning with increased primary and secondary branching. Moreover, TH-positive neurons exhibited distorted and fragmented neurites indicative of neurodegeneration, as previously reported [420]. DCX is a microtubule-associated protein known for its involvement in neuronal migration and, more particularly, in the maintenance of bipolar shape in migrating neurons [518]. DCX is also important for proper dendritic development and remodeling [519]. Interestingly, it has been shown that DCX-positive immature neurons with LRRK2 deficiency, a gene associated with monogenetic PD, exhibit extended neuritic development and more complex arborization [520], a phenotype similar to our current observations.

Given the presence of intracellular protein aggregates detected here in both DCX-positive and TH-positive neurons, it is not surprising that PD cultures exhibited overt degeneration traits, in agreement with our previous observations [420] and other reports [247, 259, 428]. Emerging evidence suggests that a number of underlying mechanisms in neurodegenerative diseases are closely linked to neuritic maintenance, synaptic transmission and neuronal connectivity. Our electrophysiological analysis showed similar active and passive membrane properties between control and PD cells, in agreement with our previous observations [420]. Yet calcium imaging in p.A53T-neurons that was performed here for the first time, revealed higher frequency and amplified calcium transients, which is likely to impact on the identified phenotypes of p.A53T cells. It is known that calcium oscillations play critical roles in neuronal development and differentiation affecting neurite outgrowth

and the formation of synaptic connections [521, 522]. Previous studies have shown calcium dysregulation in hiPSC-derived neurons from PD patients carrying the LRRK2 G2019S mutation [523] or mutations in the PD-linked gene GBA1 [415] as well as in hiPSC-derived neurons from patients with frontotemporal lobar degeneration tauopathy [524]. The observed altered network activity, along with the aberrant neurite branching observed in PD neurons, are in line with a defect in synaptic maturation and plasticity [525].

We next addressed whether the *in vitro* observed vulnerability of p.A53T neurons would be retained *in vivo*. The 6-OHDA lesion that results in loss of nigral dopamine neurons has been first established in rats as a PD model [526] and later in mice due to development of a large number transgenic mouse models for PD studies [463, 527, 528]. The majority of studies engaging differentiated derivatives of human pluripotent stem cells for transplantation use immunosuppressed rodent models where integration and functionality are assessed both histologically and behaviorally. Our data from two different tests for evaluation of motor activity in the 6-OHDA lesioned NOD/SCID mice were rather unexpected. In both tests a significant restoration of behavioral deficits occurred spontaneously in mice without transplantation. We postulate a cross-hemispheric contribution of dopaminergic fiber sprouting. Contrary to the long-standing belief that dopamine neurons project unilaterally, a recent study has demonstrated that dopamine neurons have cross-hemispheric projections with functional significance [529]. Most interestingly, and in support of our findings, the authors of this study showed that in animals with a unilateral 6-OHDA lesion, contralateral projections could be stimulated with amphetamine to evoke dopamine release in the lesioned striatum, raising important concerns when using this experimental approach to evaluate the efficacy of transplanted cells in pre-clinical studies.

Subsequently we focused on immunohistochemical analysis of the graft and the surrounding host environment. Assessment of the graft at 12 weeks after transplantation suggested that both control and PD cells survived and could differentiate to a similar extent despite the pathological features that these cells displayed *in vitro*. One difference we noted was an increased number of DCX-positive cells in PD grafts, suggesting that PD neurons might be stalled at this immature differentiation state, an observation that might account for their

compromised ability to extend neurites and form contacts with host neurons. Considering the limited numbers of TH-positive neurons present in both control and PD grafts it is desirable to examine in future studies longer time points, exceeding 6 months after transplantation, which is a challenging task taking into consideration the increased mortality rate of the 6-OHDA lesioned NOD/SCID mice. Long-term studies are also needed to clarify whether the elevation in  $\alpha$ Syn immunoreactivity seen in PD grafts (this study with p.A53T- $\alpha$ Syn grafts and [468] with LRRK2-G2019S grafts) - a phenotype that cannot be attributed to their more immature state - would eventually result in a pathological phenotype with formation of protein aggregates in mature neurons. Another issue is whether p.A53T pathology can spread from the graft to the host environment. Cell to cell seeding of  $\alpha$ Syn and transmission of pathology from patient to healthy human neurons has been recently observed *in vitro* [428]. Whether this may also occur *in vivo* remains to be seen.

Despite similarities, the observed differences between control and PD grafts should not be overlooked as they may be intensified overtime affecting their integration within the tissue. Control-derived grafts tended to intermingle more efficiently at 12 weeks with the host tissue whilst PD grafts retained sharply demarcated boundaries. This was accompanied by a decreased number of PD graft-derived projections onto host medium spiny neurons. This may be explained either by an increased permissiveness of the host tissue to healthy human neurons or by the compromised ability of human PD neurons to form synaptic contacts [420]. Under this light, further analysis of the phenotypes that patient cells acquire over longer periods of time as well as the use of multiple iPSC clones from different patients should extend our current proof-of-concept study and provide additional evidence for *in vivo* disease modeling.

## **6.2 Limitations of the study**

As already mentioned, the results presented in this study are based on an iPSC line from one PD patient carrying the p.A53T mutation (PD) and an iPSC line from one age-matched healthy individual (control). This is a limitation, since iPSCs are known to exhibit line-to-line variations (rev. by [357, 530] and therefore we recognize that in the future the use of multiple iPSC clones from different patients should extend our “case study”. Nevertheless,

we would like to stress the challenging nature of such studies, which are particularly labor intensive and also require a large number of animals to yield meaningful results while it is a major task to synchronize human iPSC-derived immature neurons with the mice.

The past few years, genome editing technologies have enabled the introduction of genetic changes into iPSCs in a site-specific manner, including correction of disease-causing gene mutations in patient-derived cells. These approaches enable the generation of genetically matched, isogenic corrected iPSC lines, enabling identification of pathological features in cells with an identical genetic background (rev. by [357]). In line with this, gene corrected iPSC clones are being generated in our laboratory, which should enable direct comparisons between isogenic lines. This strategy should also limit the number of clones to be tested and hence the number of animals required.

The use of immunocompromised NOD/SCID mice, which is necessary for xenotransplantation to avoid graft rejection, presented an additional constraint. These animals are very fragile by their nature and experiments were conducted in the SPF-free part of the Institute's Animal Facility. Mice had to weigh at least 25 gr for these experiments so that they would withstand surgery and 6-OHDA treatment while they required specific post-operative care, otherwise they would die because of wasting and dehydration due to lack of appetite for food and water. Therefore the 6-OHDA lesion was introduced in adult mice of 3 months of age (younger animals did not reach the right weight) and transplantation was performed after 3 weeks, which allowed on one hand animals to recover and on the other, cells to be introduced into a less toxic environment. These mandatory manipulations left us with a relatively short time window (up to 12 weeks) to study the cells *in vivo* due to the leakage in the immunodeficiency phenotype in this particular mouse strain ([www.envigo.com](http://www.envigo.com)). So, for a longer time period analysis, an alternative mouse strain or animal model may be employed.

Finally, despite the great animal care that was taken in this study, the lethality after unilateral injection of 6-OHDA in the medial forebrain bundle was so high (>85%) that we had to change our model to the milder unilateral intrastriatal lesion. Even so the lethality rate was above 40%. Moreover, from the animals that did survive the lesion only 50% developed the desired

phenotype. Thus, the overall *in vivo* analysis was performed in a relatively small number of transplanted animals up to 12 weeks which is a rather short time for human neurons to differentiate *in vivo*.

Despite the difficulties encountered, some quite unexpected results emerged such as the spontaneous motor recovery of the lesioned animals. Moreover, our study has laid the background for future investigations towards development of *in vivo* models to study the properties of patient-derived A53T cells.

### **6.3 Future research directions**

The present study is the first to provide evidence of the survival and behavior of the mutant A53T cells in the lesioned striatum of immunocompromised mice. However, because of the limitations described above we sought to develop an alternative mouse model that involves the generation of a chimeric human-mouse brain after intracerebral transplantation of iPSC-derived neuronal precursors in neonatal (at postnatal day 1) immunocompromised NOD/SCID mice. This model should give us the opportunity to investigate the ability of p.A53T-derived cells to integrate and differentiate *in vivo* during longer periods of time, up to 6 months. Stem cell derived neuronal precursors have been already shown to integrate efficiently in the mouse brain resulting in specific patterns of neuronal maturation, connectivity, and synaptic activity after transplantation in neonatal mice [531-533], allowing for the *in vivo* study of these cells. It remains, indeed, crucial to complement *in vitro* approaches with *in vivo* experiments to study human neurons in the context of the brain. Towards these lines we performed some initial studies that should pave the way towards development of such hybrid A53T human-mouse brains. In particular, iPSCs from control lines were differentiated to neuroepithelial stem/progenitor cells with dual SMAD inhibition to promote neural induction, (based on [376]). The cells were injected in the cortex of neonatal mice (postnatal day 1, p1) of the NOD/SCID strain and immunohistochemical analysis followed after 3 weeks. The cells managed to survive and integrate into the host brain and analysis of longer time points is in progress.

Another approach would be the development of brain organoids that would allow the study of A53T pathology in an environment closer to the human situation. Although brain organoids can be maintained only for a limited time *in vitro*, we anticipate that they may be useful for investigating A53T pathology in a more complex environment. Our *in vitro* data where we could identify pathological traits in rather young neurons support our expectations. Finally, it has been shown that brain organoids generated *in vitro* can survive for longer after transplantation in the mouse brain as they become vascularized and do not die of hypoxia (ref). We envisage that these state-of-the-art approaches should shed light into the early mechanisms of PD pathogenesis and provide novel disease targets as well as potential disease-modifying treatments.

## 7. EXTENDED ABSTRACT

Parkinson's disease (PD) is the second most common neurodegenerative disorder characterized by motor and non-motor symptoms arising from loss of striatal-projecting dopaminergic neurons of the substantia nigra pars compacta as well as of other types of neurons throughout the brain. Even though it is still unknown whether dopamine neuron degeneration is an initial disease feature or the inevitable consequence of multiple dysfunctions throughout the brain, it represents a common pathological manifestation in PD and is responsible for many of the clinical symptoms. A major neuropathological hallmark of PD is the presence of intracellular protein aggregates in the cell bodies and neurites of affected neurons, respectively termed Lewy bodies and Lewy neurites, which are mainly composed of  $\alpha$ -synuclein ( $\alpha$ Syn). This is a small pre-synaptic protein whose physiological function is still under investigation, yet its pathological involvement in PD is widely accepted.  $\alpha$ Syn is the major sporadic PD linked gene, whereas point mutations and multiplications of the locus cause an autosomal dominant form of the disease, often characterized by early onset and a generally severe phenotype. The best-studied  $\alpha$ Syn mutation is p.A53T (G209A in the *SNCA* gene), first identified in families of Italian and Greek ancestry. Although the majority of PD cases are sporadic, studies on familial forms that are clinically and neuropathologically similar to sporadic PD have assisted in gaining insights into PD etiopathology.

Although 200 years have elapsed since the disease was first described and despite intensive research efforts towards understanding the disease using animal models and post-mortem human brain tissues, the causes that lead to the appearance and progression of PD remain largely unresolved. Moreover, there is an unmet need for the development of effective therapies since currently available treatments address the symptoms, but do not cure the disease. A major drawback has been the lack of appropriate models simulating efficiently the human disease. As a consequence several therapeutic approaches that appeared promising at a preclinical level, failed to deliver the expected results when tested in clinical trials. Nowadays the advent of cell reprogramming technologies and the generation of induced pluripotent stem cells (iPSCs) have opened up new prospects for understanding PD

pathogenesis and progression in a patient-specific setting. These approaches allow the generation of patient-derived disease models by directed differentiation of iPSCs to the desired cell types of the brain and also offer the possibility for drug discovery or repositioning in a human setting.

In recent years several studies have used iPSC-based cellular systems generated from patient cells as a valuable means for modeling PD *in vitro*. These investigations revealed a number of disease-associated phenotypes, including increased sensitivity to oxidative and nitrosative stress, mitochondrial deficits, and axonal defects and synaptopathy. In a 2017 collaborative study led by Kouroupi et al. at the Laboratory of Cellular and Molecular Neurobiology – Stem Cells of the Hellenic Pasteur Institute, a disease-in-a-dish model for familial PD was developed using induced pluripotent stem cells (iPSCs) from two patients carrying the p.A53T  $\alpha$ -synuclein ( $\alpha$ Syn) mutation. By directed differentiation, a PD model was generated that displays protein aggregation, compromised neurite outgrowth, axonal neuropathology and synaptic defects [420].

In this work we aimed to answer whether the vulnerability of these p.A53T (designated PD) iPSC-derived neurons is also retained in an *in vivo* setting after transplantation in the rodent brain. Towards this, we investigated the *in vivo* phenotypes of iPSC-derived cells from one p.A53T patient in comparison to control iPSCs derived from a healthy donor, after transplantation in a lesion mouse model established by unilateral intrastriatal 6-hydroxydopamine (6-OHDA) injection in the immunosuppressed NOD/SCID strain. To direct the differentiation of control and PD iPSC lines towards the dopaminergic lineage, we applied a floor plate induction protocol that involves the use of a cocktail of small molecules that either inhibit the BMP/ TGF- $\beta$ / Activin pathways or activate the sonic hedgehog pathway and WNT signaling followed by neuronal differentiation-promoting factors. At the end of floor plate induction (11 days *in vitro*; DIV), practically all cells were LMX1A-positive floor plate neuroepithelial cells and about 50% were LMX1A/FOXA2-positive dopaminergic precursors. Engraftable neurons were obtained with this protocol after 25 DIV, and in order to avoid cellular overgrowth, further enrichment in PSA-NCAM-positive neuronal cells was achieved at 28 DIV by isolation on magnetic beads covered with an antibody against PSA-NCAM. Sorted cells comprised primarily of

immature neurons (approximately 70%) as assessed by expression of the neuronal lineage markers doublecortin (DCX) and  $\beta$ III-Tubulin while a proportion were nestin-positive neuronal precursors, with no statistically significant differences between control and PD cells.

Because the differentiation protocol used in this work was different from that previously reported in the Kouroupi study [420], before proceeding to *in vivo* transplantation we addressed the phenotype of PD cultures maintained for longer periods of time *in vitro*, in terms of cell morphology and functionality that included electrophysiological recordings and calcium imaging. In PD cells analyzed between 45-70 DIV, degeneration signs became apparent. DCX-positive immature PD neurons exhibited aberrant neuritic growth whilst intracellular protein aggregates were detected in both DCX- and tyrosine hydroxylase-positive (TH) dopaminergic PD neurons. Additionally TH-positive PD cells, which formed a dense network at 70 DIV, displayed dystrophic neurites with swollen varicosities that quite often ended up in fragmented processes. Up-regulation of  $\alpha$ Syn protein, indicative of pathology, was also noted in PD neurons as compared to controls. In terms of functionality, electrophysiological recordings did not reveal statistically significant differences on active and passive membrane properties between control and PD cells. Interestingly, however, calcium imaging demonstrated a higher frequency of spontaneous calcium transients in PD cells with a significantly larger mean amplitude. As calcium dynamics regulate neurite growth and synaptic connectivity, the observed alterations in calcium signaling should impact on, and explain, the morphological phenotypes of PD neurons.

To investigate the *in vivo* phenotype of PSA-NCAM-enriched iPSC-derived cells at 30 DIV, we established a 6-hydroxydopamine (6-OHDA) lesioned mouse model in the NOD/SCID strain that supports xenograft survival. A unilateral lesion was induced by intrastriatal injection of 6-OHDA in 9-10 week old mice and the resulting functional deficit was confirmed 2 weeks later using drug-induced and drug-free behavioral analysis. However, functional analysis in longer time periods up to 15 weeks revealed a spontaneous behavioral recovery in the lesioned animals. Although a 60% loss of TH-positive neurons was verified by immunohistochemistry in the substantia nigra which remained stable over 15 weeks, striatal dopaminergic reinnervation was observed in

agreement with the concurrent behavioral recovery. This phenomenon could be explained by sprouting of remaining undamaged dopaminergic fibers within the ipsilateral lesioned striatum and/or by a cross-hemispheric compensatory mechanism by which TH fibers originating in the contralateral substantia nigra are induced to project into the ipsilateral striatum.

Next, we proceeded to cell transplantation and immunohistochemical analysis of the graft and the surrounding host environment. To investigate their phenotypic characteristics *in vivo*, control and PD iPSC-derived PSA-NCAM-enriched cells (30 DIV) were transplanted 3 weeks after 6-OHDA injection and immunohistochemical analysis followed after another 12 weeks. The analysis revealed that despite the disease-related characteristics that PD cells displayed when maintained up to 70 DIV, they could survive and differentiate *in vivo* over a 12-week period. However, interesting differences were noted between patient-derived and control grafts. First, a significant rise in  $\alpha$ Syn immunoreactivity was noted in PD grafted cells indicative of a first step towards pathology. Second, control-derived grafts appeared to integrate better than PD grafts within the host tissue extending projections that formed more contacts with host striatal neurons. Third, significantly more DCX-positive immature neurons were found in PD derived grafts as compared to controls, suggesting that PD neurons are stalled at this immature differentiation state. This observation is likely to account for their compromised ability to extend neurites and form contacts with host neurons.

Overall our data suggest that the distinct disease-related characteristics which p.A53T cells develop *in vitro*, may be attenuated or take longer to emerge *in vivo* after transplantation within the mouse brain. Considering the limited numbers of TH-positive neurons present in both control and PD grafts it is desirable to examine in future studies longer time points, exceeding 6 months after transplantation, which is a challenging task given the increased mortality rate of the 6-OHDA lesioned NOD/SCID mice. Long-term studies are also needed to clarify whether the elevation in  $\alpha$ Syn immunoreactivity seen in PD grafts - a phenotype that cannot be attributed to their more immature state - would eventually result in a pathological phenotype with formation of protein aggregates in mature neurons. Another issue is whether p.A53T pathology can spread from the graft to the host environment. Cell to cell seeding of  $\alpha$ Syn and

transmission of pathology from patient to healthy human neurons has been recently observed *in vitro*. Whether this may also occur *in vivo* remains to be seen.

To conclude, further analysis of the phenotypes that patient cells acquire over longer periods of time as well as the use of multiple iPSC clones from different patients should extend our current proof-of-concept study and provide additional evidence for *in vivo* disease modeling.

## 8. ΕΚΤΕΤΑΜΕΝΗ ΠΕΡΙΛΗΨΗ

Η νόσος Πάρκινσον (ΝΠ) είναι η δεύτερη σε συχνότητα νευροεκφυλιστική διαταραχή και χαρακτηρίζεται από την απώλεια των ντοπαμινεργικών νευρώνων της συμπαγούς μοίρας της μέλαινας ουσίας που προβάλλουν τις απολήξεις τους στο ραβδωτό σώμα, καθώς και άλλων τύπων νευρώνων σε όλη την έκταση του εγκεφάλου. Μέχρι σήμερα δεν γνωρίζουμε αν η εκφύλιση των ντοπαμινεργικών νευρώνων είναι η αιτία της έναρξης της ασθένειας ή αποτελεί την αναπόφευκτη συνέπεια πολλαπλών δυσλειτουργιών στον εγκέφαλο, ωστόσο αντιπροσωπεύει ένα κοινό παθολογικό χαρακτηριστικό που ευθύνεται για πολλά από τα κλινικά συμπτώματα. Μείζον νευροπαθολογικό γνώρισμα της ΝΠ είναι η συσσώρευση ενδοκυττάριων πρωτεϊνικών συσσωματωμάτων στα σώματα και τους νευρίτες των προσβεβλημένων νευρώνων, στα οποία εντοπίζεται κατά κύριο λόγο η πρωτεΐνη α-συνουκλεΐνη (αSyn). Η αSyn είναι μικρή προσυναπτική πρωτεΐνη της οποίας η φυσιολογική λειτουργία δεν έχει διαλευκανθεί επαρκώς, ωστόσο η συμμετοχή της στην παθολογία της ΝΠ είναι ευρέως αποδεκτή. Στη συντριπτική πλειοψηφία των περιπτώσεων, η νόσος είναι σποραδική και πιθανώς οφείλεται στο συνδυασμό γενετικών και περιβαλλοντικών παραγόντων κινδύνου. Σε μια μειοψηφία περιπτώσεων (5-10%) η νόσος είναι κληρονομική με την ύπαρξη μεταλλάξεων σε συγκεκριμένα γονίδια. Το γονίδιο *SNCA* που κωδικοποιεί την πρωτεΐνη αSyn συνδέεται με τη ΝΠ ενώ σημειακές μεταλλάξεις και διπλασιασμός ή τριπλασιασμός του γονιδιακού τόπου προκαλούν μία αυτοσωμική επικρατή μορφή της νόσου, που συχνά χαρακτηρίζεται από πρόωμη έναρξη και γενικά σοβαρό φαινότυπο. Η σημειακή μετάλλαξη αντικατάστασης G209A στο γονίδιο *SNCA* που συνεπάγεται τη σύνθεση της παθολογικής πρωτεΐνης p.A53T αSyn προσδιορίστηκε για πρώτη φορά σε οικογένειες ιταλικής και ελληνικής καταγωγής και αποτελεί την καλύτερα μελετημένη μετάλλαξη. Αν και η πλειοψηφία των περιπτώσεων της νόσου είναι σποραδικές, οι μελέτες σε οικογενείς μορφές που είναι κλινικά και νευροπαθολογικά παρόμοιες με τις σποραδικές συνέβαλαν σημαντικά στην κατανόηση της ΝΠ.

Παρότι η ΝΠ περιγράφηκε για πρώτη φορά πριν 200 χρόνια και παρά τις έκτοτε εντατικές έρευνες σε ζωικά πειραματικά μοντέλα ή μεταθανάτιους ιστούς ανθρώπινου εγκεφάλου, οι αιτίες που ευθύνονται για την εμφάνιση και την

εξέλιξη της νόσου παραμένουν σε μεγάλο βαθμό αδιευκρίνιστες. Ένας σημαντικός ανασταλτικός παράγοντας ήταν η έλλειψη κατάλληλων μοντέλων που προσομοιάζουν επαρκώς τα χαρακτηριστικά της ασθένειας στον άνθρωπο. Έτσι θεραπευτικές προσεγγίσεις, πολλά υποσχόμενες σε προκλινικό επίπεδο, απέτυχαν όταν έφτασαν σε κλινικές δοκιμές. Σήμερα η επαναστατική τεχνολογία του κυτταρικού επαναπρογραμματισμού και η κατασκευή επαγόμενων πολυδύναμων βλαστικών κυττάρων (iPSCs) από ενήλικα σωματικά κύτταρα ασθενών άνοιξαν νέες προοπτικές για την κατανόηση της ΝΠ. Οι προσεγγίσεις αυτές επιτρέπουν τη δημιουργία εξατομικευμένων κυτταρικών μοντέλων για τη μελέτη της παθογένειας και της εξέλιξης της ΝΠ και δίνουν μοναδικές ευκαιρίες για την ανακάλυψη ή επανατοποθέτηση φαρμάκων.

Σε διάφορα μοντέλα που αναπτύχθηκαν την τελευταία επταετία με βάση την τεχνολογία των iPSCs από κύτταρα ασθενών και τη στοχευμένη διαφοροποίηση τους σε νευρώνες, αναδείχθηκαν φαινότυποι που σχετίζονται με τη ΝΠ, όπως αυξημένη ευαισθησία σε οξειδωτικό ή νιτρώδες στρες, μιτοχονδριακές ανωμαλίες, νευραξονική παθολογία και μειωμένη συναπτική συνδεσιμότητα. Στο Εργαστήριο Κυτταρικής και Μοριακής Νευροβιολογίας και Βλαστικών Κυττάρων του Ελληνικού Ινστιτούτου Παστέρ, αναπτύχθηκε ένα *in vitro* μοντέλο για οικογενή ΝΠ με χρήση iPSCs από δύο ασθενείς που φέρουν τη μεταλλαγή p.A53T- $\alpha$ Syn. Με κατευθυνόμενη διαφοροποίηση δημιουργήθηκε ένα κυτταρικό σύστημα που εμφανίζει νευροεκφυλιστικούς φαινοτύπους σχετιζόμενους με τη ΝΠ, όπως συσσώρευση πρωτεϊνικών συσσωματωμάτων, μειωμένη συναπτική συνδεσιμότητα και παθολογία των νευραξόνων [420]. Στην παρούσα μελέτη διερευνήσαμε τους *in vivo* φαινοτύπους των κυττάρων αυτών μετά από μεταμόσχευση σε μοντέλο ποντικού στο οποίο είχε προκληθεί βλάβη με μονόπλευρη έγχυση 6-υδροξυνοτοπαμίνης (6-OHDA) στο ραβδωτό σώμα του εγκεφάλου ποντικών του ανοσοκατασταλμένου στελέχους NOD/SCID. Για τον σκοπό αυτό, εφαρμόσαμε ένα πρωτόκολλο επαγωγής εδαφιαίου νευρικού πετάλου σε iPSC κυτταρικές σειρές προερχόμενες από έναν p.A53T ασθενή και έναν υγιή δότη προκειμένου να διαφοροποιηθούν προς τη ντοπαμινεργική γενεαλογία. Το πρωτόκολλο αυτό περιλαμβάνει μείγμα μικρών μορίων που αποτελούν είτε αναστολείς των μονοπατιών BMP/ TGF- $\beta$ / Activin είτε επαγωγείς του μονοπατιού sonic hedgehog και του μονοπατιού

σηματοδότησης WNT, ακολουθούμενο από παράγοντες που ευνοούν τη στοχευμένη διαφοροποίηση σε νευρώνες. Με αυτό το πρωτόκολλο, την ημέρα 11 *in vitro* (11 DIV) πρακτικά όλα τα κύτταρα στην καλλιέργεια είναι θετικά για τον μεταγραφικό παράγοντα LMX1A που χαρακτηρίζει τα νευροεπιθηλιακά κύτταρα του εδαιφιαίου πετάλου ενώ περίπου τα μισά είναι διπλά θετικά για τους παράγοντες LMX1A και FOXA2 που χαρακτηρίζουν τα πρόδρομα κύτταρα της ντοπαμινεργικής γενεαλογίας. Νευρώνες κατάλληλοι για μεταμόσχευση αποκτήθηκαν μετά από 25 DIV και για να αποφευχθούν φαινόμενα υπερπλασίας *in vivo*, εφαρμόστηκε ανοσοεμπλουτισμός σε νευρωνικά κύτταρα με τη βοήθεια μαγνητικών σφαιριδίων επικαλυμμένων με αντίσωμα έναντι PSA-NCAM κατά την ημέρα 28 DIV. Πειράματα ανοσοφθορισμού την ημέρα 30 DIV, ακριβώς κατά τον χρόνο της μεταμόσχευσης, έδειξαν ότι η καλλιέργεια απαρτιζόταν κατά 70% από ανώριμους νευρώνες θετικούς για τους μάρτυρες της πρώιμης νευρικής διαφοροποίησης διπλοκορτίνη (DCX) και βIII-τουμπουλίνη ενώ σημαντικό ποσοστό παρέμενε θετικό για τον μάρτυρα των πρόδρομων νευρικών κυττάρων, νεστίνη. Δεν βρέθηκαν στατιστικά σημαντικές διαφορές μεταξύ των δύο καλλιεργειών.

Δεδομένου ότι το πρωτόκολλο στοχευμένης διαφοροποίησης που εφαρμόστηκε στην παρούσα μελέτη διέφερε από αυτό που εφαρμόστηκε στην εργασία των Κουρουρί και συνεργατών [420], κρίναμε σκόπιμο να διερευνήσουμε τα χαρακτηριστικά που αποκτούν οι καλλιέργειες από PD και υγιή δότη σε διάστημα μακρότερο των 30 ημερών, πριν προχωρήσουμε στη μεταμόσχευσή τους. Εξετάσαμε παραμέτρους που αφορούν στη μορφολογία και τη λειτουργικότητα των κυττάρων με ανοσοφθορισμό, ηλεκτροφυσιολογικές καταγραφές και απεικόνιση ιόντων ασβεστίου. Ανάλυση μεταξύ των ημερών 45-70 DIV έδειξε ότι τα PD κύτταρα παρουσίασαν εμφανή σημάδια εκφύλισης. Ανώριμοι PD νευρώνες θετικοί για διπλοκορτίνη (DCX) εμφάνισαν αυξημένες νευριτικές εκφύσεις και δευτερογενείς διακλαδώσεις ενώ ανιχνεύθηκε ενδοκυττάρια συσσώρευση πρωτεϊνών τόσο σε DCX-θετικούς νευρώνες όσο και σε ώριμους ντοπαμινεργικούς νευρώνες θετικούς για το ένζυμο υδροξυλάση της τυροσίνης (TH). Σε PD καλλιέργειες των 70 DIV, τα πυκνά δίκτυα των TH-θετικών νευρώνων παρουσίαζαν δυστροφικούς και κατακερματισμένους νευρίτες. Παρατηρήθηκε επίσης αυξημένη έκφραση της πρωτεΐνης αSyn, που αποτελεί παθολογική ένδειξη. Όσον αφορά τη λειτουργικότητα, οι

ηλεκτροφυσιολογικές καταγραφές δεν έδειξαν στατιστικά σημαντικές διαφορές μεταξύ των PD και υγιών νευρώνων στις ενεργητικές και παθητικές μεμβρανικές ιδιότητες. Η ακεραιότητα του νευρωνικού δικτύου σε PD και υγιείς καλλιέργειες αξιολογήθηκε με απεικόνιση των ιόντων ασβεστίου. Η μέθοδος φανέρωσε συχνότερες αυθόρμητες διακυμάνσεις στις συγκεντρώσεις του ενδοκυττάρου ασβεστίου στις PD καλλιέργειες σε σύγκριση με αυτές από υγιή δότη, με μεγαλύτερο μέσο εύρος διακύμανσης. Η παρατήρηση αυτή έχει ιδιαίτερο ενδιαφέρον, δεδομένου ότι οι διακυμάνσεις των ιόντων ασβεστίου ρυθμίζουν πλήθος βιολογικών διεργασιών, μεταξύ των οποίων την αύξηση των νευριτών και τη συναπτική συνδεσιμότητα, όπου παρατηρούνται σημαντικές διαφορές μεταξύ PD και υγιών κυττάρων.

Στη συνέχεια, προκειμένου να διερευνήσουμε τις ιδιότητες των PD κυττάρων *in vivo* μετά από μεταμόσχευση στον εγκέφαλο, χρησιμοποιήσαμε ένα μοντέλο χημικής βλάβης που αναπτύχθηκε μετά από στερεοτακτική έγχυση της τοξίνης 6-υδροξυνοτοπαμίνης (6-OHDA) στο ραβδωτό σώμα ποντικών του στελέχους NOD/SCID, το οποίο υποστηρίζει την επιβίωση ξενομοσχεύματος. Η 6-OHDA προκαλεί την ανάδρομη εκφύλιση των TH θετικών νευρώνων της μέλαινας ουσίας με αποτέλεσμα την εμφάνιση κινητικής δυσλειτουργίας. Δύο εβδομάδες μετά την έγχυση της τοξίνης, η συμπεριφορική ανάλυση των ποντικών επιβεβαίωσε την προκαλούμενη καταστροφή τόσο με αξιολόγηση της επαγόμενης με αμφεταμίνη στροφικής ασυμμετρίας όσο και με καταγραφή της κινητικής δραστηριότητας των προσθίων και οπισθίων άκρων χωρίς τη χορήγηση αμφεταμίνης. Ωστόσο η λειτουργική ανάλυση σε μεγαλύτερο χρόνο, έως 15 εβδομάδες μετά την πρόκληση της βλάβης, αποκάλυψε την αυθόρμητη ανάκαμψη της κινητικής συμπεριφοράς των ποντικών. Ακόμη, αν και η απώλεια των ντοπαμινεργικών νευρώνων της μέλαινας ουσίας παρέμεινε σταθερή σε ποσοστό 60% σε διάστημα 15 εβδομάδων, παρατηρήθηκε επανέγερση του ραβδωτού σώματος, όπου προβάλλουν οι ντοπαμινεργικοί νευρώνες της μέλαινας ουσίας. Η παρατηρούμενη επανέγερση του ραβδωτού είναι σύμφωνη με τη συμπεριφορική βελτίωση και μπορεί να εξηγηθεί με πιθανή εκβλάση/ ανάπτυξη των υπολειπομένων ντοπαμινεργικών απολήξεων που δεν καταστράφηκαν με τη χορήγηση 6-OHDA στο ραβδωτό ή/ και με συνεισφορά ντοπαμινεργικών ινών από το ετερόπλευρο ημισφαίριο.

Για τη μελέτη των *in vivo* χαρακτηριστικών τους, PSA-NCAM ανοσοεμπλουτισμένες καλλιέργειες νευρικών κυττάρων τόσο από PD όσο και από υγιή δότη (30 DIV), μεταμοσχεύθηκαν 3 εβδομάδες μετά την έγχυση 6-OHDA στο ραβδωτό σώμα του εγκεφάλου ποντικών του στελέχους NOD/SCID. Ανοσοϊστοχημική ανάλυση 12 εβδομάδες μετά τη μεταμόσχευση έδειξε ότι τα PD κύτταρα, παρά τα σχετιζόμενα με τη νόσο χαρακτηριστικά που παρουσίασαν έως και 70 DIV, επιβίωσαν και διαφοροποιήθηκαν *in vivo* παρόμοια με τα κύτταρα του υγιούς δότη. Ωστόσο, παρατηρήθηκαν διαφορές μεταξύ των μοσχευμάτων. Συγκεκριμένα, διαπιστώθηκε αύξηση της πρωτεΐνης αSyn στα μοσχεύματα του ασθενούς, που αποτελεί μία πρώτη παθολογική ένδειξη. Σε συμφωνία με την παρατήρηση αυτή, φάνηκε ότι τα υγιή κύτταρα ενσωματώνονται καλύτερα στον εγκέφαλο του ξενιστή σε σύγκριση με τα PD, καθώς εξέτειναν προεκβολές που σχημάτιζαν περισσότερες συνδέσεις με τους μεσαίους ακανθώδεις νευρώνες του ραβδωτού σώματος του ξενιστή. Τέλος, τα PD κύτταρα είχαν την τάση να παραμένουν σε μία πιο αδιαφοροποίητη κατάσταση σε σύγκριση με τα υγιή. Το γεγονός αυτό πιθανά εξηγεί την περιορισμένη ικανότητά τους να σχηματίζουν συνδέσεις με τα κύτταρα του ξενιστή.

Συνολικά τα αποτελέσματα της μελέτης μας δείχνουν ότι τα διακριτά χαρακτηριστικά εκφύλισης που παρουσιάζουν τα PD κύτταρα *in vitro*, εξασθενούν ή ενδεχομένως απαιτούν περισσότερο χρόνο για να εμφανιστούν *in vivo* μετά από μεταμόσχευση στον εγκέφαλο του ποντικού. Λαμβάνοντας υπόψιν το περιορισμένο ποσοστό ώριμων ντοπαμινεργικών νευρώνων στα μοσχεύματα τόσο του ασθενούς όσο και του υγιούς, είναι επιθυμητή η εξέταση των μοσχευμάτων σε μεγαλύτερα χρονικά διαστήματα, άνω του εξαμήνου, προκειμένου να δοθεί ικανός χρόνος για να διαφοροποιηθούν τα ανθρώπινα κύτταρα. Αυτό αποτελεί αρκετά δύσκολο στόχο με βάση το ποσοστό θνησιμότητας των NOD/SCID ζώων μετά τη χορήγηση 6-OHDA. Μακροχρόνιες μελέτες απαιτούνται επίσης για να διαλευκανθεί αν η αύξηση της αSyn στα μοσχεύματα του ασθενούς – χαρακτηριστικό που δεν σχετίζεται με την πιο ανώριμη κατάσταση των PD κυττάρων σε σύγκριση με τα υγιή- θα προκαλέσει εντέλει την εμφάνιση πρωτεϊνικών συσσωματωμάτων μέσα στο μόσχευμα. Ένα ακόμα ζήτημα είναι κατά πόσον η παθολογική p.A53T αSyn μπορεί να

εξαπλωθεί από το μόσχευμα στον εγκέφαλο του ξενιστή, όπως έχει δειχθεί σε *in vitro* καλλιέργειες.

Συγκεφαλαιώνοντας, η παρούσα μελέτη αποτελεί την πρώτη προσπάθεια να μελετηθεί η νόσος Πάρκινσον σε χιμαιρικό μοντέλο εγκεφάλου με μεταμόσχευση ανθρώπινων κυττάρων ασθενούς στον ποντικό. Περαιτέρω ανάλυση των φαινοτύπων που αποκτούν τα κύτταρα ασθενών σε μεγαλύτερα χρονικά διαστήματα, ενδεχομένως με τη χρήση εναλλακτικού ζωικού μοντέλου, καθώς και η ανάλυση πολλαπλών iPSC κλώνων από διαφορετικούς ασθενείς θα επεκτείνει την τρέχουσα μελέτη με σκοπό την ανάπτυξη *in vivo* χιμαιρικών μοντέλων για τη μελέτη της νόσου Πάρκινσον.

## 9. REFERENCES

1. Tysnes, O.B. and A. Storstein, *Epidemiology of Parkinson's disease*. J Neural Transm (Vienna), 2017. **124**(8): p. 901-905.
2. Odekerken, V.J., et al., *Subthalamic nucleus versus globus pallidus bilateral deep brain stimulation for advanced Parkinson's disease (NSTAPS study): a randomised controlled trial*. Lancet Neurol, 2013. **12**(1): p. 37-44.
3. Alves, G., et al., *Epidemiology of Parkinson's disease*. J Neurol, 2008. **255** Suppl 5: p. 18-32.
4. Parkinson, J., *Essay on the shaking palsy*. 1817.
5. Charcot, J.-M., *On Parkinson's disease*. In *Lectures on diseases of the nervous system delivered at the Salpêtrière*. 1872. 155-188.
6. Tretiakoff, C., *Contribution a l'etude de l'anatomie pathologique du locus niger de Soemmering avec quelques deductions relatives a la pathogenie des troubles du tonus musculaire et de la maladie de Parkinson*. 1919.
7. Carlsson, A., M. Lindqvist, and T. Magnusson, *3,4-Dihydroxyphenylalanine and 5-hydroxytryptophan as reserpine antagonists*. Nature, 1957. **180**(4596): p. 1200.
8. Dauer, W. and S. Przedborski, *Parkinson's disease: mechanisms and models*. Neuron, 2003. **39**(6): p. 889-909.
9. Jankovic, J. and R. Tintner, *Dystonia and parkinsonism*. Parkinsonism Relat Disord, 2001. **8**(2): p. 109-21.
10. Pohar, S.L. and C. Allyson Jones, *The burden of Parkinson disease (PD) and concomitant comorbidities*. Arch Gerontol Geriatr, 2009. **49**(2): p. 317-21.
11. Quencer, K., et al., *Limb-kinetic apraxia in Parkinson disease*. Neurology, 2007. **68**(2): p. 150-1.
12. Sveinbjornsdottir, S., *The clinical symptoms of Parkinson's disease*. J Neurochem, 2016. **139** Suppl 1: p. 318-324.
13. Perez-Lloret, S., et al., *Oro-buccal symptoms (dysphagia, dysarthria, and sialorrhea) in patients with Parkinson's disease: preliminary analysis from the French COPARK cohort*. Eur J Neurol, 2012. **19**(1): p. 28-37.
14. Hughes, A.J., et al., *Accuracy of clinical diagnosis of idiopathic Parkinson's disease: a clinico-pathological study of 100 cases*. J Neurol Neurosurg Psychiatry, 1992. **55**(3): p. 181-4.
15. Lees, A.J., J. Hardy, and T. Revesz, *Parkinson's disease*. Lancet, 2009. **373**(9680): p. 2055-66.
16. Schrag, A., et al., *Prediagnostic presentations of Parkinson's disease in primary care: a case-control study*. Lancet Neurol, 2015. **14**(1): p. 57-64.
17. Chaudhuri, K.R., *Autonomic dysfunction in movement disorders*. Curr Opin Neurol, 2001. **14**(4): p. 505-11.
18. Siddiqui, M.F., et al., *Autonomic dysfunction in Parkinson's disease: a comprehensive symptom survey*. Parkinsonism Relat Disord, 2002. **8**(4): p. 277-84.
19. Jost, W.H., *Autonomic dysfunctions in idiopathic Parkinson's disease*. J Neurol, 2003. **250** Suppl 1: p. 128-30.
20. Jost, W.H., *Gastrointestinal dysfunction in Parkinson's Disease*. J Neurol Sci, 2010. **289**(1-2): p. 69-73.
21. Gower, W., *A Manual of Diseases of the Nervous System*. 2nd ed. 1893, London: J. & A. Churchill. 648.
22. Doty, R.L., D.A. Deems, and S. Stellar, *Olfactory dysfunction in parkinsonism: a general deficit unrelated to neurologic signs, disease stage, or disease duration*. Neurology, 1988. **38**(8): p. 1237-44.

23. Doty, R.L., P. Shaman, and M. Dann, *Development of the University of Pennsylvania Smell Identification Test: a standardized microencapsulated test of olfactory function*. *Physiol Behav*, 1984. **32**(3): p. 489-502.
24. Mehta, S.H., J.C. Morgan, and K.D. Sethi, *Sleep disorders associated with Parkinson's disease: role of dopamine, epidemiology, and clinical scales of assessment*. *CNS Spectr*, 2008. **13**(3 Suppl 4): p. 6-11.
25. Porter, B., R. Macfarlane, and R. Walker, *The frequency and nature of sleep disorders in a community-based population of patients with Parkinson's disease*. *Eur J Neurol*, 2008. **15**(1): p. 50-4.
26. Monderer, R. and M. Thorpy, *Sleep disorders and daytime sleepiness in Parkinson's disease*. *Curr Neurol Neurosci Rep*, 2009. **9**(2): p. 173-80.
27. Onofrj, M., A. Thomas, and L. Bonanni, *New approaches to understanding hallucinations in Parkinson's disease: phenomenology and possible origins*. *Expert Rev Neurother*, 2007. **7**(12): p. 1731-50.
28. Thanvi, B.R., T.C. Lo, and D.P. Harsh, *Psychosis in Parkinson's disease*. *Postgrad Med J*, 2005. **81**(960): p. 644-6.
29. Reijnders, J.S., et al., *A systematic review of prevalence studies of depression in Parkinson's disease*. *Mov Disord*, 2008. **23**(2): p. 183-9; quiz 313.
30. Broen, M.P., et al., *Prevalence of pain in Parkinson's disease: a systematic review using the modified QUADAS tool*. *Mov Disord*, 2012. **27**(4): p. 480-4.
31. Goetz, C.G., et al., *Pain in Parkinson's disease*. *Mov Disord*, 1986. **1**(1): p. 45-9.
32. Ford, B., *Pain in Parkinson's disease*. *Mov Disord*, 2010. **25** Suppl 1: p. S98-103.
33. Dickson, D.W., et al., *Neuropathological assessment of Parkinson's disease: refining the diagnostic criteria*. *Lancet Neurol*, 2009. **8**(12): p. 1150-7.
34. Nagatsu, T., *Tyrosine hydroxylase: human isoforms, structure and regulation in physiology and pathology*. *Essays Biochem*, 1995. **30**: p. 15-35.
35. Cheng, H.C., C.M. Ulane, and R.E. Burke, *Clinical progression in Parkinson disease and the neurobiology of axons*. *Ann Neurol*, 2010. **67**(6): p. 715-25.
36. Dickson, D.W., *Neuropathology of Parkinson disease*. *Parkinsonism Relat Disord*, 2018. **46** Suppl 1: p. S30-S33.
37. Lewy, F., *Paralysis agitans. 1. Pathologische Anatomie*. 2nd ed. 1912, Berlin: Julius Springer.
38. Goedert, M., et al., *100 years of Lewy pathology*. *Nat Rev Neurol*, 2013. **9**(1): p. 13-24.
39. Kalia, L.V., et al., *Clinical correlations with Lewy body pathology in LRRK2-related Parkinson disease*. *JAMA Neurol*, 2015. **72**(1): p. 100-5.
40. Gibb, W.R. and A.J. Lees, *The relevance of the Lewy body to the pathogenesis of idiopathic Parkinson's disease*. *J Neurol Neurosurg Psychiatry*, 1988. **51**(6): p. 745-52.
41. Gomez-Tortosa, E., et al., *alpha-Synuclein immunoreactivity in dementia with Lewy bodies: morphological staging and comparison with ubiquitin immunostaining*. *Acta Neuropathol*, 2000. **99**(4): p. 352-7.
42. Kusanuki, K., et al., *Diffuse Lewy body disease manifesting as corticobasal syndrome: A rare form of Lewy body disease*. *Neurology*, 2018. **91**(3): p. e268-e279.
43. Sakamoto, M., et al., *Heterogeneity of nigral and cortical Lewy bodies differentiated by amplified triple-labeling for alpha-synuclein, ubiquitin, and thiazin red*. *Exp Neurol*, 2002. **177**(1): p. 88-94.
44. Halliday, G., et al., *The progression of pathology in longitudinally followed patients with Parkinson's disease*. *Acta Neuropathol*, 2008. **115**(4): p. 409-15.
45. Poewe, W., *Parkinson's disease and the quest for preclinical diagnosis: an interview with Professor Werner Poewe*. *Neurodegener Dis Manag*, 2017. **7**(5): p. 273-277.

46. Witt, M., et al., *Biopsies of olfactory epithelium in patients with Parkinson's disease*. *Mov Disord*, 2009. **24**(6): p. 906-14.
47. Janvin, C.C., et al., *Cognitive profiles of individual patients with Parkinson's disease and dementia: comparison with dementia with lewy bodies and Alzheimer's disease*. *Mov Disord*, 2006. **21**(3): p. 337-42.
48. Kalinderi, K., S. Bostantjopoulou, and L. Fidani, *The genetic background of Parkinson's disease: current progress and future prospects*. *Acta Neurol Scand*, 2016. **134**(5): p. 314-326.
49. Braak, H., et al., *Idiopathic Parkinson's disease: possible routes by which vulnerable neuronal types may be subject to neuroinvasion by an unknown pathogen*. *J Neural Transm (Vienna)*, 2003. **110**(5): p. 517-36.
50. Braak, H., et al., *Staging of brain pathology related to sporadic Parkinson's disease*. *Neurobiol Aging*, 2003. **24**(2): p. 197-211.
51. Braak, H., et al., *Stages in the development of Parkinson's disease-related pathology*. *Cell Tissue Res*, 2004. **318**(1): p. 121-34.
52. Hawkes, C.H., K. Del Tredici, and H. Braak, *Parkinson's disease: a dual-hit hypothesis*. *Neuropathol Appl Neurobiol*, 2007. **33**(6): p. 599-614.
53. Visanji, N.P., et al., *The prion hypothesis in Parkinson's disease: Braak to the future*. *Acta Neuropathol Commun*, 2013. **1**: p. 2.
54. Rietdijk, C.D., et al., *Exploring Braak's Hypothesis of Parkinson's Disease*. *Front Neurol*, 2017. **8**: p. 37.
55. Beach, T.G., et al., *Multi-organ distribution of phosphorylated alpha-synuclein histopathology in subjects with Lewy body disorders*. *Acta Neuropathol*, 2010. **119**(6): p. 689-702.
56. Sulzer, D., *Multiple hit hypotheses for dopamine neuron loss in Parkinson's disease*. *Trends Neurosci*, 2007. **30**(5): p. 244-50.
57. Desplats, P., et al., *Combined exposure to Maneb and Paraquat alters transcriptional regulation of neurogenesis-related genes in mice models of Parkinson's disease*. *Mol Neurodegener*, 2012. **7**: p. 49.
58. Hutson, C.B., et al., *Traumatic brain injury in adult rats causes progressive nigrostriatal dopaminergic cell loss and enhanced vulnerability to the pesticide paraquat*. *J Neurotrauma*, 2011. **28**(9): p. 1783-801.
59. Peng, J., M.L. Oo, and J.K. Andersen, *Synergistic effects of environmental risk factors and gene mutations in Parkinson's disease accelerate age-related neurodegeneration*. *J Neurochem*, 2010. **115**(6): p. 1363-73.
60. Peng, J., et al., *Iron and paraquat as synergistic environmental risk factors in sporadic Parkinson's disease accelerate age-related neurodegeneration*. *J Neurosci*, 2007. **27**(26): p. 6914-22.
61. Ritz, B.R., et al., *Dopamine transporter genetic variants and pesticides in Parkinson's disease*. *Environ Health Perspect*, 2009. **117**(6): p. 964-9.
62. Engelender, S. and O. Isacson, *The Threshold Theory for Parkinson's Disease*. *Trends Neurosci*, 2017. **40**(1): p. 4-14.
63. Dijkstra, A.A., et al., *Evidence for Immune Response, Axonal Dysfunction and Reduced Endocytosis in the Substantia Nigra in Early Stage Parkinson's Disease*. *PLoS One*, 2015. **10**(6): p. e0128651.
64. Bereczki, E., et al., *Synaptic proteins predict cognitive decline in Alzheimer's disease and Lewy body dementia*. *Alzheimers Dement*, 2016. **12**(11): p. 1149-1158.
65. Koch, J.C., et al., *Alpha-Synuclein affects neurite morphology, autophagy, vesicle transport and axonal degeneration in CNS neurons*. *Cell Death Dis*, 2015. **6**: p. e1811.

66. Nemani, V.M., et al., *Increased expression of alpha-synuclein reduces neurotransmitter release by inhibiting synaptic vesicle recluster after endocytosis*. *Neuron*, 2010. **65**(1): p. 66-79.
67. Vargas, K.J., et al., *Synucleins Have Multiple Effects on Presynaptic Architecture*. *Cell Rep*, 2017. **18**(1): p. 161-173.
68. Burke, R.E. and K. O'Malley, *Axon degeneration in Parkinson's disease*. *Exp Neurol*, 2013. **246**: p. 72-83.
69. Hornykiewicz, O., *Biochemical aspects of Parkinson's disease*. *Neurology*, 1998. **51**(2 Suppl 2): p. S2-9.
70. Imbriani, P., et al., *Centrality of Early Synaptopathy in Parkinson's Disease*. *Front Neurol*, 2018. **9**: p. 103.
71. Taoufik, E., et al., *Synaptic dysfunction in neurodegenerative and neurodevelopmental diseases: an overview of induced pluripotent stem-cell-based disease models*. *Open Biol*, 2018. **8**(9).
72. Picillo, M., et al., *The relevance of gender in Parkinson's disease: a review*. *J Neurol*, 2017. **264**(8): p. 1583-1607.
73. Langston, J.W., et al., *Chronic Parkinsonism in humans due to a product of mepredine-analog synthesis*. *Science*, 1983. **219**(4587): p. 979-80.
74. Przedborski, S., et al., *The parkinsonian toxin MPTP: action and mechanism*. *Restor Neurol Neurosci*, 2000. **16**(2): p. 135-142.
75. Nandipati, S. and I. Litvan, *Environmental Exposures and Parkinson's Disease*. *Int J Environ Res Public Health*, 2016. **13**(9).
76. Bellou, V., et al., *Environmental risk factors and Parkinson's disease: An umbrella review of meta-analyses*. *Parkinsonism Relat Disord*, 2016. **23**: p. 1-9.
77. Jafari, S., et al., *Head injury and risk of Parkinson disease: a systematic review and meta-analysis*. *Mov Disord*, 2013. **28**(9): p. 1222-9.
78. Noyce, A.J., et al., *Meta-analysis of early nonmotor features and risk factors for Parkinson disease*. *Ann Neurol*, 2012. **72**(6): p. 893-901.
79. Olsen, Laura K., E. Dowd, and Declan P. McKernan, *A role for viral infections in Parkinson's etiology?* *Neuronal Signaling*, 2018. **2**(2).
80. Austin, K.W., S.W. Ameringer, and L.J. Cloud, *An Integrated Review of Psychological Stress in Parkinson's Disease: Biological Mechanisms and Symptom and Health Outcomes*. *Parkinsons Dis*, 2016. **2016**: p. 9869712.
81. Joshi, N. and S. Singh, *Updates on immunity and inflammation in Parkinson disease pathology*. *J Neurosci Res*, 2018. **96**(3): p. 379-390.
82. Polymeropoulos, M.H., et al., *Mutation in the alpha-synuclein gene identified in families with Parkinson's disease*. *Science*, 1997. **276**(5321): p. 2045-7.
83. Deng, H., P. Wang, and J. Jankovic, *The genetics of Parkinson disease*. *Ageing Res Rev*, 2018. **42**: p. 72-85.
84. Zarranz, J.J., et al., *The new mutation, E46K, of alpha-synuclein causes Parkinson and Lewy body dementia*. *Ann Neurol*, 2004. **55**(2): p. 164-73.
85. Kruger, R., et al., *A1a30Pro mutation in the gene encoding alpha-synuclein in Parkinson's disease*. *Nat Genet*, 1998. **18**(2): p. 106-8.
86. Khalaf, O., et al., *The H50Q mutation enhances alpha-synuclein aggregation, secretion, and toxicity*. *J Biol Chem*, 2014. **289**(32): p. 21856-76.
87. Bozi, M., et al., *Genetic assessment of familial and early-onset Parkinson's disease in a Greek population*. *Eur J Neurol*, 2014. **21**(7): p. 963-8.
88. Pasanen, P., et al., *Novel alpha-synuclein mutation A53E associated with atypical multiple system atrophy and Parkinson's disease-type pathology*. *Neurobiol Aging*, 2014. **35**(9): p. 2180 e1-5.

89. Martikainen, M.H., et al., *Clinical and imaging findings in Parkinson disease associated with the A53E SNCA mutation*. *Neurol Genet*, 2015. **1**(4): p. e27.
90. Lesage, S., et al., *G51D alpha-synuclein mutation causes a novel parkinsonian-pyramidal syndrome*. *Ann Neurol*, 2013. **73**(4): p. 459-71.
91. Kiely, A.P., et al., *alpha-Synucleinopathy associated with G51D SNCA mutation: a link between Parkinson's disease and multiple system atrophy?* *Acta Neuropathol*, 2013. **125**(5): p. 753-69.
92. Ibanez, P., et al., *Causal relation between alpha-synuclein gene duplication and familial Parkinson's disease*. *Lancet*, 2004. **364**(9440): p. 1169-71.
93. Chartier-Harlin, M.C., et al., *Alpha-synuclein locus duplication as a cause of familial Parkinson's disease*. *Lancet*, 2004. **364**(9440): p. 1167-9.
94. Hoffman-Zacharska, D., et al., *Novel A18T and pA29S substitutions in alpha-synuclein may be associated with sporadic Parkinson's disease*. *Parkinsonism Relat Disord*, 2013. **19**(11): p. 1057-1060.
95. Campelo, C. and R.H. Silva, *Genetic Variants in SNCA and the Risk of Sporadic Parkinson's Disease and Clinical Outcomes: A Review*. *Parkinsons Dis*, 2017. **2017**: p. 4318416.
96. Nalls, M.A., et al., *Large-scale meta-analysis of genome-wide association data identifies six new risk loci for Parkinson's disease*. *Nat Genet*, 2014. **46**(9): p. 989-93.
97. Chang, D., et al., *A meta-analysis of genome-wide association studies identifies 17 new Parkinson's disease risk loci*. *Nat Genet*, 2017. **49**(10): p. 1511-1516.
98. Mata, I.F., et al., *The discovery of LRRK2 p.R1441S, a novel mutation for Parkinson's disease, adds to the complexity of a mutational hotspot*. *Am J Med Genet B Neuropsychiatr Genet*, 2016. **171**(7): p. 925-30.
99. Zimprich, A., et al., *Mutations in LRRK2 cause autosomal-dominant parkinsonism with pleomorphic pathology*. *Neuron*, 2004. **44**(4): p. 601-7.
100. Taymans, J.M., C. Van den Haute, and V. Baekelandt, *Distribution of PINK1 and LRRK2 in rat and mouse brain*. *J Neurochem*, 2006. **98**(3): p. 951-61.
101. Parisiadou, L., et al., *LRRK2 regulates synaptogenesis and dopamine receptor activation through modulation of PKA activity*. *Nat Neurosci*, 2014. **17**(3): p. 367-76.
102. Shin, N., et al., *LRRK2 regulates synaptic vesicle endocytosis*. *Exp Cell Res*, 2008. **314**(10): p. 2055-65.
103. Winner, B., et al., *Adult neurogenesis and neurite outgrowth are impaired in LRRK2 G2019S mice*. *Neurobiol Dis*, 2011. **41**(3): p. 706-16.
104. Do, C.B., et al., *Web-based genome-wide association study identifies two novel loci and a substantial genetic component for Parkinson's disease*. *PLoS Genet*, 2011. **7**(6): p. e1002141.
105. Edwards, T.L., et al., *Genome-wide association study confirms SNPs in SNCA and the MAPT region as common risk factors for Parkinson disease*. *Ann Hum Genet*, 2010. **74**(2): p. 97-109.
106. Fung, H.C., et al., *Genome-wide genotyping in Parkinson's disease and neurologically normal controls: first stage analysis and public release of data*. *Lancet Neurol*, 2006. **5**(11): p. 911-6.
107. Hamza, T.H., et al., *Common genetic variation in the HLA region is associated with late-onset sporadic Parkinson's disease*. *Nat Genet*, 2010. **42**(9): p. 781-5.
108. Sandor, C., et al., *Whole-exome sequencing of 228 patients with sporadic Parkinson's disease*. *Sci Rep*, 2017. **7**: p. 41188.
109. Satake, W., et al., *Genome-wide association study identifies common variants at four loci as genetic risk factors for Parkinson's disease*. *Nat Genet*, 2009. **41**(12): p. 1303-7.

110. Simon-Sanchez, J., et al., *Genome-wide association study reveals genetic risk underlying Parkinson's disease*. Nat Genet, 2009. **41**(12): p. 1308-12.
111. Maiti, P., J. Manna, and G.L. Dunbar, *Current understanding of the molecular mechanisms in Parkinson's disease: Targets for potential treatments*. Transl Neurodegener, 2017. **6**: p. 28.
112. Jucker, M. and L.C. Walker, *Self-propagation of pathogenic protein aggregates in neurodegenerative diseases*. Nature, 2013. **501**(7465): p. 45-51.
113. Sweeney, P., et al., *Protein misfolding in neurodegenerative diseases: implications and strategies*. Transl Neurodegener, 2017. **6**: p. 6.
114. Hunn, B.H., et al., *Impaired intracellular trafficking defines early Parkinson's disease*. Trends Neurosci, 2015. **38**(3): p. 178-88.
115. Wang, X., et al., *Dysregulation of protein trafficking in neurodegeneration*. Mol Neurodegener, 2014. **9**: p. 31.
116. Bennett, M.C., et al., *Degradation of alpha-synuclein by proteasome*. J Biol Chem, 1999. **274**(48): p. 33855-8.
117. Ebrahimi-Fakhari, D., et al., *Distinct roles in vivo for the ubiquitin-proteasome system and the autophagy-lysosomal pathway in the degradation of alpha-synuclein*. J Neurosci, 2011. **31**(41): p. 14508-20.
118. Rivero-Rios, P., et al., *Targeting the Autophagy/Lysosomal Degradation Pathway in Parkinson's Disease*. Curr Neuropharmacol, 2016. **14**(3): p. 238-49.
119. Tofaris, G.K., et al., *Ubiquitin ligase Nedd4 promotes alpha-synuclein degradation by the endosomal-lysosomal pathway*. Proc Natl Acad Sci U S A, 2011. **108**(41): p. 17004-9.
120. Webb, J.L., et al., *Alpha-Synuclein is degraded by both autophagy and the proteasome*. J Biol Chem, 2003. **278**(27): p. 25009-13.
121. Holmes, B.B. and M.I. Diamond, *Cellular mechanisms of protein aggregate propagation*. Curr Opin Neurol, 2012. **25**(6): p. 721-6.
122. Murrow, L. and J. Debnath, *Autophagy as a stress-response and quality-control mechanism: implications for cell injury and human disease*. Annu Rev Pathol, 2013. **8**: p. 105-37.
123. Low, P., *The role of ubiquitin-proteasome system in ageing*. Gen Comp Endocrinol, 2011. **172**(1): p. 39-43.
124. Tanaka, K. and N. Matsuda, *Proteostasis and neurodegeneration: the roles of proteasomal degradation and autophagy*. Biochim Biophys Acta, 2014. **1843**(1): p. 197-204.
125. Lim, K.L. and C.W. Zhang, *Molecular events underlying Parkinson's disease - an interwoven tapestry*. Front Neurol, 2013. **4**: p. 33.
126. Ebrahimi-Fakhari, D., L. Wahlster, and P.J. McLean, *Protein degradation pathways in Parkinson's disease: curse or blessing*. Acta Neuropathol, 2012. **124**(2): p. 153-72.
127. Moors, T., et al., *Lysosomal Dysfunction and alpha-Synuclein Aggregation in Parkinson's Disease: Diagnostic Links*. Mov Disord, 2016. **31**(6): p. 791-801.
128. Gan-Or, Z., P.A. Dion, and G.A. Rouleau, *Genetic perspective on the role of the autophagy-lysosome pathway in Parkinson disease*. Autophagy, 2015. **11**(9): p. 1443-57.
129. Bose, A. and M.F. Beal, *Mitochondrial dysfunction in Parkinson's disease*. J Neurochem, 2016. **139 Suppl 1**: p. 216-231.
130. Bender, A., et al., *High levels of mitochondrial DNA deletions in substantia nigra neurons in aging and Parkinson disease*. Nat Genet, 2006. **38**(5): p. 515-7.
131. Scarffe, L.A., et al., *Parkin and PINK1: much more than mitophagy*. Trends Neurosci, 2014. **37**(6): p. 315-24.

132. Blesa, J., et al., *Oxidative stress and Parkinson's disease*. *Front Neuroanat*, 2015. **9**: p. 91.
133. Chung, C.Y., et al., *Cell type-specific gene expression of midbrain dopaminergic neurons reveals molecules involved in their vulnerability and protection*. *Hum Mol Genet*, 2005. **14**(13): p. 1709-25.
134. Guo, J.D., et al., *Damage to dopaminergic neurons by oxidative stress in Parkinson's disease (Review)*. *Int J Mol Med*, 2018. **41**(4): p. 1817-1825.
135. Chan, C.S., et al., *'Rejuvenation' protects neurons in mouse models of Parkinson's disease*. *Nature*, 2007. **447**(7148): p. 1081-6.
136. Guzman, J.N., et al., *Robust pacemaking in substantia nigra dopaminergic neurons*. *J Neurosci*, 2009. **29**(35): p. 11011-9.
137. Guzman, J.N., et al., *Oxidant stress evoked by pacemaking in dopaminergic neurons is attenuated by DJ-1*. *Nature*, 2010. **468**(7324): p. 696-700.
138. Wang, Q., Y. Liu, and J. Zhou, *Neuroinflammation in Parkinson's disease and its potential as therapeutic target*. *Transl Neurodegener*, 2015. **4**: p. 19.
139. McGeer, P.L., et al., *Reactive microglia are positive for HLA-DR in the substantia nigra of Parkinson's and Alzheimer's disease brains*. *Neurology*, 1988. **38**(8): p. 1285-91.
140. Ferreira, S.A. and M. Romero-Ramos, *Microglia Response During Parkinson's Disease: Alpha-Synuclein Intervention*. *Front Cell Neurosci*, 2018. **12**: p. 247.
141. Gelders, G., V. Baekelandt, and A. Van der Perren, *Linking Neuroinflammation and Neurodegeneration in Parkinson's Disease*. *J Immunol Res*, 2018. **2018**: p. 4784268.
142. Kannarkat, G.T., J.M. Boss, and M.G. Tansey, *The role of innate and adaptive immunity in Parkinson's disease*. *J Parkinsons Dis*, 2013. **3**(4): p. 493-514.
143. Hirsch, E.C. and S. Hunot, *Neuroinflammation in Parkinson's disease: a target for neuroprotection?* *Lancet Neurol*, 2009. **8**(4): p. 382-97.
144. Joers, V., et al., *Microglial phenotypes in Parkinson's disease and animal models of the disease*. *Prog Neurobiol*, 2017. **155**: p. 57-75.
145. Tansey, M.G. and M.S. Goldberg, *Neuroinflammation in Parkinson's disease: its role in neuronal death and implications for therapeutic intervention*. *Neurobiol Dis*, 2010. **37**(3): p. 510-8.
146. Yun, S.P., et al., *Block of A1 astrocyte conversion by microglia is neuroprotective in models of Parkinson's disease*. *Nat Med*, 2018. **24**(7): p. 931-938.
147. Mattson, M.P., *Calcium and neurodegeneration*. *Aging Cell*, 2007. **6**(3): p. 337-50.
148. Pchitskaya, E., E. Popugaeva, and I. Bezprozvanny, *Calcium signaling and molecular mechanisms underlying neurodegenerative diseases*. *Cell Calcium*, 2018. **70**: p. 87-94.
149. Hyland, B.I., et al., *Firing modes of midbrain dopamine cells in the freely moving rat*. *Neuroscience*, 2002. **114**(2): p. 475-92.
150. Mercuri, N.B., et al., *Effects of dihydropyridine calcium antagonists on rat midbrain dopaminergic neurones*. *Br J Pharmacol*, 1994. **113**(3): p. 831-8.
151. Carreras-Sureda, A., P. Pihan, and C. Hetz, *Calcium signaling at the endoplasmic reticulum: fine-tuning stress responses*. *Cell Calcium*, 2018. **70**: p. 24-31.
152. Giorgi, C., et al., *Mitochondrial calcium homeostasis as potential target for mitochondrial medicine*. *Mitochondrion*, 2012. **12**(1): p. 77-85.
153. Kilpatrick, B.S., et al., *Direct mobilisation of lysosomal Ca<sup>2+</sup> triggers complex Ca<sup>2+</sup> signals*. *J Cell Sci*, 2013. **126**(Pt 1): p. 60-6.
154. Hurley, M.J., et al., *Parkinson's disease is associated with altered expression of CaV1 channels and calcium-binding proteins*. *Brain*, 2013. **136**(Pt 7): p. 2077-97.
155. Millecamps, S. and J.P. Julien, *Axonal transport deficits and neurodegenerative diseases*. *Nat Rev Neurosci*, 2013. **14**(3): p. 161-76.

156. Saha, A.R., et al., *Parkinson's disease alpha-synuclein mutations exhibit defective axonal transport in cultured neurons*. J Cell Sci, 2004. **117**(Pt 7): p. 1017-24.
157. Abou-Sleiman, P.M., M.M. Muqit, and N.W. Wood, *Expanding insights of mitochondrial dysfunction in Parkinson's disease*. Nat Rev Neurosci, 2006. **7**(3): p. 207-19.
158. Chu, Y., et al., *Alterations in axonal transport motor proteins in sporadic and experimental Parkinson's disease*. Brain, 2012. **135**(Pt 7): p. 2058-73.
159. Maroteaux, L. and R.H. Scheller, *The rat brain synucleins; family of proteins transiently associated with neuronal membrane*. Brain Res Mol Brain Res, 1991. **11**(3-4): p. 335-43.
160. Goedert, M., *Alpha-synuclein and neurodegenerative diseases*. Nat Rev Neurosci, 2001. **2**(7): p. 492-501.
161. Jakes, R., M.G. Spillantini, and M. Goedert, *Identification of two distinct synucleins from human brain*. FEBS Lett, 1994. **345**(1): p. 27-32.
162. Goedert, M., R. Jakes, and M.G. Spillantini, *The Synucleinopathies: Twenty Years On*. J Parkinsons Dis, 2017. **7**(s1): p. S53-S71.
163. Iwai, A., et al., *The precursor protein of non-A beta component of Alzheimer's disease amyloid is a presynaptic protein of the central nervous system*. Neuron, 1995. **14**(2): p. 467-75.
164. Kahle, P.J., et al., *Subcellular localization of wild-type and Parkinson's disease-associated mutant alpha -synuclein in human and transgenic mouse brain*. J Neurosci, 2000. **20**(17): p. 6365-73.
165. Kamp, F., et al., *Inhibition of mitochondrial fusion by alpha-synuclein is rescued by PINK1, Parkin and DJ-1*. EMBO J, 2010. **29**(20): p. 3571-89.
166. Devi, L., et al., *Mitochondrial import and accumulation of alpha-synuclein impair complex I in human dopaminergic neuronal cultures and Parkinson disease brain*. J Biol Chem, 2008. **283**(14): p. 9089-100.
167. Zhang, L., et al., *Semi-quantitative analysis of alpha-synuclein in subcellular pools of rat brain neurons: an immunogold electron microscopic study using a C-terminal specific monoclonal antibody*. Brain Res, 2008. **1244**: p. 40-52.
168. Guardia-Laguarta, C., et al., *alpha-Synuclein is localized to mitochondria-associated ER membranes*. J Neurosci, 2014. **34**(1): p. 249-59.
169. Barbour, R., et al., *Red blood cells are the major source of alpha-synuclein in blood*. Neurodegener Dis, 2008. **5**(2): p. 55-9.
170. Bottner, M., et al., *Expression pattern and localization of alpha-synuclein in the human enteric nervous system*. Neurobiol Dis, 2012. **48**(3): p. 474-80.
171. Ulmer, T.S., et al., *Structure and dynamics of micelle-bound human alpha-synuclein*. J Biol Chem, 2005. **280**(10): p. 9595-603.
172. Ueda, K., et al., *Molecular cloning of cDNA encoding an unrecognized component of amyloid in Alzheimer disease*. Proc Natl Acad Sci U S A, 1993. **90**(23): p. 11282-6.
173. Weinreb, P.H., et al., *NACP, a protein implicated in Alzheimer's disease and learning, is natively unfolded*. Biochemistry, 1996. **35**(43): p. 13709-15.
174. Eliezer, D., et al., *Conformational properties of alpha-synuclein in its free and lipid-associated states*. J Mol Biol, 2001. **307**(4): p. 1061-73.
175. Davidson, W.S., et al., *Stabilization of alpha-synuclein secondary structure upon binding to synthetic membranes*. J Biol Chem, 1998. **273**(16): p. 9443-9.
176. Viennet, T., et al., *Structural insights from lipid-bilayer nanodiscs link alpha-Synuclein membrane-binding modes to amyloid fibril formation*. Communications Biology, 2018. **1**(1): p. 44.
177. Fortin, D.L., et al., *Lipid rafts mediate the synaptic localization of alpha-synuclein*. J Neurosci, 2004. **24**(30): p. 6715-23.

178. Wang, W., et al., *A soluble alpha-synuclein construct forms a dynamic tetramer*. Proc Natl Acad Sci U S A, 2011. **108**(43): p. 17797-802.
179. Bartels, T., J.G. Choi, and D.J. Selkoe, *alpha-Synuclein occurs physiologically as a helically folded tetramer that resists aggregation*. Nature, 2011. **477**(7362): p. 107-10.
180. Dettmer, U., et al., *KTKEGV repeat motifs are key mediators of normal alpha-synuclein tetramerization: Their mutation causes excess monomers and neurotoxicity*. Proc Natl Acad Sci U S A, 2015. **112**(31): p. 9596-601.
181. Gould, N., et al., *Evidence of native alpha-synuclein conformers in the human brain*. J Biol Chem, 2014. **289**(11): p. 7929-34.
182. Middleton, E.R. and E. Rhoades, *Effects of curvature and composition on alpha-synuclein binding to lipid vesicles*. Biophys J, 2010. **99**(7): p. 2279-88.
183. Shen, H., M. Pirruccello, and P. De Camilli, *SnapShot: membrane curvature sensors and generators*. Cell, 2012. **150**(6): p. 1300, 1300 e1-2.
184. Fusco, G., et al., *Structural basis of synaptic vesicle assembly promoted by alpha-synuclein*. Nat Commun, 2016. **7**: p. 12563.
185. Burre, J., M. Sharma, and T.C. Sudhof, *alpha-Synuclein assembles into higher-order multimers upon membrane binding to promote SNARE complex formation*. Proc Natl Acad Sci U S A, 2014. **111**(40): p. E4274-83.
186. Burre, J., et al., *Alpha-synuclein promotes SNARE-complex assembly in vivo and in vitro*. Science, 2010. **329**(5999): p. 1663-7.
187. Han, J., K. Pluhackova, and R.A. Bockmann, *The Multifaceted Role of SNARE Proteins in Membrane Fusion*. Front Physiol, 2017. **8**: p. 5.
188. Thayanidhi, N., et al., *Alpha-synuclein delays endoplasmic reticulum (ER)-to-Golgi transport in mammalian cells by antagonizing ER/Golgi SNAREs*. Mol Biol Cell, 2010. **21**(11): p. 1850-63.
189. Gitler, A.D., et al., *The Parkinson's disease protein alpha-synuclein disrupts cellular Rab homeostasis*. Proc Natl Acad Sci U S A, 2008. **105**(1): p. 145-50.
190. Cooper, A.A., et al., *Alpha-synuclein blocks ER-Golgi traffic and Rab1 rescues neuron loss in Parkinson's models*. Science, 2006. **313**(5785): p. 324-8.
191. Sharma, M., J. Burre, and T.C. Sudhof, *CSPalpha promotes SNARE-complex assembly by chaperoning SNAP-25 during synaptic activity*. Nat Cell Biol, 2011. **13**(1): p. 30-9.
192. Chandra, S., et al., *Double-knockout mice for alpha- and beta-synucleins: effect on synaptic functions*. Proc Natl Acad Sci U S A, 2004. **101**(41): p. 14966-71.
193. Scott, D.A., et al., *A pathologic cascade leading to synaptic dysfunction in alpha-synuclein-induced neurodegeneration*. J Neurosci, 2010. **30**(24): p. 8083-95.
194. Scott, D. and S. Roy, *alpha-Synuclein inhibits intersynaptic vesicle mobility and maintains recycling-pool homeostasis*. J Neurosci, 2012. **32**(30): p. 10129-35.
195. Larsen, K.E., et al., *Alpha-synuclein overexpression in PC12 and chromaffin cells impairs catecholamine release by interfering with a late step in exocytosis*. J Neurosci, 2006. **26**(46): p. 11915-22.
196. Cabin, D.E., et al., *Synaptic vesicle depletion correlates with attenuated synaptic responses to prolonged repetitive stimulation in mice lacking alpha-synuclein*. J Neurosci, 2002. **22**(20): p. 8797-807.
197. Lautenschlager, J., et al., *C-terminal calcium binding of alpha-synuclein modulates synaptic vesicle interaction*. Nat Commun, 2018. **9**(1): p. 712.
198. Vargas, K.J., et al., *Synucleins regulate the kinetics of synaptic vesicle endocytosis*. J Neurosci, 2014. **34**(28): p. 9364-76.
199. Xu, J., et al., *alpha-Synuclein Mutation Inhibits Endocytosis at Mammalian Central Nerve Terminals*. J Neurosci, 2016. **36**(16): p. 4408-14.

200. Busch, D.J., et al., *Acute increase of alpha-synuclein inhibits synaptic vesicle recycling evoked during intense stimulation*. Mol Biol Cell, 2014. **25**(24): p. 3926-41.
201. Lautenschlager, J., C.F. Kaminski, and G.S. Kaminski Schierle, *alpha-Synuclein - Regulator of Exocytosis, Endocytosis, or Both?* Trends Cell Biol, 2017. **27**(7): p. 468-479.
202. Wu, N., et al., *Alpha-synuclein overexpression in mice alters synaptic communication in the corticostriatal pathway*. J Neurosci Res, 2010. **88**(8): p. 1764-76.
203. Janezic, S., et al., *Deficits in dopaminergic transmission precede neuron loss and dysfunction in a new Parkinson model*. Proc Natl Acad Sci U S A, 2013. **110**(42): p. E4016-25.
204. Watson, J.B., et al., *Alterations in corticostriatal synaptic plasticity in mice overexpressing human alpha-synuclein*. Neuroscience, 2009. **159**(2): p. 501-13.
205. Liu, S., et al., *alpha-Synuclein produces a long-lasting increase in neurotransmitter release*. EMBO J, 2004. **23**(22): p. 4506-16.
206. Abeliovich, A., et al., *Mice lacking alpha-synuclein display functional deficits in the nigrostriatal dopamine system*. Neuron, 2000. **25**(1): p. 239-52.
207. Greten-Harrison, B., et al., *alphabetagamma-Synuclein triple knockout mice reveal age-dependent neuronal dysfunction*. Proc Natl Acad Sci U S A, 2010. **107**(45): p. 19573-8.
208. Park, S.M., et al., *Distinct roles of the N-terminal-binding domain and the C-terminal-solubilizing domain of alpha-synuclein, a molecular chaperone*. J Biol Chem, 2002. **277**(32): p. 28512-20.
209. Chen, R.H., et al., *alpha-Synuclein membrane association is regulated by the Rab3a recycling machinery and presynaptic activity*. J Biol Chem, 2013. **288**(11): p. 7438-49.
210. Peng, X., et al., *Alpha-synuclein activation of protein phosphatase 2A reduces tyrosine hydroxylase phosphorylation in dopaminergic cells*. J Cell Sci, 2005. **118**(Pt 15): p. 3523-30.
211. Papp, M.I., J.E. Kahn, and P.L. Lantos, *Glial cytoplasmic inclusions in the CNS of patients with multiple system atrophy (striatonigral degeneration, olivopontocerebellar atrophy and Shy-Drager syndrome)*. J Neurol Sci, 1989. **94**(1-3): p. 79-100.
212. Larson, M.E., et al., *Soluble alpha-synuclein is a novel modulator of Alzheimer's disease pathophysiology*. J Neurosci, 2012. **32**(30): p. 10253-66.
213. Klein, A.D. and J.R. Mazzulli, *Is Parkinson's disease a lysosomal disorder?* Brain, 2018.
214. Sidransky, E., et al., *Multicenter analysis of glucocerebrosidase mutations in Parkinson's disease*. N Engl J Med, 2009. **361**(17): p. 1651-61.
215. Wong, Y.C. and D. Krainc, *alpha-synuclein toxicity in neurodegeneration: mechanism and therapeutic strategies*. Nat Med, 2017. **23**(2): p. 1-13.
216. Der-Sarkissian, A., et al., *Structural organization of alpha-synuclein fibrils studied by site-directed spin labeling*. J Biol Chem, 2003. **278**(39): p. 37530-5.
217. Heise, H., et al., *Molecular-level secondary structure, polymorphism, and dynamics of full-length alpha-synuclein fibrils studied by solid-state NMR*. Proc Natl Acad Sci U S A, 2005. **102**(44): p. 15871-6.
218. Vilar, M., et al., *The fold of alpha-synuclein fibrils*. Proc Natl Acad Sci U S A, 2008. **105**(25): p. 8637-42.
219. Barrett, P.J. and J. Timothy Greenamyre, *Post-translational modification of alpha-synuclein in Parkinson's disease*. Brain Res, 2015. **1628**(Pt B): p. 247-253.
220. Fujiwara, H., et al., *alpha-Synuclein is phosphorylated in synucleinopathy lesions*. Nat Cell Biol, 2002. **4**(2): p. 160-4.
221. Oueslati, A., M. Fournier, and H.A. Lashuel, *Role of post-translational modifications in modulating the structure, function and toxicity of alpha-synuclein: implications for*

- Parkinson's disease pathogenesis and therapies*. Prog Brain Res, 2010. **183**: p. 115-45.
222. Negro, A., et al., *Multiple phosphorylation of alpha-synuclein by protein tyrosine kinase Syk prevents eosin-induced aggregation*. FASEB J, 2002. **16**(2): p. 210-2.
223. Good, P.F., et al., *Protein nitration in Parkinson's disease*. J Neuropathol Exp Neurol, 1998. **57**(4): p. 338-42.
224. Giasson, B.I., et al., *Oxidative damage linked to neurodegeneration by selective alpha-synuclein nitration in synucleinopathy lesions*. Science, 2000. **290**(5493): p. 985-9.
225. Li, W., et al., *Aggregation promoting C-terminal truncation of alpha-synuclein is a normal cellular process and is enhanced by the familial Parkinson's disease-linked mutations*. Proc Natl Acad Sci U S A, 2005. **102**(6): p. 2162-7.
226. Games, D., et al., *Reducing C-terminal-truncated alpha-synuclein by immunotherapy attenuates neurodegeneration and propagation in Parkinson's disease-like models*. J Neurosci, 2014. **34**(28): p. 9441-54.
227. Lashuel, H.A., et al., *The many faces of alpha-synuclein: from structure and toxicity to therapeutic target*. Nat Rev Neurosci, 2013. **14**(1): p. 38-48.
228. Conway, K.A., et al., *Acceleration of oligomerization, not fibrillization, is a shared property of both alpha-synuclein mutations linked to early-onset Parkinson's disease: implications for pathogenesis and therapy*. Proc Natl Acad Sci U S A, 2000. **97**(2): p. 571-6.
229. Sharon, R., et al., *The formation of highly soluble oligomers of alpha-synuclein is regulated by fatty acids and enhanced in Parkinson's disease*. Neuron, 2003. **37**(4): p. 583-95.
230. Dettmer, U., et al., *Parkinson-causing alpha-synuclein missense mutations shift native tetramers to monomers as a mechanism for disease initiation*. Nat Commun, 2015. **6**: p. 7314.
231. Pieri, L., et al., *Fibrillar alpha-synuclein and huntingtin exon 1 assemblies are toxic to the cells*. Biophys J, 2012. **102**(12): p. 2894-905.
232. Peelaerts, W., et al., *alpha-Synuclein strains cause distinct synucleinopathies after local and systemic administration*. Nature, 2015. **522**(7556): p. 340-4.
233. Guo, J.L., et al., *Distinct alpha-synuclein strains differentially promote tau inclusions in neurons*. Cell, 2013. **154**(1): p. 103-17.
234. Bousset, L., et al., *Structural and functional characterization of two alpha-synuclein strains*. Nat Commun, 2013. **4**: p. 2575.
235. Prusiner, S.B., et al., *Evidence for alpha-synuclein prions causing multiple system atrophy in humans with parkinsonism*. Proc Natl Acad Sci U S A, 2015. **112**(38): p. E5308-17.
236. Choi, B.K., et al., *Large alpha-synuclein oligomers inhibit neuronal SNARE-mediated vesicle docking*. Proc Natl Acad Sci U S A, 2013. **110**(10): p. 4087-92.
237. Wang, L., et al., *alpha-synuclein multimers cluster synaptic vesicles and attenuate recycling*. Curr Biol, 2014. **24**(19): p. 2319-26.
238. Burre, J., M. Sharma, and T.C. Sudhof, *Systematic mutagenesis of alpha-synuclein reveals distinct sequence requirements for physiological and pathological activities*. J Neurosci, 2012. **32**(43): p. 15227-42.
239. Diao, J., et al., *Native alpha-synuclein induces clustering of synaptic-vesicle mimics via binding to phospholipids and synaptobrevin-2/VAMP2*. Elife, 2013. **2**: p. e00592.
240. Martin, L.J., et al., *Parkinson's disease alpha-synuclein transgenic mice develop neuronal mitochondrial degeneration and cell death*. J Neurosci, 2006. **26**(1): p. 41-50.

241. Choubey, V., et al., *Mutant A53T alpha-synuclein induces neuronal death by increasing mitochondrial autophagy*. J Biol Chem, 2011. **286**(12): p. 10814-24.
242. Chen, L., et al., *A53T human alpha-synuclein overexpression in transgenic mice induces pervasive mitochondria macroautophagy defects preceding dopamine neuron degeneration*. J Neurosci, 2015. **35**(3): p. 890-905.
243. Nakamura, K., et al., *Direct membrane association drives mitochondrial fission by the Parkinson disease-associated protein alpha-synuclein*. J Biol Chem, 2011. **286**(23): p. 20710-26.
244. Di Maio, R., et al., *alpha-Synuclein binds to TOM20 and inhibits mitochondrial protein import in Parkinson's disease*. Sci Transl Med, 2016. **8**(342): p. 342ra78.
245. Outeiro, T.F. and S. Lindquist, *Yeast cells provide insight into alpha-synuclein biology and pathobiology*. Science, 2003. **302**(5651): p. 1772-5.
246. Chung, C.Y., et al., *Identification and rescue of alpha-synuclein toxicity in Parkinson patient-derived neurons*. Science, 2013. **342**(6161): p. 983-7.
247. Oaks, A.W., et al., *Synucleins antagonize endoplasmic reticulum function to modulate dopamine transporter trafficking*. PLoS One, 2013. **8**(8): p. e70872.
248. Tanik, S.A., et al., *Lewy body-like alpha-synuclein aggregates resist degradation and impair macroautophagy*. J Biol Chem, 2013. **288**(21): p. 15194-210.
249. Xilouri, M., et al., *alpha-synuclein degradation by autophagic pathways: a potential key to Parkinson's disease pathogenesis*. Autophagy, 2008. **4**(7): p. 917-9.
250. Xilouri, M., et al., *Abberant alpha-synuclein confers toxicity to neurons in part through inhibition of chaperone-mediated autophagy*. PLoS One, 2009. **4**(5): p. e5515.
251. Xilouri, M., O.R. Brekk, and L. Stefanis, *alpha-Synuclein and protein degradation systems: a reciprocal relationship*. Mol Neurobiol, 2013. **47**(2): p. 537-51.
252. Mazzulli, J.R., et al., *alpha-Synuclein-induced lysosomal dysfunction occurs through disruptions in protein trafficking in human midbrain synucleinopathy models*. Proc Natl Acad Sci U S A, 2016. **113**(7): p. 1931-6.
253. Martinez-Vicente, M., et al., *Dopamine-modified alpha-synuclein blocks chaperone-mediated autophagy*. J Clin Invest, 2008. **118**(2): p. 777-88.
254. Wong, Y.C. and D. Krainc, *Lysosomal trafficking defects link Parkinson's disease with Gaucher's disease*. Mov Disord, 2016. **31**(11): p. 1610-1618.
255. Mazzulli, J.R., et al., *Gaucher disease glucocerebrosidase and alpha-synuclein form a bidirectional pathogenic loop in synucleinopathies*. Cell, 2011. **146**(1): p. 37-52.
256. Kontopoulos, E., J.D. Parvin, and M.B. Feany, *Alpha-synuclein acts in the nucleus to inhibit histone acetylation and promote neurotoxicity*. Hum Mol Genet, 2006. **15**(20): p. 3012-23.
257. Fares, M.B., et al., *The novel Parkinson's disease linked mutation G51D attenuates in vitro aggregation and membrane binding of alpha-synuclein, and enhances its secretion and nuclear localization in cells*. Hum Mol Genet, 2014. **23**(17): p. 4491-509.
258. Zheng, B., et al., *PGC-1alpha, a potential therapeutic target for early intervention in Parkinson's disease*. Sci Transl Med, 2010. **2**(52): p. 52ra73.
259. Ryan, S.D., et al., *Isogenic human iPSC Parkinson's model shows nitrosative stress-induced dysfunction in MEF2-PGC1alpha transcription*. Cell, 2013. **155**(6): p. 1351-64.
260. Luo, J., et al., *A calcineurin- and NFAT-dependent pathway is involved in alpha-synuclein-induced degeneration of midbrain dopaminergic neurons*. Hum Mol Genet, 2014. **23**(24): p. 6567-74.
261. Caraveo, G., et al., *Calcineurin determines toxic versus beneficial responses to alpha-synuclein*. Proc Natl Acad Sci U S A, 2014. **111**(34): p. E3544-52.

262. Cali, T., et al., *alpha-Synuclein controls mitochondrial calcium homeostasis by enhancing endoplasmic reticulum-mitochondria interactions*. J Biol Chem, 2012. **287**(22): p. 17914-29.
263. Krols, M., et al., *Mitochondria-associated membranes as hubs for neurodegeneration*. Acta Neuropathol, 2016. **131**(4): p. 505-23.
264. Volpicelli-Daley, L.A., et al., *Formation of alpha-synuclein Lewy neurite-like aggregates in axons impedes the transport of distinct endosomes*. Mol Biol Cell, 2014. **25**(25): p. 4010-23.
265. Prots, I., et al., *alpha-Synuclein oligomers impair neuronal microtubule-kinesin interplay*. J Biol Chem, 2013. **288**(30): p. 21742-54.
266. Tilve, S., F. Difato, and E. Chieragatti, *Cofilin 1 activation prevents the defects in axon elongation and guidance induced by extracellular alpha-synuclein*. Sci Rep, 2015. **5**: p. 16524.
267. Ordonez, D.G., M.K. Lee, and M.B. Feany, *alpha-synuclein Induces Mitochondrial Dysfunction through Spectrin and the Actin Cytoskeleton*. Neuron, 2018. **97**(1): p. 108-124 e6.
268. Borghi, R., et al., *Full length alpha-synuclein is present in cerebrospinal fluid from Parkinson's disease and normal subjects*. Neurosci Lett, 2000. **287**(1): p. 65-7.
269. El-Agnaf, O.M., et al., *Alpha-synuclein implicated in Parkinson's disease is present in extracellular biological fluids, including human plasma*. FASEB J, 2003. **17**(13): p. 1945-7.
270. Lee, H.J., S. Patel, and S.J. Lee, *Intravesicular localization and exocytosis of alpha-synuclein and its aggregates*. J Neurosci, 2005. **25**(25): p. 6016-24.
271. Emmanouilidou, E., et al., *Cell-produced alpha-synuclein is secreted in a calcium-dependent manner by exosomes and impacts neuronal survival*. J Neurosci, 2010. **30**(20): p. 6838-51.
272. Paillusson, S., et al., *Activity-dependent secretion of alpha-synuclein by enteric neurons*. J Neurochem, 2013. **125**(4): p. 512-7.
273. Abounit, S., et al., *Tunneling nanotubes spread fibrillar alpha-synuclein by intercellular trafficking of lysosomes*. EMBO J, 2016. **35**(19): p. 2120-2138.
274. Volpicelli-Daley, L.A., et al., *Exogenous alpha-synuclein fibrils induce Lewy body pathology leading to synaptic dysfunction and neuron death*. Neuron, 2011. **72**(1): p. 57-71.
275. Luk, K.C., et al., *Exogenous alpha-synuclein fibrils seed the formation of Lewy body-like intracellular inclusions in cultured cells*. Proc Natl Acad Sci U S A, 2009. **106**(47): p. 20051-6.
276. Desplats, P., et al., *Inclusion formation and neuronal cell death through neuron-to-neuron transmission of alpha-synuclein*. Proc Natl Acad Sci U S A, 2009. **106**(31): p. 13010-5.
277. Luk, K.C., et al., *Intracerebral inoculation of pathological alpha-synuclein initiates a rapidly progressive neurodegenerative alpha-synucleinopathy in mice*. J Exp Med, 2012. **209**(5): p. 975-86.
278. Luk, K.C., et al., *Pathological alpha-synuclein transmission initiates Parkinson-like neurodegeneration in nontransgenic mice*. Science, 2012. **338**(6109): p. 949-53.
279. Trigo-Damas, I., N.L. Del Rey, and J. Blesa, *Novel models for Parkinson's disease and their impact on future drug discovery*. Expert Opin Drug Discov, 2018. **13**(3): p. 229-239.
280. Ungerstedt, U., T. Ljungberg, and G. Steg, *Behavioral, physiological, and neurochemical changes after 6-hydroxydopamine-induced degeneration of the nigro-striatal dopamine neurons*. Adv Neurol, 1974. **5**: p. 421-6.

281. Glinka, Y., K.F. Tipton, and M.B. Youdim, *Nature of inhibition of mitochondrial respiratory complex I by 6-Hydroxydopamine*. J Neurochem, 1996. **66**(5): p. 2004-10.
282. Ungerstedt, U., *Adipsia and aphagia after 6-hydroxydopamine induced degeneration of the nigro-striatal dopamine system*. Acta Physiol Scand Suppl, 1971. **367**: p. 95-122.
283. Sauer, H. and W.H. Oertel, *Progressive degeneration of nigrostriatal dopamine neurons following intrastriatal terminal lesions with 6-hydroxydopamine: a combined retrograde tracing and immunocytochemical study in the rat*. Neuroscience, 1994. **59**(2): p. 401-15.
284. Przedborski, S., et al., *Dose-dependent lesions of the dopaminergic nigrostriatal pathway induced by intrastriatal injection of 6-hydroxydopamine*. Neuroscience, 1995. **67**(3): p. 631-47.
285. Alves da Costa, C., et al., *6-Hydroxydopamine but not 1-methyl-4-phenylpyridinium abolishes alpha-synuclein anti-apoptotic phenotype by inhibiting its proteasomal degradation and by promoting its aggregation*. J Biol Chem, 2006. **281**(14): p. 9824-31.
286. Bove, J. and C. Perier, *Neurotoxin-based models of Parkinson's disease*. Neuroscience, 2012. **211**: p. 51-76.
287. Glajch, K.E., et al., *Sensorimotor assessment of the unilateral 6-hydroxydopamine mouse model of Parkinson's disease*. Behav Brain Res, 2012. **230**(2): p. 309-16.
288. Blesa, J.T.-D., I.; Quiroga-Varela, A.; Lopez-Gonzalez del Rey, N., *Animal Models of Parkinson's Disease*. 2016: Intechopen.
289. Iravani, M.M., et al., *A modified MPTP treatment regime produces reproducible partial nigrostriatal lesions in common marmosets*. Eur J Neurosci, 2005. **21**(4): p. 841-54.
290. Bergman, H., T. Wichmann, and M.R. DeLong, *Reversal of experimental parkinsonism by lesions of the subthalamic nucleus*. Science, 1990. **249**(4975): p. 1436-8.
291. Cannon, J.R., et al., *A highly reproducible rotenone model of Parkinson's disease*. Neurobiol Dis, 2009. **34**(2): p. 279-90.
292. Day, B.J., et al., *A mechanism of paraquat toxicity involving nitric oxide synthase*. Proc Natl Acad Sci U S A, 1999. **96**(22): p. 12760-5.
293. Manning-Bog, A.B., et al., *The herbicide paraquat causes up-regulation and aggregation of alpha-synuclein in mice: paraquat and alpha-synuclein*. J Biol Chem, 2002. **277**(3): p. 1641-4.
294. Xiong, Y., T.M. Dawson, and V.L. Dawson, *Models of LRRK2-Associated Parkinson's Disease*. Adv Neurobiol, 2017. **14**: p. 163-191.
295. Yao, C., et al., *LRRK2-mediated neurodegeneration and dysfunction of dopaminergic neurons in a Caenorhabditis elegans model of Parkinson's disease*. Neurobiol Dis, 2010. **40**(1): p. 73-81.
296. Saha, S., et al., *LRRK2 modulates vulnerability to mitochondrial dysfunction in Caenorhabditis elegans*. J Neurosci, 2009. **29**(29): p. 9210-8.
297. Tong, Y., et al., *Loss of leucine-rich repeat kinase 2 causes impairment of protein degradation pathways, accumulation of alpha-synuclein, and apoptotic cell death in aged mice*. Proc Natl Acad Sci U S A, 2010. **107**(21): p. 9879-84.
298. Lin, X., et al., *Leucine-rich repeat kinase 2 regulates the progression of neuropathology induced by Parkinson's-disease-related mutant alpha-synuclein*. Neuron, 2009. **64**(6): p. 807-27.
299. Herzig, M.C., et al., *LRRK2 protein levels are determined by kinase function and are crucial for kidney and lung homeostasis in mice*. Hum Mol Genet, 2011. **20**(21): p. 4209-23.

300. Baptista, M.A., et al., *Loss of leucine-rich repeat kinase 2 (LRRK2) in rats leads to progressive abnormal phenotypes in peripheral organs*. PLoS One, 2013. **8**(11): p. e80705.
301. Ramonet, D., et al., *Dopaminergic neuronal loss, reduced neurite complexity and autophagic abnormalities in transgenic mice expressing G2019S mutant LRRK2*. PLoS One, 2011. **6**(4): p. e18568.
302. Chen, C.Y., et al., *(G2019S) LRRK2 activates MKK4-JNK pathway and causes degeneration of SN dopaminergic neurons in a transgenic mouse model of PD*. Cell Death Differ, 2012. **19**(10): p. 1623-33.
303. Lee, B.D., et al., *Inhibitors of leucine-rich repeat kinase-2 protect against models of Parkinson's disease*. Nat Med, 2010. **16**(9): p. 998-1000.
304. Dusonchet, J., et al., *A rat model of progressive nigral neurodegeneration induced by the Parkinson's disease-associated G2019S mutation in LRRK2*. J Neurosci, 2011. **31**(3): p. 907-12.
305. Kitada, T., et al., *Impaired dopamine release and synaptic plasticity in the striatum of parkin-/- mice*. J Neurochem, 2009. **110**(2): p. 613-21.
306. Von Coelln, R., et al., *Loss of locus coeruleus neurons and reduced startle in parkin null mice*. Proc Natl Acad Sci U S A, 2004. **101**(29): p. 10744-9.
307. Goldberg, M.S., et al., *Parkin-deficient mice exhibit nigrostriatal deficits but not loss of dopaminergic neurons*. J Biol Chem, 2003. **278**(44): p. 43628-35.
308. Lu, X.H., et al., *Bacterial artificial chromosome transgenic mice expressing a truncated mutant parkin exhibit age-dependent hypokinetic motor deficits, dopaminergic neuron degeneration, and accumulation of proteinase K-resistant alpha-synuclein*. J Neurosci, 2009. **29**(7): p. 1962-76.
309. Gispert, S., et al., *Parkinson phenotype in aged PINK1-deficient mice is accompanied by progressive mitochondrial dysfunction in absence of neurodegeneration*. PLoS One, 2009. **4**(6): p. e5777.
310. Gautier, C.A., T. Kitada, and J. Shen, *Loss of PINK1 causes mitochondrial functional defects and increased sensitivity to oxidative stress*. Proc Natl Acad Sci U S A, 2008. **105**(32): p. 11364-9.
311. Kim, R.H., et al., *Hypersensitivity of DJ-1-deficient mice to 1-methyl-4-phenyl-1,2,3,6-tetrahydropyridine (MPTP) and oxidative stress*. Proc Natl Acad Sci U S A, 2005. **102**(14): p. 5215-20.
312. Goldberg, M.S., et al., *Nigrostriatal dopaminergic deficits and hypokinesia caused by inactivation of the familial Parkinsonism-linked gene DJ-1*. Neuron, 2005. **45**(4): p. 489-96.
313. Pham, T.T., et al., *DJ-1-deficient mice show less TH-positive neurons in the ventral tegmental area and exhibit non-motoric behavioural impairments*. Genes Brain Behav, 2010. **9**(3): p. 305-17.
314. Rousseaux, M.W., et al., *Progressive dopaminergic cell loss with unilateral-to-bilateral progression in a genetic model of Parkinson disease*. Proc Natl Acad Sci U S A, 2012. **109**(39): p. 15918-23.
315. Visanji, N.P., et al., *alpha-Synuclein-Based Animal Models of Parkinson's Disease: Challenges and Opportunities in a New Era*. Trends Neurosci, 2016. **39**(11): p. 750-762.
316. Bodhicharla, R., et al., *Effects of alpha-synuclein overexpression in transgenic Caenorhabditis elegans strains*. CNS Neurol Disord Drug Targets, 2012. **11**(8): p. 965-75.
317. Feany, M.B. and W.W. Bender, *A Drosophila model of Parkinson's disease*. Nature, 2000. **404**(6776): p. 394-8.

318. Auluck, P.K., et al., *Chaperone suppression of alpha-synuclein toxicity in a Drosophila model for Parkinson's disease*. Science, 2002. **295**(5556): p. 865-8.
319. Mizuno, H., et al., *alpha-Synuclein Transgenic Drosophila As a Model of Parkinson's Disease and Related Synucleinopathies*. Parkinsons Dis, 2010. **2011**: p. 212706.
320. Karpinar, D.P., et al., *Pre-fibrillar alpha-synuclein variants with impaired beta-structure increase neurotoxicity in Parkinson's disease models*. EMBO J, 2009. **28**(20): p. 3256-68.
321. Auluck, P.K. and N.M. Bonini, *Pharmacological prevention of Parkinson disease in Drosophila*. Nat Med, 2002. **8**(11): p. 1185-6.
322. Takahashi, M., et al., *Phosphorylation of alpha-synuclein characteristic of synucleinopathy lesions is recapitulated in alpha-synuclein transgenic Drosophila*. Neurosci Lett, 2003. **336**(3): p. 155-8.
323. Xun, Z., et al., *Lifetime proteomic profiling of an A30P alpha-synuclein Drosophila model of Parkinson's disease*. J Proteome Res, 2007. **6**(9): p. 3729-38.
324. Xun, Z., et al., *Quantitative proteomics of a presymptomatic A53T alpha-synuclein Drosophila model of Parkinson disease*. Mol Cell Proteomics, 2008. **7**(7): p. 1191-203.
325. Varga, S.J., et al., *A new Drosophila model to study the interaction between genetic and environmental factors in Parkinson's disease*. Brain Res, 2014. **1583**: p. 277-86.
326. Abul Khair, S.B., et al., *Silencing of Glucocerebrosidase Gene in Drosophila Enhances the Aggregation of Parkinson's Disease Associated alpha-Synuclein Mutant A53T and Affects Locomotor Activity*. Front Neurosci, 2018. **12**: p. 81.
327. Prabhudesai, S., et al., *A novel "molecular tweezer" inhibitor of alpha-synuclein neurotoxicity in vitro and in vivo*. Neurotherapeutics, 2012. **9**(2): p. 464-76.
328. O'Donnell, K.C., et al., *Axon degeneration and PGC-1alpha-mediated protection in a zebrafish model of alpha-synuclein toxicity*. Dis Model Mech, 2014. **7**(5): p. 571-82.
329. Masliah, E., et al., *Dopaminergic loss and inclusion body formation in alpha-synuclein mice: implications for neurodegenerative disorders*. Science, 2000. **287**(5456): p. 1265-9.
330. Chesselet, M.F., et al., *A progressive mouse model of Parkinson's disease: the Thy1-aSyn ("Line 61") mice*. Neurotherapeutics, 2012. **9**(2): p. 297-314.
331. Martin, L.J., et al., *Mitochondrial permeability transition pore regulates Parkinson's disease development in mutant alpha-synuclein transgenic mice*. Neurobiol Aging, 2014. **35**(5): p. 1132-52.
332. Giasson, B.I., et al., *Neuronal alpha-synucleinopathy with severe movement disorder in mice expressing A53T human alpha-synuclein*. Neuron, 2002. **34**(4): p. 521-33.
333. Oaks, A.W., et al., *Age-dependent effects of A53T alpha-synuclein on behavior and dopaminergic function*. PLoS One, 2013. **8**(4): p. e60378.
334. Yamakado, H., et al., *alpha-Synuclein BAC transgenic mice as a model for Parkinson's disease manifested decreased anxiety-like behavior and hyperlocomotion*. Neurosci Res, 2012. **73**(2): p. 173-7.
335. Kuo, Y.M., et al., *Extensive enteric nervous system abnormalities in mice transgenic for artificial chromosomes containing Parkinson disease-associated alpha-synuclein gene mutations precede central nervous system changes*. Hum Mol Genet, 2010. **19**(9): p. 1633-50.
336. Mougnot, A.L., et al., *Prion-like acceleration of a synucleinopathy in a transgenic mouse model*. Neurobiol Aging, 2012. **33**(9): p. 2225-8.
337. Masuda-Suzukake, M., et al., *Prion-like spreading of pathological alpha-synuclein in brain*. Brain, 2013. **136**(Pt 4): p. 1128-38.
338. Recasens, A., et al., *Lewy body extracts from Parkinson disease brains trigger alpha-synuclein pathology and neurodegeneration in mice and monkeys*. Ann Neurol, 2014. **75**(3): p. 351-62.

339. Rutherford, N.J., et al., *Comparison of the in vivo induction and transmission of alpha-synuclein pathology by mutant alpha-synuclein fibril seeds in transgenic mice.* Hum Mol Genet, 2017. **26**(24): p. 4906-4915.
340. He, Q., et al., *Treatment with Trehalose Prevents Behavioral and Neurochemical Deficits Produced in an AAV alpha-Synuclein Rat Model of Parkinson's Disease.* Mol Neurobiol, 2016. **53**(4): p. 2258-68.
341. Shahaduzzaman, M., et al., *Anti-human alpha-synuclein N-terminal peptide antibody protects against dopaminergic cell death and ameliorates behavioral deficits in an AAV-alpha-synuclein rat model of Parkinson's disease.* PLoS One, 2015. **10**(2): p. e0116841.
342. Nuber, S., et al., *A progressive dopaminergic phenotype associated with neurotoxic conversion of alpha-synuclein in BAC-transgenic rats.* Brain, 2013. **136**(Pt 2): p. 412-32.
343. Phan, J.A., et al., *Early synaptic dysfunction induced by alpha-synuclein in a rat model of Parkinson's disease.* Sci Rep, 2017. **7**(1): p. 6363.
344. Yamasaki, T., et al., *Dynamic Changes in Striatal mGluR1 But Not mGluR5 during Pathological Progression of Parkinson's Disease in Human Alpha-Synuclein A53T Transgenic Rats: A Multi-PET Imaging Study.* J Neurosci, 2016. **36**(2): p. 375-84.
345. Koprach, J.B., et al., *Towards a Non-Human Primate Model of Alpha-Synucleinopathy for Development of Therapeutics for Parkinson's Disease: Optimization of AAV1/2 Delivery Parameters to Drive Sustained Expression of Alpha Synuclein and Dopaminergic Degeneration in Macaque.* PLoS One, 2016. **11**(11): p. e0167235.
346. Lazaro, D.F., et al., *Systematic comparison of the effects of alpha-synuclein mutations on its oligomerization and aggregation.* PLoS Genet, 2014. **10**(11): p. e1004741.
347. Goncalves, S. and T.F. Outeiro, *Assessing the subcellular dynamics of alpha-synuclein using photoactivation microscopy.* Mol Neurobiol, 2013. **47**(3): p. 1081-92.
348. Lazaro, D.F., M.A.S. Pavlou, and T.F. Outeiro, *Cellular models as tools for the study of the role of alpha-synuclein in Parkinson's disease.* Exp Neurol, 2017. **298**(Pt B): p. 162-171.
349. Zhou, W., et al., *Overexpression of human alpha-synuclein causes dopamine neuron death in primary human mesencephalic culture.* Brain Res, 2002. **926**(1-2): p. 42-50.
350. Tonges, L., et al., *Alpha-synuclein mutations impair axonal regeneration in models of Parkinson's disease.* Front Aging Neurosci, 2014. **6**: p. 239.
351. Sacino, A.N., et al., *Conformational templating of alpha-synuclein aggregates in neuronal-glia cultures.* Mol Neurodegener, 2013. **8**: p. 17.
352. Takahashi, K. and S. Yamanaka, *Induction of pluripotent stem cells from mouse embryonic and adult fibroblast cultures by defined factors.* Cell, 2006. **126**(4): p. 663-76.
353. Yu, J., et al., *Induced pluripotent stem cell lines derived from human somatic cells.* Science, 2007. **318**(5858): p. 1917-20.
354. Takahashi, K., et al., *Induction of pluripotent stem cells from adult human fibroblasts by defined factors.* Cell, 2007. **131**(5): p. 861-72.
355. Nakagawa, M., et al., *Generation of induced pluripotent stem cells without Myc from mouse and human fibroblasts.* Nat Biotechnol, 2008. **26**(1): p. 101-6.
356. Yamanaka, S., *Induced pluripotent stem cells: past, present, and future.* Cell Stem Cell, 2012. **10**(6): p. 678-84.
357. Shi, Y., et al., *Induced pluripotent stem cell technology: a decade of progress.* Nat Rev Drug Discov, 2017. **16**(2): p. 115-130.
358. Takahashi, K. and S. Yamanaka, *A decade of transcription factor-mediated reprogramming to pluripotency.* Nat Rev Mol Cell Biol, 2016. **17**(3): p. 183-93.

359. Raab, S., et al., *A Comparative View on Human Somatic Cell Sources for iPSC Generation*. *Stem Cells Int*, 2014. **2014**: p. 768391.
360. Dolmetsch, R. and D.H. Geschwind, *The human brain in a dish: the promise of iPSC-derived neurons*. *Cell*, 2011. **145**(6): p. 831-4.
361. McKinney, C.E., *Using induced pluripotent stem cells derived neurons to model brain diseases*. *Neural Regen Res*, 2017. **12**(7): p. 1062-1067.
362. Studer, L., E. Vera, and D. Cornacchia, *Programming and Reprogramming Cellular Age in the Era of Induced Pluripotency*. *Cell Stem Cell*, 2015. **16**(6): p. 591-600.
363. Mertens, J., et al., *Evaluating cell reprogramming, differentiation and conversion technologies in neuroscience*. *Nat Rev Neurosci*, 2016. **17**(7): p. 424-37.
364. Nguyen, H.N., et al., *LRRK2 mutant iPSC-derived DA neurons demonstrate increased susceptibility to oxidative stress*. *Cell Stem Cell*, 2011. **8**(3): p. 267-80.
365. Cooper, O., et al., *Pharmacological rescue of mitochondrial deficits in iPSC-derived neural cells from patients with familial Parkinson's disease*. *Sci Transl Med*, 2012. **4**(141): p. 141ra90.
366. Ho, R., et al., *ALS disrupts spinal motor neuron maturation and aging pathways within gene co-expression networks*. *Nat Neurosci*, 2016. **19**(9): p. 1256-67.
367. Gunhanlar, N., et al., *A simplified protocol for differentiation of electrophysiologically mature neuronal networks from human induced pluripotent stem cells*. *Mol Psychiatry*, 2018. **23**(5): p. 1336-1344.
368. Darville, H., et al., *Human Pluripotent Stem Cell-derived Cortical Neurons for High Throughput Medication Screening in Autism: A Proof of Concept Study in SHANK3 Haploinsufficiency Syndrome*. *EBioMedicine*, 2016. **9**: p. 293-305.
369. Qi, Y., et al., *Combined small-molecule inhibition accelerates the derivation of functional cortical neurons from human pluripotent stem cells*. *Nat Biotechnol*, 2017. **35**(2): p. 154-163.
370. Shi, Y., P. Kirwan, and F.J. Livesey, *Directed differentiation of human pluripotent stem cells to cerebral cortex neurons and neural networks*. *Nat Protoc*, 2012. **7**(10): p. 1836-46.
371. Shi, Y., et al., *Human cerebral cortex development from pluripotent stem cells to functional excitatory synapses*. *Nat Neurosci*, 2012. **15**(3): p. 477-86, S1.
372. Sun, A.X., et al., *Direct Induction and Functional Maturation of Forebrain GABAergic Neurons from Human Pluripotent Stem Cells*. *Cell Rep*, 2016. **16**(7): p. 1942-53.
373. Yang, N., et al., *Generation of pure GABAergic neurons by transcription factor programming*. *Nat Methods*, 2017. **14**(6): p. 621-628.
374. Lu, J., et al., *Generation of serotonin neurons from human pluripotent stem cells*. *Nat Biotechnol*, 2016. **34**(1): p. 89-94.
375. Abud, E.M., et al., *iPSC-Derived Human Microglia-like Cells to Study Neurological Diseases*. *Neuron*, 2017. **94**(2): p. 278-293 e9.
376. Chambers, S.M., et al., *Highly efficient neural conversion of human ES and iPS cells by dual inhibition of SMAD signaling*. *Nat Biotechnol*, 2009. **27**(3): p. 275-80.
377. Douvaras, P., et al., *Directed Differentiation of Human Pluripotent Stem Cells to Microglia*. *Stem Cell Reports*, 2017. **8**(6): p. 1516-1524.
378. Kirkeby, A., et al., *Generation of regionally specified neural progenitors and functional neurons from human embryonic stem cells under defined conditions*. *Cell Rep*, 2012. **1**(6): p. 703-14.
379. Kriks, S., et al., *Dopamine neurons derived from human ES cells efficiently engraft in animal models of Parkinson's disease*. *Nature*, 2011. **480**(7378): p. 547-51.
380. Pandya, H., et al., *Differentiation of human and murine induced pluripotent stem cells to microglia-like cells*. *Nat Neurosci*, 2017. **20**(5): p. 753-759.

381. Jones, V.C., et al., *Aberrant iPSC-derived human astrocytes in Alzheimer's disease*. *Cell Death Dis*, 2017. **8**(3): p. e2696.
382. Oksanen, M., et al., *PSEN1 Mutant iPSC-Derived Model Reveals Severe Astrocyte Pathology in Alzheimer's Disease*. *Stem Cell Reports*, 2017. **9**(6): p. 1885-1897.
383. Shaltouki, A., et al., *Efficient generation of astrocytes from human pluripotent stem cells in defined conditions*. *Stem Cells*, 2013. **31**(5): p. 941-52.
384. Tcw, J., et al., *An Efficient Platform for Astrocyte Differentiation from Human Induced Pluripotent Stem Cells*. *Stem Cell Reports*, 2017. **9**(2): p. 600-614.
385. Douvaras, P., et al., *Efficient generation of myelinating oligodendrocytes from primary progressive multiple sclerosis patients by induced pluripotent stem cells*. *Stem Cell Reports*, 2014. **3**(2): p. 250-9.
386. Ehrlich, M., et al., *Rapid and efficient generation of oligodendrocytes from human induced pluripotent stem cells using transcription factors*. *Proc Natl Acad Sci U S A*, 2017. **114**(11): p. E2243-E2252.
387. Wang, S., et al., *Human iPSC-derived oligodendrocyte progenitor cells can myelinate and rescue a mouse model of congenital hypomyelination*. *Cell Stem Cell*, 2013. **12**(2): p. 252-64.
388. Serio, A., et al., *Astrocyte pathology and the absence of non-cell autonomy in an induced pluripotent stem cell model of TDP-43 proteinopathy*. *Proc Natl Acad Sci U S A*, 2013. **110**(12): p. 4697-702.
389. Di Lullo, E. and A.R. Kriegstein, *The use of brain organoids to investigate neural development and disease*. *Nat Rev Neurosci*, 2017. **18**(10): p. 573-584.
390. Birey, F., et al., *Assembly of functionally integrated human forebrain spheroids*. *Nature*, 2017. **545**(7652): p. 54-59.
391. Pasca, A.M., et al., *Functional cortical neurons and astrocytes from human pluripotent stem cells in 3D culture*. *Nat Methods*, 2015. **12**(7): p. 671-8.
392. Jo, J., et al., *Midbrain-like Organoids from Human Pluripotent Stem Cells Contain Functional Dopaminergic and Neuromelanin-Producing Neurons*. *Cell Stem Cell*, 2016. **19**(2): p. 248-257.
393. Qian, X., et al., *Brain-Region-Specific Organoids Using Mini-bioreactors for Modeling ZIKV Exposure*. *Cell*, 2016. **165**(5): p. 1238-1254.
394. Pasca, S.P., *The rise of three-dimensional human brain cultures*. *Nature*, 2018. **553**(7689): p. 437-445.
395. Quadrato, G., J. Brown, and P. Arlotta, *The promises and challenges of human brain organoids as models of neuropsychiatric disease*. *Nat Med*, 2016. **22**(11): p. 1220-1228.
396. Bershteyn, M., et al., *Human iPSC-Derived Cerebral Organoids Model Cellular Features of Lissencephaly and Reveal Prolonged Mitosis of Outer Radial Glia*. *Cell Stem Cell*, 2017. **20**(4): p. 435-449 e4.
397. Lancaster, M.A., et al., *Cerebral organoids model human brain development and microcephaly*. *Nature*, 2013. **501**(7467): p. 373-9.
398. Yoon, K.J., et al., *Zika-Virus-Encoded NS2A Disrupts Mammalian Cortical Neurogenesis by Degrading Adherens Junction Proteins*. *Cell Stem Cell*, 2017. **21**(3): p. 349-358 e6.
399. Mariani, J., et al., *FOXP1-Dependent Dysregulation of GABA/Glutamate Neuron Differentiation in Autism Spectrum Disorders*. *Cell*, 2015. **162**(2): p. 375-390.
400. Conforti, P., et al., *Faulty neuronal determination and cell polarization are reverted by modulating HD early phenotypes*. *Proc Natl Acad Sci U S A*, 2018. **115**(4): p. E762-E771.

401. Raja, W.K., et al., *Self-Organizing 3D Human Neural Tissue Derived from Induced Pluripotent Stem Cells Recapitulate Alzheimer's Disease Phenotypes*. PLoS One, 2016. **11**(9): p. e0161969.
402. Pamies, D., et al., *A human brain microphysiological system derived from induced pluripotent stem cells to study neurological diseases and toxicity*. ALTEX, 2017. **34**(3): p. 362-376.
403. Monzel, A.S., et al., *Derivation of Human Midbrain-Specific Organoids from Neuroepithelial Stem Cells*. Stem Cell Reports, 2017. **8**(5): p. 1144-1154.
404. Son, M.Y., et al., *Distinctive genomic signature of neural and intestinal organoids from familial Parkinson's disease patient-derived induced pluripotent stem cells*. Neuropathol Appl Neurobiol, 2017. **43**(7): p. 584-603.
405. Lee, G., et al., *Large-scale screening using familial dysautonomia induced pluripotent stem cells identifies compounds that rescue IKBKAP expression*. Nat Biotechnol, 2012. **30**(12): p. 1244-8.
406. Hoing, S., et al., *Discovery of inhibitors of microglial neurotoxicity acting through multiple mechanisms using a stem-cell-based phenotypic assay*. Cell Stem Cell, 2012. **11**(5): p. 620-32.
407. Burkhardt, M.F., et al., *A cellular model for sporadic ALS using patient-derived induced pluripotent stem cells*. Mol Cell Neurosci, 2013. **56**: p. 355-64.
408. Naryshkin, N.A., et al., *Motor neuron disease. SMN2 splicing modifiers improve motor function and longevity in mice with spinal muscular atrophy*. Science, 2014. **345**(6197): p. 688-93.
409. Mullard, A., *Stem-cell discovery platforms yield first clinical candidates*. Nat Rev Drug Discov, 2015. **14**(9): p. 589-91.
410. Inoue, H., et al., *iPS cells: a game changer for future medicine*. EMBO J, 2014. **33**(5): p. 409-17.
411. Schwartz, M.P., et al., *Human pluripotent stem cell-derived neural constructs for predicting neural toxicity*. Proc Natl Acad Sci U S A, 2015. **112**(40): p. 12516-21.
412. Petrucci, S., M. Ginevrino, and E.M. Valente, *Phenotypic spectrum of alpha-synuclein mutations: New insights from patients and cellular models*. Parkinsonism Relat Disord, 2016. **22 Suppl 1**: p. S16-20.
413. Liu, G.H., et al., *Progressive degeneration of human neural stem cells caused by pathogenic LRRK2*. Nature, 2012. **491**(7425): p. 603-7.
414. Reinhardt, P., et al., *Genetic correction of a LRRK2 mutation in human iPSCs links parkinsonian neurodegeneration to ERK-dependent changes in gene expression*. Cell Stem Cell, 2013. **12**(3): p. 354-67.
415. Schondorf, D.C., et al., *iPSC-derived neurons from GBA1-associated Parkinson's disease patients show autophagic defects and impaired calcium homeostasis*. Nat Commun, 2014. **5**: p. 4028.
416. Woodard, C.M., et al., *iPSC-derived dopamine neurons reveal differences between monozygotic twins discordant for Parkinson's disease*. Cell Rep, 2014. **9**(4): p. 1173-82.
417. Ren, Y., et al., *Parkin mutations reduce the complexity of neuronal processes in iPSC-derived human neurons*. Stem Cells, 2015. **33**(1): p. 68-78.
418. Shaltouki, A., et al., *Mitochondrial alterations by PARKIN in dopaminergic neurons using PARK2 patient-specific and PARK2 knockout isogenic iPSC lines*. Stem Cell Reports, 2015. **4**(5): p. 847-59.
419. Burbulla, L.F., et al., *Dopamine oxidation mediates mitochondrial and lysosomal dysfunction in Parkinson's disease*. Science, 2017. **357**(6357): p. 1255-1261.

420. Kouroupi, G., et al., *Defective synaptic connectivity and axonal neuropathology in a human iPSC-based model of familial Parkinson's disease*. Proc Natl Acad Sci U S A, 2017. **114**(18): p. E3679-E3688.
421. Singh Dolt, K., F. Hammachi, and T. Kunath, *Modeling Parkinson's disease with induced pluripotent stem cells harboring alpha-synuclein mutations*. Brain Pathol, 2017. **27**(4): p. 545-551.
422. Torrent, R., et al., *Using iPSC Cells toward the Understanding of Parkinson's Disease*. J Clin Med, 2015. **4**(4): p. 548-66.
423. Matta, S., et al., *LRRK2 controls an EndoA phosphorylation cycle in synaptic endocytosis*. Neuron, 2012. **75**(6): p. 1008-21.
424. Soldner, F., et al., *Generation of isogenic pluripotent stem cells differing exclusively at two early onset Parkinson point mutations*. Cell, 2011. **146**(2): p. 318-31.
425. Byers, B., et al., *SNCA triplication Parkinson's patient's iPSC-derived DA neurons accumulate alpha-synuclein and are susceptible to oxidative stress*. PLoS One, 2011. **6**(11): p. e26159.
426. Flierl, A., et al., *Higher vulnerability and stress sensitivity of neuronal precursor cells carrying an alpha-synuclein gene triplication*. PLoS One, 2014. **9**(11): p. e112413.
427. Oliveira, L.M., et al., *Elevated alpha-synuclein caused by SNCA gene triplication impairs neuronal differentiation and maturation in Parkinson's patient-derived induced pluripotent stem cells*. Cell Death Dis, 2015. **6**: p. e1994.
428. Ryan, T., et al., *Cardiolipin exposure on the outer mitochondrial membrane modulates alpha-synuclein*. Nat Commun, 2018. **9**(1): p. 817.
429. Koprach, J.B., L.V. Kalia, and J.M. Brotchie, *Animal models of alpha-synucleinopathy for Parkinson disease drug development*. Nat Rev Neurosci, 2017. **18**(9): p. 515-529.
430. Spillantini, M.G., et al., *Alpha-synuclein in Lewy bodies*. Nature, 1997. **388**(6645): p. 839-40.
431. Appel-Cresswell, S., et al., *Alpha-synuclein p.H50Q, a novel pathogenic mutation for Parkinson's disease*. Mov Disord, 2013. **28**(6): p. 811-3.
432. Pasanen, P., et al., *SNCA mutation p.Ala53Glu is derived from a common founder in the Finnish population*. Neurobiol Aging, 2017. **50**: p. 168 e5-168 e8.
433. Proukakis, C., et al., *A novel alpha-synuclein missense mutation in Parkinson disease*. Neurology, 2013. **80**(11): p. 1062-4.
434. Ibanez, P., et al., *Absence of NR4A2 exon 1 mutations in 108 families with autosomal dominant Parkinson disease*. Neurology, 2004. **62**(11): p. 2133-4.
435. Singleton, A.B., M.J. Farrer, and V. Bonifati, *The genetics of Parkinson's disease: progress and therapeutic implications*. Mov Disord, 2013. **28**(1): p. 14-23.
436. Kotzbauer, P.T., et al., *Fibrillization of alpha-synuclein and tau in familial Parkinson's disease caused by the A53T alpha-synuclein mutation*. Exp Neurol, 2004. **187**(2): p. 279-88.
437. Spira, P.J., et al., *Clinical and pathological features of a Parkinsonian syndrome in a family with an Ala53Thr alpha-synuclein mutation*. Ann Neurol, 2001. **49**(3): p. 313-9.
438. Fogel, B.L., et al., *RBFOX1 regulates both splicing and transcriptional networks in human neuronal development*. Hum Mol Genet, 2012. **21**(19): p. 4171-86.
439. Soldner, F., et al., *Parkinson's disease patient-derived induced pluripotent stem cells free of viral reprogramming factors*. Cell, 2009. **136**(5): p. 964-77.
440. Duda, J.E., et al., *Concurrence of alpha-synuclein and tau brain pathology in the Contursi kindred*. Acta Neuropathol, 2002. **104**(1): p. 7-11.
441. Lin, L., et al., *Molecular Features Underlying Neurodegeneration Identified through In Vitro Modeling of Genetically Diverse Parkinson's Disease Patients*. Cell Rep, 2016. **15**(11): p. 2411-26.

442. Allen, N.J. and C. Eroglu, *Cell Biology of Astrocyte-Synapse Interactions*. Neuron, 2017. **96**(3): p. 697-708.
443. Gonzalez, D.M., J. Gregory, and K.J. Brennand, *The Importance of Non-neuronal Cell Types in hiPSC-Based Disease Modeling and Drug Screening*. Front Cell Dev Biol, 2017. **5**: p. 117.
444. Djelloul, M., et al., *Alpha-Synuclein Expression in the Oligodendrocyte Lineage: an In Vitro and In Vivo Study Using Rodent and Human Models*. Stem Cell Reports, 2015. **5**(2): p. 174-84.
445. Muffat, J., et al., *Efficient derivation of microglia-like cells from human pluripotent stem cells*. Nat Med, 2016. **22**(11): p. 1358-1367.
446. Haenseler, W., et al., *Excess alpha-synuclein compromises phagocytosis in iPSC-derived macrophages*. Sci Rep, 2017. **7**(1): p. 9003.
447. Moreno, E.L., et al., *Differentiation of neuroepithelial stem cells into functional dopaminergic neurons in 3D microfluidic cell culture*. Lab Chip, 2015. **15**(11): p. 2419-28.
448. Cotzias, G.C., P.S. Papavasiliou, and R. Gellene, *Modification of Parkinsonism--chronic treatment with L-dopa*. N Engl J Med, 1969. **280**(7): p. 337-45.
449. Katzenschlager, R., et al., *Apomorphine subcutaneous infusion in patients with Parkinson's disease with persistent motor fluctuations (TOLEDO): a multicentre, double-blind, randomised, placebo-controlled trial*. Lancet Neurol, 2018.
450. Fox, S.H., et al., *International Parkinson and movement disorder society evidence-based medicine review: Update on treatments for the motor symptoms of Parkinson's disease*. Mov Disord, 2018.
451. Ory-Magne, F., et al., *Withdrawing amantadine in dyskinetic patients with Parkinson disease: the AMANDYSK trial*. Neurology, 2014. **82**(4): p. 300-7.
452. Sardi, S.P., J.M. Cedarbaum, and P. Brundin, *Targeted Therapies for Parkinson's Disease: From Genetics to the Clinic*. Mov Disord, 2018. **33**(5): p. 684-696.
453. McIntyre, C.C. and R.W. Anderson, *Deep brain stimulation mechanisms: the control of network activity via neurochemistry modulation*. J Neurochem, 2016. **139** Suppl 1: p. 338-345.
454. Suarez-Cedeno, G., J. Suescun, and M.C. Schiess, *Earlier Intervention with Deep Brain Stimulation for Parkinson's Disease*. Parkinsons Dis, 2017. **2017**: p. 9358153.
455. Favre, J., et al., *Outcome of unilateral and bilateral pallidotomy for Parkinson's disease: patient assessment*. Neurosurgery, 2000. **46**(2): p. 344-53; discussion 353-5.
456. Cahan, L.D., R.F. Young, and F. Li, *Radiosurgical Pallidotomy for Parkinson's Disease*. Prog Neurol Surg, 2018. **33**: p. 149-157.
457. Li, W., et al., *Extensive graft-derived dopaminergic innervation is maintained 24 years after transplantation in the degenerating parkinsonian brain*. Proc Natl Acad Sci U S A, 2016. **113**(23): p. 6544-9.
458. Kefalopoulou, Z., et al., *Long-term clinical outcome of fetal cell transplantation for Parkinson disease: two case reports*. JAMA Neurol, 2014. **71**(1): p. 83-7.
459. Barker, R.A., J. Drouin-Ouellet, and M. Parmar, *Cell-based therapies for Parkinson disease--past insights and future potential*. Nat Rev Neurol, 2015. **11**(9): p. 492-503.
460. Trzaska, K.A. and P. Rameshwar, *Dopaminergic neuronal differentiation protocol for human mesenchymal stem cells*. Methods Mol Biol, 2011. **698**: p. 295-303.
461. Hallett, P.J., et al., *Successful function of autologous iPSC-derived dopamine neurons following transplantation in a non-human primate model of Parkinson's disease*. Cell Stem Cell, 2015. **16**(3): p. 269-74.
462. Caiazzo, M., et al., *Direct generation of functional dopaminergic neurons from mouse and human fibroblasts*. Nature, 2011. **476**(7359): p. 224-7.

463. Rivetti di Val Cervo, P., et al., *Induction of functional dopamine neurons from human astrocytes in vitro and mouse astrocytes in a Parkinson's disease model*. Nat Biotechnol, 2017. **35**(5): p. 444-452.
464. Barker, R.A., et al., *Human Trials of Stem Cell-Derived Dopamine Neurons for Parkinson's Disease: Dawn of a New Era*. Cell Stem Cell, 2017. **21**(5): p. 569-573.
465. Hargus, G., et al., *Differentiated Parkinson patient-derived induced pluripotent stem cells grow in the adult rodent brain and reduce motor asymmetry in Parkinsonian rats*. Proc Natl Acad Sci U S A, 2010. **107**(36): p. 15921-6.
466. Kikuchi, T., et al., *Human iPS cell-derived dopaminergic neurons function in a primate Parkinson's disease model*. Nature, 2017. **548**(7669): p. 592-596.
467. Kikuchi, T., et al., *Idiopathic Parkinson's disease patient-derived induced pluripotent stem cells function as midbrain dopaminergic neurons in rodent brains*. J Neurosci Res, 2017. **95**(9): p. 1829-1837.
468. Hemmer, K., et al., *In Vivo Phenotyping Of Parkinson-Specific Stem Cells Reveals Increased  $\alpha$ -Synuclein Levels But No Spreading*. bioRxiv, 2017.
469. Koros, C., et al., *Selective cognitive impairment and hyposmia in p.A53T SNCA PD vs typical PD*. Neurology, 2018. **90**(10): p. e864-e869.
470. Papadimitriou, D., et al., *Motor and Nonmotor Features of Carriers of the p.A53T Alpha-Synuclein Mutation: A Longitudinal Study*. Mov Disord, 2016. **31**(8): p. 1226-30.
471. Wrasidlo, W., et al., *A de novo compound targeting alpha-synuclein improves deficits in models of Parkinson's disease*. Brain, 2016. **139**(Pt 12): p. 3217-3236.
472. Papastefanaki, F., et al., *Grafts of Schwann cells engineered to express PSA-NCAM promote functional recovery after spinal cord injury*. Brain, 2007. **130**(Pt 8): p. 2159-74.
473. Von Voigtlander, P.F. and K.E. Moore, *Involvement of nigro-striatal neurons in the in vivo release of dopamine by amphetamine, amantadine and tyramine*. J Pharmacol Exp Ther, 1973. **184**(3): p. 542-52.
474. Koutsoudaki, P.N., et al., *Neural stem/progenitor cells differentiate into oligodendrocytes, reduce inflammation, and ameliorate learning deficits after transplantation in a mouse model of traumatic brain injury*. Glia, 2016. **64**(5): p. 763-79.
475. Mitsui, K., et al., *The homeoprotein Nanog is required for maintenance of pluripotency in mouse epiblast and ES cells*. Cell, 2003. **113**(5): p. 631-42.
476. Masui, S., et al., *Pluripotency governed by Sox2 via regulation of Oct3/4 expression in mouse embryonic stem cells*. Nat Cell Biol, 2007. **9**(6): p. 625-35.
477. Schopperle, W.M. and W.C. DeWolf, *The TRA-1-60 and TRA-1-81 human pluripotent stem cell markers are expressed on podocalyxin in embryonal carcinoma*. Stem Cells, 2007. **25**(3): p. 723-30.
478. Ross, L.L., ED., *Human Ontogeny: Gastrulation, Neurulation, and Somite Formation". Atlas of anatomy: general anatomy and musculoskeletal system*. 2006: Thieme.
479. Sanchez-Danes, A., et al., *Disease-specific phenotypes in dopamine neurons from human iPS-based models of genetic and sporadic Parkinson's disease*. EMBO Mol Med, 2012. **4**(5): p. 380-95.
480. Sundberg, M., et al., *Improved cell therapy protocols for Parkinson's disease based on differentiation efficiency and safety of hESC-, hiPSC-, and non-human primate iPSC-derived dopaminergic neurons*. Stem Cells, 2013. **31**(8): p. 1548-62.
481. Zhang, P., N. Xia, and R.A. Reijo Pera, *Directed dopaminergic neuron differentiation from human pluripotent stem cells*. J Vis Exp, 2014(91): p. 51737.
482. Ye, W., et al., *FGF and Shh signals control dopaminergic and serotonergic cell fate in the anterior neural plate*. Cell, 1998. **93**(5): p. 755-66.

483. Kadkhodaei, B., et al., *Nurr1 is required for maintenance of maturing and adult midbrain dopamine neurons*. J Neurosci, 2009. **29**(50): p. 15923-32.
484. El Maarouf, A. and U. Rutishauser, *Removal of polysialic acid induces aberrant pathways, synaptic vesicle distribution, and terminal arborization of retinotectal axons*. J Comp Neurol, 2003. **460**(2): p. 203-11.
485. Quartu, M., et al., *Polysialylated-neural cell adhesion molecule (PSA-NCAM) in the human trigeminal ganglion and brainstem at prenatal and adult ages*. BMC Neurosci, 2008. **9**: p. 108.
486. Friocourt, G., et al., *Doublecortin functions at the extremities of growing neuronal processes*. Cereb Cortex, 2003. **13**(6): p. 620-6.
487. Gleeson, J.G., et al., *Doublecortin is a microtubule-associated protein and is expressed widely by migrating neurons*. Neuron, 1999. **23**(2): p. 257-71.
488. Lee, D.R., et al., *PSA-NCAM-negative neural crest cells emerging during neural induction of pluripotent stem cells cause mesodermal tumors and unwanted grafts*. Stem Cell Reports, 2015. **4**(5): p. 821-34.
489. Doi, D., et al., *Prolonged maturation culture favors a reduction in the tumorigenicity and the dopaminergic function of human ESC-derived neural cells in a primate model of Parkinson's disease*. Stem Cells, 2012. **30**(5): p. 935-45.
490. Kim, D.S., et al., *Highly pure and expandable PSA-NCAM-positive neural precursors from human ESC and iPSC-derived neural rosettes*. PLoS One, 2012. **7**(7): p. e39715.
491. Shin, S., et al., *Long-term proliferation of human embryonic stem cell-derived neuroepithelial cells using defined adherent culture conditions*. Stem Cells, 2006. **24**(1): p. 125-38.
492. Hargus, G., et al., *Origin-dependent neural cell identities in differentiated human iPSCs in vitro and after transplantation into the mouse brain*. Cell Rep, 2014. **8**(6): p. 1697-1703.
493. Smith, G.H., A., *Animal Models of Movement Disorders: 6-OHDA toxin models of PD in mice*. . Vol. 61. 2011: Springer / Humana.
494. Doi, D., et al., *Isolation of human induced pluripotent stem cell-derived dopaminergic progenitors by cell sorting for successful transplantation*. Stem Cell Reports, 2014. **2**(3): p. 337-50.
495. Lehnen, D., et al., *IAP-Based Cell Sorting Results in Homogeneous Transplantable Dopaminergic Precursor Cells Derived from Human Pluripotent Stem Cells*. Stem Cell Reports, 2017. **9**(4): p. 1207-1220.
496. Lendahl, U., L.B. Zimmerman, and R.D. McKay, *CNS stem cells express a new class of intermediate filament protein*. Cell, 1990. **60**(4): p. 585-95.
497. Shen, D., et al., *Novel cell- and tissue-based assays for detecting misfolded and aggregated protein accumulation within aggregates and inclusion bodies*. Cell Biochem Biophys, 2011. **60**(3): p. 173-85.
498. Berridge, M.J., M.D. Bootman, and H.L. Roderick, *Calcium signalling: dynamics, homeostasis and remodelling*. Nat Rev Mol Cell Biol, 2003. **4**(7): p. 517-29.
499. Liu, L., et al., *Palmitate induces transcriptional regulation of BACE1 and presenilin by STAT3 in neurons mediated by astrocytes*. Exp Neurol, 2013. **248**: p. 482-90.
500. Zundorf, G. and G. Reiser, *Calcium dysregulation and homeostasis of neural calcium in the molecular mechanisms of neurodegenerative diseases provide multiple targets for neuroprotection*. Antioxid Redox Signal, 2011. **14**(7): p. 1275-88.
501. Nedergaard, M. and A. Verkhratsky, *Calcium dyshomeostasis and pathological calcium signalling in neurological diseases*. Cell Calcium, 2010. **47**(2): p. 101-2.
502. Spitzer, N.C., C.M. Root, and L.N. Borodinsky, *Orchestrating neuronal differentiation: patterns of Ca<sup>2+</sup> spikes specify transmitter choice*. Trends Neurosci, 2004. **27**(7): p. 415-21.

503. Rothman, R.B. and M.H. Baumann, *Monoamine transporters and psychostimulant drugs*. Eur J Pharmacol, 2003. **479**(1-3): p. 23-40.
504. Fleckenstein, A.E., et al., *New insights into the mechanism of action of amphetamines*. Annu Rev Pharmacol Toxicol, 2007. **47**: p. 681-98.
505. Labandeira-Garcia, J.L., et al., *Time course of striatal changes induced by 6-hydroxydopamine lesion of the nigrostriatal pathway, as studied by combined evaluation of rotational behaviour and striatal Fos expression*. Exp Brain Res, 1996. **108**(1): p. 69-84.
506. Behrstock, S., et al., *Lesion-induced increase in survival and migration of human neural progenitor cells releasing GDNF*. Cell Transplant, 2008. **17**(7): p. 753-62.
507. Tcherepanov, A.A. and B.P. Sokolov, *Age-related abnormalities in expression of mRNAs encoding synapsin 1A, synapsin 1B, and synaptophysin in the temporal cortex of schizophrenics*. J Neurosci Res, 1997. **49**(5): p. 639-44.
508. Wiedenmann, B. and W.W. Franke, *Identification and localization of synaptophysin, an integral membrane glycoprotein of Mr 38,000 characteristic of presynaptic vesicles*. Cell, 1985. **41**(3): p. 1017-28.
509. Calhoun, M.E., et al., *Comparative evaluation of synaptophysin-based methods for quantification of synapses*. J Neurocytol, 1996. **25**(12): p. 821-8.
510. Masliah, E., et al., *Quantitative immunohistochemistry of synaptophysin in human neocortex: an alternative method to estimate density of presynaptic terminals in paraffin sections*. J Histochem Cytochem, 1990. **38**(6): p. 837-44.
511. Le, W., J. Wu, and Y. Tang, *Protective Microglia and Their Regulation in Parkinson's Disease*. Front Mol Neurosci, 2016. **9**: p. 89.
512. Tang, Y. and W. Le, *Differential Roles of M1 and M2 Microglia in Neurodegenerative Diseases*. Mol Neurobiol, 2016. **53**(2): p. 1181-94.
513. Mogi, M., et al., *Transforming growth factor-beta 1 levels are elevated in the striatum and in ventricular cerebrospinal fluid in Parkinson's disease*. Neurosci Lett, 1995. **193**(2): p. 129-32.
514. Mogi, M., et al., *Interleukin (IL)-1 beta, IL-2, IL-4, IL-6 and transforming growth factor-alpha levels are elevated in ventricular cerebrospinal fluid in juvenile parkinsonism and Parkinson's disease*. Neurosci Lett, 1996. **211**(1): p. 13-6.
515. Mogi, M., et al., *Tumor necrosis factor-alpha (TNF-alpha) increases both in the brain and in the cerebrospinal fluid from parkinsonian patients*. Neurosci Lett, 1994. **165**(1-2): p. 208-10.
516. Gerhard, A., et al., *In vivo imaging of microglial activation with [11C](R)-PK11195 PET in idiopathic Parkinson's disease*. Neurobiol Dis, 2006. **21**(2): p. 404-12.
517. Qiu, L., et al., *Immature Midbrain Dopaminergic Neurons Derived from Floor-Plate Method Improve Cell Transplantation Therapy Efficacy for Parkinson's Disease*. Stem Cells Transl Med, 2017. **6**(9): p. 1803-1814.
518. Koizumi, H., et al., *Doublecortin maintains bipolar shape and nuclear translocation during migration in the adult forebrain*. Nat Neurosci, 2006. **9**(6): p. 779-86.
519. Shin, E., et al., *Doublecortin-like kinase enhances dendritic remodelling and negatively regulates synapse maturation*. Nat Commun, 2013. **4**: p. 1440.
520. Paus, M., et al., *Enhanced dendritogenesis and axogenesis in hippocampal neuroblasts of LRRK2 knockout mice*. Brain Res, 2013. **1497**: p. 85-100.
521. Rosenberg, S.S. and N.C. Spitzer, *Calcium signaling in neuronal development*. Cold Spring Harb Perspect Biol, 2011. **3**(10): p. a004259.
522. van Ooyen, A. and J. van Pelt, *Activity-dependent neurite outgrowth and neural network development*. Prog Brain Res, 1994. **102**: p. 245-59.

523. Schwab, A.J. and A.D. Ebert, *Neurite Aggregation and Calcium Dysfunction in iPSC-Derived Sensory Neurons with Parkinson's Disease-Related LRRK2 G2019S Mutation*. Stem Cell Reports, 2015. **5**(6): p. 1039-1052.
524. Imamura, K., et al., *Calcium dysregulation contributes to neurodegeneration in FTLD patient iPSC-derived neurons*. Sci Rep, 2016. **6**: p. 34904.
525. Lohmann, C. and R.O. Wong, *Regulation of dendritic growth and plasticity by local and global calcium dynamics*. Cell Calcium, 2005. **37**(5): p. 403-9.
526. Ungerstedt, U., *6-Hydroxy-dopamine induced degeneration of central monoamine neurons*. Eur J Pharmacol, 1968. **5**(1): p. 107-10.
527. Brundin, P., et al., *The rotating 6-hydroxydopamine-lesioned mouse as a model for assessing functional effects of neuronal grafting*. Brain Res, 1986. **366**(1-2): p. 346-9.
528. Thiele, S.L., R. Warre, and J.E. Nash, *Development of a unilaterally-lesioned 6-OHDA mouse model of Parkinson's disease*. J Vis Exp, 2012(60).
529. Fox, M.E., et al., *Cross-hemispheric dopamine projections have functional significance*. Proc Natl Acad Sci U S A, 2016. **113**(25): p. 6985-90.
530. Liang, G. and Y. Zhang, *Genetic and epigenetic variations in iPSCs: potential causes and implications for application*. Cell Stem Cell, 2013. **13**(2): p. 149-59.
531. Espuny-Camacho, I., et al., *Hallmarks of Alzheimer's Disease in Stem-Cell-Derived Human Neurons Transplanted into Mouse Brain*. Neuron, 2017. **93**(5): p. 1066-1081 e8.
532. Espuny-Camacho, I., et al., *Pyramidal neurons derived from human pluripotent stem cells integrate efficiently into mouse brain circuits in vivo*. Neuron, 2013. **77**(3): p. 440-56.
533. Gaspard, N., et al., *An intrinsic mechanism of corticogenesis from embryonic stem cells*. Nature, 2008. **455**(7211): p. 351-7.



